BMR JOURNAL
OF AUSTRALIAN GEOLOGY & GEOPHYSICS

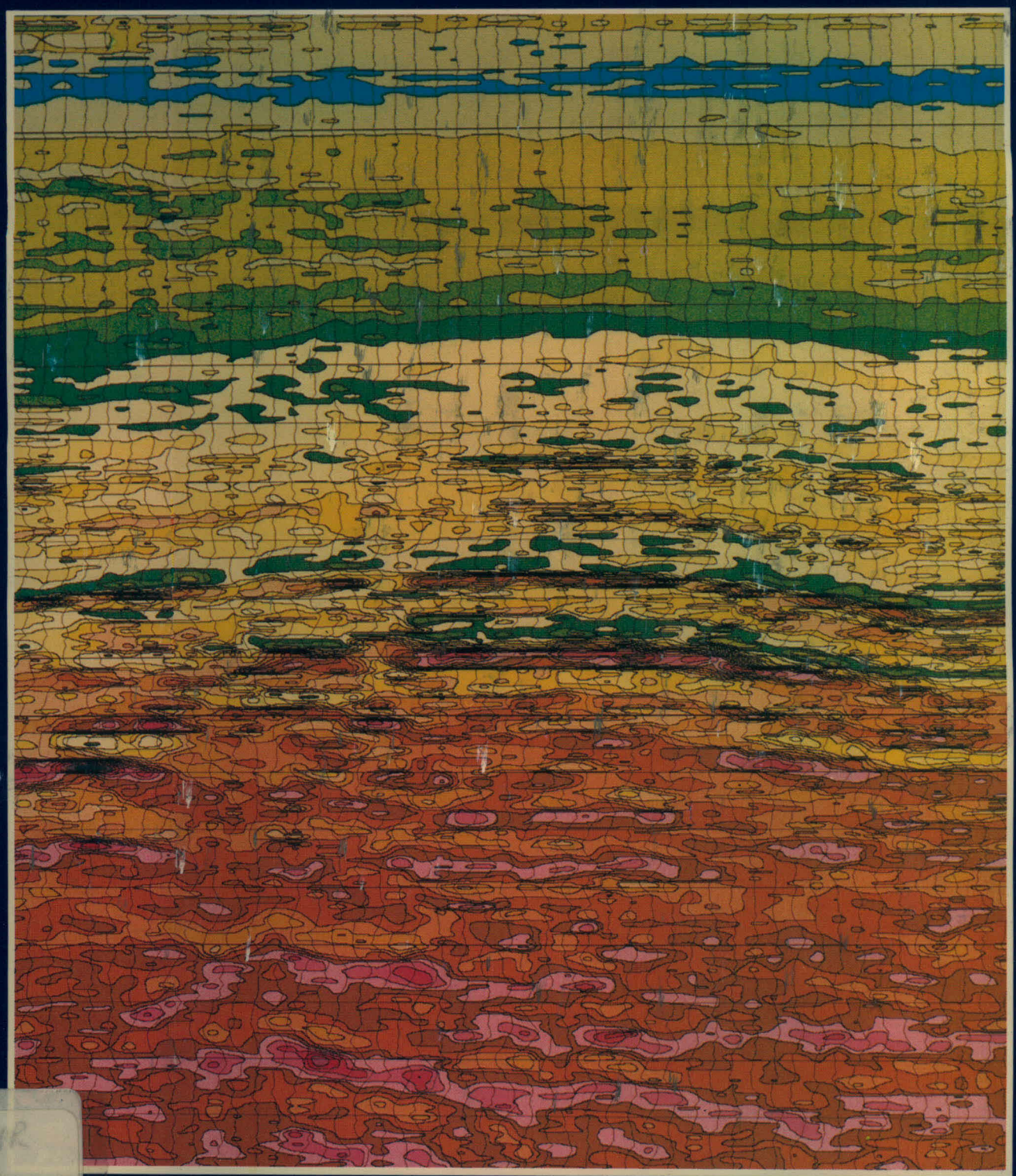

VOLUME 9 NUMBER 3 SEPTEMBER 1984

BMR JOURNAL

OF AUSTRALIAN GEOLOGY & GEOPHYSICS

VOLUME 9 NUMBER 3 SEPTEMBER 1984

CONTENTS

Front Cover: Colour contour displays of velocity log (Glog) information can be generated from seismic data and well logs to show broad and narrow velocity variations within the subsurface. The cover illustration is a 7.2 km section from BMR 1982 Line 11, south of Bass-1 well in the Bass Basin. A possible zone of direct hydrocarbon detection occurs as two flat events made up of a narrow doublet of colour, indicating a low velocity followed immediately by a high velocity. These flat events occur across the upper part of a general arch in the colour bands. Increasing velocity within the section starts with low velocity blues, greens, and yellows through to high velocities in browns, reds, and purples. The vertical scale is two-way time at 10 cm per second, commencing at 0.8 seconds at the top of the illustration. A paper by Etheridge & others in this issue describes major basin-forming structures in the Bass Basin and their relevance to hydrocarbon exploration.

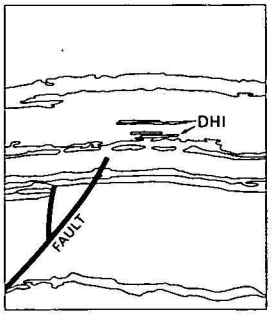

AUSTRALIAN GOVERNMENT PUBLISHING SERVICE CANBERRA 1985

Department of Resources and Energy

Minister: Senator the Hon. Gareth Evans, Q.C.

Secretary: A. J. Woods, A.O.

Bureau of Mineral Resources, Geology and Geophysics

Director: R. W. R. Rutland

Editor, BMR Journal: I. M. Hodgson

The BMR Journal of Australian Geology & Geophysics is a quarterly journal of research. It contains papers and shorter notes by scientists of the BMR or others who are collaborating with BMR. Discussion of papers is invited from anyone.

Subscriptions to the BMR Journal are managed by the Australian Government Publishing Service (Mail Order Sales, GPO Box 84, Canberra, ACT 2601; telephone (062) 95 4485), to which enquiries should be directed.

Other matters concerning the Journal should be sent to the Director, marked for the attention of the Editor, BMR Journal.

Month of issue: March 1985

ISSN 0312-9608

Printed by Graphic Services Pty Ltd, 516-518 Grand Junction Road, Northfield, S.A. 5085

BMR Journal of Australian Geology & Geophysics, 9, 197–206

Basin-forming structures and their relevance to hydrocarbon exploration in Bass Basin, southeastern Australia

M.A. Etheridge[1], J.C. Branson[2], D.A. Falvey[2], K.L. Lockwood[2], P.G. Stuart-Smith[1] & A.S. Scherl[2]

Interpretation of high-quality seismic reflection data from Bass Basin, southeastern Australia, has led to the recognition of major Early Cretaceous extensional normal faults segmented by contemporaneous transfer faults. The normal faults, which initiated development of the basin, are rotational, have low to moderate dips, and were produced by 60–80% horizontal extension ($\beta = 1.6$–2.0) of the crust beneath the basin. There are three major normal faults, with trends of 290° to 300° – one along each margin and one near the centre of the basin. The transfer faults are vertical and trend 020° to 030°. They are predominantly of right-lateral offset, giving rise to the northwesterly trend of the basin. The normal faults and associated tilt-block edges have had a major influence on structural evolution in the overlying hydrocarbon-prospective Eastern View Coal Measures (EVCM). A play concept is presented that relates the mid-basin tilt-block/normal fault system and associated transfer faults to structures, facies variations, and source maturity within the EVCM. A geohistory analysis of a specific location containing such a structure associated with possible direct hydrocarbon indicators shows that the lower EVCM has been oil-mature since the Oligocene, and it is suggested, therefore, that the prospectivity of the Bass Basin should be upgraded.

Introduction

In 1982, the Australian Bureau of Mineral Resources (BMR) contracted (with Geophysical Services International) a regional marine geophysical survey, comprising 3200 km of seismic, gravity, and magnetic traverse in Bass Strait, between southeastern mainland Australia and Tasmania. The survey was centred on the Bass Basin, with ties to the adjacent Gippsland and Otway Basins and the continental slopes (Fig. 1).

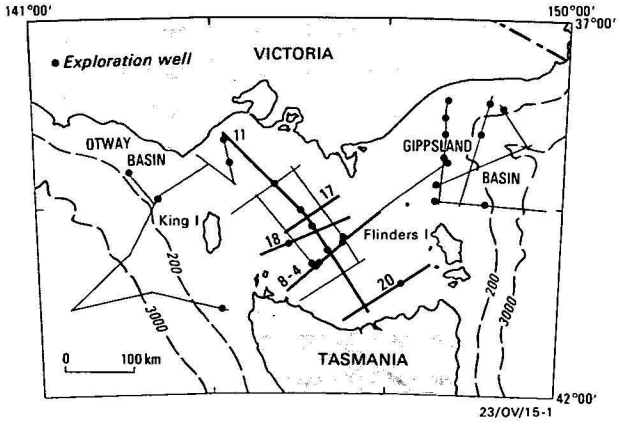

Figure 1. Track map for BMR 1982 Bass Strait geophysical survey.
Survey lines referred to in the text are heavily drawn and numbered.

The Gippsland Basin, which is substantially similar in stratigraphy, reservoir and source characteristics, and maturation levels to the Bass Basin, is Australia's major oil producer. However, despite these similarities, exploration in the Bass Basin to date (19 wells) has proved disappointing, resulting in one small uncommercial gas/condensate accumulation (Pelican) and only a few other minor hydrocarbon shows. Mid-Eocene to younger structures, which contain most of the hydrocarbons in the Gippsland Basin, are poorly developed or absent in the Bass Basin. Development of structures in the Bass Basin is mainly associated with deep-seated fault blocks of Cretaceous age, and, consequently, the BMR seismic survey was designed to provide superior quality data in the Cretaceous to early Tertiary section. Reverberation from and within the extensive Eocene coal measures severely reduced the quality of earlier seismic data from these lower stratigraphic levels.

This paper outlines the results of a detailed analysis of the Cretaceous fault structures within the Bass Basin, and presents a general kinematic model for the early basin history. The structural picture that emerges from the new data is quite different from previously published interpretations, and it provides a new framework for evaluating hydrocarbon plays associated with the deep-seated structures. Development of this play concept leads to an explanation of the known distribution of hydrocarbons within the basin and identification of untested targets.

[1]Division of Petrology & Geochemistry, BMR
[2]Division of Marine Geosciences & Petroleum Geology, BMR

Regional setting

Tectonic and structural setting

The Bass Basin is a Mesozoic to Late Tertiary basin related to Gondwanaland breakup along Australia's southern and eastern margins. It is separated from the Gippsland and Otway Basins by narrow ridges of Late Proterozoic to Palaeozoic rocks of the Lachlan Fold Belt.

In most published accounts (Robinson, 1974; Brown, 1976; Davidson & others, 1984) the Bass Basin and its major structures have been shown to have a northwesterly trend, which differs from the westerly trend in the Gippsland Basin and the west-northwesterly trend of the Otway Basin (Robinson, 1974; Davidson & others, 1984, fig. 6). There has been little agreement as to the tectonic relationships that gave rise to the trends and positions of the three basins, except that they resulted from rifting and sea-floor spreading along one or both of Australia's southern and eastern margins (e.g. Burke & Dewey, 1973; Mutter & Jongsma, 1978; Davidson, 1970; Davidson & others, 1984). A model for the structural evolution of the three basins is described by Etheridge & others (in press).

Generalised lithostratigraphy

The sediments of the Bass Basin comprise three principal components: the late Tertiary marine sequences, a Late Cretaceous to late Eocene alluvial and coastal plain sequence, and an Early Cretaceous rift valley sequence. The Late Cretaceous to late Eocene section is known as the Eastern View Coal Measures (EVCM), and is comparable to the Latrobe Group in the Gippsland Basin.

Brown (1976) divided the EVCM into upper and lower sequences separated by an early Eocene partial unconformity, of possible regional significance. In general, the lower sequence consists of a silty shale section with thin fine sandstones and rare coals, but important local variations were emphasised by Brown (1976). We regard these local variations to be largely induced by the major structures described below. The upper se-

quence is characterised by thick coal sections in the centre of the basin, which decrease in abundance upwards and westwards. Both upper and lower sequences become more shaly northwards, a generalisation influenced by the sand-rich lithologies encountered near the southeast basin extremity in Durroon-1. However, the presence in the southeast of a discrete structural province or sub-basin provides a new model for regional facies trends along the NW-SE axis. To date, the implied control has been simple relative proximity to regional sources of clastic material. Evidence for local structural control of lithology in the upper sequence seems confined to major high-standing horsts.

Hydrocarbons in the Bass Basin

Nineteen wells have been drilled in the Bass Basin (two others, Snail-1 and Nerita-1 were drilled in the Torquay Embayment, the northwest extension of the Bass Basin), and hydrocarbon shows or indications have been recorded in nine of them (Pelican-1,2,3 and 4, Cormorant-1, Aroo-1, Bass-3, Dondu-1 and Poonboon-1). The main results from this drilling are as follows:

1) No significant shows or indications have been found in structures mapped at the top of the Eastern View Coal Measures, which is by far the most productive level in the Gippsland Basin. Structures, albeit of lower amplitude, mapped on the unconformity between lower and upper Eastern View Coal Measures appear to be more prospective in Bass Basin (Brown, 1976).

2) Most of the structures drilled are located above the uplifted edges and corners of major Cretaceous tilt blocks.

3) Post-Eocene structures are largely restricted to the northwestern part of the basin, as in Cormorant-1, Snail-1 and Nerita-1.

4) The upper coal measures contain good reservoir sands throughout the basin, but the lower coal measures grade from dominantly shale/siltstone in the northwest (Cormorant-1, Konkon-1) to sand-rich in the southeast (Durroon-1) (Brown 1976; Nicholas & others, 1981).

Brown (1976) developed a model involving long-range migration of hydrocarbons from the shaly source rocks in the northwest towards reservoirs in the sandier sequences in the southeast. Nicholas & others (1981) demonstrated that suitable source rocks exist throughout the basin, and that hydrocarbon generation would have been mostly from lower Eastern View Coal Measures (to which they assigned a good to very good source potential) below the explored levels. Their conclusion (p.210) that 'the Eastern View Coal Measures in the deeper parts of the Bass Basin seem to meet all the prerequisites for successful petroleum exploration' provided strong support for Brown's (1976, p.81) contention that 'it appears important now to search for deeper structures beneath the blanketing upper coal measures in areas where good reservoir conditions may exist', and gave much of the impetus to the BMR seismic survey and this study of the deep structure and stratigraphy.

Cretaceous structure of Bass Basin

Large Early Cretaceous normal faults dominate the deep structure of the Bass Basin (Brown, 1976; Robinson, 1974). Coal measures and volcanics in the overlying Tertiary sequence commonly obscure the detailed structures at the Cretaceous level.

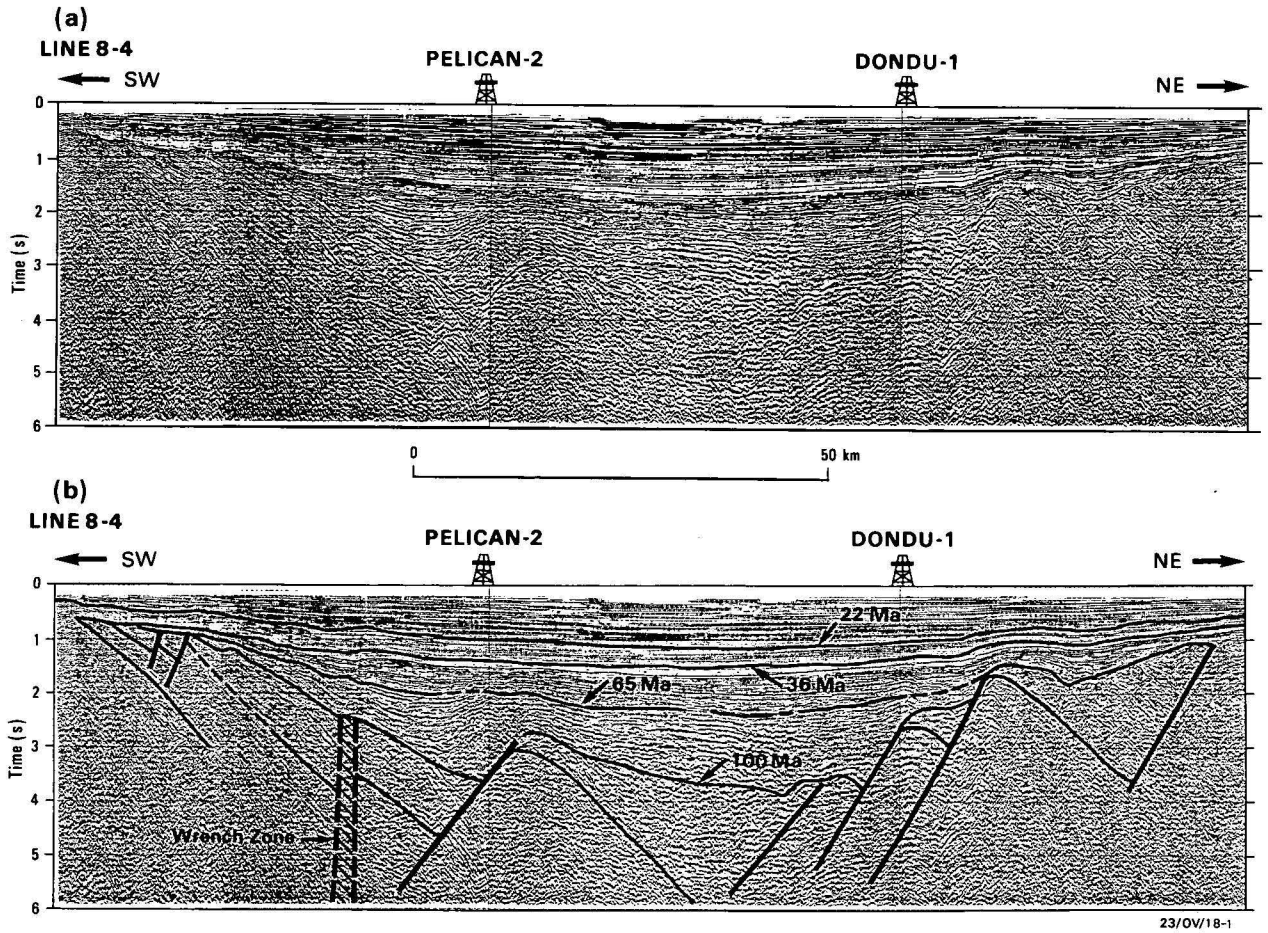

Figure 2. (a) Compressed seismic section, and (b) structural interpretation of the Bass Basin portion of line 8/4, showing the major Early Cretaceous normal faults.

The wrench zone is one of the transfer faults that affect the normal faults. Vertical exaggeration at the Cretaceous level is approximately 3.

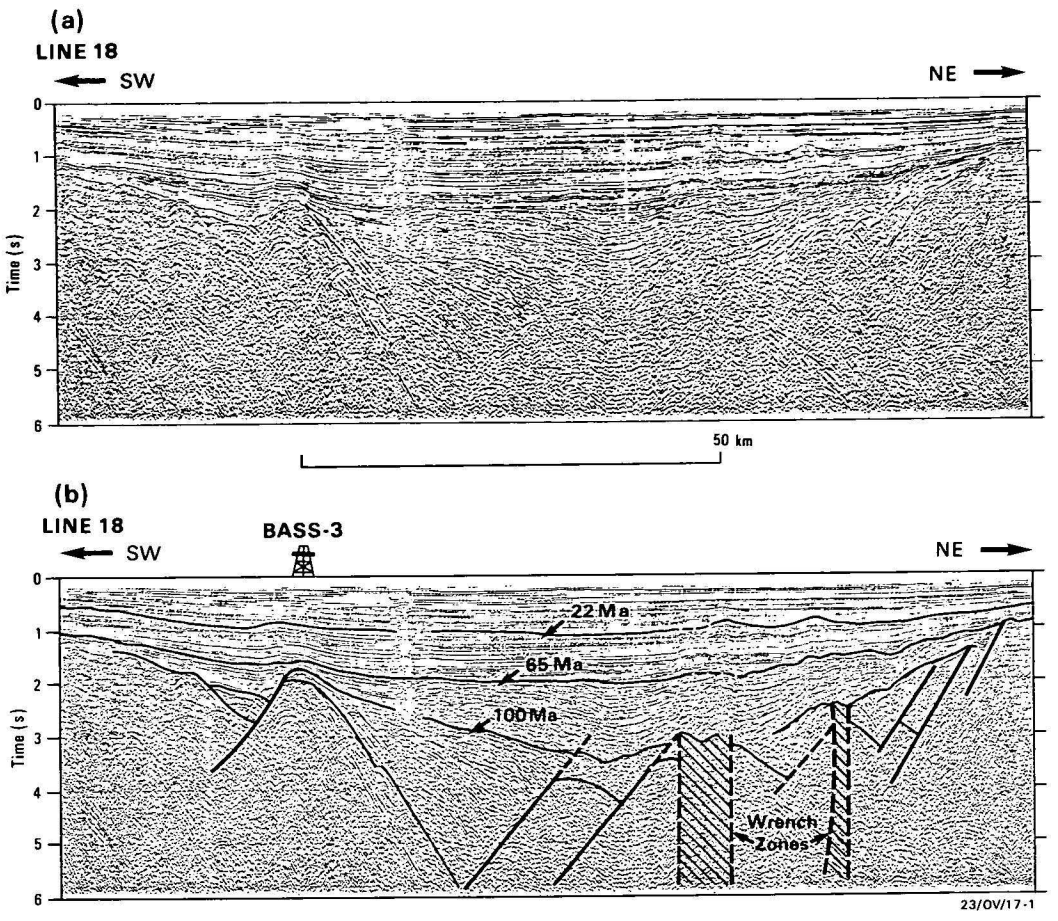

Figure 3. (a) Compressed seismic section, and (b) structural interpretation of line 18.
This section crosses the major transfer fault (shown in Figs. 5 and 6a) near its intersection with line 11. The accumulation of volcanics in the section above the transfer fault, and complex offside reflections adjacent to the fault make interpretation difficult in that region. Vertical exaggeration at the Cretaceous level is approximately 3.

but seismic sections along BMR survey lines 8/4 and 18 (Figs. 2, 3; see Fig. 1 for line locations) illustrate their main features.

The most striking features of the Early Cretaceous faults in cross-section are their shallow dips and the magnitude of displacement on them (Figs. 2–4): the true dip of most faults is 20–40°, with up to 10 km displacement. The faults are planar (at least to 6 secs TWT, approx 12 km) and rotational (Wernicke & Burchfiel, 1982), producing tilts of the pre-Cretaceous surface of up to 30° during 'domino-style' slip and rotation.

The fault spacing ranges from 20 to 50 km, and the depth of the half graben may be 6 km or more. Erosion of the tilt blocks ranges from very limited in the basin centre to substantial nearer the margins (compare the central region of line 18 with the northeast end of line 8/4, Figs. 2,3). Rotation and displacement on the faults must have been accompanied by substantial horizontal extension perpendicular to their strike (Wernicke & Burchfiel, 1982). Whereas movement on these faults was largely completed before the Late Cretaceous, there is some evidence that faults in the basin centre were initiated before those nearer the margins. Compare, for example, the prograding and wedge-shaped fill in the half-graben near the left-centre of line 18 (Fig. 3) with the more slab-like geometry in the eroded Early Cretaceous blocks at either end of line 8/4 (Fig. 2).

A large number of company seismic data were examined to supplement the BMR survey, in order to map the major Cretaceous normal faults on the immediately overlying unconformity surface (Fig. 5). Accurate mapping of these structures is difficult because of their depth (commonly below 3 secs TWT), and because of the poor quality of many of the data below the Eocene coal measures. In particular, many of the company data provided little or no useful information at the Early Cretaceous level. Further, detailed horizon mapping was not carried out at this stage. Consequently, Figure 5 should be regarded as somewhat schematic. However, the traces of most of the large faults at this level are relatively straight, and the larger displacement faults must terminate at a transfer fault. A detailed analysis of these structures is given by Etheridge & others (in press).

The basin can be divided into two regions, based on the orientation, age, and style of faulting. In the central and northwest parts of the basin, the Early Cretaceous faults are predominantly south-southwest dipping, rotational normal faults, trending 290–300° (Figs. 2,3,4). However, in the southeastern-most portion of the basin, they are more steeply dipping (60–75°), mainly irrotational, and bound one or two roughly symmetrical graben, which also trend west-northwest. Superimposed on these in the southeastern region (well illustrated on BMR line 20) are Late Cretaceous rotational normal faults, trending 315–325° (Fig. 5). Robinson (1974), Brown (1976), Weaver & others (1981), and Davidson & others (1984) described these as major basin-forming structures. However, the age and geographic restriction of these structures suggest that they are unrelated to gross basin evolution. This conclusion is supported by the southeastwards thinning of the Tertiary thermal sag sequence, independent of the late Cretaceous extensional structures. We tentatively interpret these structures as bottoming on a fairly shallow crustal decollement, which developed during the early rift phase in the Tasman Sea. The structural trend in the southeastern region is within 10° of the magnetic trend in the Tasman Sea.

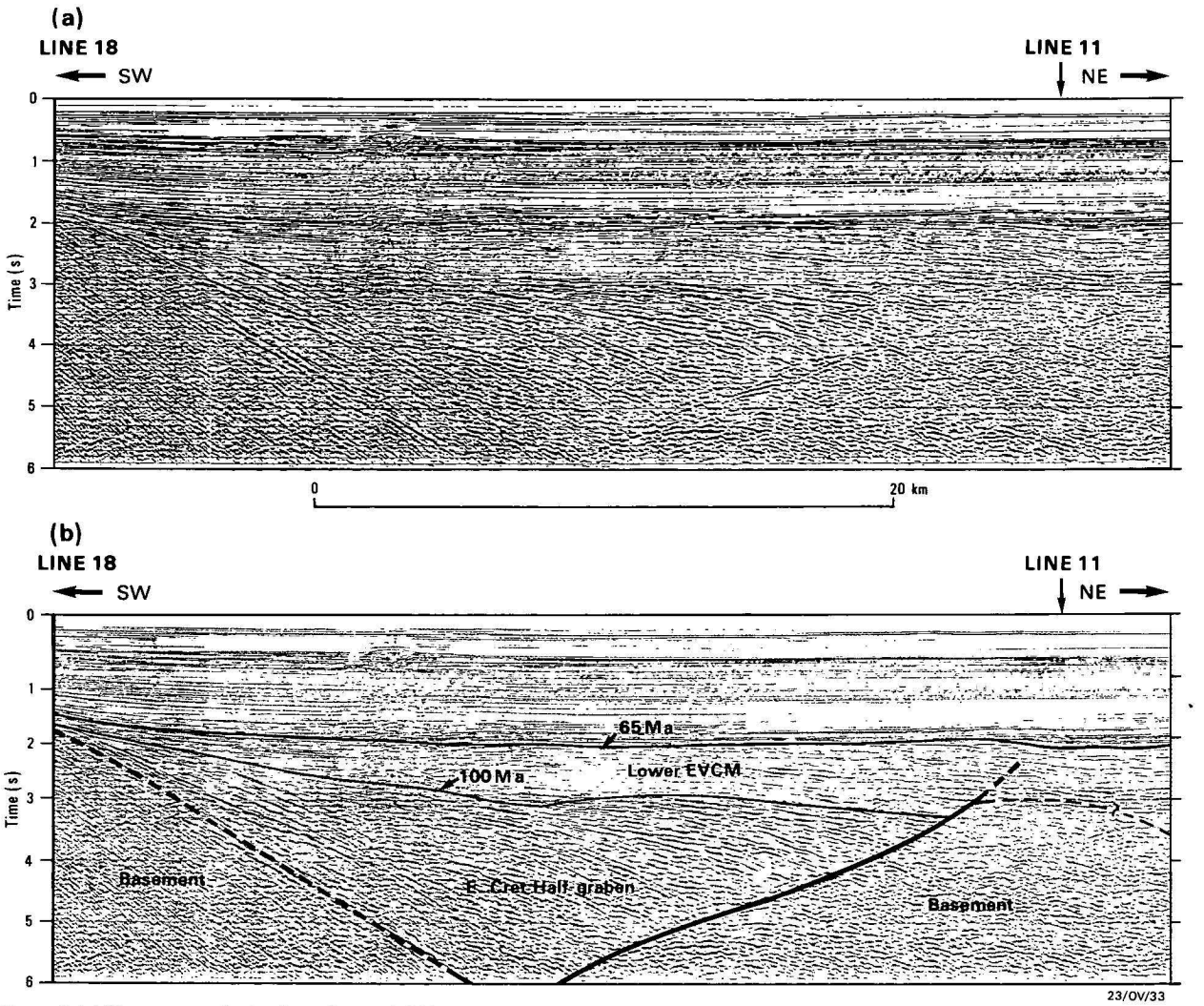

Figure 4. (a) Uncompressed seismic section, and (b) interpretation of portion of line 18 (left centre of Fig. 3), showing the shallow-dipping fault (heavy solid line) and rotated basement surface (heavy dashed line) bounding a wedge-shaped half-graben of prograding Early Cretaceous sediment.

The Early Cretaceous is at least 6 km thick in this section, and extends below 6 secs TWT (12–15 km). This section has approximately equal vertical and horizontal scales, but is about 40 degrees clockwise from a true dip section with respect to the Early Cretaceous structures. The true dips are marked on the section.

The Early Cretaceous normal faults generally extend less than 40 km along strike, and are segmented by an orthogonal set of transfer faults (Gibbs, 1984), which extend across the whole basin (Figs. 5,6)*. The transfer faults are not simple wrench faults, because the normal faults cannot all be matched across them. Rather they are geometrically equivalent to transform faults, in that they allow different distributions of horizontal extension on either side of them (Bally, 1981, figs 21–24). Just as modern oceanic transforms do not generally pass into the continental lithosphere, so the Bass Basin transfer faults probably do not extend into its bounding rises. However, the horizontal extension under the basin decreases rapidly towards the southeast, and transfer of that extension either to the Gippsland Basin or to the Southern Ocean west of Tasmania would require one or more transfers to extend to those basins across the intervening rises.

In summary, the major part of the Bass Basin was initiated by extension in a north-northeast to south-southwest direction during the Early Cretaceous. The overall northwesterly trend of the basin is the result of dominantly right-lateral transfer faulting (Fig. 5). In the upper 10 km or so, extension was accomplished by movement on domino-style, planar, rotational normal faults. The overall extension based on this fault geometry was 60–80% (β=1.6–1.8).

The Early Cretaceous faults and tilt blocks played a key role in the development of structures in the overlying rocks. Compaction over tilt-block edges and/or rejuvenation of normal or transfer faults have been the primary means of structure development.

Play concepts

Relation between deep structure and plays within the EVCM

Broadly, the play concept developed here requires the coincidence of a thick, mature Late Cretaceous to Paleocene source section with some form of structural closure in the EVCM related to the underlying Early Cretaceous structures described above.

Anticlinal and fault-related closures of this type are particularly well developed over tilt-block edges along the margins of the Bass Basin, but their exploration has been without success (e.g.

*Gibbs (1984) introduced the term 'transfer fault' to describe analogous structures in the North Sea basin, and we follow his usage here, rather than use the term 'transform fault', which tends to be associated with sea-floor spreading.

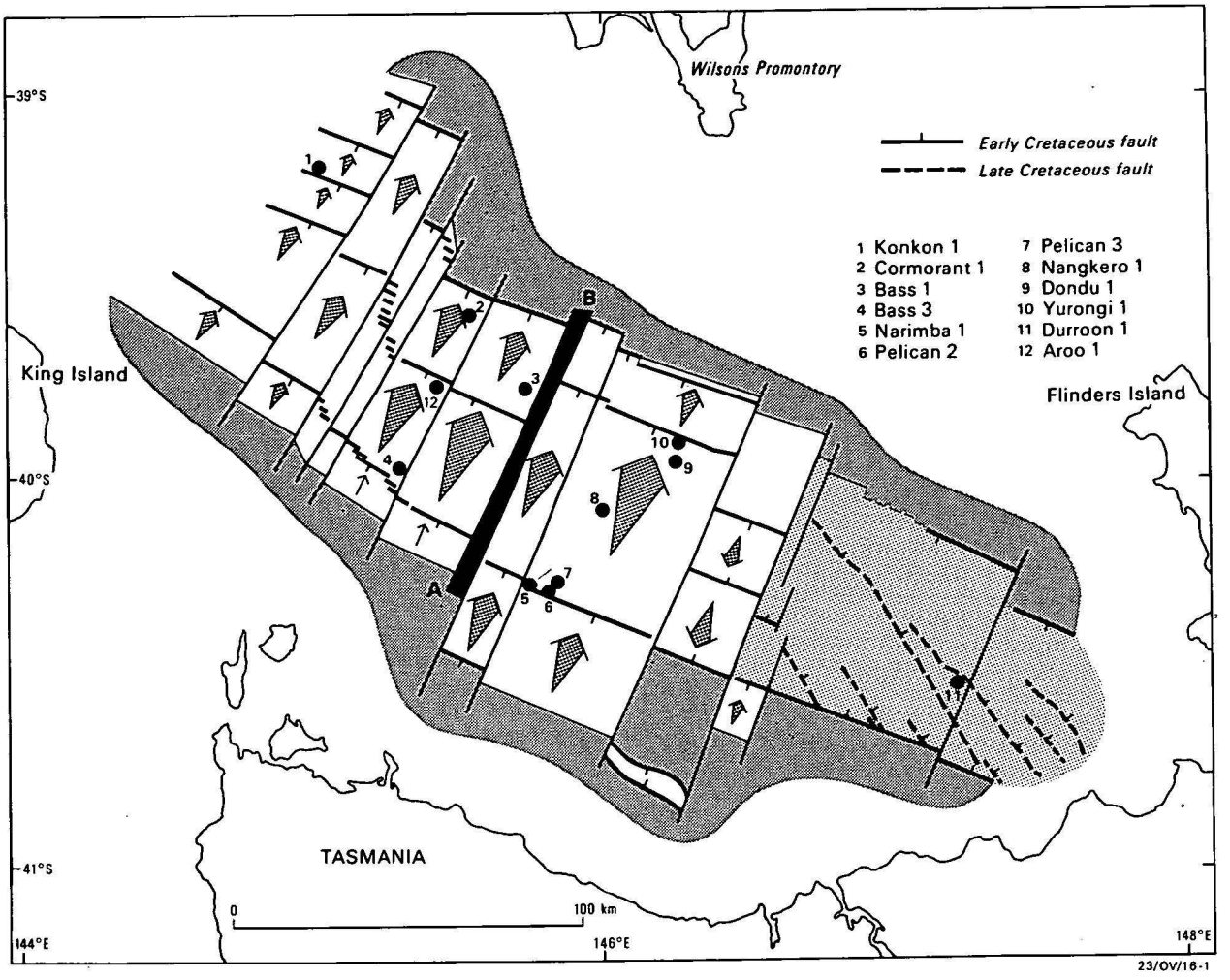

Figure 5. Map of major Cretaceous structures throughout the Bass Basin.
The lightly shaded region in the southeast corner has steep, irrotational Early Cretaceous faults overprinted by rotational Late Cretaceous faults (see text for explanation). The filled arrows represent the size and asymmetry of the Early Cretaceous half-graben. The thickest transfer fault (A–B) is illustrated in Figure 6a.

Bass-2, Bass-3, Yurongi-1, Dondu-1). Nicholas & others (1981) showed, however, that the lower parts of the EVCM are generally oil mature in the centre of the basin. We therefore conclude that long-range migration from the basin centre to its margins has not taken place, and that any hydrocarbons produced in the basin centre are likely either to have been trapped close to the source or to have escaped directly to the surface. Drilling results to date certainly confirm the presence of hydrocarbons nearer the basin centre (e.g. Pelican, Cormorant, Aroo), but we suggest that potentially important plays in this central region remain virtually unexplored.

A major Early Cretaceous normal fault and associated tilt-block edge have been mapped throughout the centre of the basin. Only the Pelican wells could be considered to have adequately tested this structure (Fig. 7), and they discovered a significant gas/condensate reserve, whose evaluation was severely hampered by overpressuring. The Pelican accumulation, however, represents less than 10 per cent of the strike length of this important structure, and we will illustrate the play concept further with examples from elsewhere along it.

First, however, it is important to clarify the significant role of the transfer faults in the development of younger structures in the Bass Basin. There are three main ways in which the old transfer faults can influence structure development with the EVCM. 1 – on a basin-wide scale, they offset and change the geometry of the normal faults and tilt blocks (Figs. 5, 6). In particular, the major transfer fault depicted in Figures 5 and 6a has substantially offset the mid-basin normal fault on which our main play concept is based. This has resulted in the Pelican–Narimba structure being correlated with that in the vicinity of Bass-1 and Aroo, rather than with the basin-marginal structure that is approximately along strike (i.e. Bass-3). 2 – more locally, the transfer faults can provide along-strike closure of structures generated by drape over, or reactivation of, the normal faults/tilt-block edges (Fig. 6b). 3 – the transfer faults represent major vertical zones of weakness in the basement. They extend across the full width of the basin and to the maximum depth of the normal faults (at least 12–15 km), and are, therefore, likely to have been reactivated during subsequent movements in the basin. Dip-slip reactivation would have aided along-strike closure of the structures associated with tilt blocks. More importantly, strike-slip reactivation would have produced in the overlying blanket the whole range of structures commonly associated with wrench-fault zones (Harding & Lowell, 1979; Harding, 1973). Such structures are rare in Bass Basin, although the Cormorant and Konkon structures may well be of this type. However, subtle domes in the deeper parts of the basin away from the tilt blocks may have been generated in such a fashion (e.g. fig. 3 of Weaver & others, 1981).

Davidson & others (1984) have attributed a number of Tertiary structures within the Bass Basin to reactivation of older faults. However, without the advantage of the deep BMR data, they were unable to recognise the large-scale Early Cretaceous nor-

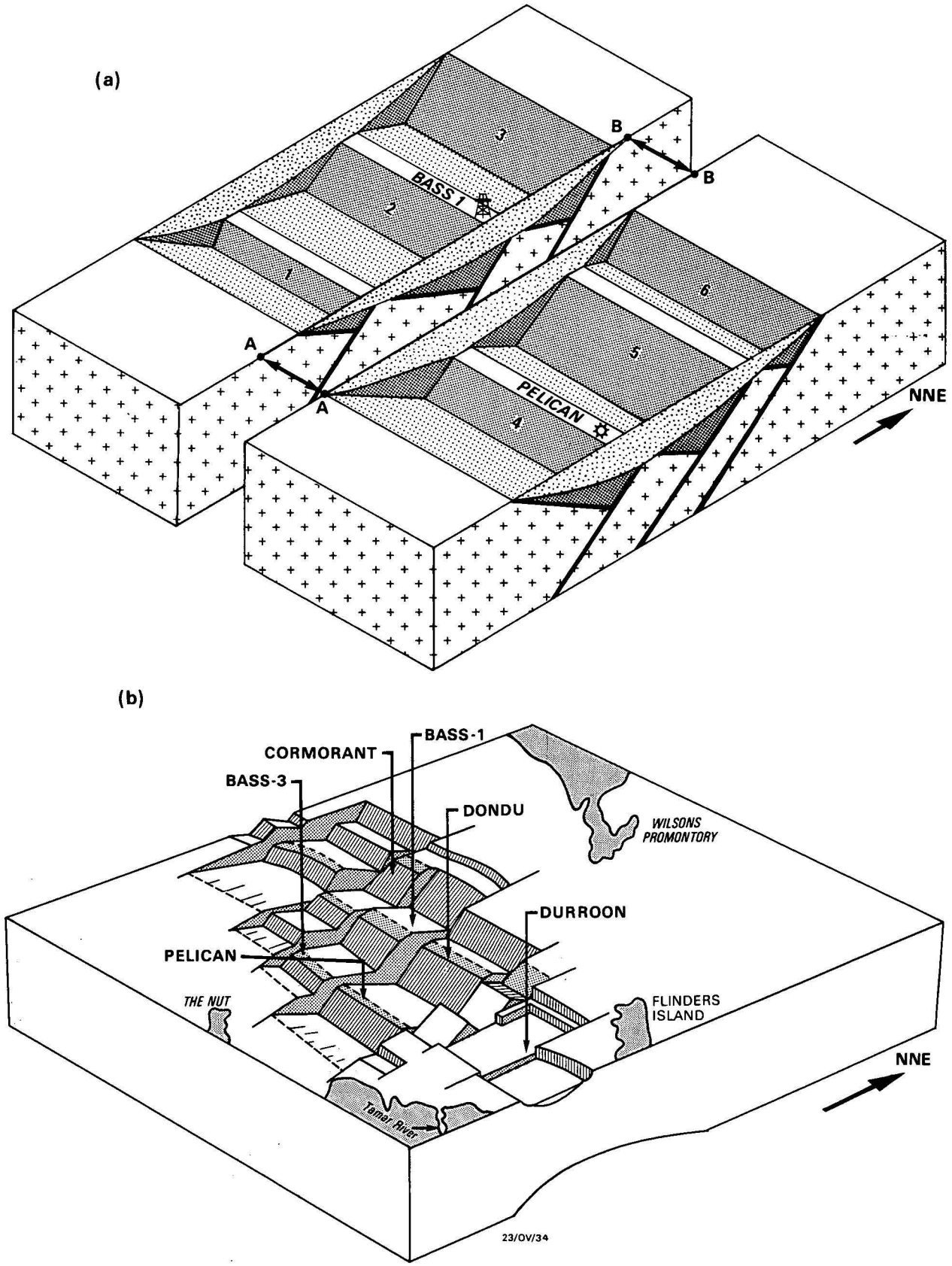

Figure 6. (a) Isometric projection of the central region of the basin, showing the geometry of the major Early Cretaceous structures.
The projection has been exploded along the transfer A–B (Fig. 5), and one or two of the lesser transfers have been omitted for clarity. Note that there is no match of the size of the respective half-graben (1,2,3 versus 4,5,6) across the fault, and that the transfer A–B does not extend beyond the margins of the half-graben.

(b) A simplified sketch of the Bass Basin basement topography, showing the major fault-bounded Early Cretaceous depocentres and the consistent right-lateral offset across the transfer faults.
The north-northeast to south-southeast extension is shown schematically by the arrows and the crustal thinning.

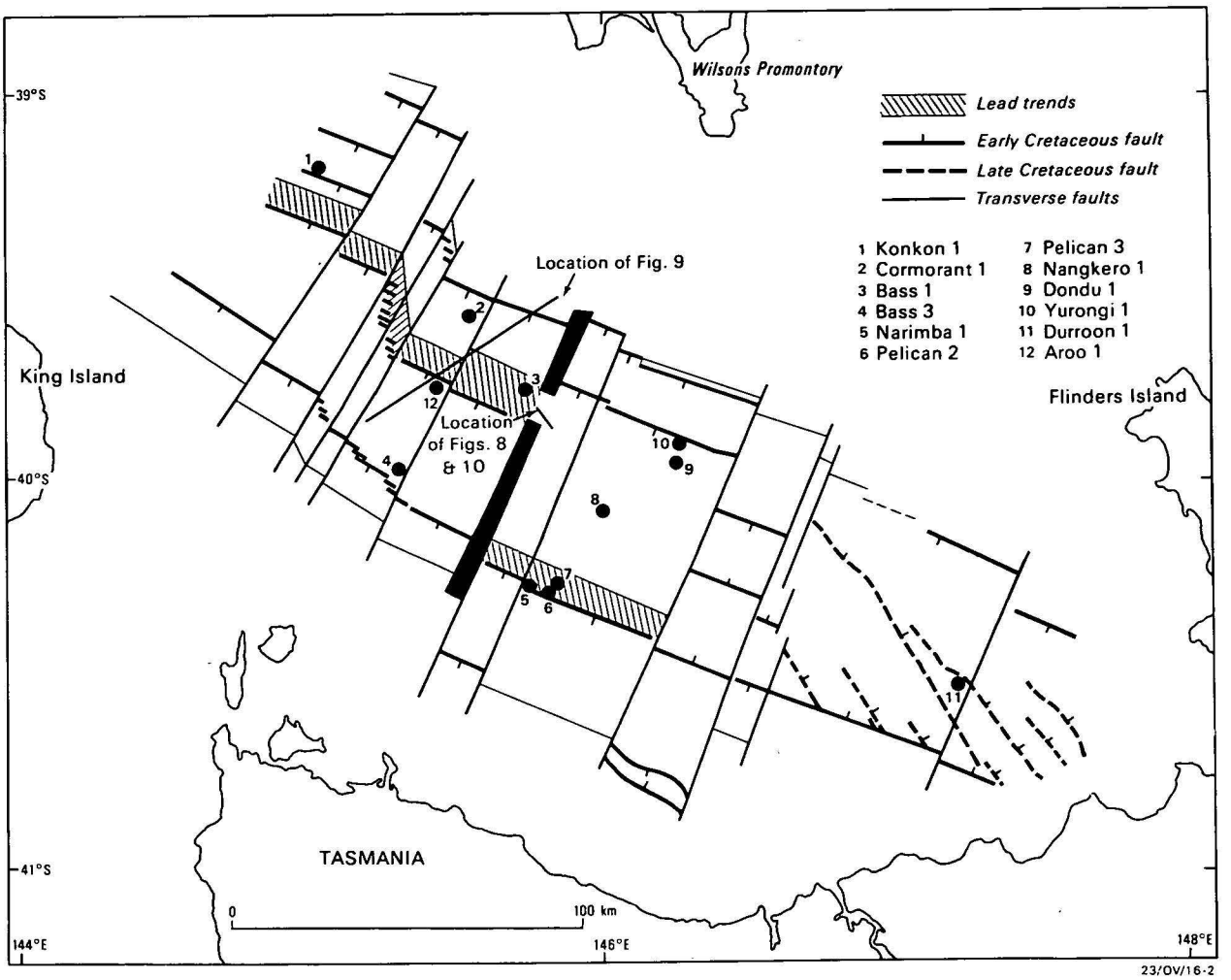

Figure 7. Gross lead map of Bass Basin, showing the extent of the mid-basin Early Cretaceous tilt blocks and the location of the exploration wells to date.

The locations of Figures 8, 9, and 10 are indicated.

mal and transfer faults. Rather, they applied the complex wrench 'ice' model of Davidson (1980) and interpreted what we consider to be relatively minor faults of Late Cretaceous to early Tertiary age as the major basin-forming structures. Basically, we agree with their emphasis on the importance of reactivation of early faults during post mid-Eocene northwest-southeast compression, but differ somewhat on the nature and geometry of the early structures.

Plays related to mid-basin tilt blocks

We regard the most important plays related to deep structures in the Bass Basin to be those developed over the major mid-basin tilt blocks. An example of a number of such plays occurs in the vicinity of Bass-1, and is best illustrated by data from BMR lines 11, 17, and 18. In this region, a possible multiple play is associated with several features that may be widespread in equivalent structural settings (Fig. 8). The basement high blocks and associated early structures served two important functions. First, the high block may have influenced sedimentation, particularly in the immediately overlying Late Cretaceous to Paleocene sequence. Second, drape over the highs and reactivation of the major faults led to structuring at various levels throughout the EVCM.

The lithology of the 'lower' EVCM at Cormorant and Pelican localities has been described as argillaceous and arenaceous, respectively (Brown, 1976). In a quantitative study, Aquing (1980) derived sand–shale ratios in the range 0–0.2 at Cormorant, and in the range 1.1–3.2 at Pelican-3, for the latest Paleocene and early Eocene. This lithological contrast correlates well with position relative to major Cretaceous structures. Cormorant-1 is located several kilometres on the

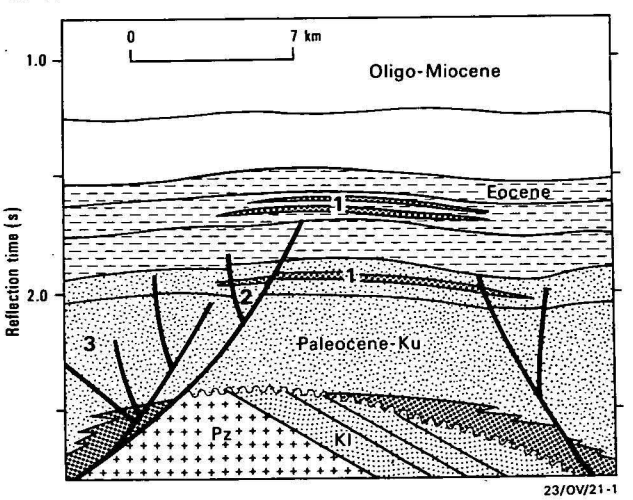

Figure 8. Play concept diagram for the mid-basin tilt blocks, based on geology near the intersections of lines 11 and 18.

The various shadings refer to the chronostratigraphic intervals indicated, except that the heavy stipple indicates more sand-rich facies spatially related to the basement high. Numbers 1 to 3 refer to specific plays described in the text.

downthrown side of one of the major Cretaceous normal faults in a Late Cretaceous–Paleocene basinal zone that was later deformed. Pelican-3, however, was drilled just on the upthrown side of another major normal fault close to a Late Cretaceous–Paleocene hinge zone. Aquing (1980) recognised lacustrine shales in a number of wells near the Late Cretaceous–Paleocene depocentres. Core and log comparisons of Narimba-1 and Dondu-1 (earliest Eocene), Yurongi-1 (early Paleocene) and Poonboon-1 (Late Cretaceous) contain evidence of lacustrine shales, but the deepest cores from Pelican-1, 2, and 4 have coarser facies, ascribed by Aquing (1980) to 'lower alluvial plain-overbank flow'.

It now appears possible to modify the generalised basin-wide facies trends discussed under **'generalised lithostratigraphy'** above. Cretaceous fault blocks may have significantly controlled nearby lithologies, perhaps generating thick shale-prone sequences on their downthrown sides, probably in lacustrine environments, and thinner sand-prone sequences adjacent to the hinge zones on their upthrown sides, probably in flood-plain

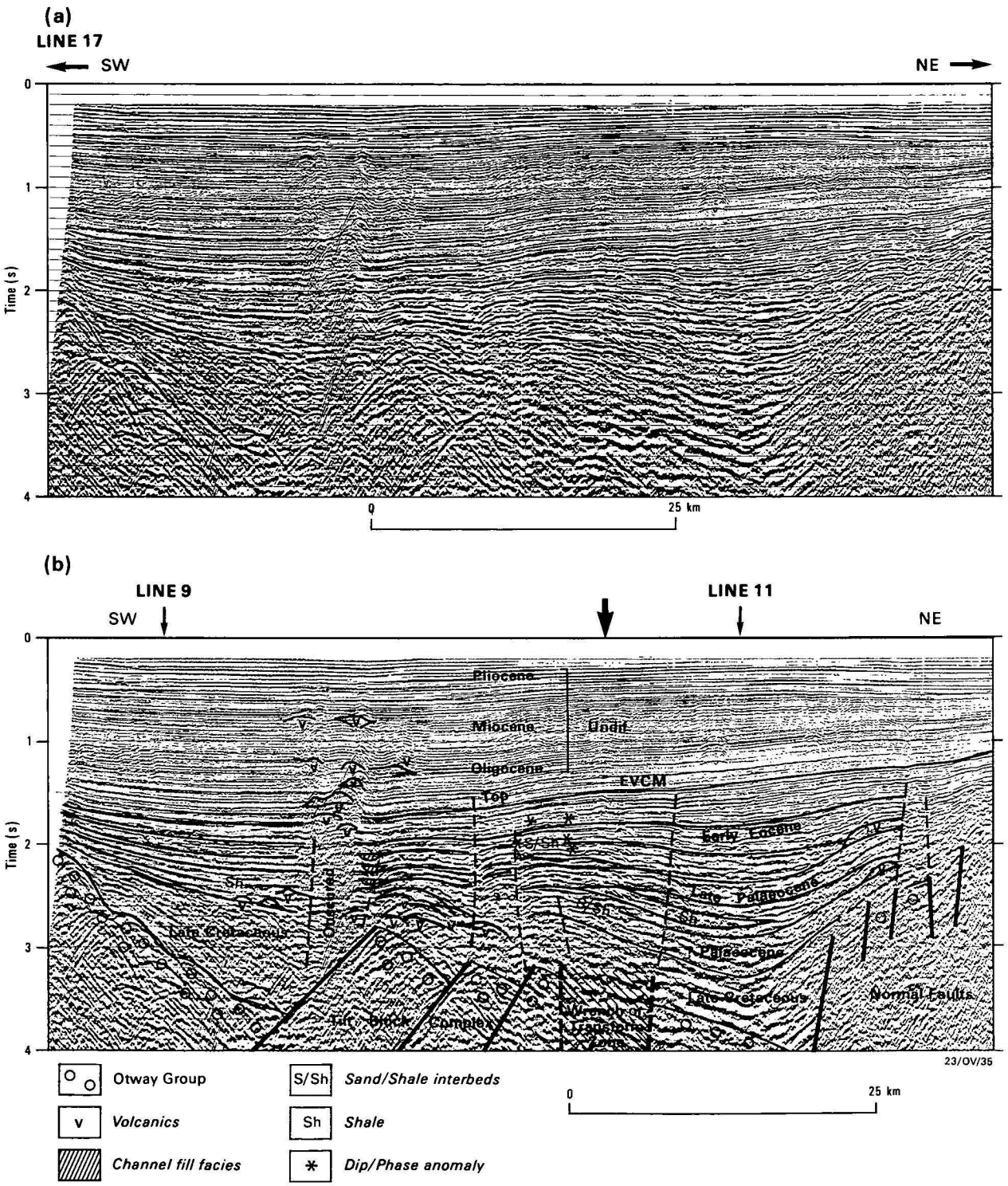

Figure 9. (a) Seismic section, and (b) interpretation of portion of line 17, showing relation between major Early Cretaceous structures and the overlying stratigraphy.

Vertical exaggeration of the section is approximately x3. The arrow shows where the mid-basin tilt-block complex is truncated by a transfer fault. Asterisks indicate small-scale dip anomalies (flat spots) and phase anomalies.

and braided-river environments. This interpretation may be cautiously extended to the case of transfer faults, where these mark a significant change in basement elevation. Such localities, however, are more difficult to detect in section than those of normal faults. Detailed seismic mapping on a finer grid is required to detect the local direction of basement downstepping and hence the local direction of clastic fining. We recognise that this is a simple model of basin sedimentology that needs modification to accommodate local variations in environment.

Seismic data from a portion of Line 17 are presented in Figure 9 with a structural and preliminary litho-environmental interpretation. There is evidence of reactivation of the Early Cretaceous transfer and normal faults that have produced structures in this region of thick mature EVCM.

A monotonous and massive lithology is interpreted for some of the bland seismic sequences in the main basin (on the right in Fig. 9), where the environment is analogous to that at Cormorant, and shale-rich sequences are expected. These sequences grade laterally across the transfer zone (and up-dip) into lithologies interpreted as vertically alternating sands and shales. This character persists laterally across a tilt-block complex, but reverts to the more bland type in the main basin (on the southwest in the section).

Small-scale dip anomalies (flat spots) and phase anomalies associated with structuring warrant further investigation. We note that there is no suggestion of structuring at the top EVCM.

Structuring over the tilt-block edges may be of three main types. First, anticlinal closure may result from drape over the basement high (see 1 on Fig. 8). This type of stucture is well developed near the intersection of BMR lines 11 and 18, and well illustrated on the synthetic sonic log/seismic trace inversion record section at this location (Fig. 10). Possible direct hydrocarbon indicators (DHIs) can also be seen on this section. They occur at various levels as both velocity anomalies and 'flat spots' (Fig. 10).

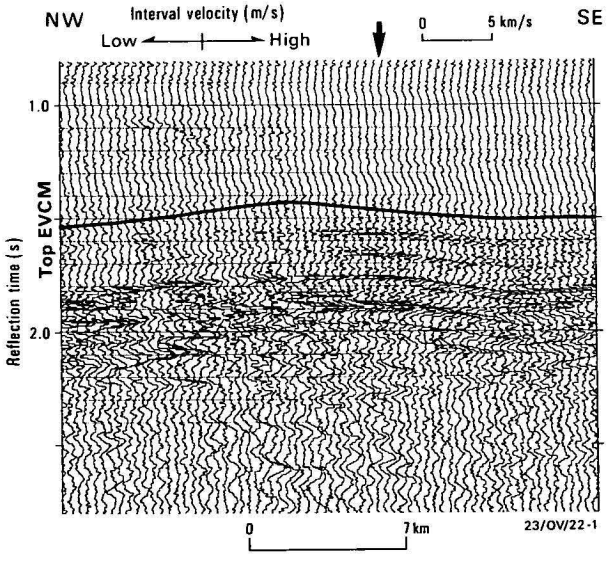

Figure 10. Interval velocities for the location given in Figure 7.
Within 0.2s reflection time measured from the top EVCM at the point indicated by the arrow, thin flat-lying anomalously low velocity zones are evident. Horizontal and vertical scales are the same as for Figure 8.

The second type of structural closure involves reactivation of the early normal and adjacent transfer faults to produce fault and/or fold closure of sand bodies against a shale/siltstone-rich part of the sequence (see 2 on Fig. 8). Such reactivation could involve wrench, reverse, or normal fault movements on early structures, depending on the orientation of the stress field at the time. Davidson & others (1984, figs. 11,12) identified structural closure in the EVCM a short distance towards the southeast, and described it as a 'wrench-modified normal fault' (p. 107). They emphasised the importance of post-middle Eocene northwest-southeast compression in this general region. We agree that this compression event is likely to be important, but add that reactivation of the major Early Cretaceous structures is likely to control the evolution of the younger structures.

The third possibility is for shale diapirism in an overpressured sequence, especially within the seemingly shale-rich Late Cretaceous-Paleocene section on the downthrown side of the major normal faults (see 3 in Fig. 8). Bishop (1978) discussed in general terms the mechanism by which thin sandstone reservoirs deposited in fluvio-lacustrine enviroments may be ruptured and sealed by mobile clays.

Seismic data extending 15 km west of Pelican show a disrupted sequence of reflections (Fig. 2) in the Late Cretaceous-Paleocene sequence, forming a dome, which may have been caused by diapiric structuring. In the core of this dome, a thick, seismically featureless sequence is interpreted as a mobilised shale mass. Normal velocity analysis over this section reveals only that it is probably clay-prone.

Geohistory analysis

A computer-generated geohistory diagram (Fig. 11) was prepared for the location illustrated in Figure 10, using the method described by Van Hinte (1978) and Falvey & Deighton (1982). Cenozoic isochrons were extrapolated from Bass-1 by standard seismic-stratigraphic techniques, whereas the Cretaceous intervals were obtained from the regional basin interpretation. In this mid-basin location, no period of erosion/non-deposition is proposed during the late

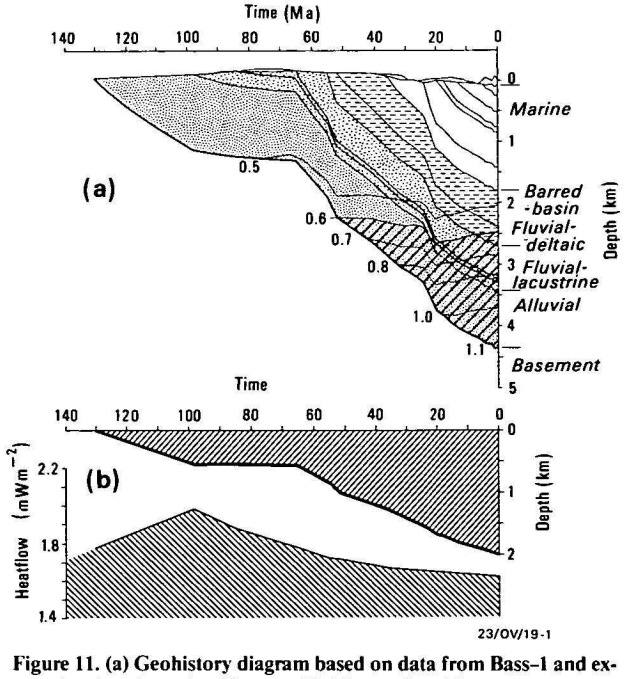

Figure 11. (a) Geohistory diagram based on data from Bass-1 and extrapolated to the region illustrated in Figures 8 and 9.
The various shadings correspond to the chronostratigraphic intervals shown in Figure 8. The cross-hatched region represents the 'oil-window', and demonstrates the maturity of the lower EVCM sequence during the last 20 Ma.

(b) Sediment-stripped basement subsidence curve or tectonic subsidence, and heat flow history derived from geohistory model.

Cretaceous/Paleocene, unlike the marginal highs. Palaeowater-depths from late Eocene to Recent were also extrapolated from Bass-1 (B. Radke, personal communication). The thermal analysis and maturation prediction (Falvey & Deighton, 1982) are based on compaction parameters, thermal conductivity, and heat flow derived from Bass-1, and use the values of anomalous palaeoheat-flow derived for this structural location by Karner (personal communication).

The analysis shows that late Cretaceous and Paleocene source rocks would have started to become mature for oil (R_o = 0.6%) towards the end of the Oligocene. At present, this interval lies wholly within the oil window (R_o = 0.76%-0.90%). In the absence of significant structuring since the Miocene, the existing stuctures should have acted as effective traps. The occurrence of the direct hydrocarbon indicators at a depth of about 2 km (R_o = 0.5%) is at least consistent with their being gas-filled sands.

The sediment-stripped basement subsidence curve ('tectonic subsidence') clearly shows the two separate tectonic episodes that formed the Bass Basin. The Early Cretaceous crustal extension/subsidence phase would appear to have involved continued but decreasing block movement through to the end of the Cretaceous. A well-defined thermal cooling subsidence cycle that began at 65 Ma can be described by an exponential curve with a time constant of about 50 Ma. The onset of this cooling cannot be simply related to the onset of sea-floor spreading in the Southern Ocean or Tasman Sea.

Conclusions

1) The Bass Basin originated by north-northeast to south-southwest crustal extension during the Early Cretaceous. Extension took place on shallowly dipping, rotational faults trending 290-300° and a contemporaneous perpendicular set of transfer faults. The offset across the transfer faults is consistently right-lateral, producing the overall northwesterly trend of the basin, oblique to its extensional faults.

2) Three major normal faults and associated basement tilt-block highs have been traced throughout the main part of the basin, one close to each margin and one approximately coincident with the basin depocentre.

3) Structures are commonly developed within the Eastern View Coal Measures over normal faults and tilt-block edges, and their mid-basin coincidence with mature Late Cretaceous/Paleocene source sequences has led to the development of a new play concept, which has been poorly tested by exploration to date. Drape folding, early fault reactivation, and possible shale diapirism may all produce up-dip closure in sand reservoirs overlying the mid-basin high. In addition, the high block may have given rise to sandier facies in the Late Cretaceous to Paleocene section over and adjacent to it.

4) Reactivation of the major transfers may also have led to structuring in the overlying Eastern View Coal Measures, especially next to major basement tilt blocks.

5) A geohistory analysis of the tilt-block play in the vicinity of Bass-1 confirms the maturity of the Late Cretaceous to Paleocene source section. Maturity was achieved in the late Oligocene, well after most of the structuring developed, and much of the sequence is oil-mature at the present day. Similar structures that have proved unprospective along the basin margin are unlikely to have underlying mature sources, suggesting that hydrocarbon migration has been relatively local.

6) The only significant exploration of this lead in the Bass Basin has been in the Pelican-Narimba region, where the major hydrocarbon discovery in Bass Basin is located. A substantial strike length of the prospective basement high is untested, and the hydrocarbon potential of the Bass Basin, at least for modest reservoirs, remains good.

Acknowledgements

We would like to thank Jim Colwell for specialist advice on various aspects of fluvial sedimentology, and Bruce Radke for information on the Late Tertiary marine sequence in Bass-1. Ian Deighton of Paltech Ltd kindly ran the computer geohistory analysis. Paul Williamson provided useful comments on an earlier draft. The figures were drawn by Gill Clarke.

References

Aquing, R.R., 1980 - Geology of the Eastern View Coal Measures - Bass basin. *M.Sc. thesis, Macquarie University* (unpublished).

Bally, A.W., 1981 - Atlantic-type margins. *In* Geology of passive continental margins. *American Association of Petroleum Geologists, Education Course Note Series* No.19, 1-48.

Bishop, R.S., 1978 - Mechanism for emplacement of piercement diapirs. *American Association of Petroleum Geologists, Bulletin*, 62(9), 1561-1583.

Brown, B.R., 1976 - Bass Basin, some aspects of petroleum geology - *In* Economic geology of Australia and Papua New Guinea. Vol. 3 - Petroleum. *Australasian Institute of Mining and Metallurgy, Monograph* 7, 67-82.

Burke, K. & Dewey, J.F., 1973 - Plume-generated triple junctions: key indicators in applying plate tectonics to old rocks. *Journal of Geology*, 81, 406-433.

Davidson, J.K., 1980 - Rotational displacements in southeastern Australia and their influences on hydrocarbon occurrence. *Tectonophysics*, 63, 139-153.

Davidson, J.K., Blackburn, G.J., & Morrison, K.C., 1984 - Bass & Gippsland basins: a comparison. *APEA Journal*, 24(1), 101-109.

Denham, J., & Brown, B.R., 1976 - A new look at the Otway Basin. *APEA Journal*, 16, 91-98.

Etheridge, M.A., Branson, J.C., & Stuart-Smith, P.G., in press - Extensional basin-forming structures in Bass Strait and their importance for hydrocarbon exploration. *APEA Journal*, 25(1).

Falvey, D.A., & Deighton, I., 1982 - Recent advances in burial and thermal geohistory analysis. *APEA Journal*, 22, 65-81.

Gibbs, A.D., 1984 - Structural evolution of extensional basin margins. *Journal of the Geological Society, London*, 141, 609-620.

Harding, T.P., & Lowell, J.D., 1979 - Structural styles, their plate tectonic habitats and hydrocarbon traps in petroleum provinces. *American Association of Petroleum Geologists, Bulletin*, 63, 1016-1058.

Kingston, D.R., Dishroon, C.P., & Williams, P.A., 1983 - Hydrocarbon plays and global basin classification. *American Association of Petroleum Geologists, Bulletin*, 67(12), 2194-2198.

Mutter, J.C., & Jongsma, D., 1978 - The pattern of the pre-Tasman Sea rift system and the geometry of break-up. *Bulletin of the American Society of Exploration Geophysicists*, 9(3), 70-75.

Nicholas, E., Lockwood, K.L., Martin, A.R. & Jackson, K.S., 1981 - Petroleum potential of the Bass Basin. *BMR Journal of Australian Geology & Geophysics* 6, 199-212.

Robinson, V.A., 1974 - Geological history of the Bass Basin. *APEA Journal* 14, 44-49.

Threlfall, W.F., Brown, B.R. & Griffith, B.R., 1976 - Gippsland Basin, Offshore. *In* Economic Geology of Australia and Papua New Guinea. Vol. 3 - Petroleum. *Australasian Institute of Mining and Metallurgy, Monograph* 7, 41-67.

Van Hinte, J.E., 1978 - Geohistory analysis - Application of micropaleontology in exploration geology. *American Association of Petroleum Geologists, Bulletin* 62(2), 201-222.

Weaver, O.D., Houde, Y., Smitherman J., & Nettels, C., 1982 - Bass Basin set for new exploration. *Oil and Gas Journal*, (Jan 4) 80(1), 154-161.

Wernicke, B., & Burchfeil, B.C., 1982 - Modes of extensional tectonics. *Journal of Structural Geology*, 4(2), 105-115.

BMR Journal of Australian Geology & Geophysics, 9, 207–218

Rare-earth element geochemistry of Archaean orthogneisses and evolution of the East Antarctic shield

J.W. Sheraton[1], D.J. Ellis[2], & S.M. Kuehner[2]

Two distinct suites of Archaean (about 3100 Ma) granulite-facies orthogneisses, predominantly of intrusive origin, have been recognised in the Napier Complex of Enderby Land, Antarctica. One, mainly of tonalitic to granodioritic composition, is strongly depleted in Y and HREE, and is characterised by positive Eu anomalies. It probably represents new continental crust derived by hydrous partial melting of a hornblende and/or garnet-bearing mafic source. A generally younger 'undepleted' suite, predominantly of trondhjemitic to granitic composition, has higher TiO_2, P_2O_5, Y, Zr, Nb, REE, and Ga/Al, lower CaO, Sr, Ti/Y, Ce/Y, and Mg/(Mg + total Fe), and commonly negative Eu anomalies. It apparently originated by relatively dry, lower-pressure melting of mainly felsic crustal rocks. Compositional differences between depleted tonalites and granodiorites are almost entirely confined to LIL elements (K, Rb, Ba, Pb, Th, and U), and can be explained by interaction of either the source material or the magma (during generation or, less likely, emplacement) with an LIL-element-enriched fluid phase. Such an enrichment process is difficult to model in detail because of LIL-element depletion during granulite-facies metamorphism. Depleted granitoids may be representative of a deeper crustal level than undepleted granitoids, which, together with a variety of metasediments, predominate in adjacent lower-grade (amphibolite to low granulite facies) late Archaean and Proterozoic terrains. The Archaean granitoids are dominated by two I-type (igneous-derived) suites, whereas those of post-Archaean age are largely undepleted I-type or S-type (sediment-derived).

Introduction

The Archaean Napier Complex of Enderby Land, Antarctica (Fig. 1) is of particular petrological interest, owing to the unique occurrence on a regional scale of the rare associations sapphirine+quartz, orthopyroxene+sillimanite, and osumilite. These mineral assemblages imply extremely high temperatures of metamorphism (800–900°C at 8–10 kb) and very low P_{H_2O} (Ellis, 1980; Ellis & others, 1980; Sheraton & others, 1980). The Napier Complex is one of the oldest high-grade metamorphic terrains; Rb-Sr and Sm-Nd whole-rock and U-Pb zircon dating have indicated an age for the granulite-facies metamorphism of approximately 3070 Ma, and also suggest a crustal history extending back to 3700–3800 Ma (Black & others, 1983; Sheraton & Black, 1983; McCulloch & Black, 1984).

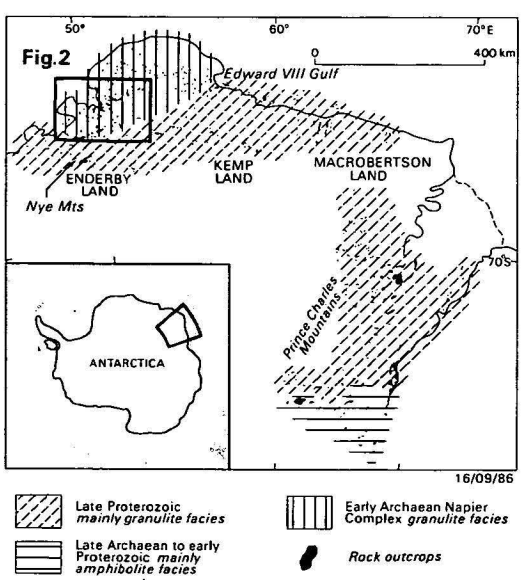

Figure 1. Map showing metamorphic complexes of Enderby, Kemp, and MacRobertson Lands.

By far the most abundant rock type in the Napier Complex is massive felsic orthogneiss (orthopyroxene-quartz-feldspar gneiss), although subordinate garnet-quartz-feldspar gneiss, mafic granulite, and a variety of metasedimentary rocks are also present (Fig. 2). Strong deformation during high-grade

Table 1. Average compositions of depleted and undepleted granitoids, garnet gneisses, and representative post-orogenic intrusives from the Napier Complex (A-J), and biotite-ferrohastingsite granite from the southern Prince Charles Mountains.

	A	B	C	D	E	F	G	H	I	J	K
SiO_2	68.52	69.83	74.69	62.95	73.95	70.00	70.53	73.62	57.28	69.66	71.06
TiO_2	0.47	0.32	0.19	0.98	0.59	0.85	0.75	0.23	1.93	0.61	0.79
Al_2O_3	14.90	14.87	13.20	13.90	11.27	12.35	12.42	13.20	14.17	14.15	12.20
Fe_2O_3	1.63	1.01	0.77	2.56	1.57	1.79	1.86	1.21	3.26	1.01	1.35
FeO	2.57	2.08	0.89	6.48	3.04	3.42	3.31	1.59	7.32	2.66	3.43
MnO	0.05	0.05	0.03	0.12	0.05	0.08	0.06	0.05	0.13	0.03	0.08
MgO	1.87	1.39	0.52	2.44	1.32	1.01	0.85	0.75	1.79	0.76	0.65
CaO	4.11	2.98	1.71	4.94	2.10	2.13	2.31	1.59	5.93	1.72	2.28
Na_2O	4.22	4.09	3.23	3.69	4.00	2.70	2.93	3.14	2.75	2.67	2.80
K_2O	1.10	2.78	4.59	0.97	1.89	4.82	4.54	4.21	2.84	5.87	4.40
P_2O_5	0.12	0.07	0.02	0.22	0.08	0.22	0.15	0.05	1.12	0.21	0.22
CIPW Norms											
q	27.53	26.05	33.70	21.34	36.23	29.17	29.44	34.11	15.54	26.02	31.23
c	—	—	—	—	—	—	—	0.71	—	0.78	—
or	6.50	16.43	27.13	5.73	11.17	28.49	26.83	24.88	16.78	34.69	26.18
ab	35.71	34.61	27.33	31.23	33.85	22.85	24.79	26.57	23.27	22.59	23.69
an	18.46	14.00	7.96	18.50	7.21	7.34	7.33	7.56	17.93	7.16	7.64
di	0.93	0.26	0.32	3.82	2.22	1.50	2.65	—	3.52	—	1.91
hy	6.90	5.88	1.88	12.55	5.59	5.31	4.20	3.50	10.49	4.99	4.67
mt	2.36	1.46	1.12	3.71	2.28	2.60	2.70	1.75	4.73	1.46	1.96
il	0.89	0.61	0.36	1.86	1.12	1.61	1.42	0.44	3.67	1.16	1.50
ap	0.28	0.17	0.05	0.52	0.19	0.52	0.36	0.12	2.65	0.50	0.52
Trace elements (ppm)											
V	45	37	13	121	17	27	32	17	73	24	25
Cr	40'	41'	16'	25	8	13	35	33	14	10	10
Ni	22'	21'	10'	16	15'	6	15	11	9	5	6
Cu	11	10	8	15	7	12	17	8	22	9	16
Zn	50	40	22	96	42	62	49	22	132	46	65
Ga	16	16	12	19	17	16	18	14	21	19	16
Rb	14	50	117	13	22	102	117	123	65	197	171
Sr	360	330	166	166	132	130	76	140	379	128	80
Y	10	7	4	43	41	26	61	35	72	32	93
Zr	152	126	106	269	379	586	358	150	776	473	643
Nb	4	4	3	14	14	19	22	5	51	26	64
Ba	692	1163	1373	704	792	2310	1131	911	1675	1019	789
La	29	30	68	57	60	108	48	47	161	190	107
Ce	44	44	84	96	97	166	90	74	297	336	208
Pb	10	20	29	11	10	23	10	38	19	52	23
Th	4	7	18	18	14	24	2	16	5	134	31
U	~0.4	~0.7	~0.8'	1.4	1.4	1.0	~0.5	1.5	0.9	3.9	4.0
F[2]	143	73	195	110	105	123	150	130	545	550	723
mg	0.45	0.45	0.36	0.33	0.34	0.26	0.23	0.33	0.24	0.27	0.20
K/Rb	650	461	326	619	713	392	322	284	363	247	215
Rb/Sr	0.039	0.15	0.70	0.078	0.17	0.78	1.54	0.88	0.172	1.54	2.14
Ba/Sr	1.92	3.52	8.27	4.24	6.00	17.8	14.9	6.51	4.42	7.96	9.86
Al/Ga	4900	4900	5800	3900	3500	4100	3650	5000	3600	3900	4000
Ce/Y	4.4	6.3	21.0	2.2	2.4	6.4	1.48	2.1	4.1	10.5	2.2
Th/U	~10	~10	~11	13	10	24	~4	11	6	34	8
Ti/Y	282	274	285	137	86	196	74	39	161	114	5

1. Single high values omitted when calculating means. 2. Fluorine averages based on fewer analyses. Analyses by XRF and AA in Bureau of Mineral Resources Laboratory (see Sheraton & Labonne (1978) for details of methods).

A. 21 depleted tonalites
B. 12 depleted granodiorites
C. 7 depleted granites
D. 4 undepleted tonalites
E. 6 undepleted trondhjemites
F. 6 undepleted granites
G. 6 undepleted granites from Proclamation Island.
H. 24 garnet-quartz-feldspar gneisses.
I. 4 orthopyroxene granodiorites.
J. 5 biotite granites.
K. 8 biotite-ferrohastingsite granites.

[1]Division of Petrology & Geochemistry, BMR
[2]Department of Geology,
University of Tasmania,
PO Box 252C, Hobart, TAS 7001

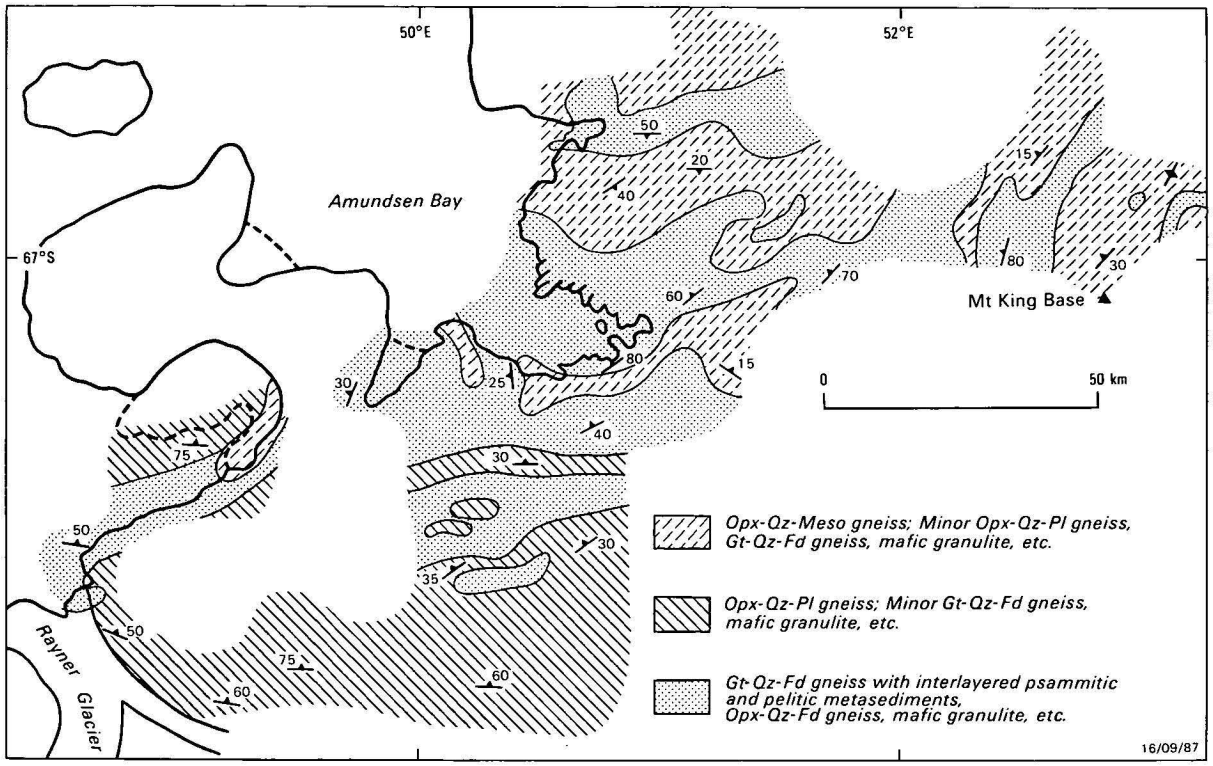

Figure 2. Generalised geological map of western part of the Napier Complex.
Opx-Qz-Pl gneiss and much of the Opx-Qz-Meso gneiss belong to the depleted granitoid suite, but Opx-Qz-Meso gneiss north of Mount King is predominantly of undepleted type. Mineral abbreviations: Fd, feldspar; Gt, garnet; Meso, mesoperthite; Opx, orthopyroxene; Pl, plagioclase; Qz, quartz.

metamorphism has generally obliterated intrusive relationships, but the common absence of compositional layering, localised presence of xenoliths, mostly diopside-normative compositions, and well-defined chemical trends are good evidence for a mainly intrusive igneous origin. Sheraton & Black (1983), who made a detailed geochemical and isotopic study of these rocks, considered that their chemical characteristics are not consistent with them being residues of partial melting, a conclusion reached by many other workers on the basis of data from similar high-grade terrains (Cooper & Field, 1977; Tarney & Windley, 1977; Collerson & Fryer, 1978; Wells, 1979; Rollinson & Windley, 1980b; Weaver & Tarney, 1980, 1981). Partial melting during granulite-facies metamorphism was apparently not extensive, possibly owing to the presence of a fluid phase rich in CO_2 (Newton & others, 1980), and, although localised melting clearly occurred, the resulting melts did not migrate far (cf. Sighinolfi & Gorgoni, 1978). Hence, the overall compositions of the orthogneisses are thought to be essentially representative of their original igneous compositions, apart from some loss of large-ion lithophile (LIL) elements during metamorphism. Igneous rock names (after O'Connor, 1965) are therefore used in this paper.

Sheraton & Black (1983) recognised two chemically distinct suites of orthogneiss, termed depleted[1] and undepleted, according to the degree of depletion in Y (and, by implication, heavy rare-earth elements, HREE), following the work of Ewing (1979) on Archaean volcanics from Canada. Apart from Y, many other elements and element ratios show systematic differences, when allowance is made for variations in SiO_2 content (Table 1, Fig. 3). Depleted granitoids, mainly of tonalitic to granodioritic composition, but including some granite (s.s.), were considered to represent new continental crust derived from the mantle by a two-stage melting process involving mafic crustal rocks. The Y depletion was explained in terms of hydrous partial melting of a garnet-bearing source (garnet amphibolite or possibly eclogite). Undepleted granitoids (predominantly of trondhjemitic and granitic composition, but including minor tonalite) have, for a given SiO_2 content, higher TiO_2, P_2O_5, Y, Zr, Nb, La, Ce, and Ga/Al, lower Sr, Ti/Y, Ce/Y and Mg/(Mg + total Fe), and slightly lower CaO (Table 1; Fig. 3). They probably originated by melting of predominantly felsic crustal rocks at relatively low P_{H_2O}. Widespread leucocratic garnet-quartz-feldspar gneiss was also thought to be of igneous (possibly extrusive) origin, and is compositionally similar to the undepleted granites. Both depleted and undepleted suites show evidence for loss of Rb (relative to K), Th, and U during granulite-facies metamorphism.

This paper presents rare-earth element (REE) data for a representative selection of depleted and undepleted granitoids, which allows further constraints to be applied to the petrogenesis of these Napier Complex rocks. Implications regarding the evolution of the East Antarctic shield are also considered.

Rare-earth element data

A total of 20 whole-rock samples was analysed for 10 rare-earth elements, using the ion-exchange thin-film X-ray fluorescence technique of Fryer (1977). Analyses were carried out at the University of Tasmania on a Philips PW 1410 X-ray spectrometer. In all cases, yields of more than 70 per cent (monitored by a Tm spike) were obtained. Three samples were run in duplicate and gave consistent results for all elements. Details of the calibration with international standard rocks are given by Fryer (1977); precision is reported as better than 10 per cent for all elements. REE data are given in Table 2, and chondrite-normalised REE patterns in Fig. 4. Normalising values used are those of Taylor & Gorton (1977).

[1]This terminology refers specifically to depletion in Y and HREE, and should not be confused with the common depletion of granulites in LIL elements (Th,U,K, and Rb).

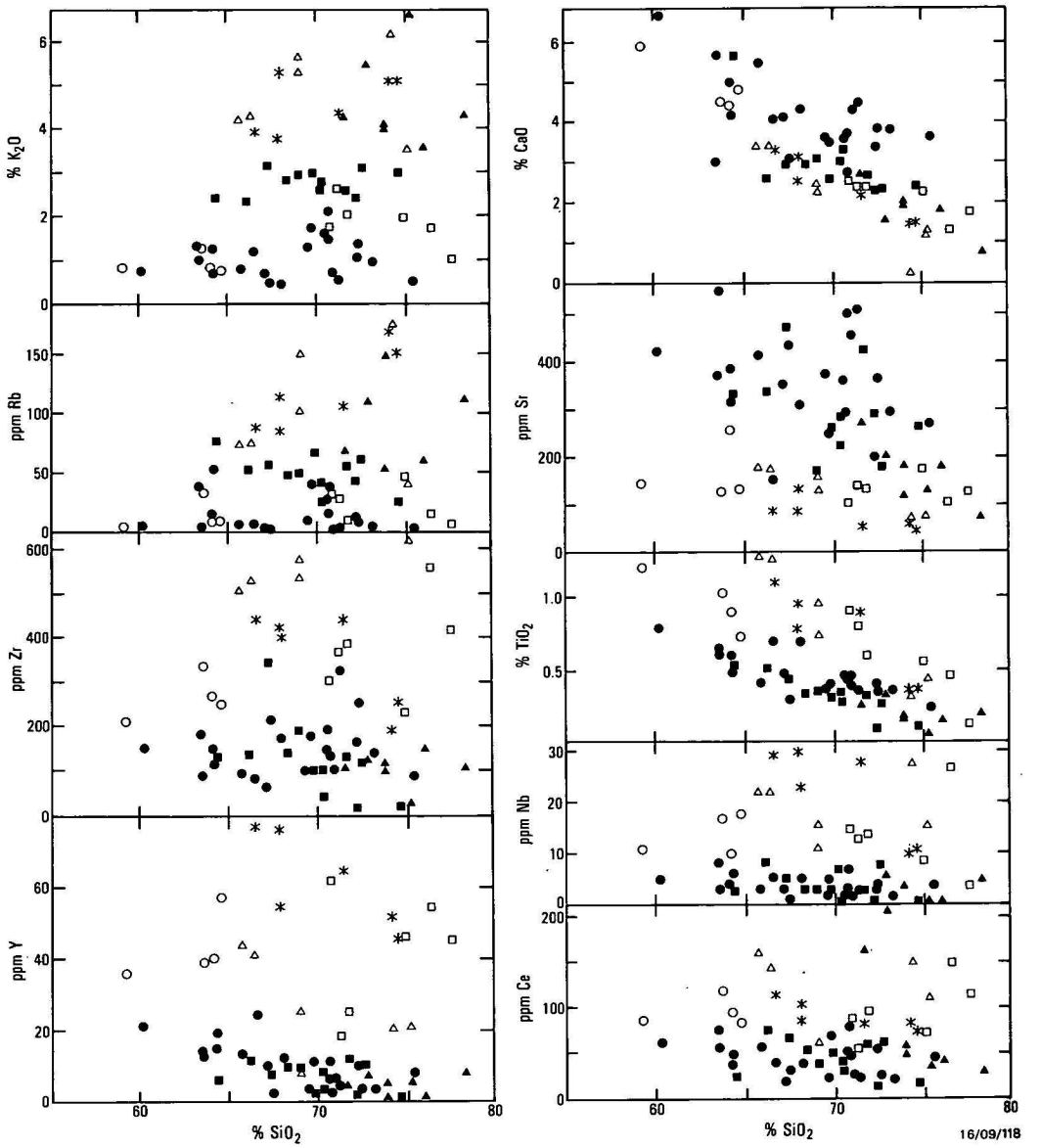

Figure 3. SiO_2 variation diagrams for gneisses from Napier Complex (after Sheraton & Black, 1983).
Depleted tonalites—solid circles; depleted granodiorites—solid squares; depleted granites—solid triangles; undepleted tonalites—open circles; undepleted trondhjemites—open squares; undepleted granites—open triangles; undepleted granites from Proclamation Island—stars.

Depleted granitoids

Tonalites and granodiorites have similar, moderately to strongly fractionated patterns (Ce_N/Yb_N = 3–17), with low HREE (1–8 times chondritic) and Eu anomalies that range from strongly positive to zero. There is a negative correlation between the Eu anomaly and HREE concentration, samples with the highest Eu/Eu* having lower HREE (Fig. 5) as well as generally lower LREE. Two depleted granites have more strongly fractionated patterns (Ce_N/Yb_N = 14 and 87), very low HREE (2–3 times chondritic), and positive Eu anomalies. As a group, the depleted granitoids show a tendency for Ce_N/Yb_N and Eu/Eu* to increase, and HREE and total REE to decrease with increasing SiO_2.

Tonalitic gneisses from many other Archaean high-grade terrains, as well as many unmetamorphosed tonalites, have very similar REE characteristics to those of the depleted suite, in particular positive Eu anomalies (e.g., Compton, 1978; O'Nions & Pankhurst, 1978; Arth, 1979; Tarney & others, 1979; Field & others, 1980; Hanson, 1980; Rollinson & Windley, 1980a; Weaver & Tarney, 1980; Longstaffe & others, 1982). Petrogenetic modelling by these authors has shown that such features are produced by partial melting of mafic rocks (amphibolite, garnet amphibolite, or eclogite) leaving residual garnet, hornblende, or both. Residual hornblende, garnet, and clinopyroxene may each contribute to a positive Eu anomaly in a partial melt (Hanson, 1978; Irving & Frey, 1978), with more extreme degrees of HREE depletion requiring residual garnet. Tarney & others (1980) have shown that the REE characteristics of tonalitic gneisses of the Scottish Lewisian, compositionally very similar to those of the Napier Complex, can best be explained by progressive partial melting involving residual garnet.

Equilibrium batch melting calculations (Arth, 1976) were carried out to assess possible residual phases and hence conditions of magma generation; mineral-melt distribution coefficients of Arth (1976) for felsic rocks were used. A tholeiite source with a slightly fractionated (LREE-enriched) pattern and LREE contents similar to those of mafic granulites and Proterozoic tholeiite dykes in the Napier Complex was assumed. 20–40 per cent melting of such a mafic source at 5–8 kb and high P_{H_2O} ($\geq 0.6\ P_{total}$) gives tonalitic liquids and residues of mainly horn-

Table 2. Major and trace-element (including REE) contents of representative depleted and undepleted granitoids and biotite-ferrohastingsite granite (73281015) from the southern Prince Charles Mountains.

	Depleted Suite										Undepleted Suite									
	Tonalites					Granodiorites			Granites		Tonalites		Tondhjemites		Granites		Garnet Gneisses			Granite
	7728 4114	7728 4658	7728 4374	7628 3203	7728 3428	7628 3023	7628 3246	7628 3057	7628 3001	7728 4313	7628 3074	7728 3985	7628 3274	7728 3980	7628 3006	7628 3228	7628 3064	7628 3211	7628 3272	7328 1015
SiO_2	64.2	65.8	67.2	70.8	73.3	68.4	72.4	72.7	71.7	76.2	63.7	64.7	71.9	75.1	66.4	75.3	74.3	74.5	76.2	72.1
TiO_2	0.60	0.40	0.47	0.43	0.35	0.33	0.10	0.27	0.26	0.15	1.05	0.74	0.61	0.56	1.28	0.44	0.09	0.10	0.44	0.76
Al_2O_3	15.28	14.88	15.06	14.76	13.94	15.79	14.31	14.19	14.48	12.40	12.78	15.14	11.14	11.35	12.92	10.55	13.30	13.40	10.98	12.22
Fe_2O_3	1.94	1.45	1.88	1.18	0.90	1.41	0.39	1.05	0.73	0.64	2.90	2.28	1.10	2.44	2.70	1.61	1.16	0.87	2.23	1.09
FeO	3.37	2.68	3.35	1.67	1.88	2.07	1.12	1.21	1.30	0.94	8.01	4.73	4.43	2.28	4.18	2.55	0.67	0.67	2.80	3.50
MnO	0.07	0.06	0.08	0.03	0.04	0.07	0.03	0.03	0.03	0.03	0.16	0.11	0.04	0.06	0.13	0.04	0.04	0.04	0.09	0.07
MgO	2.63	2.89	1.99	0.84	1.04	1.38	0.38	0.42	0.91	0.62	2.46	2.37	1.69	0.56	1.16	0.77	0.17	0.22	0.18	0.57
CaO	5.05	5.48	4.14	3.72	3.82	2.95	2.27	2.30	2.67	1.82	4.52	4.87	2.37	2.27	3.35	1.19	1.33	1.05	1.71	2.31
Na_2O	4.30	4.02	4.31	4.53	4.08	4.31	5.23	4.34	3.04	3.22	2.23	3.70	4.09	3.64	3.07	3.03	3.71	3.77	2.15	2.75
K_2O	1.30	0.86	0.76	1.52	0.98	2.84	2.42	3.12	4.24	3.57	1.32	0.81	2.06	1.99	4.26	3.50	4.56	5.27	3.23	4.47
P_2O_5	0.17	0.14	0.08	0.07	0.08	0.13	0.03	0.03	0.02	0.03	0.14	0.28	0.08	0.15	0.39	0.02	<0.01	0.02	0.01	0.21
Trace elements (ppm)																				
V	72	72	64	12	46	36	6	11	9	19	195	96	11	4	51	<2	2	2	<2	28
Cr	100	91	47	13	20	33	8	5	42	7	8	66	13	4	9	6	3	9	<3	11
Ni	25	54	18	5	19	15	6	3	28	9	16	20	26	10	7	<2	<2	9	4	6
Cu	9	21	24	6	6	5	3	3	8	28	9	9	8	7	18	6	3	3	6	20
Zn	68	42	66	33	32	47	20	39	25	21	150	85	33	58	57	73	25	5	56	53
Ga	19	16	18	15	14	18	15	16	15	12	19	20	17	17	16	16	14	14	17	16
Rb	14	6	2	15	4	47	43	60	67	59	33	8	9	46	74	40	120	191	65	144
Sr	386	412	349	292	295	727	289	177	274	181	128	134	134	176	174	77	101	61	76	103
Y	19	16	14	10	10	16	4	18	9	7	41	43	30	56	50	29	52	22	68	77
Zr	153	97	64	196	144	145	21	122	107	153	337	253	386	234	529	619	82	65	334	516
Nb	4	3	3	7	2	3	<1	8	3	1	17	18	14	9	22	16	2	1	4	60
Ba	741	680	456	713	674	1610	898	1060	1170	1150	1240	530	1060	740	2480	984	1410	613	1360	766
La	15.7	29.6	9.5	35.9	9.1	18.7	5.1	26.0	114	20.1	68.9	31.3	64.3	32.0	59.8	66.3	19.4	34.1	35.7	57.6
Ce	33.8	61.5	17.2	63.4	16.6	43.3	8.1	51.8	178	34.1	137	82.3	124	68.8	143	134	36.0	67.1	57.6	144
Pr	4.2	7.3	1.9	6.5	1.4	5.5	0.6	6.5	17.1	3.3	14.8	11.0	13.3	8.6	16.6	16.6	4.3	6.8	6.0	16.7
Nd	15.7	22.3	6.5	16.4	5.3	18.6	2.9	20.3	39.7	9.2	49.8	40.9	44.9	30.7	61.8	52.6	15.0	19.2	19.4	53.2
Sm	3.6	4.3	1.6	2.3	1.3	3.9	0.6	4.4	4.3	1.4	9.1	9.9	7.8	7.7	11.9	9.4	3.7	3.5	4.1	11.6
Eu	1.2	1.4	0.9	1.0	1.1	1.2	0.7	1.2	1.3	1.2	2.4	1.7	1.9	2.4	2.5	2.1	0.8	0.7	2.1	2.2
Gd	3.2	3.5	1.8	1.5	1.2	2.9	0.4	3.9	2.3	1.0	7.8	8.6	6.3	8.3	9.6	7.4	5.4	3.4	7.0	11.4
Dy	3.0	2.8	1.9	0.7	1.0	2.0	0.3	2.7	1.0	0.7	7.5	7.5	5.5	8.4	9.0	4.7	7.1	3.7	12.7	13.9
Er	1.9	2.0	1.6	0.8	1.3	1.6	0.4	1.8	0.5	0.6	4.3	4.1	3.0	5.2	4.3	2.8	6.0	1.9	8.5	8.5
Yb	1.6	1.5	1.4	0.9	1.3	1.4	0.2	1.4	0.5	0.6	4.3	3.6	2.9	4.5	3.8	2.6	5.9	1.4	8.2	8.5
Pb	10	8	5	9	9	25	10	23	24	19	14	19	9	17	19	10	36	45	27	18
Th	1	12	<1	4	<1	9	<1	20	18	<1	21	39	16	18	1	17	46	6	3	25
U	<0.5	<0.5	<0.5	<0.5	<0.5	<0.5	0.5	1.0	<0.5	<0.5	1.0	4.0	0.5	2.0	0.5	1.5	3.5	0.5	1.0	3.0
Ce_N/Yb_N	5.3	10	3.3	17	3.3	8.0	10	9.5	87	14	8.2	5.8	10.8	3.9	9.7	13.0	1.6	12.5	1.8	4.3
Eu/Eu*	1.07	1.06	1.7	1.6	2.6	1.05	4.2	0.92	1.16	2.9	0.87	0.54	0.80	0.93	0.70	0.76	0.57	0.66	1.22	0.59

Ce_N and Yb_N are chondrite-normalised values; Eu/Eu* is ratio of measured to interpolated Eu contents, also chondrite-normalised.

blende with subordinate clinopyroxene, plagioclase, olivine, and/or Fe-Ti oxide (Holloway & Burnham, 1972; Helz, 1976). Typical results of these calculations, assuming 30 per cent equilibrium melting, are shown in Figure 6. A residue predominantly of hornblende gives the best approximation to the observed patterns (Fig. 4), particularly the concave-upwards curve of many samples (Hanson, 1980), and is consistent, in terms of bulk composition, with removal of 30 per cent of a tonalitic melt from a tholeiitic source. Up to 20 per cent of residual garnet results in patterns similar to those of the most strongly REE-fractionated (high Ce_N/Yb_N) samples, whereas an increasing proportion of clinopyroxene gives less fractionated patterns with smaller positive Eu anomalies. In fact, virtually the entire range of patterns shown by the depleted suite can be produced through melting of a single source by varying the proportions of residual hornblende and clinopyroxene. At relatively low pressures (5–8 kb), at least, increasing percentage melting and P_{total}, and decreasing P_{H_2O} would all result in smaller proportions of residual hornblende and less siliceous melts (Holloway & Burnham, 1972; Helz, 1976).

Garnet would be a possible residual phase at somewhat higher pressures (Green & Ringwood, 1967, 1972). The presence of residual olivine would not affect the shape of the REE pattern significantly, but would result in proportionally higher concentrations of all REE in the melt. Residual eclogite (clinopyroxene + garnet) would give rise to melts with even more fractionated patterns, but smaller positive Eu anomalies, although the considerable variation in patterns of the depleted suite and uncertainties in source composition do not allow the complete elimination of this possibility. However, melting of a less LREE-enriched source, such as oceanic tholeiite, would require correspondingly greater proportions of residual garnet to produce the observed degrees of REE fractionation (Ce_N/Yb_N) in some of the samples. Relatively high Sr contents and positive Eu anomalies of the depleted tonalites and granodiorites are inconsistent with major residual plagioclase, effectively eliminating melting of any likely felsic source. Partial melting of mafic granulite at lower P_{H_2O} with residual pyroxene + olivine ± plagioclase would produce insufficient fractionation of REE, even if all Ti not in these phases was incorporated in sphene, which, in any case, would be more probable under hydrous melting conditions (Hellman & Green, 1979).

Calculated Eu/Eu* ratios are similar to that of the average depleted granitoid, but significantly smaller than the more extreme values (Fig. 4). Any plagioclase preferentially entering the partial melt would tend to enhance the positive Eu anomaly, but only if melt and residual phases did not fully equilibrate. Residual apatite (about 0.3%, assuming 0.13% P_2O_5 in the source) would contribute to a positive Eu anomaly (Watson & Capobianco, 1981; Watson & Green, 1981), particularly under high P_{H_2O} conditions (Saunders & others, 1980), but the net effect would be insignificant. However, the ratio Eu^{2+}/Eu^{3+} and hence Eu/Eu* in residual minerals and coexisting liquid would be strongly dependent on oxygen fugacity (Drake, 1975). The fact that samples with the largest Eu anomalies tend to be the most siliceous, and the lack of a positive correlation between normative plagioclase content and Eu/Eu* are inconsistent with their being either plagioclase-rich cumulates (cf. Field & others, 1980) or residues of partial melting (cf. Weaver, 1980).

Similar equilibrium melting calculations for other elements, using a range of mineral-melt distribution coefficients (Arth, 1976; Pearce & Norry, 1979; Gill, 1981), are consistent with an amphibole-rich residue; moreover, the good correlation of TiO_2 with Y (Sheraton & Black, 1983) is consistent with horn-

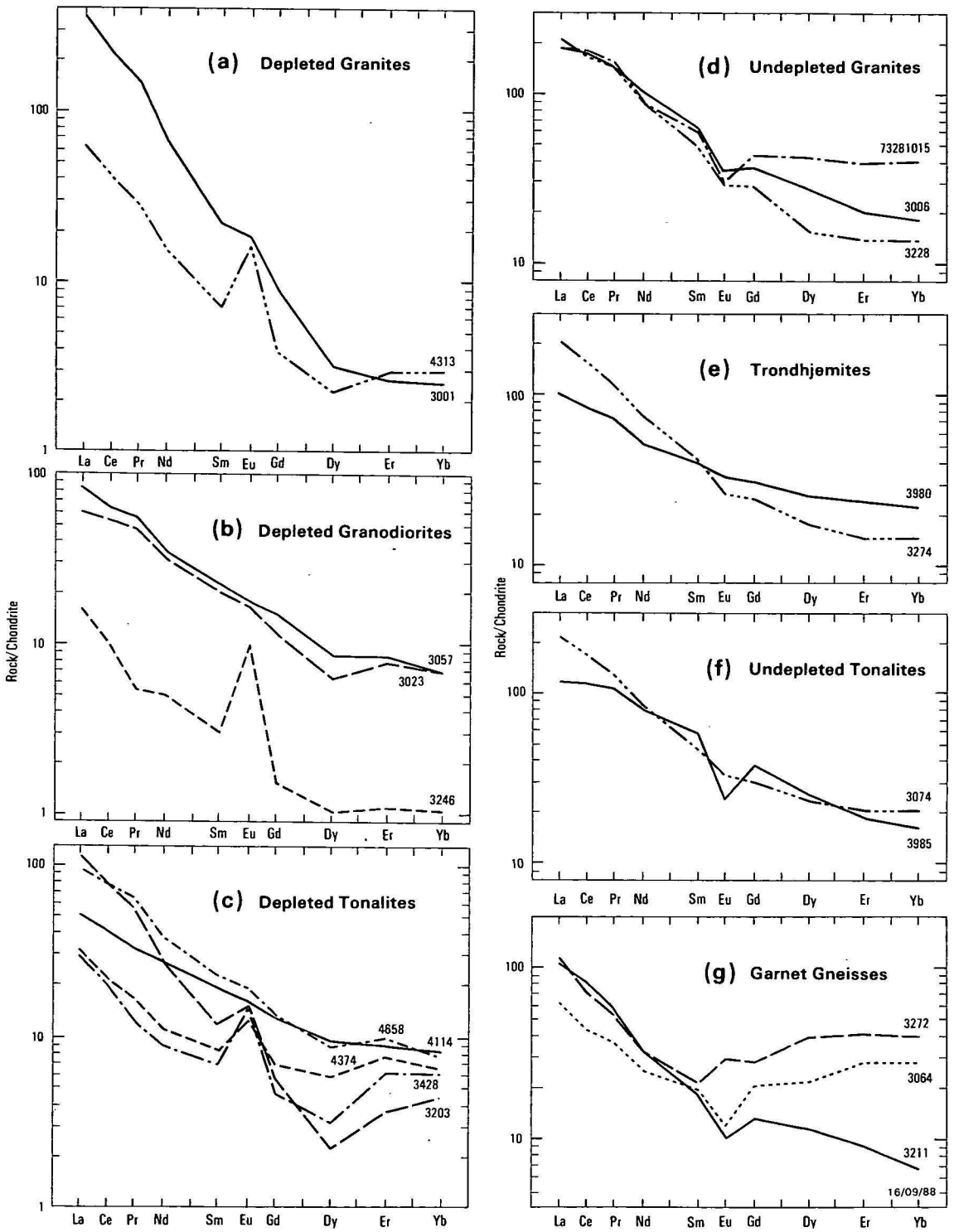

Figure 4. Chondrite-normalised rare-earth element abundances in depleted and undepleted granitoids, garnet gneisses, and a late Archaean biotite-ferrohastingsite granite (73281015).

Sample numbers from 3001 to 3274 are prefixed 7628, and those from 3428 to 4658 are prefixed 7728.

blende control. Pyroxene ± olivine residues would equilibrate with liquids insufficiently depleted in Y, whereas liquids in equilibrium with an eclogitic residue would generally be too depleted in Y; in both cases, the liquids would be too high in Ti and V unless a residual Ti or Fe oxide was also present (Green, 1981; Green & Pearson, 1983). A hornblende-rich residue would not require significant amounts of a Ti-rich mineral (sphene or ilmenite), even if the source contained as much as 2 per cent TiO_2. Plagioclase-rich residues would result in liquids too low in Sr. Concentrations of other minor elements (Cr, Ni, Zr, Nb, and Ba) do not impose significant constraints on residual mineralogy.

The alternative explanation that the HREE depletion results from hornblende fractionation (Arth & others, 1978; Frey & others, 1978) is inconsistent with the observed trend shown by most tonalites and granodiorites of slightly increasing normative diopside with SiO_2 (Fig. 7) (Cawthorn & Brown, 1976).

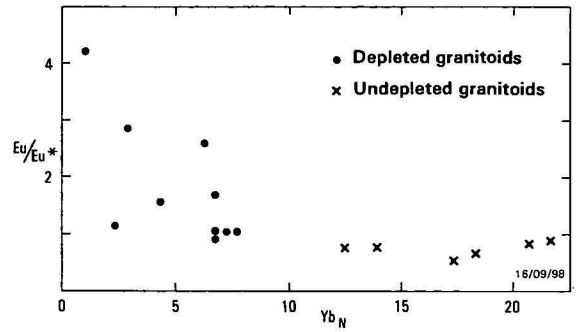

Figure 5. Chondrite-normalised Yb against Eu/Eu* plot for depleted and undepleted granitoids.

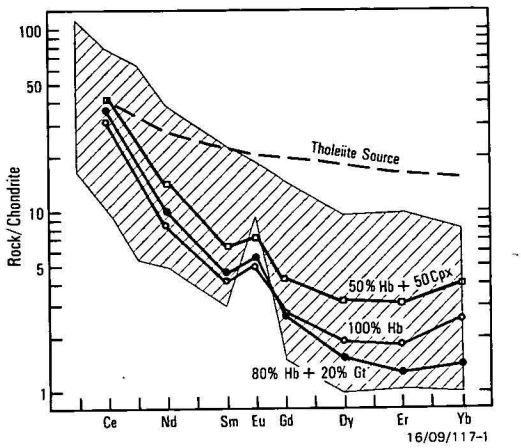

Figure 6. Calculated REE abundances in partial melts in equilibrium with residues consisting of 50% hornblende + 50% clinopyroxene, 100% hornblende, and 80% hornblende + 20% garnet.
Distribution coefficients used are those of Arth (1976) for felsic rocks. Dashed line indicates assumed tholeiitic source composition; shaded area is field of depleted tonalites and granodiorites.

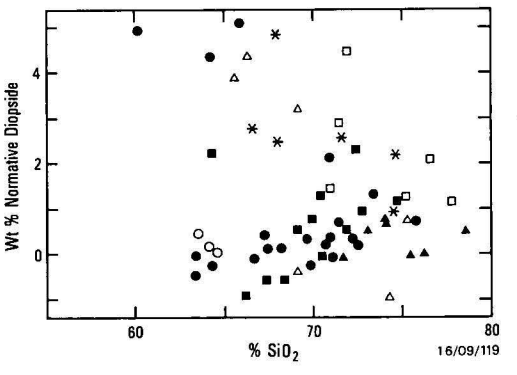

Figure 7. Plot of normative diopside against SiO_2 for Napier Complex granitoids.
Rocks with normative corundum are plotted as negative values on the ordinate. Symbols as in Figure 3.

Sheraton & Black (1983) explained this tendency for normative corundum to increase with degree of melting by the presence, in addition to hornblende, of a corundum-normative mineral such as garnet in the source. A decreasing proportion of residual garnet with increasing degree of melting would also explain the trends of increasing HREE and Y and decreasing Eu/Eu* with decreasing SiO_2 (and increasing total FeO). The overall chemical trends are therefore considered to be essentially controlled by partial melting, although a limited degree of hornblende fractionation may be necessary to account for the largest positive Eu anomalies. Moreover, depleted granites have compositions consistent with derivation from granodioritic magma by fractionation of plagioclase, hornblende, and possibly biotite, with a consequent reduction in CaO, Sr, Y, and HREE (Fig. 3). Their high Ba/Sr ratios are difficult to produce directly by any reasonable degree of melting of a mafic source (Sheraton & Black, 1983).

Undepleted granitoids

Undepleted tonalites, trondhjemites, and granites have moderately fractionated (Ce_N/Yb_N = 4–11) REE patterns, but much less depleted HREE (13–22 times chondritic) and small to moderate negative Eu anomalies (Fig. 4). LREE contents are mostly higher than those of the depleted suite (Table 2). Garnet-quartz-feldspar gneisses, mostly of granitic composition, have generally similar characteristics, but rather variable HREE contents. The trondhjemites are compositionally similar to low Al_2O_3 trondhjemites of Arth (1979). They are quite different from those in the Lewisian, most of which have strongly fractionated patterns with large positive Eu anomalies (Tarney & others, 1979; Weaver & Tarney, 1980), and are thus more like depleted Napier Complex tonalites.

REE patterns like those of the undepleted suite are typical of a wide range of Archaean to Recent granitoids and are generally considered to be consistent with partial melting of continental crustal rocks of various types (e.g., Condie & Hunter, 1976; Albuquerque, 1977; Condie, 1978; Hanson, 1978; O'Nions & Pankhurst, 1978).

Mostly diopside-normative compositions, with molecular $Al_2O_3/(Na_2O + K_2O + CaO)$ ratios consistently less than 1.1, indicate derivation of the undepleted, like the depleted, suite from igneous rather than sedimentary source materials, i.e. they are I-type granitoids on the classification of Chappell & White (1974). Even the slightly corundum-normative leucocratic garnet-bearing granitic gneisses are I-type on this basis, although an origin by melting of immature greywackes or a mixed igneous/sedimentary source cannot be entirely ruled out. However, in spite of their similar REE characteristics, the considerable compositional differences between the undepleted tonalites, trondhjemites, and granites (Table 1, Fig. 3) preclude a common origin; in particular, they cannot plausibly be related either by fractionation of any combination of pyroxene, hornblende, biotite, and plagioclase, or by progressive partial melting of the same source material. SiO_2 variation trends are inconsistent with either process, so that, for example, the granites could not be derived from a more siliceous trondhjemitic magma by crystal fractionation.

Partial melting of a mafic source under relatively low P_{total} and P_{H_2O} conditions could account for the REE characteristics of the undepleted tonalites (Fig. 4). For example, about 30 per cent melting of a tholeiite source with the same REE contents as that used in Figure 6, leaving a residue of plagioclase (50%), clinopyroxene (25%), and olivine (25%), would produce a melt of appropriate bulk composition and REE characteristics (i.e. a negative Eu anomaly and relative enrichment in LREE). An even closer match is achieved if the source has a slightly more fractionated REE pattern (higher Ce_N/Yb_N). Little or no residual hornblende or garnet are possible or the partial melt becomes markedly depleted in middle and HREE and has a smaller negative, or even a positive, Eu anomaly; residual plagioclase is compatible with comparatively low Sr in the melt. Alternatively, melting of a somewhat more siliceous source, with a pyroxene + plagioclase ± quartz residue, is possible and would result in similar REE patterns. Derivation from a mafic to intermediate granulite source would partly explain the higher TiO_2, Y, Zr, Nb, and REE contents of the undepleted, compared to the depleted, tonalites (Tables 1, 2; Fig. 3), particularly if relatively low P_{H_2O} tended to destabilise

residual accessory phases such as ilmenite, rutile, sphene, and zircon (Hellman & Green, 1979; Saunders & others, 1980), as well as hornblende. In addition, a more incompatible-element enriched source is likely. However, some residual apatite and an Fe-Ti oxide (or possibly minor (<10%) hornblende) would be necessary to account for the P_2O_5, TiO_2, and V contents of the tonalites. Whatever the exact composition of the source, the geochemistry of the undepleted tonalites implies relatively low-pressure melting within the crust (<15 kb for a mafic source: Green & Ringwood, 1972). The more siliceous trondhjemites have mostly similar minor-element contents to the tonalites, consistent with somewhat lower degrees of melting (10–20%) of a similar source. However, their lower TiO_2, P_2O_5, and V contents (Table 1) require greater proportions of residual apatite and Fe-Ti oxide, more extensive crystal fractionation, or both.

A more siliceous source is probable for the more abundant undepleted granites (Sheraton & Black, 1983), but simple remelting of depleted granitoids cannot easily account for their rather lower Ce/Y and Ti/Y and higher HREE contents (see e.g., Weaver, 1980), which suggest an additional unfractionated component (such as mafic granulite) in the source region. Hence, a source consisting of one-third tholeiite (as in Fig. 6) plus two-thirds average depleted gneiss, with a small positive Eu anomaly, was used in model melting calculations. Such a bimodal lower crust, of average intermediate composition, is in line with both geophysical (e.g., Smithson & Brown, 1977) and geochemical (e.g., Taylor & McLennan, 1981) data. For example, 30 per cent melting of this source, leaving a granulite residue (64% plagioclase, 15% orthopyroxene, 9% clinopyroxene, and 12% quartz), would give a granitic liquid of similar bulk composition to the average undepleted granite (Table 1F) and with REE characteristics shown in Figure 8. Clearly, an even closer match could be obtained by juggling the source composition, percentage melting, and proportions of residual phases, but in view of the large uncertainties in published distribution coefficients, calculations of this type can only model natural processes to a first approximation. Equilibrium batch melting calculations for other minor elements are in reasonable agreement with this model, although a source somewhat more enriched (by factors of about 1.5 to 2) in certain incompatible elements (Zr, Nb, and Ba), as well as LREE, is probable, and some residual apatite (probably <0.1%) and a Fe-Ti oxide are necessary to explain the TiO_2, P_2O_5, and V contents of the granites. It is apparent, however, that, unless the source was considerably more enriched in HREE than that used in the calculations, hornblende could not have been a major residual mineral, whereas considerable residual plagioclase is required. Even a source with similar HREE contents to the tholeiite of Figure 6 would not allow more than 5 or 10 per cent residual hornblende or significant residual sphene.

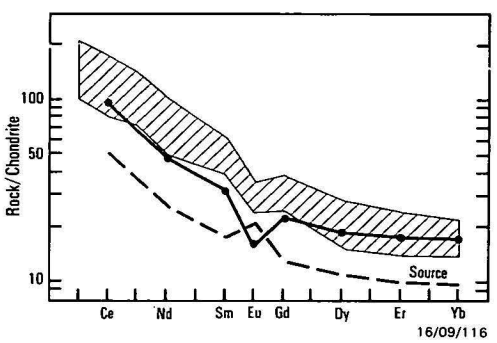

Figure 8. Calculated REE abundances in partial melt in equilibrium with a residue consisting of plagioclase (64%), orthopyroxene (15%), clinopyroxene (9%), and quartz (12%).

Dashed line indicates assumed source composition (1/3 tholeiite as Figure 6, 2/3 average depleted granitoid); shaded area is field of undepleted granitoids.

The possible role of crystal fractionation (either fractional crystallisation or separation of restite phases from the magma) is difficult to assess. Although most of the major-element variation can be explained in terms of variations in the proportions of plagioclase and pyroxene, model melting calculations indicate that progressive partial melting involving only residual pyroxene and plagioclase cannot account for the marked depletion in Y (Fig. 3) and, presumably, HREE with increasing SiO_2 shown by the undepleted granites. Similarly, fractionation of only plagioclase and pyroxene cannot explain this trend. Major-element variations of undepleted granites from one locality (Proclamation Island) can be approximated by about 30 per cent fractionation of plagioclase + orthopyroxene + hornblende + biotite (in the approximate proportions 4:2:2:1) or plagioclase + orthopyroxene + clinopyroxene + biotite (5:3:1:1). The trends are not sufficiently well defined to distinguish between these possibilities; either would be consistent with the observed decrease in normative diopside with increasing SiO_2 (Fig. 7). Rayleigh fractionation calculations (Arth, 1976), using distribution coefficients of Arth (1976), Pearce & Norry (1979), and Hanson (1980), confirm that the additional separation of minor zircon and apatite (≈0.06% and 0.5%, respectively, based on the observed depletions in Zr and P_2O_5) as well as a Ti-rich phase, is required to account for much of the minor-element variation. Fractionation of 0.4–1.0 per cent sphene (depending on whether or not hornblende was also a fractionating phase) would account for the depletion in Ti, REE, Y, and probably Nb (Fig. 3). Sphene is a common accessory in I-type granitoids (Chappell & White, 1974). Such minor phases are known to play a significant part in controlling REE behaviour during production and fractionation of felsic magmas (McCarthy & Kable, 1978; Tindle & Pearce, 1981). Other undepleted granites show greater compositional variations, but generally similar trends (Fig. 3 and 7).

These calculations do not prove, but are at least consistent with, some degree of crystal fractionation. Probable fractionating phases are, of course, difficult to identify directly, owing to the metamorphosed state of the rocks. The predominant mafic mineral in the Proclamation Island granite is orthopyroxene (up to 7%), with only minor (up to 1%) hornblende, biotite, and clinopyroxene. However, hornblende may well have been the major mafic phase present during emplacement, probably with subordinate biotite. During subsequent granulite-facies metamorphism, it would undergo a reaction to give mainly orthopyroxene, clinopyroxene, and plagioclase, whereas biotite would break down to orthopyroxene + K-feldspar. Any sphene present must also have become unstable, as ilmenite is now the only Ti-rich phase present. The apparent degree of orthopyroxene control may partly reflect its modal variation, resulting from deformation and recrystallisation under granulite-facies conditions, superimposed on the original trends due to plagioclase + hornblende ± biotite fractionation. Alternatively, both hornblende and orthopyroxene may have been stable during emplacement under synmetamorphic conditions. The Rb-Sr isochron age of the Proclamation Island granite (3072^{+35}_{-33} Ma, initial $^{87}Sr/^{86}Sr$ 0.70091 ± 0.00004) is thought to be that of emplacement and to closely approach that of the peak of metamorphism in the Napier Complex (Sheraton & Black, 1983).

Late and post-orogenic granitoids

A late Archaean biotite-ferrohastingsite granite (73281015) from the southern Prince Charles Mountains (MacRobertson Land) is typical of late to post-orogenic granodioritic to granitic intrusives of Enderby Land and adjacent areas of East Antarctica. Such intrusives are characterised by Fe-rich mafic minerals (including fayalite locally) and are commonly rather melanocratic with abundant accessory minerals (including

apatite, zircon, sphene, allanite, chevkinite or perrierite, fluorite, and monazite); hence, they have relatively low Mg/(Mg + total Fe) and higher minor-element contents (Ti, P, Y, Zr, Nb, REE) than the undepleted granitoids (Table 1). Sample 73281015 has an even less fractionated pattern, with similar LREE contents but higher HREE than the latter (Fig. 4). These granitoids thus more closely resemble the undepleted than the depleted suite, but show still greater enrichment in Fe and many minor elements.

LIL-element metasomatism

Sheraton & Black (1983) pointed out that the depleted tonalites and granodiorites have virtually identical compositional trends, except that the latter have considerably higher K_2O, Rb, Ba, Pb, Th, and U, and lower CaO (Table 1; Fig. 3). REE data are consistent with this feature, showing a very similar range of patterns for both groups. These chemical characteristics may be illustrated by means of incompatible-element abundances normalised to estimated primordial mantle concentrations (mostly chondritic), with elements arranged in order of decreasing incompatibility with respect to a mantle source of basaltic magma (Fig. 9) (Sun & others, 1979; Wood & others, 1979). Average concentrations were used for LIL (large ion lithophile) elements (which show considerable scatter) and REE (for which only limited data are available), but other elements, which show systematic variations with SiO_2, were normalised on variation diagrams to a SiO_2 content of 70 per cent. The latter value is close to the average SiO_2 contents of both groups and to the average of samples for which REE data are available. In the average granodiorite, Pb, Rb, Ba, Th, U, and K are enriched by factors of 1.7 or more, relative to the average tonalite; P is lower by a factor of 0.65, and Ca (not shown) and Yb by 0.75. All other analysed elements (including V, Cr, Ni, Cu, Zn, Ga, and majors) differ by less than ± 20 percent, probably insignificant in view of their considerable scatter within each group. Similar Sr contents indicate that the granodiorites could not have been derived from a tonalitic magma by fractionation of plagioclase, and the similar major-element compositions (K excepted) and range of SiO_2 contents militate against very different degrees of partial melting. The fact that the compositional differences are almost entirely confined to LIL elements makes it tempting to invoke the involvement of a fluid phase enriched in those elements. LIL elements show little correlation with SiO_2, but fairly good correlations with one another (e.g., K and Ba), also suggesting that their variations were determined by some process other than progressive partial melting or crystal fractionation. The 'decoupling' of LIL elements from other trace and major elements has been noted by Weaver & others (1979) and Ringwood (1982).

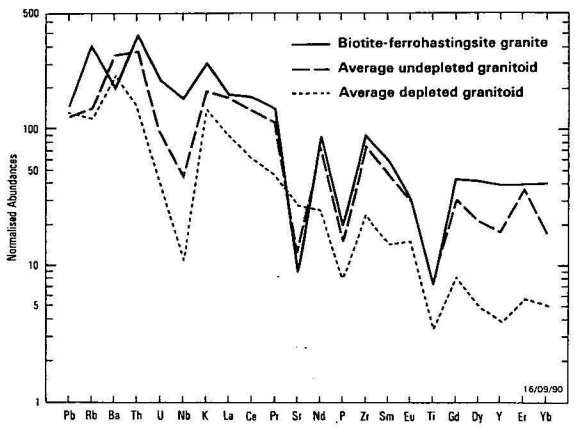

Figure 9. Normalised incompatible-element abundances in average depleted tonalite and granodiorite.
Normalising values are estimated primordial mantle concentrations (mostly chondritic) of Sun (1980). See text for further discussion.

A complicating factor is the metamorphic depletion in Rb, Th, U, and, to a lesser extent, K, which is difficult to quantify, but cannot, in isolation, account for the distinct compositional gap in K_2O and Rb between the tonalites and granodiorites (Fig. 3). K and Rb show the greatest differences (Fig. 9), but may have been preferentially lost from the tonalites (Tarney & Windley, 1977). Thus, if LIL-element ratios were similar in the tonalites and granodiorites prior to metamorphism (i.e., if essentially all LIL-element variation in both was determined by a single metasomatic component), and if there was no significant net loss of Ba during metamorphism - and various studies (e.g., Tarney & others, 1972; Sheraton & others, 1973; Cooper & Field, 1977, and Rollinson & Windley, 1980b) suggest that this is usually the case - then there were additional losses of about 16 ppm Rb and 0.56 per cent K_2O from the average tonalite over those expected had both tonalites and granodiorites undergone similar degrees of depletion. On this model, any losses of Th and U must have been to similar extents from each group, although the degree of depletion in Th was not necessarily the same as that of U. Alternatively, the postulated metasomatic fluid phase could have contributed significantly different proportions of K, Rb, Ba, etc. to the tonalite and granodiorite magmas, making estimation of degrees of metamorphic depletion impossible. However, it is worth pointing out that the mantle source of a suite of Proterozoic tholeiite dykes in Enderby Land was apparently metasomatically enriched in K, Rb, Ba, and Th (and possibly U and Pb) to similar extents relative to their estimated abundances in primordial mantle (Sheraton & Black, 1981).

One possible source of such a metasomatic fluid during magma generation would be from the dehydration of subducted oceanic crust (Tarney & Saunders, 1979; Saunders & others, 1980). Another would be from dehydration of older sialic crust during magma emplacement; isotopic Pb evidence indicates that such a fluid, derived from 3700 Ma Amitsoq-type continental crust in West Greenland, contaminated 3000–2800 Ma Nuk gneiss precursors during their emplacement (Taylor & others, 1980). However, the present rather limited isotopic data suggest that much of the depleted tonalite and granodiorite could be the oldest felsic crustal component of the Napier Complex (Sheraton & Black, 1983). Alternatively, the granodioritic magmas may have been generated by partial melting of a mafic source relatively enriched in LIL elements, although this would imply derivation from a separate source region to that of the tonalites. In theory, it should be possible to distinguish isotopically between partial melting in association with a metasomatic fluid and partial melting of a previously metasomatised source, if the metasomatising phase produced variable enrichment in Rb (cf. Sheraton & Black, 1981). But isotopic resetting during high-grade metamorphism make this impossible (Sheraton & Black, 1983). The strong negative Nb anomalies of the tonalites and granodiorites (Fig. 9) are certainly consistent with LIL-element metasomatism of either the source region or the magmas themselves, but, with similar anomalies shown by P and Ti, would be enhanced by the stability of hornblende and possibly Ti oxides and apatite under hydrous melting conditions. In detail, the LIL-element patterns of Figure 9 could be taken to imply significant depletion of K, Pb, Th, and particularly Rb and U, relative to Ba during metamorphism. It is clear that both tonalitic and granodioritic magmas must have been derived by similar degrees of melting of sources with very similar compositions, LIL elements excepted.

Discussion and conclusions

REE data for Napier Complex felsic orthogneisses support the presence of two compositionally distinct suites of I-type (igneous-derived) granitoid, as proposed by Sheraton & Black (1983). Similarly, O'Nions & Pankhurst (1978) subdivided the Archaean Amitsoq gneiss of West Greenland into a mainly tonalitic group with strong HREE depletion and positive Eu anomalies, and a predominantly granitic group with negative Eu anomalies; Ewing (1979) showed that both depleted (in Y and HREE) and undepleted trends exist in Archaean intermediate to felsic volcanics.

Depleted granitoids (predominantly tonalite and granodiorite) from Enderby Land apparently represent new continental crust, ultimately derived from the mantle by a two-stage melting process involving mafic crustal rocks, and thus may be an example of Glikson's (1972, 1979) 'sialic nuclei'. Their fractionated REE patterns, with marked HREE depletion, positive Eu anomalies, and other chemical characteristics can be explained by various degrees of relatively high-pressure hydrous partial melting of a hornblende or garnet-bearing mafic source (amphibolite, garnet amphibolite or, less likely, eclogite); only the subordinate granites (s.s.) have compositions that suggest significant crystal fractionation. One possible source of depleted magma – if subduction processes occurred in the Archaean, as suggested by Arndt (1983) and Nisbett & Fowler (1983) – would be subducted hydrated oceanic crust, which could also have contributed LIL-element-enriched fluids, which apparently played a significant part in determining magma composition.

The generally less-fractionated REE patterns, negative Eu anomalies, and, on average, more potassic (i.e. granitic, s.s.) compositions of the undepleted suite are compatible with relatively low-pressure melting of predominantly felsic continental crustal rocks, in which plagioclase rather than garnet or hornblende has played a major role. Melting under generally lower P_{H_2O} conditions would increase partition of minor elements such as Ti, P, Y, Zr, Nb, and REE, all of which are considerably higher in the undepleted suite (Fig. 10), into the melt, although a more enriched source is also probable. Crystal fractionation (predominantly of plagioclase, hornblende, and possibly orthopyroxene) may have played an important part in determining the compositional trends of the relatively abundant undepleted granites. Plagioclase fractionation (as well as residual plagioclase) would lead to the development of a marked negative Sr anomaly (Fig. 10). Nb, P, and Ti anomalies of the undepleted suite may have been partially inherited from a predominantly depleted source, but would also be enhanced by low-pressure fractionation of minor phases such as apatite and sphene. The relatively fractionated, leucocratic garnet gneisses have lower contents of these elements than other undepleted granitoids (Table 1). Magma generation by remelting of older, predominantly depleted granitoids (plus an unfractionated mafic component) is not inconsistent with Rb-Sr isotopic data, although variable resetting during high-grade metamorphism makes interpretation difficult (Sheraton & Black, 1983). However, both depleted and undepleted suites were apparently intruded over a considerable time, and may be partly contemporaneous, as in Canada (Ewing, 1979).

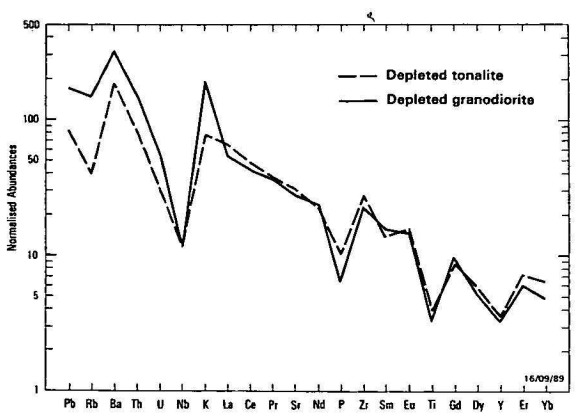

Figure 10. Normalised incompatible-element abundances in (1) biotite-ferrohastingsite granite (73281015), (2) average of 16 undepleted granitoids, and (3) average of 40 depleted granitoids.

Both depleted and undepleted granitoids now contain virtually anhydrous mineral assemblages, which imply thorough dehydration during metamorphism, probably as a result of introduction of a CO_2-rich fluid phase and accompanied by loss of LIL elements (Rb, Th, U, and K) (Tarney & Windley, 1977; Newton & others, 1980; Weaver & Tarney, 1981). However, like other Archaean high-grade terrains (e.g., Tarney & others, 1972), Ba is relatively high.

Late and post-orogenic granitoids in Enderby Land and adjacent areas are characterised by greater Fe-enrichment, commonly have high K_2O/Na_2O, and have even higher minor-element contents (Fig. 10) than undepleted granitoids; they resemble the latter in REE patterns, and, if the granite from the southern Prince Charles Mountains (73281015) is typical, have marked negative Eu anomalies. Similar granitoids have been termed 'A-type' (anorogenic) by Loiselle & Wones (1979) who, in common with White (1979) and Collins & others (1982), considered them to be derived by melting of relatively anhydrous (possibly residual) lower crustal rocks. The unusually anhydrous Napier Complex country rocks would provide a suitable source for magmas of this type. Rapakivi granites, which display similar REE characteristics and have particularly low Mg/(Mg + total Fe) (Anderson & Cullers, 1979; Hubbard & Whitley, 1979), are a related suite. Emslie (1978) suggested that such magmas are generated by melting of lower crustal rocks during emplacement of mafic magma.

Depleted orthogneiss terrains (and comparable granitoids of greenstone belts) are characteristic of the Archaean (Glikson, 1979) and commonly differ from typical younger sodic intrusives in the presence of marked positive Eu anomalies (cf. Albuquerque, 1977; Lopez-Escobar & others, 1979), although plagioclase-rich cumulates, regardless of age, are likely to have such anomalies (e.g., Field & others, 1980; Demaiffe & Hertogen, 1981). Archaean granitoids include both depleted and undepleted I-types, whereas undepleted I-type, together with S (sediment-derived) and A-types, are more typical of the Proterozoic and Phanerozoic, in part reflecting the development of thick sedimentary sequences (Ronov, 1972). Isotopic evidence (Moorbath, 1977; Patchett & others, 1981) shows that new felsic continental crust has been generated throughout geological time, so the question arises of why depleted granitoids are not more abundant in post-Archaean terrains. Tarney & Saunders (1979) have suggested that higher Archaean geothermal gradients would lead to more extensive melting of a (hypothetical) garnet-bearing downgoing slab, and hence to an increased production of depleted magma at that time. Alternatively, their relative abundance in Archaean terrains may partly reflect systematic differences in the present erosion levels.

Gneisses of the late Proterozoic Rayner Complex (Fig. 1), immediately adjacent to the Napier Complex in Enderby Land, appear, on chemical and isotopic evidence, to be largely remetamorphosed Napier Complex rocks (Sheraton & Black, 1983). In contrast, late Proterozoic granulite-facies metamorphics in MacRobertson Land and Princess Elizabeth Land in-

clude a high proportion with a relatively short previous crustal history (Tingey, 1982; Sheraton & Collerson, 1983; Sheraton & others, 1984). Metasediments and S-type granitoids are much more common, but depleted granitoids, as evidenced by low Y and high Ti/Y and Ce/Y, are rare (Sheraton & Black, 1983). Similarly, late Archaean amphibolite-facies orthogneisses of the southern Prince Charles Mountains are almost exclusively of undepleted type, and include many 'A-type' granitoids. Thus, undepleted granitoids, as well as being comparable with typical post-Archaean I-type granitoids, may well be representative of a higher crustal level than the depleted suite; the Napier Complex, with particularly high temperatures of metamorphism, clearly represents a very deep crustal level. Moreover, the southern part of the Napier Complex, which is largely made up of depleted tonalite and granodiorite (Fig. 2), was at a deeper crustal level during the high-grade metamorphism (as indicated by higher-pressure mineral assemblages in mafic rocks and metapelites, and P-T estimates) than the northeastern part, which includes a much higher proportion of undepleted granitoids and metasediments (Sheraton & others, 1980). Holland & Lambert (1975), Tarney & Windley (1977), and Weaver & Tarney (1981) have proposed models in which primary hydrous tonalitic magmas (with positive Eu anomalies) were emplaced by an underplating mechanism at the base of the crust. Such liquids, in contrast to relatively dry partial melts of lower crustal rocks, would not be able to rise to high crustal levels before crystallising (Cann, 1970).

Acknowledgements

We thank B.I. Cruikshank, K.H. Ellingsen, G.R. Ewers, J. Fitzsimmons, C. Madden, J.G. Pyke, and T.I. Slezak for chemical analyses; A.Y. Glikson for assistance with REE modelling computer programs; and J. Tarney, S-S Sun, J. Ferguson and A.Y. Glikson for invaluable comments on the manuscript. Logistic support in the field was provided by the Antarctic Division, Department of Science and Technology, Hobart. The figures were drafted by Phil Jorritsma and Norma Price.

References

Albuquerque, C.A.R. de, 1977 - Geochemistry of the tonalitic and granitic rocks of the Nova Scotia southern plutons. *Geochimica et Cosmochimica Acta*, 41, 1-13.

Anderson, J.L., & Cullers, R.L., 1979 - Geochemistry and evolution of the Wolf River Batholith, a late Precambrian rapakivi massif in North Wisconsin, U.S.A. *Precambrian Research*, 7, 287-324.

Arndt, N.T., 1983 - Role of a thin komatiite-rich oceanic crust in the Archean plate-tectonic process. *Geology*, 11, 372-375.

Arth, J.G., 1976 - Behaviour of trace elements during magmatic processes - a summary of theoretical models and their applications. *Journal of Research of the U.S. Geological Survey*, 4, 41-47.

Arth, J.G., 1979 - Some trace elements in trondhjemites - their implications to magma genesis and paleotectonic setting. *In* Barker, F. (editor), Trondhjemites, dacites, and related rocks. *Elsevier, Amsterdam*, 123-132.

Arth, J.G., Barker, F., Peterman, Z.E., & Friedman, I., 1978 - Geochemistry of the gabbro-diorite-tonalite-trondhjemite suite of southwest Finland and its implications for the origin of tonalitic and trondhjemitic magmas. *Journal of Petrology*, 19, 289-316.

Black, L.P., James, P.R., & Harley, S.L., 1983 - Geochronology, structure, and petrology of early Archaean rocks at Fyfe Hills, Enderby Land, Antarctica. *Precambrian Research*, 21, 197-222.

Cann, J.R., 1970 - Upward movement of granitic magma. *Geological Magazine*, 107, 335-340.

Cawthorn, R.G., & Brown, P.A., 1976 - A model for the formation and crystallization of corundum-normative calc-alkaline magmas through amphibole fractionation. *Journal of Geology*, 84, 467-476.

Chappell, B.W., & White, A.J.R., 1974 - Two contrasting granite types. *Pacific Geology*, 8, 173-174.

Collerson, K.D., & Fryer, B.J., 1978 - The role of fluids in the formation and subsequent development of early continental crust. *Contributions to Mineralogy and Petrology*, 67, 151-167.

Collins, W.J., Beams, S.D., White, A.J.R., & Chappell, B.W., 1982 - Nature and origin of A-type granites with particular reference to southeastern Australia. *Contributions to Mineralogy and Petrology*, 80, 189-200.

Compton, P., 1978 - Rare earth evidence for the origin of the Nuk gneisses, Buksefjorden region, southern West Greenland. *Contributions to Mineralogy and Petrology*, 66, 283-293.

Condie, K.C., 1978 - Geochemistry of Proterozoic granitic plutons from New Mexico, U.S.A. *Chemical Geology*, 21, 131-149.

Condie, K.C., & Hunter, D.R., 1976 - Trace element geochemistry of Archaean granitic rocks from the Barberton region, South Africa. *Earth and Planetary Science Letters*, 29, 383-400.

Cooper, D.C., & Field, D., 1977 - The chemistry and origins of Proterozoic low-potash, high-iron, charnockitic gneisses from Tromoy, south Norway. *Earth and Planetary Science Letters*, 35, 105-115.

Demaiffe, D., & Hertogen, J., 1981 - Rare earth element geochemistry and strontium isotopic composition of a massif-type anorthositic-charnockitic body: the Hidra Massif (Rogaland, SW Norway). *Geochimica et Cosmochimica Acta*, 45, 1545-1561.

Drake, M.J., 1975 - The oxidation state of europium as an indicator of oxygen fugacity. *Geochimica et Cosmochimica Acta*, 39, 55-64.

Ellis, D.J., 1980 - Osumilite-sapphirine-quartz granulites from Enderby Land, Antarctica: P-T conditions of metamorphism, implications for garnet-cordierite equilibria and the evolution of the deep crust. *Contributions to Mineralogy and Petrology*, 74, 201-210.

Ellis, D.J., Sheraton, J.W., England, R.N., & Dallwitz, W.B., 1980 - Osumilite-sapphirine-quartz granulites from Enderby Land, Antarctica-mineral assemblages and reactions. *Contributions to Mineralogy and Petrology*, 72, 123-143.

Emslie, R.F., 1978 - Anorthosite massifs, rapakivi granites, and late Proterozoic rifting of North America. *Precambrian Research*, 7, 61-98.

Ewing, T.E., 1979 - Two calc-alkaline volcanic trends in the Archaean: trace element evidence. *Contributions to Mineralogy and Petrology*, 70, 1-7.

Field, D., Drury, S.A., & Cooper, D.C., 1980 - Rare-earth and LIL element fractionation in high-grade charnockitic gneisses, south Norway. *Lithos*, 13, 281-289.

Frey, F.A., Chappell, B.W., & Roy, S.D., 1978 - Fractionation of rare-earth elements in the Tuolumne Intrusive Series, Sierra Nevada batholith, California. *Geology*, 6, 239-242.

Fryer, B.J., 1977 - Rare earth evidence in iron-formations for changing Precambrian oxidation states. *Geochimica et Cosmochimica Acta*, 41, 361-367.

Gill, J., 1981 - Orogenic andesites and plate tectonics. *Springer-Verlag, Berlin.*

Glikson, A.Y., 1972 - Early Precambrian evidence of a primitive ocean crust and island nuclei of sodic granite. *Geological Society of America Bulletin*, 83, 3323-3344.

Glikson, A.Y., 1979 - Early Precambrian tonalite-trondhjemite sialic nuclei. *Earth-Science Reviews*, 15, 1-73.

Green, D.H., & Ringwood, A.E., 1967 - An experimental investigation of the gabbro to eclogite transformation and its petrological applications. *Geochimica et Cosmochimica Acta*, 31, 767-833.

Green, D.H., & Ringwood, A.E., 1972 - A comparison of recent experimental data on the gabbro-garnet granulite-eclogite transition. *Journal of Geology*, 80, 277-288.

Green, T.H., 1981 - Experimental evidence for the role of accessory phases in magma genesis. *Journal of Volcanology and Geothermal Research*, 10, 405-422.

Green, T.H., & Pearson, N.J., 1983 - Ti-rich accessory phase stability in hydrous mafic-felsic compositions at high P,T. *Geological Society of Australia Inc., 6th Australian Geological Convention, Canberra (Abstracts)* 144-145.

Hanson, G.N., 1978 - The application of trace elements to the petrogenesis of igneous rocks of granitic composition. *Earth and Planetary Science Letters*, 38, 26-43.

Hanson, G.N., 1980 - Rare-earth elements in petrogenetic studies of igneous systems. *Annual Reviews of Earth and Planetary Sciences*, 8, 371-406.

Hellman, P.L., & Green, T.H., 1979 - The role of sphene as an accessory phase in the high-pressure partial melting of hydrous mafic compositions. *Earth and Planetary Science Letters*, 42, 191-201.

Helz, R.T., 1976 - Phase relations of basalts in their melting ranges at P_{H_2O} = 5kb. Part II. Melt compositions. *Journal of Petrology*, 17, 139-193.

Holland, J.G., & Lambert, R. St. J., 1975 - The chemistry and origin of the Lewisian gneisses of the Scottish mainland: the Scourie and Inver assemblages and sub-crustal accretion. *Precambrian Research*, 2, 161-188.

Holloway, J.R., & Burnham, C.W., 1972 - Melting relations of basalt with equilibrium water pressure less than total pressure. *Journal of Petrology*, 13, 1-29.

Hubbard, F.H., & Whitley, J.E., 1979 - REE in charnockite and associated rocks, southwest Sweden. *Lithos*, 12, 1-11.

Irving, A.J., & Frey, F.A., 1978 - Distribution of trace elements between garnet megacrysts and host volcanic liquids of kimberlitic to rhyolitic composition. *Geochemica et Cosmochimica Acta*, 42, 771-787.

Loiselle, M.C., & Wones, D.R., 1979 - Characteristics and origin of anorogenic granites. *Geological Society of America, 92nd Annual Meeting, Abstracts with Programs*, 11(7), 468.

Longstaffe, F.J., McNutt, R.H., & Crockett, J.H., 1982 - Rare-earth element modelling of Archaean meta-igneous and igneous rocks, Lake Despair area, northwestern Ontario. *Precambrian Research*, 17, 275-296.

Lopez-Escobar, L., Frey, F.A., & Oyarzun, J., 1979 - Geochemical characteristics of Central Chile (33°-34°S) granitoids. *Contributions to Mineralogy and Petrology*, 70, 439-450.

McCarthy, T.S., & Kable, E.J.D., 1978 - On the behaviour of rare-earth elements during partial melting of granitic rock. *Chemical Geology*, 22, 21-29.

McCulloch, M.T., & Black, L.P., 1984 - Sm-Nd isotopic systematics of Enderby Land granulites and evidence for the redistribution of Sm and Nd during metamorphism. *Earth and Planetary Science Letters*, 71, 46-58.

Moorbath, S., 1977 - Ages, isotopes and evolution of Precambrian continental crust. *Chemical Geology*, 20, 151-187.

Newton, R.C., Smith, J.V., & Windley, B.F., 1980 - Carbonic metamorphism, granulites and crustal growth. *Nature*, 288, 45-50.

Nisbett, E.G., & Fowler, C.M.R., 1983 - Model for Archean plate tectonics. *Geology*, 11, 376-379.

O'Connor, J.T., 1965 - A classification for quartz-rich igneous rocks based on feldspar ratios. *U.S. Geological Survey Professional Paper* 525B, B79-84.

O'Nions, R.K., & Pankhurst, R.F., 1978 - Early Archaean rocks and geochemical evolution of the earth's crust. *Earth and Planetary Science Letters*, 38, 211-236.

Patchett, P.J., Kouvo, O., Hedge, C.E., & Tatsumoto, M., 1981 - Evolution of continental crust and mantle heterogeneity: evidence from Hf isotopes. *Contributions to Mineralogy and Petrology*, 78, 279-297.

Pearce, J.A., & Norry, J., 1979 - Petrogenetic implications of Ti, Zr, Y and Nb variations in volcanic rocks. *Contributions to Mineralogy and Petrology*, 69, 33-47.

Ringwood, A.E., 1982 - Phase transformations and differentiation in subducted lithosphere: implications for mantle dynamics, basalt petrogenesis, and crustal evolution. *Journal of Geology*, 90, 611-643.

Rollinson, H.R., & Windley, B.F., 1980a - An Archaean granulite-grade tonalite-trondhjemite-granite suite from Scourie, NW Scotland: geochemistry and origin. *Contributions to Mineralogy and Petrology*, 72, 265-281.

Rollinson, H.R., & Windley, B.F., 1980b - Selective elemental depletion during metamorphism of Archaean granulites, Scourie, NW Scotland. *Contributions to Mineralogy and Petrology*, 72, 257-263.

Ronov, A.B., 1972 - Evolution of rock composition and geochemical processes in the sedimentary shell of the Earth. *Sedimentology*, 19, 157-172.

Saunders, A.D., Tarney, J., & Weaver, S.D., 1980 - Transverse geochemical variations across the Antarctic Peninsula: implications for the genesis of calc-alkaline magmas. *Earth and Planetary Science Letters*, 46, 344-360.

Sheraton, J.W., & Black, L.P., 1981 - Geochemistry and geochronology of Proterozoic tholeiite dykes of East Antarctica: evidence for mantle metasomatism. *Contributions to Mineralogy and Petrology*, 78, 305-317.

Sheraton, J.W., & Black, L.P., 1983 - Geochemistry of Precambrian gneisses: relevance for the evolution of the East Antarctic Shield. *Lithos*, 16, 273-296.

Sheraton, J.W., & Collerson, K.D., 1983 - Archaean and Proterozoic geological relationships in the Vestfold Hills-Prydz Bay area, Antarctica. *BMR Journal of Australian Geology & Geophysics*, 8, 119-128.

Sheraton, J.W., & Labonne, B., 1978 - Petrology and geochemistry of acid igneous rocks of northeast Queensland. *Bureau of Mineral Resources, Australia, Bulletin*, 169.

Sheraton, J.W., Skinner, A.C., & Tarney, J., 1973 - The geochemistry of the Scourian gneisses of the Assynt district. *In* Park, R.G., & Tarney, J. (editors), The early Precambrian of Scotland and related rocks of Greenland. *University of Keele*, 13-30.

Sheraton, J.W., Offe, L.A., Tingey, R.J., & Ellis, D.J., 1980 - Enderby Land, Antarctica - an unusual Precambrian high-grade metamorphic terrain. *Journal of the Geological Society of Australia*, 27, 1-18.

Sheraton, J.W., Black, L.P., & McCulloch, M.T., 1984 - Regional geochemical and isotopic characteristics of high-grade metamorphics of the Prydz Bay area: the extent of Proterozoic reworking of Archaean continental crust in East Antarctica. *Precambrian Research*, 26, 169-198.

Sighinolfi, G.P., & Gorgoni, C., 1978 - Chemical evolution of high-grade metamorphic rocks - anatexis and remotion of material from granulite terrains. *Chemical Geology*, 22, 157-176.

Smithson, S.B., & Brown, S.K., 1977 - A model for lower continental crust. *Earth and Planetary Science Letters*, 35, 134-144.

Sun, S-S., 1980 - Lead isotopic study of young volcanic rocks from mid-ocean ridges, ocean islands and island arcs. *Philosophical Transactions of the Royal Society of London, Series A*, 297, 409-445.

Sun, S-S., Nesbitt, R.W., & Sharaskin, A.Y., 1979 - Geochemical characteristics of mid-ocean ridge basalts. *Earth and Planetary Science Letters*, 44, 119-138.

Tarney, J., & Saunders, A.D., 1979 - Trace element constraints on the origin of cordilleran batholiths. *In* Atherton, M.P., & Tarney, J. (editors), Origin of granite batholiths: geochemical evidence. *Shiva, Orpington, Kent*, 90-105.

Tarney, J., Skinner, A.C., & Sheraton, J.W., 1972 - A geochemical comparison of major Archaean gneiss units from northwest Scotland and East Greenland. *24th International Geological Congress*, Section 1, 162-174.

Tarney, J., Weaver, B., & Drury, S.A., 1979 - Geochemistry of Archaean trondhjemitic and tonalitic gneisses from Scotland and East Greenland. *In* Barker, F. (editor), Trondhjemites, dacites, and related rocks. *Elsevier, Amsterdam*, 275-299.

Tarney, J., & Windley, B.F., 1977 - Chemistry, thermal gradients and evolution of the lower continental crust. *Journal of the Geological Society of London*, 134, 153-172.

Taylor, P.N., Moorbath, S., Goodwin, R., & Petrykowski, A.C., 1980 - Crustal contamination as an indicator of the extent of early Archaean continental crust: Pb isotopic evidence from the late Archaean gneisses of West Greenland. *Geochimica et Cosmochimica Acta*, 44, 1437-1453.

Taylor, S.R., & Gorton, M.P., 1977 - Geochemical application of spark source mass spectrography-III. Element sensitivity, precision and accuracy. *Geochimica et Cosmochimica Acta*, 41, 1375-1380.

Taylor, S.R., & McLennan, S.M., 1981 - The rare earth element evidence in Precambrian sedimentary rocks: implications for crustal evolution. *In* Kroner, A. (editor), Precambrian plate tectonics. *Elsevier, Amsterdam*, 527-548.

Tindle, A.G., & Pearce, J.A., 1981 - Petrogenetic modelling of in situ fractional crystallisation in the zoned Loch Doon pluton, Scotland. *Contributions to Mineralogy and Petrology*, 78, 196-207.

Tingey, R.J., 1982 - The geological evolution of the Prince Charles Mountains an Antarctic Archaean cratonic block. *In* Craddock, C. (editor), Antarctic geoscience. *University of Wisconsin Press, Madison*, 455-464.

Watson, E.B., & Capobianco, C.J., 1981 - Phosphorus and the rare-earth elements in felsic magmas: an assessment of the role of apatite. *Geochimica et Cosmochimica Acta*, 45, 2349-2358.

Watson, E.B., & Green, T.H., 1981 - Apatite/liquid partition coefficients for the rare-earth elements and strontium. *Earth and Planetary Science Letters*, 56, 405-421.

Weaver, B.L., 1980 - Rare-earth element geochemistry of Madras granulites. *Contributions to Mineralogy and Petrology*, 71, 271-279.

Weaver, B.L., & Tarney, J., 1980 - Rare-earth geochemistry of Lewisian granulite-facies gneisses, northwest Scotland: implications for the petrogenesis of the Archaean lower continental crust. *Earth and Planetary Science Letters*, 51, 279-296.

Weaver, B.L., & Tarney, J., 1981 - Lewisian gneiss geochemistry and Archaean crustal development models. *Earth and Planetary Science Letters*, 55, 171-180.

Weaver, S.D., Saunders, A.D., Pankhurst, R.J., & Tarney, J., 1979 - A geochemical study of magmatism associated with the initial stages of back arc spreading. *Contributions to Mineralogy and Petrology*, 68, 151-169.

Wells, P.R.A., 1979 - Chemical and thermal evolution of Archaean sialic crust, southern West Greenland. *Journal of Petrology*, 20, 187–226.

White, A.J.R., 1979 - Sources of granitic magmas. *Geological Society of America 92nd Annual Meeting, Abstracts with Programs*, 11(7), 539.

Wood, D.A., Tarney, J., Varet, J., Saunders, A.D., Bougault, H., Joron, J-L., Treuill, M., & Cann, J.R., 1979 - Geochemistry of basalts drilled in the North Atlantic by IPOD Leg 49: implications for mantle heterogeneity, *Earth and Planetary Science Letters*, 42, 77–97.

BMR Journal of Australian Geology & Geophysics, 9, 219–223

An isotopic study of granitoids in the Litchfield Block, Northern Territory

R.W. Page[1], M.J. Bower[1], & D.B. Guy[1]

The Litchfield Block contains a variety of granitoids, gneissic rocks, and migmatites that are intrusive into metasediments of probable Early Proterozoic age at the western margin of the Pine Creek Inlier. Isotopic data, which include U-Pb measurements on cogenetic zircon and xenotime and Rb-Sr total-rock measurements on the least metamorphosed granodiorites, show that these rocks crystallised from mantle-derived melts between 1840 Ma and 1850 Ma ago. Radiogenic Pb was lost from zircon in the early Palaeozoic (about 435 Ma), but xenotime remained a closed system until recent time. Many granitoids in the Litchfield Block have a gneissic fabric imposed during greenschist to amphibolite-grade regional metamorphism. This disturbance allowed partial isotopic re-equilibration of Rb-Sr total-rock systems, at about 1770 ± 16 Ma. As this igneous and metamorphic evolution is mirrored in other parts of the Pine Creek Inlier, the Halls Creek Inlier, and many other orogenic belts in northern Australia, its recognition and isotopic definition in the Litchfield Block further emphasise the magnitude and chronological integrity of this early Proterozoic tectonic event.

Introduction

U-Pb and Rb-Sr isotopic studies have been made on various granitoid rocks from the Litchfield Block southwest of Darwin, Northern Territory (Fig. 1). The block is composed of granitoids and metamorphic rocks forming a meridionally trending elongate belt about 50 km across and 150 km long on the western margin of the Pine Creek Geosyncline (Walpole & others, 1968). This study focuses only on the granitoid rocks, which, although perhaps continuous at depth, are divided at the surface into a number of separate masses by Proterozoic metamorphic rocks and younger Proterozoic and Phanerozoic cover.

Some parts of the block were studied in moderate detail and others on a reconnaissance basis, in order to find the age of emplacement of the granitoids and, possibly, the age of the subsequent metamorphism. As well as identifying any major age differences amongst the granitoids, this approach was designed particularly to address the long-standing question as to whether the Litchfield Block contains Archaean components akin to those that form the basement of the Pine Creek Inlier (such as 40 km to the east at Rum Jungle) or whether it is an extension of the Proterozoic Halls Creek Inlier. The presence or otherwise of Archaean granitoids is important to exploration strategy in the Pine Creek Inlier, as units such as the 2470 Ma Nanambu Complex in the Alligator Rivers region (Page & others, 1980) have been shown by McAndrew & Finlay (1980) to be fertile source rocks for uranium mineralisation in younger metasedimentary units.

[1]Division of Petrology & Geochemistry, BMR

Geological background and previous geochronology

Rock relationships in the Litchfield Block were first reported by Walpole & others (1968), and more recently have been studied in detail by the Northern Territory Geological Survey (NTGS). The granitoids of the Litchfield Block intrude migmatites, gneisses, and schists, some of which are differentiated as the Hermit Creek Metamorphics. Walpole & others (1968) considered the metamorphics to be Archaean, but they are equally likely to be Early Proterozoic equivalents of the Halls Creek Complex in the East Kimberley Region (Page, 1976) or the Finniss River Group further east in the Pine Creek Inlier (Needham & Stuart-Smith, 1984).

The granitoids studied in this paper range from leucocratic muscovite granites to biotite granodiorites and tonalites. Some are massive and unmetamorphosed, but many have a gneissic fabric and are migmatitic in places. Locally, there has been significant country rock assimilation, as evidenced by partially digested xenoliths. The gneissic granitoids are moderately to extensively recrystallised and some contain medium-grade metamorphic assemblages, including garnet, sillimanite, and cordierite. In places, these assemblages are restricted to xenolithic bodies, but elsewhere they are products of in-situ metamorphism of presumably sediment-influenced (S-type) granitic rocks. Their textural features and mineralogy suggest that at least some of the Litchfield granitic rocks have been affected by post-emplacement regional metamorphism. In the southern part of the block, near locality 5031, there are no obvious post-emplacement metamorphic effects, however; so either this is a younger granitic body or the metamorphism/deformation was not uniform across the block. It is

Table 1. U-Pb analytical data for zircons and xenotimes from granitoids in the Litchfield Block sample 7912.5031A.

Size (μm) and magnetic susceptibility	Weight (mg)	Concentration (ppm)			$^{206}Pb/^{204}Pb$ (measured)	Radiogenic ratios		
		Radiogenic Pb	Common Pb	U		$^{207}Pb/^{206}Pb$	$^{206}Pb/^{238}U$	$^{207}Pb/^{235}U$
Zircons								
-350 NM3	1.14	92.5	18.2	463.2	298.5	0.10002	0.19500	2.6892
-215 NM2	1.54	183.8	21.5	924.1	508.4	0.10209	0.19695	2.7724
-150 NM1	1.62	193.9	10.7	762.3	1068	0.10802	0.25650	3.8204
- 75 NMO	1.05	201.2	10.2	756.8	1138	0.10865	0.26622	3.9883
- 75 MO	1.26	229.4	12.8	896.2	1055	0.10809	0.25770	3.8407
- 45 NM2	0.58	191.4	10.7	762.5	1019	0.10786	0.25147	3.7399
Xenotimes								
-350	1.38	4669	27.0	2577	1293	0.11305	0.26970	4.2040
-215	2.48	4287	28.9	2209	1200	0.11306	0.26584	4.1443
-215	1.68	4396	35.5	2413	1002	0.11312	0.25002	3.8997
-215	2.19	4569	37.1	2463	980	0.11214	0.25106	3.8820

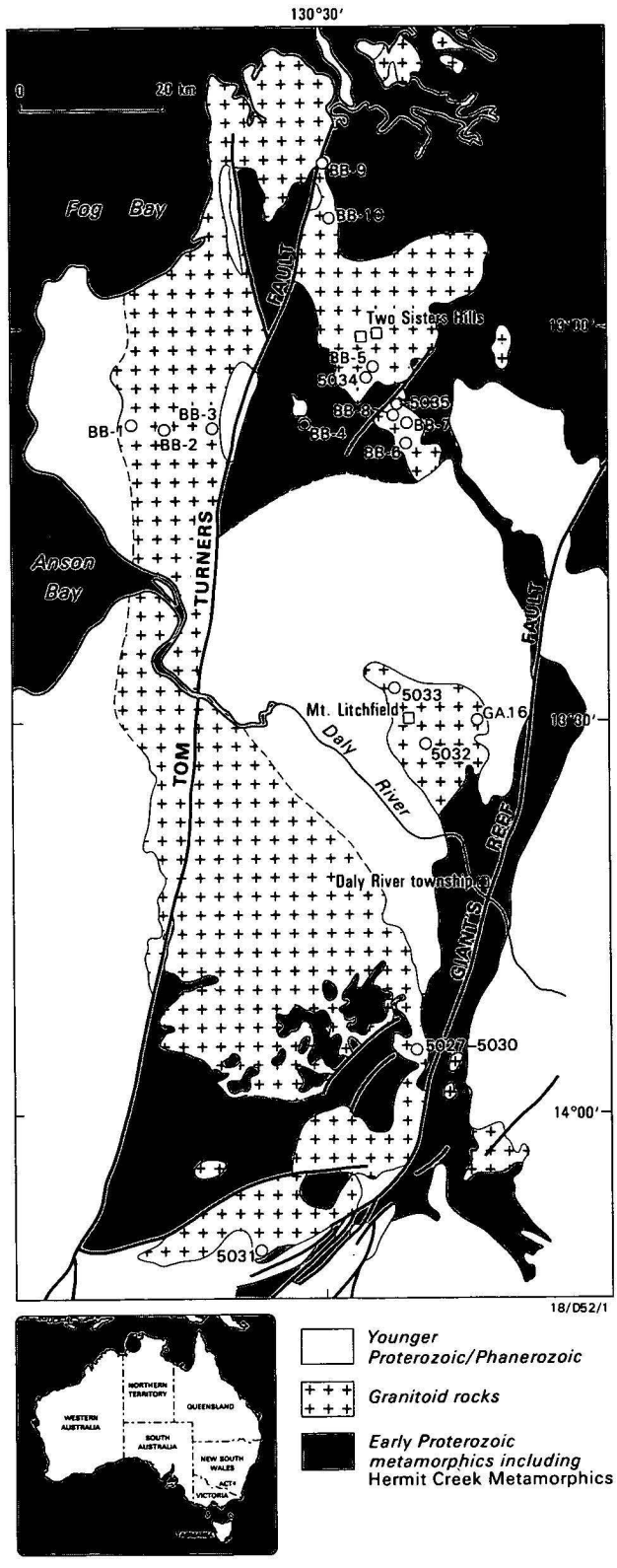

Figure 1. Distribution of Early Proterozoic metamorphic rocks, granitoid rocks, and younger cover rocks in the Litchfield Block, after Needham & Stuart-Smith (1984).

Also shown are locations of samples in Tables 1 and 2, and sample GA.16 from Walpole & others (1968).

noted that NTGS workers (D.L. Dundas, written communication, 1984) do not consider the Litchfield granitoids to have been metamorphically overprinted, but believe that the above features result from country-rock contamination. Relatively unmetamorphosed late Early Proterozoic sandstone and volcanic rocks (Chilling Sandstone and Berinka Volcanics, or Moyle River Formation of the Fitzmaurice Group, according to correlations by NTGS workers - written communication, 1984) unconformably overlie the granitic and metamorphic rocks of the block.

The only previous geochronological results from the Litchfield Block consist of one muscovite and three biotite K-Ar ages between 1560 and 1630 Ma (Hurley & others, 1961). These are minimum ages, reflecting cooling below the threshold for argon retention. A Rb-Sr total-rock measurement from one of the same samples east of Mount Litchfield (Fig. 1; Leggo, reported in Walpole & others, 1968) gave a model age of about 1740 Ma.

Analytical methods

Samples of 2–20 kg were collected from each of the granitoid sampling sites shown in Figure 1. At some sites, a number of clustered samples were collected for Rb-Sr total-rock purposes, although in most areas the reconnaissance is based only on a single representative sample. The Rb-Sr analyses were performed by isotope dilution as described in Page & others (1976), and the U-Pb procedures for zircon and xenotime were adapted from Krogh (1973). Xenotime fractions (Table 1) were dissolved in 3N HCl in teflon 'bombs'. A ^{208}Pb tracer was used for Pb concentrations in zircons, and ^{206}Pb for xenotimes. The total Pb processing blank is about 0.25 ng.

U-Pb concordia intersection ages are given at the 2σ level, using 2σ error assignments of 0.7 per cent for U/Pb ratios, 0.2 per cent for $^{207}Pb/^{206}Pb$ ratios, and a correlation coefficient of 0.96. Errors appropriate to the Rb-Sr isochrons (McIntyre & others, 1966) are quoted at the 95 per cent confidence level. All ages have been calculated using decay constants recommended by Steiger & Jäger (1977).

U-Pb data

Zircon and xenotime were separated from one of the least deformed biotite-muscovite granodiorites near the southern end of the Litchfield Block (Fig. 1, locality 5031). The granodiorite intrudes cordierite-andalusite hornfelses, probably of the Hermit Creek Metamorphics. Other than incipient alteration of plagioclase, it shows no sign of recrystallisation. Zircons are pale brown to clear, euhedral, and have regular euhedral zonation throughout, indicative of their igneous derivation. Uranium contents of the six analysed zircon fractions range from 460 to 920 ppm (Table 1), but the pattern of Pb/U discordance (Fig. 2) appears unrelated to this or the size range of the fractions. Five of the six data points define a Model 1 discordia trajectory with concordia intercepts at 1840 ± 5 Ma and 435 ± 20 Ma. The coarsest fraction (-350μm) appears to be younger than the remainder. However, it had many inclusions and gave a relatively imprecise Pb isotopic analysis. It also has the highest common Pb correction of the suite, and its exclusion is further warranted by an increase in the mean square of weighted deviates (MSWD) by a factor of 18, should it be included in the regression. The zircon results indicate an Early Proterozoic crystallisation age of 1840 ± 5 Ma, and differential Pb loss in the Early Palaeozoic about 435 Ma ago.

Xenotime in the same rock occurs as unzoned, squat, honey-coloured euhedra. Compared to zircon, it has much higher uranium, ranging from 2210 to 2580 ppm, and is characterised by high $^{208}Pb/^{206}Pb$ of around 7.3. Zircon $^{208}Pb/^{206}Pb$ ratios are around 0.06. Three xenotime fractions have virtually identical

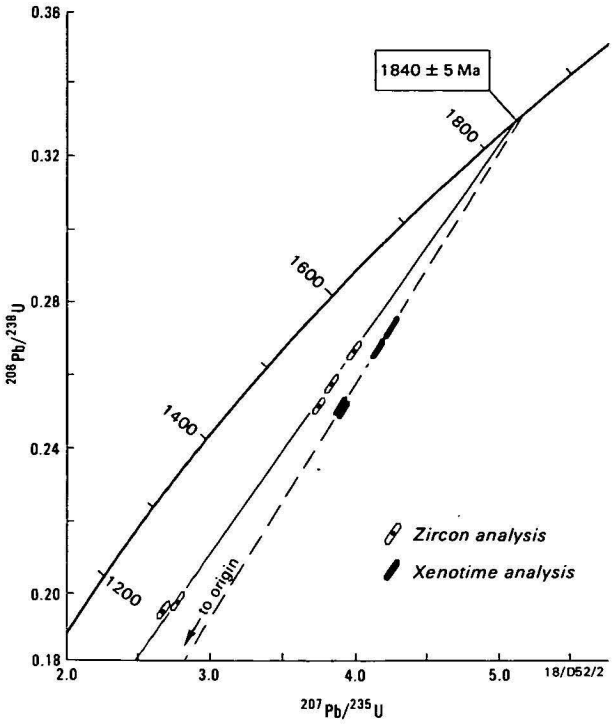

Figure 2. U-Pb concordia diagram of zircon and xenotime analytical data from sample 7912.5031.
Error envelopes define 2 σ analytical limits.

$^{207}Pb/^{206}Pb$ compositions (Table 1, Fig. 2), suggesting recent Pb loss from grains that could have initially crystallised at 1850 ± 2 Ma. This is a minimum age which might represent the time of xenotime formation. The fourth xenotime analysis has a marginally younger $^{207}Pb/^{206}Pb$ age, 1835 Ma.

There appears to be a small but discernible difference between the times of crystallisation of xenotime (at least 1850 ± 2 Ma) and zircon (1840 ± 5 Ma). The difference would be even greater if a shallower Pb-loss trajectory defined by the two most concordant xenotimes and the youngest analysis was considered. This would result in an older and less precise apparent crystallisation age of 1895 ± 20 Ma, and an inferred time of Pb loss, closer to that of the zircon system, at 304 ± 92 Ma. However, we prefer the interpretation giving the xenotime crystallisation age of 1850 ± 2 Ma, because of closer accord with the zircon U-Pb data and, as will be seen, with total-rock Rb-Sr data. Either interpretation suggests a small component of inheritance in the xenotime U-Pb system compared to the zircon U-Pb system, reflecting either the age of source components or stages of magmatic fractional crystallisation in the granodiorite.

In terms of the igneous history of this part of the Litchfield Block, the zircon and xenotime results are broadly consistent, and indicate the age of this igneous event at 1840–1850 Ma. Both xenotime and zircon suffered a single stage of later Pb loss, but at different times. Divergent Pb-loss patterns of this type have also been reported from the 1410 Ma Lawler Peak granite in central Arizona (Williams & Silver, 1979). Xenotime in the Litchfield granitoid was largely affected by Pb loss in recent times, whereas zircon, despite having much lower uranium, was susceptible to a comparable degree of Pb loss in the early Palaeozoic. Neither of these Pb-loss events is reflected in other isotopic systems; for example, regional K-Ar mica ages are much older, ranging from 1560 to 1630 Ma (Hurley & others, 1961).

Rb-Sr data

The Rb-Sr total-rock data are based on a regional coverage of several granitoid types from various parts of the Litchfield Block (Fig. 1). Granitic rocks from two of these regions (viz. the

Table 2. Rb-Sr analytical data for total-rock and biotite samples from granitoids of the Litchfield Block, Northern Territory

7912. - No.	1:100 000 grid ref.	Sample	Rb ppm	Sr ppm	$^{87}Rb/^{86}Sr$	$^{87}Sr/^{86}Sr$
5027A	Daly River 755530	Biotite-cordierite gneiss	192.5	81.4	6.936	0.86998
5027B	Daly River 755530	Biotite gneiss	196.8	120.1	4.789	0.83230
5028	Daly River 755530	Sillimanite-cordierite gneiss	201.9	122.7	4.810	0.83494
5029A	Daly River 755530	Biotite-garnet gneiss	177.1	118.0	4.376	0.80484
5029B	Daly River 755530	Biotite gneiss	183.7	126.8	4.225	0.81455
5030	Daly River 755530	Biotite-garnet gneiss	144.5	115.9	3.630	0.79415
5031A	Moyle 520300	Biotite granodiorite	235.1	99.5	6.941	0.88721
5031A	Moyle 520300	-biotite separate	908.9	7.80	2451.5	64.986
5031A	Moyle 520300	-biotite separate	911.3	7.85	2405.8	63.840
5031B	Moyle 520300	Biotite-muscovite granodiorite	249.7	78.6	9.395	0.95538
5031C	Moyle 520300	Biotite-muscovite granodiorite	247.9	77.1	9.510	0.95777
5032A	Daly River 765043	Granodiorite gneiss	129.6	211.5	1.777	0.74988
5032B	Daly River 765043	Granodiorite gneiss	118.1	234.4	1.459	0.74162
5033A	Reynolds River 735119	Granodiorite gneiss	269.0	148.2	5.310	0.84136
5033B	Reynolds River 735119	Granodiorite gneiss	202.7	238.7	2.466	0.76784
BB-1	Anson 352490	Recrystallised felsic porphyry	252.5	326.8	2.244	0.76535
BB-2	Anson 410498	Biotite granodiorite	223.4	178.5	3.647	0.80092
BB-3	Anson 478490	Porphyritic biotite granodiorite	229.8	190.8	3.508	0.79767
BB-4	Anson 593496	Foliated microgranite	80.9	246.0	0.9515	0.72813
BB-5	Reynolds River 729544	Biotite-muscovite-garnet gneiss	210.6	58.8	10.620	0.98417
BB-6	Reynolds River 747450	Muscovite-biotite-garnet gneiss	349.1	8.22	176.46	5.1908
BB-7	Reynolds River 748471	Biotite-garnet gneiss	385.0	24.1	51.988	2.02214
BB-8	Reynolds River 732485	Recrystallised biotite granodiorite	230.9	59.1	11.610	1.00490
BB-9	Bynoe 633826	Biotite-muscovite gneiss	198.2	149.0	3.878	0.80470
BB-10	Bynoe 643750	Muscovite-biotite gneiss	227.3	118.2	5.633	0.84985
			(289.6	62.7	13.788	1.05480
5034	Reynolds River 688541	Muscovite-biotite gneiss	(287.4	62.4	13.752	1.05374
5035	Reynolds River 728504	Biotite-garnet gneiss	216.4	54.8	11.739	1.01300

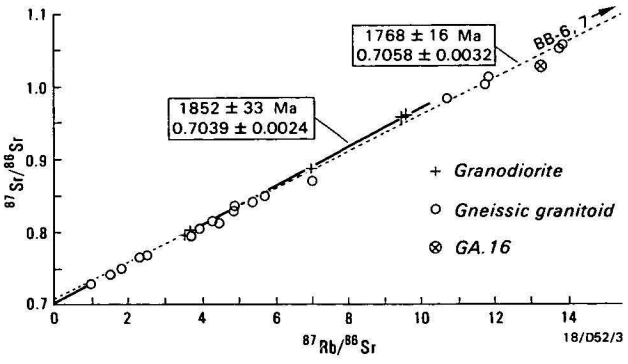

Figure 3. Rb-Sr isochron diagram, showing analytical data for five granodiorites (crosses) and twenty gneissic granitoids (circles), from the Litchfield Block.

Leggo's data point GA.16, discussed in Walpole & others (1968), is also shown (circled cross).

zircon-xenotime locality 5031 at the southern end of the block and localities BB-2, BB-3 in the northwestern mass) are petrographically dissimilar from all remaining sites. They are both massive biotite granodiorite with primary igneous textures, compared with the other sites, which are foliated to different degrees and show moderate to extensive metamorphic recrystallisation.

The five non-foliated granodiorites are from very distant localities (5031, BB-2 and BB-3) and may well have had different plutonic histories. However, assuming coevality, they appear to define a Model 1 Rb-Sr isochron (Table 2, Fig. 3) indicating a primary age of 1852 ± 33 Ma and initial $^{87}Sr/^{86}Sr$ of 0.7039 ± 0.0024. Duplicate biotite analyses from sample 5031 give younger (minimum) ages of 1823 Ma and 1824 Ma. The Rb-Sr total-rock age is in accord with the zircon and xenotime U-Pb ages from sample 5031, further verifying this as the time of igneous crystallisation of the Litchfield Block protoliths.

The indicated initial $^{87}Sr/^{86}Sr$ of 0.7039 (or maximum of 0.705) does not support significant crustal contamination in the granitoid genesis or any recycling of older crust (Hermit Creek Metamorphics), as had been suggested by Walpole & others (1968). These Rb-Sr results, together with the lack of major inheritance features in the U-Pb data, rule out the possibility that the Litchfield granitoids could be Archaean in age. Extrapolation of the initial $^{87}Sr/^{86}Sr$ value, using a depleted mantle growth line, would allow a maximum of only 60–80 Ma of crustal pre-history. It is therefore probable that these granitoids were generated during the major Early Proterozoic (1900–2100 Ma) crustal-formation event now so widely recognised in northern Australia (Wyborn & Page, 1983; Page & others, 1984).

Gneissic granitoids of granitic to tonalitic composition constitute most of the Litchfield Block. They have a foliated granoblastic fabric composed of quartz, feldspars, biotite, ±muscovite, ±garnet, ±cordierite, ±sillimanite. Twenty such gneissic granitoids, representing a variety of lithological types, from 16 sites (Fig. 1) show a predictable degree of scatter in their Rb-Sr isotopic systematics (Table 2, Fig. 3). The Model 3 isochron fit indicates an age of 1768 ± 16 Ma, initial $^{87}Sr/^{86}Sr$ being 0.7058 ± 0.0032.

The degree of scatter about this isochron, particularly for the six samples from the southeastern sites 5027–5030, indicates that the isotopic resetting has not been uniform. Deletion of the six most aberrant data points lowers the MSWD from 63.5 to 17.7, but the age (1770 ± 15 Ma) and initial $^{87}Sr/^{86}Sr$ (0.7069 ± 0.0026) are virtually unchanged. It is concluded that the Rb-Sr total-rock systems in the gneisses reflect the approximate time of the greenschist to amphibolite-grade regional metamorphism. This metamorphic event was not uniform in effect, as it is neither petrographically evident nor has it caused any isotopic resetting in the southernmost part of the block, near 5031. As the country rocks near 5031 are in fact deformed, it is possible either that an earlier deformation (pre-1850 Ma) is present or, more likely, that the granite was in a deformational strain shadow during the 1770 Ma event.

The gneisses that reflect that 1770 Ma metamorphic imprint were probably derived from granitic rocks of comparable age to the 1850 Ma massive granodiorites. However, the gneisses cannot have been directly derived from the latter, as there are significant compositional differences (L.A.I. Wyborn, personal communication). The isotopic evidence suggests quite strongly that neither the gneisses nor the massive granodiorites of the Litchfield Block have any significant Archaean component.

Conclusions

U-Pb data on zircon and xenotime are consistent with Rb-Sr total-rock data, and together indicate that granitoid rocks of the Litchfield Block were emplaced in the Early Proterozoic, at about 1850 Ma. Much of this material was newly accreted to the crust at this time, as indicated by the relatively primitive initial $^{87}Sr/^{86}Sr$ of 0.7039 and by the lack of any inheritance features in the U-Pb systems. Some of the Litchfield gneissic granitoids contain alumina-rich (S-type) mineral assemblages, which suggest a crustal pre-history. But, if this was so, it was relatively short-lived (60–80 Ma, or less). Most of these granitoids were affected by greenschist to amphibolite-grade regional metamorphism and deformation, which caused recrystallisation and imposition of their gneissic fabric some 50–80 Ma after igneous crystallisation.

The history of granitoid emplacement and metamorphism in the Litchfield Block is somewhat analogous to the geological development of the Nimbuwah Complex in the northeastern part of the Pine Creek Inlier (Page & others, 1980). In the latter, granitoid components were emplaced as new crustal material between 1870 and 1880 Ma, and were also affected by regional metamorphism at about 1800 Ma. This Early Proterozoic tectonism is further mirrored in the Halls Creek Inlier, although the geochronological resolution of the events is not as clear as in the Litchfield Block and Nimbuwah Complex. None of these granitoids is Archaean in age, or derived from or contaminated by Archaean crust. Between 1900 and 2100 Ma, their evolution from the mantle, as illustrated by the Nd and Sr isotopic data, formed part of a mantle/lower crustal event of continental proportions also evident in several other orogenic belts (McCulloch & Hensel, 1984; Page & others, 1984). However, the first stratigraphic geological expression of this Early Proterozoic crustal formation is that recorded in igneous crystallisation ages, typically 1850–1870 Ma, as seen in the Litchfield Block and many other felsic igneous provinces in northern Australia. The host metasediments such as the Hermit Creek Metamorphics, which are intruded by these granitoids could be significantly older than Early Proterozoic, but, from the existing isotopic data for the Halls Creek Complex and tuffaceous metasediments in the Pine Creek Inlier (see summary in Page & others, 1984), this is considered most unlikely.

Acknowledgements

We are grateful to Mr. D.A. Berkman and A.O.G. Minerals Limited, and also to Mobil Energy Minerals Australia Inc., who

provided logistic support for some of the field work. This study has benefitted from discussions with P.G. Stuart-Smith, R.S. Needham, P.G. Goldner, and L.P. Black. A review by, and communications with D.L. Dundas are gratefully acknowledged.

References

Hurley, P.M., Fisher, N.H., Pinson, W.H.Jr., & Fairbairn, H.W., 1961 - Geochronology of Proterozoic granites in Northern Territory, Australia; part 1. K-Ar and Rb-Sr age determinations. *Bulletin of the Geological Society of America*, 72, 653-662.

Krogh, T.E., 1973 - A low-contamination method for hydrothermal decomposition of zircon and extraction of U and Pb for isotopic age determination. *Geochimica et Cosmochimica Acta*, 37, 485-494.

McAndrew, J., & Finlay, C.J., 1980 - The nature and significance of the occurrence of uranium in the Nanambu Complex of the Pine Creek Geosyncline. *In* Ferguson, J., & Goleby, A.B., (editors), Uranium in the Pine Creek Geosyncline. *International Atomic Energy Agency, Vienna.* 357-362.

McCulloch, M.T., & Hensel, H.D., 1984 - Sm-Nd isotopic evidence for a major early to mid-Proterozoic episode of crustal growth in the Australian continent. *Abstract, 27th International Geological Congress, Moscow.*

McIntyre, G.A., Brooks, C., Compston, W., & Turek, A., 1966 - The statistical assessment of Rb-Sr isochrons. *Journal of Geophysical Research*, 71, 5459-5468.

Needham, R.S., & Stewart-Smith, P.G., 1984 - Geology of the Pine Creek Geosyncline. 1:500 000-scale map. *Bureau of Mineral Resources, Australia.*

Page, R.W., 1976 - Reinterpretation of isotopic ages from the Halls Creek Mobile Zone, northwestern Australia. *BMR Journal of Australian Geology & Geophysics*, 1, 79-81.

Page, R.W., Blake, D.H., & Mahon, M.W., 1976 - Geochronology and related aspects of acid volcanics, associated granites, and other Proterozoic rocks in The Granites-Tanami region, northwestern Australia. *BMR Journal of Australian Geology & Geophysics*, 1, 1-13.

Page, R.W., Compston, W., & Needham, R.S., 1980 - Geochronology and evolution of the late-Archaean basement and Proterozoic rocks in the Alligator Rivers Uranium Field, Northern Territory, Australia. *In* Ferguson, J., & Goleby, A.B. (editors), Uranium in the Pine Creek Geosyncline. *International Atomic Energy Agency, Vienna.* 39-68.

Page, R.W., McCulloch, M.T., & Black, L.P., 1984 - Isotopic record of major Precambrian events in Australia. *Proceedings, 27th International Geological Congress, Moscow*, Section C.05.

Steiger, R.H., Jager, E., 1977 - Subcommission on geochronology: convention on the use of decay constants in geo- and cosmochronology. *Earth and Planetary Science Letters*, 36, 359-362.

Walpole, B.P., Crohn, P.W., Dunn, P.R., & Randal, M.A., 1968 - Geology of the Katherine-Darwin region, Northern Territory. *Bureau of Mineral Resources, Australia, Bulletin*, 82.

Williams, I.S., & Silver, L.T., 1979 - The U-Th-Pb system compared in coexisting zircon, monazite and xenotime. *Abstract, Transactions, American Geophysical Union*, 60, 411.

Wyborn, L.A.I., & Page, R.W., 1983 - The Proterozoic Kalkadoon and Ewen Batholiths, Mount Isa Inlier, Queensland : source chemistry, age, and metamorphism. *BMR Journal of Australian Geology & Geophysics*, 8, 53-69.

BMR Journal of Australian Geology & Geophysics, 9, 225-231

Australian gravity base-station network: 1980 survey

Peter Wellman[1], Ken McConnell[2] & J.W. Williams[1]

In 1980, a gravity base-station network of 67 airports throughout Australia was surveyed with seven LaCoste & Romberg gravity meters, and tied to sites of six 1979 absolute gravity measurements. Two computer adjustments of the gravity meter observations were made, firstly with two and secondly with six absolute measurements to control scale and datum. Comparison of the adjustments shows that the absolute measurements are consistent with one another to within experimental error. The gravity values calculated in the computer adjustment using the weighted results of the six absolute sites have been adopted as the best values for the Australian National Base-station Network (Isogal 84 values). The values have a precision of 0.1 μm.s^{-2}, and an accuracy of about 0.3 μm.s^{-2}. A polynomial is derived for revising earlier gravity values to be consistent with the new base-station values.

Introduction

The Australian gravity base-station network provides the reference stations defining scale and datum for reduction of gravity meter readings made during all gravity surveys on the Australian landmass and surrounding ocean. The scale defined by the network is used to change differences in gravity meter readings to differences in acceleration; the datum is used to convert differences in acceleration to actual acceleration at each observation point.

In any measurement system, it is desirable to have standards that are of higher accuracy than required for routine measurement. An increase in accuracy of gravity standards is required because of the following advances in gravity and geoidal measurements in the last 20 years:

1) routine use of LaCoste and Romberg gravity meters in government and private company field surveys, requiring a more accurate base-station network for adequate datum control for survey integration;

2) use of groups of gravity meters in crustal movement surveys for earthquake prediction, requiring accurate scale control;

3) control of datum and scale of land gravity so that small-amplitude long-wavelength errors do not affect geoids calculated from land gravity observations; and

4) in metrology the accuracy of gravity values is a limiting factor in the standards of some quantities, such as the volt.

The base-station network used until the present was based on gravity meter observations made in 1964-67. These observations and the derived gravity values had known errors of 2 μm.s^{-2}, which was too high for a national base-station network controlling measurements of precision 0.2 μm.s^{-2}. In 1979, Soviet apparatus was used to measure absolute gravity at six sites within or near Australia (Arnautov & others, 1979) to an accuracy of 0.15 μm.s^{-2}, and in 1980, precise observations were made at 67 airports throughout Australia using seven LaCoste & Romberg gravity meters.

This report gives an adjustment of the 1979 absolute values and the 1980 regional network to give improved values of gravity at the 67 airports. These are used to obtain better values for the previous, more dense, network of 200 stations. The base-station corrections can be generalised by a polynomial and applied as a small correction to all gravity values within Australia.

Absolute measurements 1979

Absolute measurements of gravitational acceleration were carried out during April and May 1979 at five sites in Australia and one site at Port Moresby, Papua New Guinea (Fig. 1)(Arnautov & others, 1979). The measurements have a reported precision of about 0.06 μm.s^{-2}, and an accuracy of about 0.15 μm.s^{-2}. The reported absolute values have to be corrected by removing the Honkasalo correction (Uotila, 1980).

Absolute measurement of acceleration due to gravity is determined by direct observation of a body during free rise and fall in a vacuum. In practice, the effective site of the measurement is about 1.2 m above the floor, and the vertical gravity gradient at the absolute site is measured so that gravity meter observations can be made on the floor beneath the measurement site.

Table 1. The vertical gradient at absolute gravity sites (μm.s^{-2}m^{-1})

	1979		1980							Mean
	G252	G460	G20	G101	G132	G252	G460	G518	G525	
Sydney	3.23†	3.19	3.29	3.21	3.29	2.74*	3.25	3.15	2.98	3.20
Port Moresby		3.13								3.13
Hobart		2.74		2.76	2.75	2.74	2.75	2.73	2.42*	2.74
Alice Springs	2.98	3.06		3.79	2.83	2.98	2.92	2.79	2.73	2.90
Darwin	2.98	3.10		3.14	3.03	3.41*	2.96	3.09	3.17	3.07
Perth	3.45	3.41	3.41		3.80*		3.42	3.70		3.48

† meter G525 not G252
* values rejected in calculating mean

Table 1 gives the gradient measurements taken during the 1979 absolute survey (Arnautov & others, 1979) and those at the time of the 1980 gravity meter survey. The results are similar, so the 1979 results have been used in the calculations below. The measured gravity intervals at any site differ between meters by up to 0.3 μm.s^{-2} (presumably because of the circular error in the reading screw), and hence the gradient measurement has the potential for introducing significant errors into the primary gravity network. The measured gradient values differ from the theoretical gradient of 3.086 μm.s^{-2} by up to 0.4 μm.s^{-2}, and the theoretical values are clearly not accurate enough for this purpose.

1980 Australian gravity base-station survey

From 30 January to 1 April 1980, gravity meter ties were made between 67 airports and the five absolute gravity stations in Australia (Fig. 1). Flight lines were mainly north-south to try to control errors in the previous control survey of 1964-67, which had mainly east-west flights. Ties were also made to accurate geodetic position stations - the lunar laser ranging station at Orroral near Canberra, the satellite laser ranging stations at Yarragadee near Geraldton, and Orroral near Canberra, and radio telescopes used for VLBI near Alice Springs, Parkes, Narrabri, Sydney, Canberra, and Hobart.

[1]Division of Geophysics, BMR
[2]Earth Physics Branch, Energy Mines and Resources Canada, 1 Observatory Crescent, Ottawa, Ontario K1A0Y3 Canada

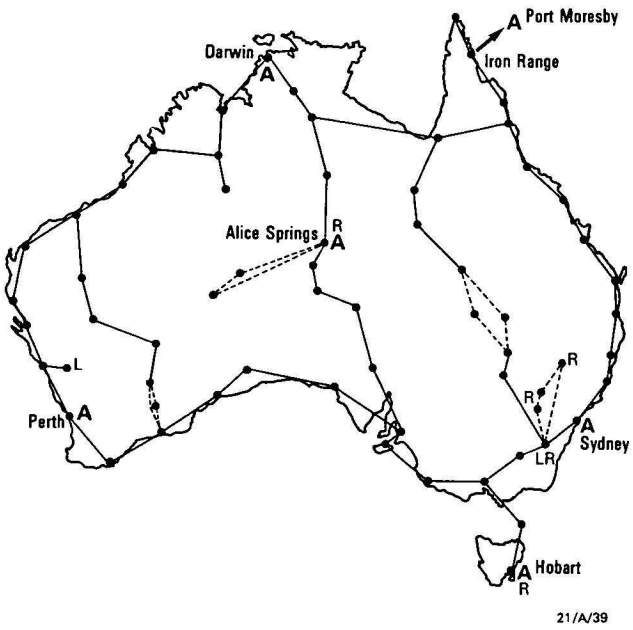

Figure 1. Traverses of the Australian gravity base-station survey of 1980.

A, absolute gravity sites; L, laser ranging sites to satellites or the Moon; R, sites of radio telescopes used for Very Long Baseline Interferometry.

Seven LaCoste & Romberg gravity meters were used: the Bureau of Mineral Resources (BMR) meters G20, G101, G132, G252, G460, G518, and a Geological Research and Development Centre (GRDC) of Indonesia meter, G525. Gravity meter readers were P. Wellman and J.W. Williams of BMR and M. Untung of GRDC. Transport between airports was by a chartered light aircraft (Piper Navajo), and took 165.2 flying hours. Transport within each town was by car.

Observations at airports A,B,C,D,.. can be made two ways: 'ladder sequence' A-B-C-D...D-C-B-A, and 'drift-control sequence' A-B-A-B-C-B-C-D-C-D... Ladder sequence was chosen for this survey for the following reasons: (a) air transport costs are lower, because each leg is flown twice, not three times; (b) observations are more symmetrical and independent, because a single set of observations is made in each direction, and, generally, observations are made during different days; and (c) a stronger network results, because a greater number of different airports is observed during one day.

At each airport, two stations were observed, if possible, outside separate buildings. The two stations were always observed in the same order. The use of two stations increases the probability that one will be recoverable in the future, and it is a check at each airport on gravity meter misreading or malfunction. After the second station at each airport was read, the gravity difference between stations was calculated for each meter. One or two readings were repeated if a discrepancy was found greater than 0.3 μm.s^{-2} from the mean value of all meters. Flights between airports averaged 1.23 hours, and time at each airport averaged 0.8 hours.

The original survey plan was modified during the survey because of the following problems: runway too wet for use - Calvert Hills; difficulty in obtaining permision to land - Meningie, Wanaaring; runway abandoned - Old Balgo Hills Mission, Mundiwindi, Katherine; destruction or partial destruction of previous gravity stations at the airport - Wiluna, Norseman, Abminga, Thargominda; and difficulty in obtaining aviation fuel during an industrial strike - Dubbo.

After the survey, the gravity meters used were tested for their sensitivity to temperature, pressure, battery voltage, and magnetic field (Williams, 1983). The effects were small, so no corrections were made to the gravity meter readings.

Reduction of gravity meter observations

The gravity meter observations were reduced at Earth Physics Branch Ottawa, using existing computer programs for tie processing and adjustment. The tie processing program applies the manufacturer's dial-response correction tables and Earth-tide corrections to calculate raw gravity intervals.

The adjustment computer program uses the following observational equation to adjust the raw gravity intervals (McConnell & Ganter,1971):

$$\sqrt{p_n}\,(g_i - g_j - k_m \Delta G_{ij} - d_m \Delta T_{ij} = e_{ij}),$$

where p_n is the observation weight, g_i is the unknown gravity value of control station i, g_j is the unknown gravity value of control station j, k_m is the unknown calibration correction factor for instrument m, ΔG_{ij} is the observed gravity difference between gravity stations i and j (raw gravity intervals), d_m is the unknown drift rate, ΔT_{ij} is the time interval between the observations at control stations i and j, and e_{ij} is the unknown observation error.

The observed intervals for each gravity meter were weighted according to an overall factor for that meter, determined from residuals of a previous adjustment. Residuals with a magnitude above three standard deviations in the final adjustment were rejected (73 intervals, 3% of all intervals) together with all intervals of more than 7 hours duration, to eliminate overnight measurements; 2358 intervals were used to solve 152 unknowns.

Two computer adjustments were made with the final data set, differing only in the number of absolute gravity stations used to control datum and scale. Adjustment one used only Hobart and Darwin absolute stations, and adjustment two used all six absolute stations, Port Moresby being included by the use of a previous tie to Iron Range airport (Table 2). The adjusted values differ by 0.11–0.20 μm.s^{-2}. These differences are caused almost solely by both Hobart and Darwin being 0.11 μm.s^{-2} higher than the datum defined by the average of the absolute stations. The calculations show that the use of all six absolute measurements, rather than just two, does not distort the gravity meter adjustment and, hence, the two sets of information are consistent within experimental error.

Table 2. Absolute sites: values from measurement and adjustments (μm.s^{-2})

	Measured value	Measured minus Adj.2	Measured minus Adj.1	Adj.1 minus Adj.2
Darwin C	9 783 009.59 ± 0.14	+0.11	-	+0.11
Iron Range K*	9 783 317.62 ± 0.28	−0.35	-0.55	+0.20
Alice Springs B	9 786 308.00 ± 0.14	+0.07	-0.04	+0.11
Perth D	9 794 036.94 ± 0.14	−0.11	-0.31	+0.20
Sydney C	9 796 376.18 ± 0.15	−0.11	-0.28	+0.17
Hobart B	9 804 178.34 ± 0.14	+0.11	-	+0.11

*The Iron Range value was calculated as follows:

Port Moresby absolute value	9 782 022.08 ± 0.14
Honkasalo correction	+0.34
Tie to 7390.0176 Port Moresby airport	−36.09 ± 0.10
Tie to 7390.1073 Iron Range airport	+ 1 328.17 ± 0.24
Tie to 6600.0025 terminal Iron Range	+3.12 ± 0.04
Value at 6600.0025 Iron Range	9 783 317.62 ± 0.28

Some separate adjustments were carried out using (i) Earth tides calculated by Longman's formula, which uses a constant amplification and zero phase lag for the various waves, and (ii) Earth tides calculated using the constants and phase lags for the waves measured by Ducarme & others (1976) and Ducarme & Melchior (1978) for Australian sites. There was no significant difference in the gravity values calculated from Longman's formula or from measured Earth-tide corrections. This was not unexpected, as the program adjusts station-to-station interval rather than actual station values.

The adjustment theory assumes that the observational errors are normally distributed and there are no other errors. The residuals of the final adjustment (adjustment 2) give a chi-square sum of 23.7 for 7 degrees of freedom, so the distribution is not normal. Relative to the normal curve, the number of residuals is higher for near-zero values and large magnitude values. The large magnitude residuals are thought to be due to misreadings, lag in instrumental recovery after flights, and errors induced by vibration during readings. It is believed that, as a result of the great redundancy of observations in this survey, these large residuals will have negligible effect on the calculated gravity values. The calculated standard error of the residuals is 0.25 $\mu m.s^{-2}$. Plotting of the errors on probability paper shows that the majority of them belong to a normal curve of standard deviation 0.22 $\mu m.s^{-2}$; this is larger than the error for short time-interval ground measurements of about 0.15 $\mu m.s^{-2}$. (Wellman & others, 1974).

The adopted values for the computer adjustment of the 1980 gravity meter survey, using the 1979 absolute gravity measurements for datum and scale, are listed in Appendix 1 (Isogal 84 values). The formal precision of the values calculated in the computer adjustment ranges from 0.091 to 0.155 $\mu m.s^{-2}$. At the 95 per cent confidence level, the accuracy of the values is thought to be better than 0.6 $\mu m.s^{-2}$. The Honkasalo correction has not been applied.

Comparison with recent international measurements

Table 3 shows that Isogal 84 values differ only slightly from IGSN 71 values (Morelli & others, 1971). Individual values differ by less than 0.9 $\mu m.s^{-2}$. The differences vary systematically with absolute gravity, so there is a slight local scale difference. A comparison with Japanese 1983 values (Nakagowa & others, 1983) shows small residuals, except -0.6 $\mu m.s^{-2}$ at Hobart. (Table 4).

Table 3. Comparison of IGSN 71 and Isogal 84 values ($\mu m.s^{-2}$)

	IGSN 71 value	Honkasalo correction	IGSN 71 + H.C. minus Isogal 84
Darwin L	9 783 006.1	+0.032	+0.18
Cairns A	9 784 862.4	+0.28	+0.42
Townsville A	9 786 097.4	+0.25	+0.82*
Mount Isa J	9 786 044.1	+0.23	−0.10*
Alice Springs J	9 786 393.9	+0.19	+0.04
Mackay J	9 787 198.8	+0.23	+0.41*
Rockhampton K	9 788 600.4	+0.19	+0.25
Maryborough A	9 790 073.2	+0.16	+0.57
Brisbane J	9 791 455.7	+0.13	+0.70*
Grafton K	9 793 153.7	+0.10	+0.00
Perth K	9 793 863.2	+0.06	−0.90
Kempsey J	9 794 123.8	+0.07	−0.23
Canberra J	9 796 063.9	+0.00	−0.25*
Sydney A	9 796 718.6	+0.02	−0.15*
Albury K	9 797 517.0	−0.02	−0.44*
Melbourne M	9 799 473.5	−0.05	−0.50

* value not based on direct reoccupation.

Table 4. Comparison of Japanese 1983 and Isogal 84 values ($\mu m.s^{-2}$)

	Japanese value	Japanese minus Isogal 84
Port Moresby D	9 782 022.74	−0.03*
Cairns A	9 784 862.13	−0.13
Townsville O	9 786 096.87	−0.17
Sydney T	9 796 856.54	−0.21
Melbourne V	9 799 317.24	−0.10
Hobart U	9 804 351.29	−0.61

* value not based on direct reoccupation.

Comparison with Isogal 65 values

The gravity values used in the present Australian national gravity data bank are based on 200 airport base stations. These base stations were established during 1964–67, and the values presently used are those calculated directly after this survey (Isogal 65 values). The main purpose of the 1980 survey was to calculate a transformation for these stations from Isogal 65 values to values correct in absolute scale and datum.

Figure 2. Australian gravity base-station network in 1980.
Thick lines and big dots are higher accuracy traverses of the 1980 survey; thin lines and small dots are the lower accuracy transverses of the 1964–67 survey. Calibration ranges are listed in Table 5.

The 1964–67 survey consisted of mainly east–west traverses between airports with similar gravity (Fig. 2), the measurements being made by three gravity meters of different type (Barlow, 1970; McCracken, 1978). A 'drift control sequence' of observations was used. The observed gravity intervals between adjacent airports were later recalculated to take into account Earth tides (Appendix 1 & 2 of McCracken, 1978). We have adjusted these intervals to the preferred gravity meter scale factors of McCracken, and, by averaging the results of the three meters, have obtained a mean observed interval.

Gravity values have been calculated as follows. Isogal 84 values (Appendix 1) have been adopted for the airports occupied in 1980. For airports not occupied in 1980 (Fig. 2) the mean observed intervals of the 1964–67 traverses have been adjusted to the Isogal 84 values by distributing errors equally between them. The magnitude of the adjustments is shown in Figure 3.

Table 5. Gravity intervals for Australian calibration ranges (μm.s^{-2}).

	Gravity stations		Gravity interval	Standard error of mean	Ref.
	IGC	BMR numbers			
Townsville	L-M	6091.0151-6091.0251	605.54	0.12	1
Brisbane	D-N	6091.0147-6091.0247	582.51	0.03	1
Sydney	N-O	6091.0105-6091.0205	590.03	0.08	1
Sydney		8291.0105-6091.0205	583.37	0.04	2
Canberra	L-K	6491.0304-6491.0204	547.72	0.02	1
Canberra	S-T	7691.0104-7691.0204	560.02	0.02	
Canberra	Q-R	7490.0001-7490.0020	2295.73	0.13	1
Melbourne	P-Q	6091.0101-6091.0201	530.26	0.10	1
Melbourne		8090.0301-8090.0401	1707.15	0.08	
Hobart	L-M	6091.0160-6091.0260	546.48	0.06	1
Adelaide	J-K	6091.0108-6091.0208	626.60	0.05	
Adelaide	J-T	6091.0108-6793.0208	1158.71	0.04	
Alice Springs	M-L	6091.0235-6091.0135	521.68	0.05	
Darwin	P-Q	8090.0332-8090.0432	314.16	0.04	
Perth	M-L	6091.0217-6091.0117	540.18	0.20	1
Perth	V-Y	7391.0117-7391.0217	542.42	0.30	1
Perth		8090.0317-7391.0217	541.82	0.05	

1. Wellman & McCracken, 1975
2. Williams & Murray, in prep.

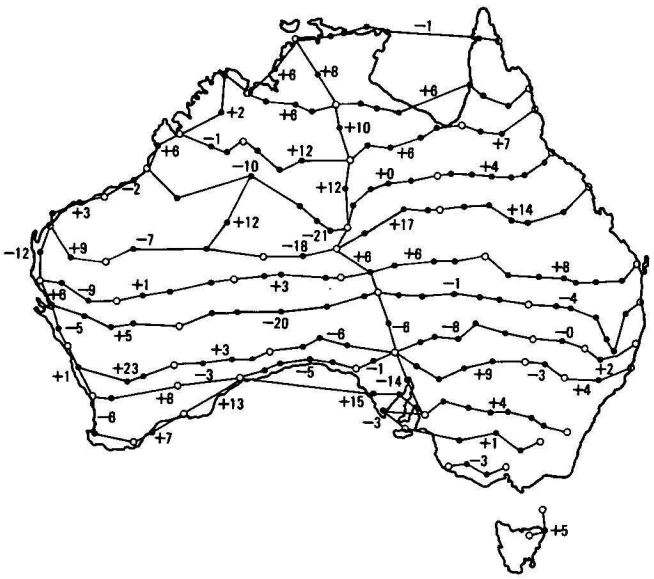

Figure 3. Differences between intervals calculated for Isogal 84 values (at airports with large dots) and intervals between these towns from 1964-67 measurements.
(Unit 0.1 μm.s^{-2}).

The differences between Isogal 65 (BMR unpublished) and Isogal 84 values have been calculated for each airport, and this difference is contoured in Figure 4. The differences are due to three factors. The main change of approximately 140 μm.s^{-2} is due to the change in the world gravity datum from Potsdam datum to IGSN 71 datum (Morelli & others, 1971). The strong north-south gradient is due to a scale change from 'the mean Australian milligal' (Dooley, 1965) to the scale defined by the weighted results of the Soviet absolute measurements (Arnautov & others, 1979). The irregularity in this gradient is due to errors in the observation and reduction of the 1964-67 survey.

Future high-accuracy field surveys should use the Isogal 84 values directly to control datum and scale. Although the gravity meter readings of old surveys could in theory be recalculated to correct scale and datum by using individual Isogal 84 values directly, this is unlikely to be done, because of the large amount of work it requires. Rather, old surveys can be corrected by a polynomial expression of the gravity change of Figure 4.

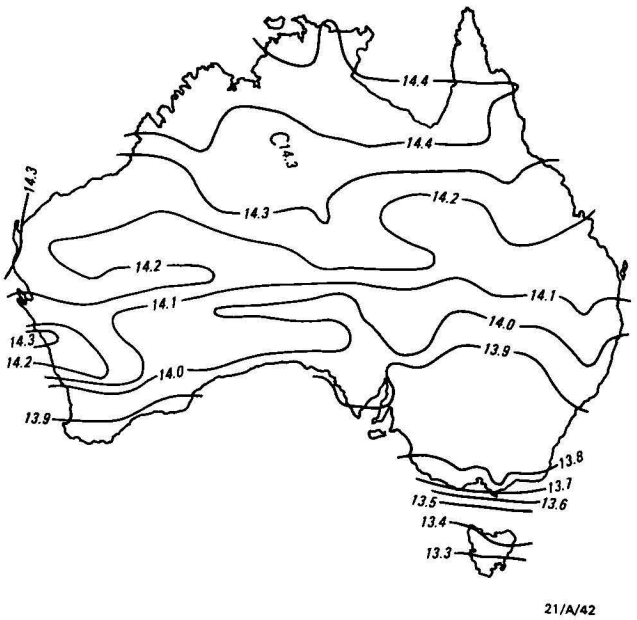

Figure 4. Differences between Isogal 65 and Isogal 84 gravity values.
(Unit 10 μm.s^{-2}).

The polynomial was derived by least-squares fitting a fifth order polynomial to the differences between the Isogal 65 and Isogal 84 values within Australia. If the difference has a value of V at latitude D°S, longitude F°E, then

$Y = (D - 25.0\,°S, X = (F - 135\,°E)$, and

$V = 14.1660 - 0.183800 \times 10^{-2}X + 0.0405366 \times Y - 0.220256 \times 10^{-3}X^2 + 0.476101 \times 10^{-3}XY + 0.709150 \times 10^{-3}Y^2 + 0.166350 \times 10^{-5}X^3 + 0.166350 \times 10^{-5}X^3 - 0.964709 \times 10^{-4}X^2Y - 0.373075 \times 10^{-4}XY^2 - 0.147880 \times 10^{-3}Y^3 + 0.915962 \times 10^{-6}X^4 + 0.764998 \times 10^{-6}X^3Y - 0.772339 \times 10^{-7}X^2Y^2 - 0.673367 \times 10^{-5}XY^3 - 0.982392 \times 10^{-5}Y^4 + 0.910128 \times 10^{-8}X^5 + 0.147126 \times 10^{-6}X^4Y + 0.666914 \times 10^{-7}X^3Y^2 + 0.568814 \times 10^{-6}X^2Y^3 + 0.456620 \times 10^{-6}XY^4 + 0.438121 \times 10^{-6}Y^5$

The standard deviation of the differences from the computed values is 0.52 μm.s^{-2}.

Observed gravity values based on Potsdam datum (Isogal 65 base-station values) should be reduced, using the 1930 International Gravity Formula for normal gravity : $g_N = 9\,780\,490.(1 + 0.005\,288\,4 \sin^2 D - 0.000\,0005\,9 \sin^2 2D)$ μm.s^{-2}, where D is latitude. Gravity values consistent with the IGSN 71 system (Isogal 73, Isogal 74, Isogal 84 base-station values) should be reduced, using the 1967 International Gravity Formula of $g_N = 9\,780\,318\,(1 + 0.005\,302\,4 \sin^2 D - 0.000\,0005\,9 \sin^2 2D)$ μm.s^{-2}.

Provided the formula for normal gravity that is appropriate to the datum used for observed gravity is employed, the computed anomalies will be similar irrespective of that datum; the difference between anomalies calculated by the two systems varies gradually from 28 μm.s^{-2} at 10°S to -32 μm.s^{-2} at 44°S. If the matching datum and formula are not used, then the calculated anomaly values will be in error by about 140 μm.s^{-2}.

Discussion

This work is a step in the continuing process of defining the gravity field more accurately. The history of Australian gravity measurements including gravity control networks has been given by Day (1966) and Dooley & Barlow (1976).

The gravity datum for Australia has been defined as 9 799 790 μm.s^{-2} at Melbourne A in 1950 (Dooley & others, 1960), as 9 796 718.6 μm.s^{-2} at Sydney A in 1973 (Boulanger & others, 1973), and as the weighted mean of six absolute measurements in this paper.

The gravity scale was defined by relative pendulum measurements as the 'mean Australian milligal' in 1965 (Dooley, 1965), was redefined from the results of GAG-2 gravity meter measurements in 1973 (Boulanger & others, 1973), was measured by OVM pendulums in 1975 (Gusev, 1975), and in this paper is redefined using the weighted results of six absolute gravity measurements.

The gravity base-station network was measured as a set of 59 relative pendulum measurements in 1950 (Dooley & others, 1960), was recalculated as a network of gravity meter readings in 1962 (Dooley, 1965), was measured as a network of sites at 200 airports in 1964–67 (Barlow, 1970), and was recalculated in 1975 (McCracken, 1978). The 1980 remeasurement at 67 of the airports is reported in this paper. The increase in accuracy and precision of the base-station values with time is shown in Table 6.

Table 6. Australian gravity base stations: approximate precision and accuracy (μm.s^{-2}).

		Precision	Accuracy
1950–51	pendulum observations	4.3	140
1962	network adjustment	1.6	140
1965–67	Isogal survey	1	140
1975	network adjustment	1	2
1984	survey and adjustment		
	stations not occupied	1	1
	stations occupied	0.1	0.2

In this paper there are several changes in the method of calculation and application of the gravity control network. Previously, datum was transferred from Potsdam in Europe or overseas using relative pendulums or gravity meters, and the 'best' value at a 'National Gravity Base Station' was adopted. Scale was defined by adopting measurements of gravity difference. In this paper, no actual measured values are adopted, because both datum and scale are defined by the weighted results of six, scattered, absolute gravity measurements.

Previously, the gravity stations with the most accurately known values were within buildings where pendulum or absolute gravity measurements had been made. In this paper, the airport stations used for comparison of the absolute stations have the most accurately known values.

Before 1973, field surveys were completely recalculated when new values of the gravity network became available. The change of datum and scale of 1973 was applied as a linear correction, g(Isogal 73)=9 796 718.6+1.000 511 8 [g(Isogal 65)−9 796 857.4][μm.s^{-2}. The new values (Isogal 84 values) are taken to be temporary, and vary gradually with position. It is recommended, therefore, that adjustments to Isogal 84 be by polynomial or approximate methods, as it is likely that further small adjustments to base-station values will be required in the future.

Acknowledgements.

We are grateful to M. Untung for his participation in the observational phase of this work, and to R.W. Bates for drafting.

References

Arnautov, G.P., Boulanger, Yu.D., Karner, G.D. & Shcheglov, S.N., 1979 - Absolute determination of gravity in Australia and Papua New Guinea during 1979. *BMR Journal of Australian Geology & Geophysics*, 4, 383–393.

Barlow, B.C., 1970 - National report on gravity in Australia, July 1965 to June 1970. *Bureau of Mineral Resources, Australia, Record*, 1970/62.

Boulanger, Yu.D., Shcheglov, S.N., Wellman, P., Coutts, D.A., & Barlow, B.C., 1973 - Soviet-Australian gravity survey along the Australian Calibration Line. *Bulletin Geodesique*, 110, 355–366.

Day, A.A., 1966 - The development of geophysics in Australia. *Journal and Proceedings, Royal Society of New South Wales*, 100, 33–60.

Dooley, J.C., 1965 - Australian gravity network adjustment, 1962. *Bureau of Mineral Resources, Australia, Report*, 72.

Dooley, J.C., & Barlow, B.C., 1976 - Gravimetry in Australia, 1819–1976. *BMR Journal of Australian Geology & Geophysics*, 1, 261–271.

Dooley, J.C., McCarthy, E., Keating, W.D., Williams, L.W., & Maddern, C.A., 1960 - Pendulum measurements of gravity in Australia. *Bureau of Mineral Resources, Australia, Bulletin* 46.

Ducarme, B. & Melchior, P., 1978 - A trans-world gravity profile. *Physics of the Earth and Planetary Interiors*, 16, 257–276.

Ducarme, B., Melchior, P., Mather, R.S., & Barlow, B.C., 1976 - Tidal gravity profiles in Australia and Papua New Guinea (1974–1976). *Unisurv* G, 25, 17–53.

Gusev, N.A., 1975 - Determination of gravity acceleration at Port Moresby (Papua New Guinea) and Hobart (Australia) with OVM pendulum apparatus. *Bureau of Mineral Resources, Australia, Record* 1975/106.

McConnell, R.K, & Ganter, C, 1971 - Adjustments and analyses of data for IGSN 71. *In* Morelli, C., & others. The international gravity standardization net 1971. *International Association of Geodesy, Paris, Special Publication* 4.

McCracken, H.M., 1978 - Australian gravity network adjustment, 1975. *Bureau of Mineral Resources, Australia, Report* 207; *BMR Microform* MF68.

Morelli, C., Ganter, C., Honkasalo, T., McConnell, R.K., Tanner, J.B., Szabo, B., Uotila, U., & Whalen, C.T., 1971 - The international gravity standardization net 1971. *International Association of Geodesy, Paris, Special Publication* 4.

Nakagawa, I., Nakai, S., Shichi, R., Tajima, H., Izutuya, S., Kono, Y., Higashi, T., Fujimoto, H., Murakami, M., Tajima, K., & Funaki, M., 1983 - Precise calibration of scale values of LaCoste & Romberg gravimeters and international gravimetric connections along the circum-Pacific zone. Final report on 'Precise calibration of scale values of LaCoste & Romberg gravimeters and contribution to the reform of the International Gravity Standardization Net 1971', 117 pp.

Wellman, P., Boulanger, Yu.D., Barlow, B.C., Shcheglov, S.N., & Coutts, D.A., 1974 - Australian and Soviet gravity surveys along the Australian Calibration Line. *Bureau of Mineral Resources, Australia, Bulletin* 161.

Wellman, P. & McCracken, H.M., 1975 - Gravity measurements on Papua New Guinea crustal movement survey markers, and along the Australian Calibration Line, 1975. *Bureau of Mineral Resources, Australia, Record* 1975/126.

Williams, J.W., 1983 - LaCoste & Romberg gravity meters; laboratory investigations into the effects of changes in air pressure, temperature, and meter supply voltage. *Bureau of Mineral Resources, Australia, Record* 1983/3.

Uotila, U.A., 1980 - Note to the users of International Gravity Standardization Net 1971. *Bureau Gravimetrique International, Bulletin d'Information*, 47, 15–16.

Appendix 1. Gravity values at stations of the 1980 survey

Airport	Station location	Station number IGC	Station number BMR	Altitude (m)	Latitude (°)(′)	Longitude (°)(′)	Gravity values Isogal 65 (μm.s^{-2})	Gravity values Isogal 84 (μm.s^{-2})
Adelaide	terminal	45548N	6491.0308	.457	34 56.5	138 32.1	9 797 190.5	9 797 051.49
Adelaide	memorial	45548U	8090.0108	5	34 56.5	138 32.1		9 797 054.32
Albany	terminal	45747J	6491.0118	69.01	34 56.6	117 47.9	9 797 066.0	9 796 927.57
Albany	hangar	45747K	8090.0118	69	34 56.6	117 47.9		9 796 927.27
Albury	terminal	45466M	7591.1136	162.09	36 04.3	146 57.5	9 797 656.2*	9 797 517.42
Albury	hire car	45466N	8090.1136	162	36 04.3	146 57.5		9 797 518.47
Alice Springs	terminal	41933J	6491.0335	542.57	23 48.4	133 53.9	9 786 537.0	9 786 394.05
Alice Springs	D.O.T.	41933N	8090.0135	542	23 48.4	133 53.9		9 786 394.02
Alice Springs	absolute	41933B	7999.0135	580	23 43	133 50		9 786 307.93
Anna Plains	apron	38491K	6792.0227	17.35	19 15.3	121 30.6	9 786 244.7	9 786 102.32
Anna Plains	windsock	38491J	6792.0127	16.65	19 15.3	121 30.6	9 786 249.9	9 786 107.44
Balgo Hills	terminal	42007M	8090.1217		20 09.0	127 58.0		9 785 215.23
Bourke	hangar	45405J	6491.9107	106.43	30 02.6	145 57.1	9 793 200.8	9 793 061.22
Bourke	terminal	45405L	8090.1107	106	30 02.6	145 57.1		9 793 060.90
Brisbane	Ansett	41773R	7213.0147	7	27 25.8	153 04.9		9 791 458.09
Brisbane	TAA	41773T	7390.0247	7	27 25.8	153 05.0	9 791 595.7*	9 791 454.93
Caiguna	motel 5/6	45626K	6491.1122		32 16.3	125 29.0	9 794 957.6	9 794 817.68
Caiguna	toilets	45626M	8090.1122		32 16.3	125 29.0		9 794 816.91
Cairns	hangar	38265A	5099.9952	2.41	16 53.4	145 45.0	9 785 006.0	9 784 862.26
Cairns	terminal	38265N	8090.0152	2	16 53.4	145 45.1		9 784 862.86
Canberra	terminal	45459U	7791.0104	566.8	35 18.5	149 11.3		9 796 066.18
Canberra	aero club	45459N	6893.0204	565.89	35 18.4	149 11.2	9 796 205.2	9 796 066.45
Canberra	laser site	45459V	8090.0104		35 38.1	148 55.7		9 794 580.64
Carnarvon	terminal	42143J	6500.0124	2.62	24 53.0	113 39.7	9 789 439.3	9 789 296.55
Carnarvon	workshop	42143K	8090.0124	2	24 53.0	113 39.7		9 789 296.06
Ceduna	DOT shed	45523L	8090.0110	16	32 07.5	133 41.9		9 794 385.94
Ceduna	tarmac	45523J	6491.0110	16.42	32 07.5	133 41.9	9 794 524.2	9 794 385.09
Cobar	B of sign	45415J	6491.0143	217.98	31 32.5	145 47.8	9 794 031.5	9 793 893.43
Cobar	terminal	45415L	8090.0143	218	31 32.5	145 47.8		9 793 892.62
Cooktown	terminal	38255L	7090.1072	5.37	15 26.8	145 11.2	9 784 422.4*	9 784 278.40
Cooktown	house	38255N	8090.1072	5	15 26.8	145 11.2		9 784 278.27
Cunnamulla	tarmac	41885J	6491.9012	188.64	28 01.9	145 37.2	9 791 316.9	9 791 176.54
Cunnamulla	terminal	41885L	8090.1012	189	28 01.9	145 37.2		9 791 176.99
Daly Waters	mast	38363J	6491.0133	210.06	16 16.0	133 22.5	9 783 891.8	9 783 747.24
Daly Waters	terminal	38363K	6793.0133	210	16 16.0	133 22.5	9 783 891.3	9 783 746.73
Darwin	hangar	38320L	6491.0132	29.78	12 25.3	130 51.8	9 783 150.0	9 783 006.24
Darwin	DCA office	38320	8090.0132	29	12 25.3	130 51.8		9 783 007.00
Darwin	terminal	38320	8090.0232	27	12 25.3	130 51.8		9 783 009.16
Darwin	cali. 1	38320	8090.0332	50	13 13.9	131 06.8		9 783 145.42
Darwin	cali. 2	38320	8090.0432	185	13 20.9	131 07.9		9 782 831.26
Darwin	absolute	38320C	7999.0132	20	12 51.	131 08.		9 783 009.48
Derby	hangar	38473J	6491.0128	6.03	17 22.3	123 39.7	9 785 207.2	9 785 063.09
Derby	terminal	38473M	6500.0128	6.88	17 22.3	123 39.7	9 785 204.2	9 785 059.76
De Rose Hill	windsock	41963J	6491.9081	410.05	26 25.6	133 15.8	9 789 754.5	9 789 612.87
De Rose Hill	strip	41963L	8090.1081	410	26 25.6	133 15.8		9 789 610.95
Dubbo	tarmac	45428J	6491.9113	280.33	32 13.0	148 34.2	9 794 318.8	9 794 179.96
Dubbo	terminal	45428M	8090.1113	280	32 13.0	148 34.2		9 794 179.48
Esperance	terminal	45631J	6491.0113	142.84	33 41.0	121 50.1	9 795 803.8	9 795 664.98
Esperance	light base	45631L	8090.0113	143	33 41.0	121 50.1		9 795 664.85
Flinders Is.	terminal	49007L	6491.9140	30.92	40 05.7	148 00.3	9 802 044.9	9 801 910.32
Flinders Is.	garage	49007J	6491.1140	30.16	40 05.7	148 00.1	9 802 046.1	9 801 911.29
Forest	hangar	45608A	5099.9912	156	30 50.8	128 06.8	9 793 062.5	9 792 922.18
Forest	hangar	45608J	6491.0112	156	30 50.8	128 06.8	9 793 062.8	9 792 922.56
Geraldton	terminal	42184L	8090.0120	33	28 47.7	114 41.9		9 792 563.91
Geraldton	hangar	42184A	5099.9920	33.95	28 47.5	114 41.8	9 792 700.5	9 792 557.19
Geraldton	D.O.T.	42184M	8090.0220	32	28 47.7	114 41.9		9 792 562.16
Geraldton	sat. laser	42184	8090.0320	268.04	29 02.9	115 20.6		9 791 449.85
Geraldton	sat. laser	42184	8090.0420	268	29 02.9	115 20.6		9 791 445.70
Giles	met. area	42058K	6792.0173	596.08	25 02.0	128 18.0	9 787 693.0	9 787 551.51
Giles	windsock	42058L	6792.0273	578.66	25 02.6	128 17.7	9 787 725.6	9 787 584.36
Grafton	terminal	41792K	6491.9110	28.91	29 45.6	153 01.8	9 793 293.3	9 793 153.80
Grafton	terminal	41792M	8090.1110	29	29 45.6	153 01.8		9 793 153.61
Halls Creek	terminal	38487J	6491.0129	409.61	18 14.2	127 40.1	9 784 616.3	9 784 473.02
Halls Creek	workshop	38487K	8090.0129	410	18 14.2	127 40.1		9 784 471.67
Hamelin Pool	windsock	42164J	6792.9207	26.60	26 25.5	114 12.4	9 790 486.3	9 790 344.39
Hamelin Pool	pump hut	42164M	8090.1207	26	26 25.5	144 12.4		9 790 346.67
Henbury	windsock	41943K	6792.1037	425.50	24 35.0	133 13.9	9 787 841.2	9 787 698.45
Henbury	road gate	41843	8090.1037	425	24 35.0	133 13.9		9 787 693.32
Hobart	hangar	49027Q	7390.0260	3	42 50.4	147 30.4	9 804 476.5*	9 804 343.87
Hobart	terminal	49027U	8090.0160	3	42 50.3	147 30.3		9 804 351.90
Hobart	absolute	49027B	7499.0160	132	42 54.5	147 19.2		9 804 178.23
Iron Range	terminal	38223K	6600.0025	18.78	12 47.2	143 18.3	9 783 461.7	9 783 317.97
Iron Range	shed	38223J	6491.9073	17.6	12 47.3	143 18.3	9 783 449.1	9 783 305.48
Kalgoorlie	concrete	45601K	6491.0214	355.46	30 46.9	121 27.7	9 792 905.0	9 792 764.30
Kalgoorlie	hangar	45601A	5099.9914	355.75	30 46.9	121 27.7	9 792 907.3	9 792 766.49
Katherine	terminal	38342M	8090.1318	129.6	14 31.	132 22.		9 783 248.59
Katherine	D.O.T.	38342N	8090.2318	129	14 31.	132 22.		9 783 247.58
Kempsey	terminal	45312J	6491.9111	14.72	31 04.2	152 46.0	9 794 361.0	9 794 124.10
Kempsey	hangar	45312O	8090.1111	14	31 04.2	152 46.0		9 794 124.66
Kingscote	terminal	45557J	6793.9306	6.1	35 42.6	137 31.5	9 798 287.1	9 798 148.34
Kingscote	light-tower	45557L	8090.1306	6.1	35 42.6	137 31.5		9 798 148.38

Laverton	windsock	42082K	6792.0215		28 37.0	122 25.0	9 790 966.4	9 790 826.31
Laverton	terminal	42082L	8090.0115		28 37.0	122 25.0		9 790 833.13
Mackay	tarmac	41819M	7390.0161	4	21 10.3	149 11.0	9 787 339.7*	9 787 197.56
Mackay	terminal	41819P	8090.0161	4	21 10.3	149 11.0		9 787 197.44
Maryborough	hangar	41752A	5099.9948	10.77	25 31.1	152 42.7	9 790 214.2	9 790 072.79
Maryborough	terminal	41752K	8090.0148	11	25 31.	152 43.		9 790 071.19
Meekatharra	terminal	42168J	6491.9090	517.07	26 36.6	118 32.7	9 789 183.0	9 789 040.60
Meekatharra	aeradio	42168K	6491.1090	517.55	26 36.7	118 32.9	9 789 194.6	9 789 051.75
Melbourne	Essendon	45474M	6491.0101	76.65	37 43.7	144 53.9	9 799 611.8	9 799 473.95
Melbourne	Essendon	45474	8090.0101	76	37 43.7	144 53.9		9 799 474.02
Melbourne	Tulla.	45474V	7213.0101		37 41.	144 51.		9 799 317.34
Melbourne	Customs	45474Z	8090.0201		37 41.	144 51.		9 799 343.80
Melbourne	Macedon	45474	8090.0301		37 30.	144 45.		9 798 834.98
Melbourne	Macedon	45474	8090.0401		37 23.	144 35.		9 797 127.83
Mount Gambier	terminal	45470J	6491.0107	63.29	37 44.7	140 47.1	9 799 772.2	9 799 634.71
Mount Gambier	hangar	45470K	8090.0107	63	37 44.7	140 47.1		9 799 628.96
Mount Isa	terminal	41909N	8090.0162	336	20 40.1	139 29.3		9 786 043.65
Mount Isa	fire stn	41909K	6491.9962	336.60	20 40.1	139 29.3	9 786 190.1	9 786 047.33
Mount Vernon	strip	42148K	6792.1210	399.53	24 13.5	118 15.0	9 787 908.1	9 787 766.99
Mount Vernon	windsock	42148J	6792.9210	398.83	24 13.4	118 15.1	9 787 911.2	9 787 769.91
Narrabri	terminal	45409J	6491.9108	222.99	30 19.1	149 49.5	9 793 113.9	9 792 974.39
Narrabri	windsock	45409M	8090.1108	223	30 19.1	149 49.5		9 792 978.43
Normanton	terminal	38271K	6491.0163	17	17 41.2	141 04.3	9 785 177.5	9 785 033.24
Normanton	DCA shed	38271M	8090.0163	17	17 41.2	141 04.3		9 785 032.02
Norseman	concrete	45621J	6491.9123	263.34	32 12.4	121 45.4	9 794 167.3	9 794 027.93
Norseman	toilet	45621K	8090.1123	263	32 12.4	121 45.4		9 794 027.68
Onslow	terminal	42115K	6792.0225	3.24	21 39.9	115 06.6	9 787 738.3	9 787 596.02
Onslow	windsock	42115L	8090.0125	3	21 39.9	115 06.6		9 787 594.91
Oodnadatta	terminal	41975J	6491.0136	112	27 33.4	135 26.1	9 790 999.4	9 790 859.16
Oodnadatta	shed	41975K	8090.0136	112	27 33.4	135 26.1		9 790 859.90
Parkes	radio tele	J	8090.0144	371	33 00.0	148 15.7		9 794 773.95
Parkes	radio tele	K	8090.0244	371.40	33 00.0	148 15.7		9 794 774.08
Perth	hangar	45715Y	8090.0117	14	31 56.0	115 57.4		9 793 861.19
Perth	catering	45715Z	8090.0217	14	31 56.0	115 57.4		9 793 862.13
Perth	absolute	45715D	7999.0117	300	31 43.	116 12.		9 794 037.05
Perth	hangar	45715K	6491.0317	15.08	31 56.2	115 57.3	9 794 004.1	9 793 864.16
Perth	terminal	45715U	6500.0117	14.44	31 56.0	115 57.4	9 794 006.9	9 793 866.83
Port Hedland	terminal	42108N	8090.0126	8	20 22.6	118 37.7		9 786 312.04
Port Hedland	D.O.T.	42108L	6792.0326	8.02	20 22.6	118 37.7	9 786 457.7	9 786 314.99
Rockhampton	fire stat.	41730K	6499.0149	9.82	23 22.7	150 28.5	9 788 742.0	9 788 600.34
Rockhampton	terminal	41730L	7090.0149	9	23 22.7	150 28.5		9 788 602.28
Sydney	Flight Fa.	45332T	6891.0305	6.37	33 56.1	151 11.2	9 796 995.5	9 796 856.75
Sydney	Air Amb.	45332Z	8090.0105	5	33 56.1	151 11.2		9 796 858.76
Sydney	absolute	45331C	7999.0105	62.7	33 52.	151 12.		9 796 376.29
Tennant Creek	terminal	38394K	6793.0134	375	19 38.5	134 10.9	9 785 289.4	9 785 145.83
Tennant Creek	power	38394A	5099.9934	375.02	19 38.5	134 10.9	9 785 289.2	9 785 145.45
Thargomindah	terminal	41873L	8090.1013	130	27 59.3	143 48.7		9 791 283.68
Thargomindah	cover	41873M	8090.2013	130	27 59.3	143 48.7		9 791 283.09
Thursday Is.	terminal	38202J	6691.9001	15.1	10 35.5	142 17.8	9 782 441.4	9 782 298.34
Thursday Is.	hangar	38202N	8090.1001	12.32	10 35.5	142 17.8		9 782 303.53
Townsville	terminal	38296O	7090.0151	4.43	19 15.4	146 46.2	9 786 240.2*	9 786 097.04
Townsville	hangar	38296S	8090.0151	4	19 15.4	146 46.2		9 786 098.68
Warburton	store	42066K	6491.9969		26 08.0	126 34.7	9 789 257.6	9 789 115.59
Windorah	terminal	41852J	6491.9023	131.71	25 24.8	142 39.8	9 789 428.3	9 789 286.59
Windorah	windsock	41852M	8090.1023	132	25 24.8	142 39.8		9 789 287.83
Woomera	terminal	45516J	6491.0138	166.78	31 09.5	136 48.3	9 793 727.5	9 793 587.81
Woomera	concrete	45516K	8090.0138	167	31 09.5	136 48.3		9 793 587.39
Wyndham	workshop	38458A	5099.9930	5.38	15 30.3	128 09.0	9 784 146.3	9 784 002.16
Wyndham	terminal	38458J	6491.0130	5.06	15 30.3	128 09.0	9 784 146.9	9 784 002.63

BMR Journal of Australian Geology & Geophysics, 9, 233-238

Revised stratigraphic nomenclature and correlation of Early Proterozoic rocks of the Darwin-Katherine region, Northern Territory

R.S. Needham[1] & P.G. Stuart-Smith[1]

New stratigraphic names and correlations are given for parts of the Early Proterozoic Pine Creek Geosyncline metasedimentary sequence and overlying felsic volcanics of the Darwin-Katherine region. They have significant implications for the stratigraphic distribution of uranium mineralisation in the Rum Jungle, Alligator Rivers, and South Alligator Valley uranium fields.

Introduction

The stratigraphy of the Pine Creek Geosyncline has undergone substantial revision following a 1:100 000-scale mapping project conducted by the Bureau of Mineral Resources since the discovery of uranium at Nabarlek in 1969. In 1980, Needham & others described the Early Proterozoic stratigraphy as a sequence that could be traced through most of the region with little facies variation. This was a radically different concept to that of earlier workers (Walpole & others, 1968) who described the sediments as several laterally disposed facies assemblages, between which there was little or no possibility of correlation. Since 1980, completion of the 1:100 000-scale mapping project has confirmed the lateral continuity of stratigraphic units in the Early Proterozoic sequence proposed by Needham & others (1980), but correlations between some units in the Rum Jungle region (Fig. 1) and those in the remainder of the geosyncline have been changed. Stratigraphic amendments have also been made in the South Alligator Valley and Oenpelli areas, and in the Katherine to South Alligator Valley region, where late Early Proterozoic felsic volcanic rocks are substantially redefined. Some of those changes have been described in map commen-

[1]Division of Petrology & Geochemistry, BMR

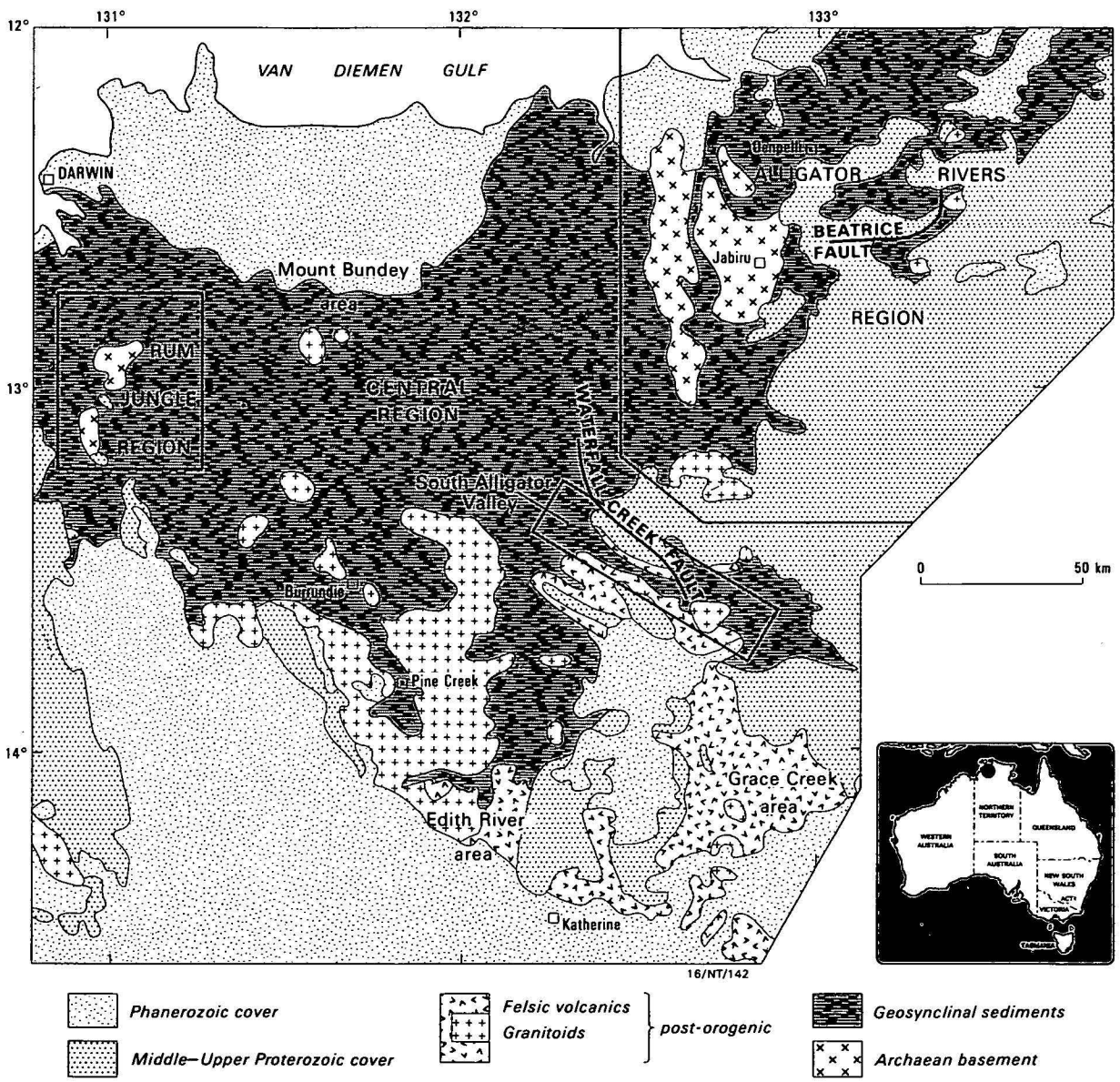

Figure 1. Generalised geology.

Table 1. New and redefined stratigraphic units and bibliographic references

Name	Remarks	Reference
Pre-orogenic geosynclinal sequence (Fig. 2)		
Acacia Gap Quartzite Member	minor name change; raised from base of Wildman Siltstone	Crick (in prep.), Stuart-Smith & others (1984a)
Batchelor Group	name dropped, formations moved to Namoona or Mount Partridge Groups	Crick (in prep.), Stuart-Smith & others (1984a)
Beestons Formation	moved from Batchelor Group to Namoona Group; facies variant of Masson Formation	Crick (in prep.), Stuart-Smith & others (1984a)
Burrell Creek Formation	extended to cover most areas of Fisher Creek Siltstone	—
Celia Dolomite	moved from Batchelor Group to Namoona Group; facies variant of Masson Formation	Crick (in prep.), Stuart-Smith & others (1984a)
Coomalie Dolomite	moved from Batchelor Group to Mount Partridge Group; facies variant of Wildman Siltstone	Crick (in prep.), Stuart-Smith & others (1984a)
Kapalga Formation	restricted to areas east of Waterfall Creek Fault; probable correlative of Koolpin and Mount Bonnie Formations and Gerowie Tuff west of fault	Needham & Stuart-Smith (1984)
Koolpin Formation	restricted to areas west of Waterfall Creek Fault	Needham & Stuart-Smith (1984)
Mount Bonnie Formation	new name; replaces Kapalga Formation west of Waterfall Creek Fault	Stuart-Smith & others (in prep.)
Myra Falls Metamorphics	reintroduction of name used by Dunn (1962). Includes Transitional and Lit-par-lit Gneiss Zones previously of the Nimbuwah Complex	Needham (1984)
Nimbuwah Complex	redefined; Transitional and Lit-par-lit Gneiss Zones moved to Myra Falls Metamorphics	Needham (1984)
Nourlangie Schist	stratigraphic range extended to include possible metamorphic equivalents of South Alligator and Finniss River Groups	Needham (1984)
Whites Formation	new name; replaces Masson Formation in Rum Jungle area, placed in Mount Partridge Group	Crick (in prep.), Stuart-Smith & others (1984a)
Post-orogenic felsic volcanic suite (Fig. 3)		
Big Sunday Formation	new name; replaces Masson Formation in southern part of South Alligator Valley; placed in El Sherana Group	Needham & Stuart-Smith (in prep.)
Coronation Sandstone	elevation to formation from member status; redefined; placed in El Sherana Group	Needham & Stuart-Smith (in prep.)
Edith River Group	new name; includes Phillips Creek, Kurrundie and Hindrance Creek Sandstones, Plum Tree Creek Volcanics, and Grace Creek Granite	Needham & Stuart-Smith (in prep.)
Edith River Volcanics	name dropped; units moved to Edith River Group or El Sherana Group	Needham & Stuart-Smith (in prep.)
El Sherana Group	new name; includes Big Sunday and Tollis Formations, Coronation Sandstone, and Pul Pul Rhyolite	Needham & Stuart-Smith (in prep.)
Grace Creek Granite	redefined; extent diminished	Needham & Stuart-Smith (in prep.)
Hindrance Creek Sandstone	elevation to formation from member status, placed in Edith River Group; change in correlation	Needham & Stuart-Smith (in prep.)
Kombolgie Formation	felsic volcanic member ('Plum Tree Creek Volcanic Member') elevated to formation status and moved to Edith River Group; intermediate to mafic members recorrelated	Needham & Stuart-Smith (in prep.)
Kurrundie Sandstone	elevation to formation from member status; placed in Edith River Group; change in correlation	Needham & Stuart-Smith (in prep.)
Phillips Creek Sandstone	elevation to formation from member status; placed in Edith River Group; change in correlation	Needham & Stuart-Smith (in prep.)
Plum Tree Creek Volcanics	elevation to formation from member status; moved from Kombolgie Formation to Edith River Group; redefined	Needham & Stuart-Smith (in prep.)
Pul Pul Rhyolite	elevation to formation from member status; redefined	Needham & Stuart-Smith (in prep.)
Tollis Formation	new name, replaces Burrell Creek Formation in Katherine–Grace Creek area; placed in El Sherana Group	Needham & Stuart-Smith (in prep.)

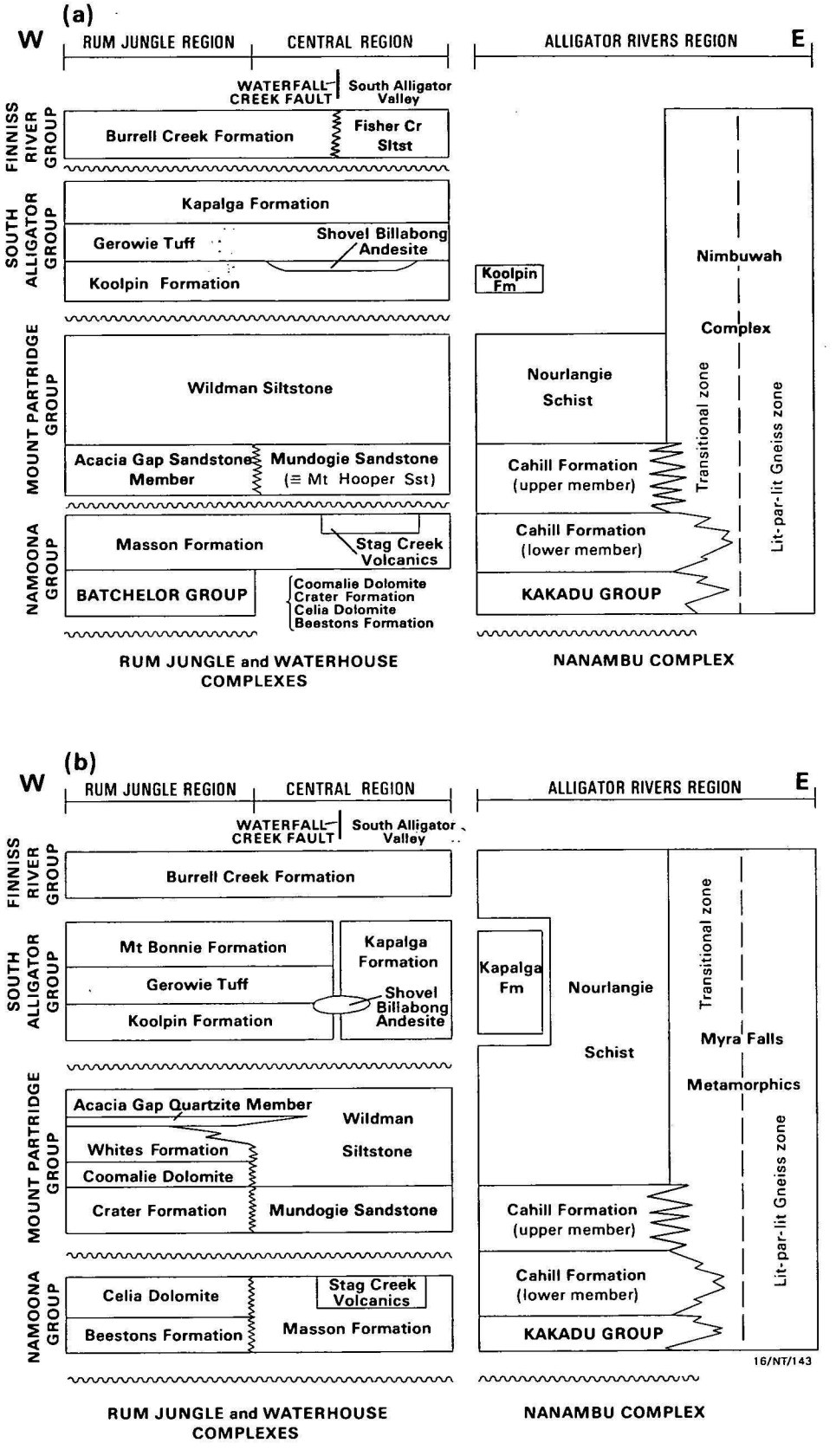

Figure 2. Diagrammatic stratigraphy of the Early Proterozoic Pine Creek Geosyncline sequence: (a) Needham & others, 1980; (b) this paper.

taries and papers (Crick, in preparation; Needham, 1982; Needham, 1984; Needham & Stuart-Smith, in preparation; Stuart-Smith & others, 1984a, 1984b). Changes to the nomenclature have been approved by the Territories Stratigraphic Nomenclature Committee and have been published or are in press (Table 1).

This paper summarises these changes and concludes the

mapping phase of the work. The updated stratigraphy raises significant implications for the stratigraphic distribution of uranium mineralisation.

Rum Jungle and central region

Needham & others (1980) correlated the **Mundogie Sandstone** with the **Acacia Gap Sandstone Member** (sic) of the **Wildman Siltstone** (Fig. 2a). However, following recent recognition of a lens of quartzite lithologically similar to the **Acacia Gap Quartzite Member** in the Mount Bundey area near the base of the Wildman Siltstone (Stuart-Smith & others, 1984a, Fig. 2); the Mundogie Sandstone is now correlated with the **Crater Formation** (of the former **Batchelor Group**). Both these units consist of coarse arenite and rudite. The Acacia Gap Quartzite Member and its correlative lens are overlain by the Wildman Siltstone, which, near its base, contains andesitic volcanics (**Mount Deane Volcanic Member** in the Rum Jungle region, not named in the Mount Bundey area; Stuart-Smith & others, 1984a). These are the only known volcanics of andesitic composition anywhere in the Proterozoic sequence in these two areas, thus giving further support to the new correlation.
The calcareous and carbonaceous shale hosting the uranium and base-metal deposits at Rum Jungle was previously placed in the **Masson Formation** (Needham & others, 1980). This has now been redefined as the **Whites Formation** (Crick, in preparation), and, together with the underlying **Coomalie Dolomite**, is regarded as a facies variant of the Wildman Siltstone (Crick, in preparation; Stuart-Smith & others, 1984a).

In the central region, the Mundogie Sandstone forms the base of the **Mount Partridge Group**, resting unconformably or disconformably on older rocks. A similar relationship may be implied for the Crater Formation, which is poorly sorted, polymictic, and conglomeratic, and which invariably has a sheared lower contact. Consequently, the units beneath the Mount Partridge Group, viz. the Masson Formation and **Stag Creek Volcanics (Namoona Group)** in the central region and the **Celia Dolomite** and **Beestons Formation** in the Rum Jungle region, are now thought to be equivalents. The Celia Dolomite and Beestons Formation have been placed in the Namoona Group, and the name Batchelor Group has been dropped.

The term **Mount Hooper Sandstone** was used by Needham & others (1980) to describe outcrops of sandstone, siltstone, and conglomerate between the South Alligator River and Mary River north of the Arnhem Highway. The unit was correlated with the Mundogie Sandstone on the basis of lithological similarity and an apparently similar stratigraphic position. Later work (Stuart-Smith & others, 1984a, 1984b) has determined continuity between the two units, and the name Mundogie Sandstone has, therefore, been extended to cover both. The name Mount Hooper Sandstone has been dropped.

South Alligator Valley area of the central region

The upper unit of the **South Alligator Group**, was defined as the **Kapalga Formation** by Needham & others (1980). However, there is now known to be a distinct change in its lithology across a major northwest-trending fault, the Waterfall Creek Fault, in the South Alligator Valley (Needham & Stuart-Smith, 1984). West of the fault to the Rum Jungle area, the rocks are interbedded greywacke, ferruginous siltstone (carbonaceous at depth) with chert bands and nodules, and tuff and argillite. The tuff and argillite represent the closing stages of **Gerowie Tuff** felsic volcanism. East of the Waterfall Creek Fault, there is no tuff in the sequence: the rocks are interbedded hematitic siltstone, chert-banded siltstone (carbonaceous at depth), and greywacke, and are similar to the non-volcanic rocks west of the fault. Some outcrops lack greywacke and more closely resemble the **Koolpin Formation**, so the stratigraphic level and formational status of these rocks are, in places, equivocal. However, the sequence east of the fault is regarded as continuous from the base of the South Alligator Group, and the name Kapalga Formation has been retained for this. West of the fault, the top unit of the South Alligator Group has been redefined as the **Mount Bonnie Formation** (Stuart-Smith & others, in preparation).

The **Fisher Creek Siltstone** was a term introduced by Walpole & others (1968) to describe siltstone and sandstone in the east of the central region, grading into schist in the Alligator Rivers Region, which they placed in the South Alligator Group. Needham & others (1980) regarded these rocks as part of the **Finniss River Group**, and in view of the similarity in lithology, dropped the name Fisher Creek Sandstone and extended the **Burrell Creek Formation** to include them. At that time, the type area of the Fisher Creek Siltstone had not been examined in the 1:100 000-scale mapping program, so in deference to earlier workers this name was perpetuated on some maps (e.g. Needham, 1984; Stuart-Smith & others, 1984b). Recent work has indicated that the type area consists of Burrell Creek Formation with anticlinal inliers of Kapalga Formation; so the term Fisher Creek Siltstone has been dropped.

Alligator Rivers region

Needham (1982) renamed the **Transitional** and **Lit-par-lit Gneiss Zones** of the **Nimbuwah Complex** (Needham & others, 1980) the **Myra Falls Metamorphics**, on the presence of resisters of sedimentary rock, which indicated a sedimentary origin. He retained the name Nimbuwah Complex for the **Migmatite Zone** and **Granitoid Core**, whose igneous origin was indicated by isotopic studies (Page & others, 1980).

We have since found that the broad gradation to less obvious migmatite structures northeastwards is due mainly to less compositional difference between the leucosome and melanosome components of the rocks in the northeast part of the Granitoid Core. We therefore recommend that no zonal distinction be made in the Nimbuwah Complex from the presence or otherwise of migmatite structures. The locally distinct granite plugs that lack migmatite structures (delineated on the 1:500 000 geological map accompanying Needham & others, 1980, and included in their Nimbuwah Complex) may be unrelated to the development of the migmatite.

Iron-rich chert-banded carbonaceous schist west and southwest of Oenpelli in the Alligator Rivers region, regarded by Needham (1984) as metamorphosed Koolpin Formation, is now placed in the Kapalga Formation, to reflect its uncertain stratigraphic position in the South Alligator Group. For the same reason, the stratigraphic range of the **Nourlangie Schist** has been extended to include all levels above the **Cahill Formation**, implying that it may be a metamorphosed equivalent of any or all of the Wildman Siltstone, South Alligator Group (specifically Kapalga Formation), and Burrell Creek Formation.

Felsic volcanic suite

Walpole & others (1968) defined the **Edith River Volcanics** and placed them in the Middle Proterozoic **Katherine River Group**. Needham & others (1980) removed them from the Katherine River Group, recognising that, between their formation and the deposition of the overlying **Kombolgie Formation**, there was a time break of at least 50 Ma, during which lopoliths of Oenpelli

Dolerite (1690 Ma) were intruded and subsequently exposed by erosion.

Recently, Needham & Stuart-Smith (in preparation) have defined two groups within the felsic volcanic suite, the **Edith River Group** and the **El Sherana Group**, separated by an unconformity and intrusion of syn-orogenic to post-orogenic granitoid plutons, dated at about 1760–1800 Ma (Page & others, 1980; Riley, 1980).

The older El Sherana Group rests unconformably on the geosynclinal sequence, which was deformed and metamorphosed between 1870 and 1800 Ma. Valley-fill sandstone and volcanics of the **Coronation Sandstone** form the basal part of the sequence and, with the overlying **Pul Pul Rhyolite**, are restricted to the South Alligator Valley. These two formations include rocks mapped previously as the **Coronation Member** and **Pul Pul Rhyolite Member** and undifferentiated Edith River Volcanics (Walpole & others, 1968), and are, in places, hornfelsed by the post-orogenic **Malone Creek Granite**. The uppermost part of the group is named the **Big Sunday Formation** in the South Alligator Valley. Elsewhere, it is named the **Tollis Formation**.

The El Sherana Group is overlain unconformably by the Edith River Group. The **Phillips Creek Sandstone**, **Kurrundie Sandstone**, and **Hindrance Creek Sandstone** form the base of the group. The Kurrundie Sandstone was previously the **Kurrundie Member** of the Kombolgie Formation (Walpole & others, 1968).

The greatest part of the Edith River Group consists of the **Plum Tree Creek Volcanics**, an extensive predominantly ignimbrite body stretching from west of the Edith River area, over most of the Grace Creek area, and north to the South Alligator Valley. It includes rocks from Walpole & others' (1968) **Plum Tree Creek Volcanic Member** of the Kombolgie Formation, parts of their Grace Creek Granite, and their Edith River Volcanics in the west of the Edith River area. In the Grace Creek area, the ignimbrite sheet surrounds a zoned granite/ microgranite known as the **Grace Creek Granite**, which is probably a subvolcanic intrusion. This is essentially the same granite as that of the same name described by Walpole & others (1968), although its definition and extent have been modified.

Other changes in stratigraphic interpretation

Walpole & others (1968) correlated the Plum Tree Creek Volcanics with volcanic members of the Kombolgie Formation, and this correlation was applied by Needham & others (1980). Recognition of the unconformable relationship between the Plum Tree Creek Volcanics and Kombolgie Formation has shown this correlation to be incorrect. The volcanic members of the Kombolgie Formation, which are all more mafic than the Plum Tree Creek Volcanics and contain basalt and andesite with minor tuffaceous sediments, form two levels within the sandstone sequence of the formation. The lower level contains the **McAddens**, **Callanan**, **Birdie Creek** and **Nungbalgarri Volcanic Members**, which are in the Katherine, South Alligator Valley, Grace Creek, and Alligator Rivers regions, respectively. The upper level contains the **Henwood Creek Volcanic Member** in the Katherine region and the **Gilruth Volcanic Member** in the Alligator Rivers region; elsewhere the higher levels of the Kombolgie Formation are not preserved.

Walpole & others (1968) recognised hematitic siliceous breccias in the Rum Jungle (**'HQB'** – hematite quartz breccia) and South Alligator Valley (**Scinto Breccia Member**) areas, and made several suggestions as to their genesis. We believe they

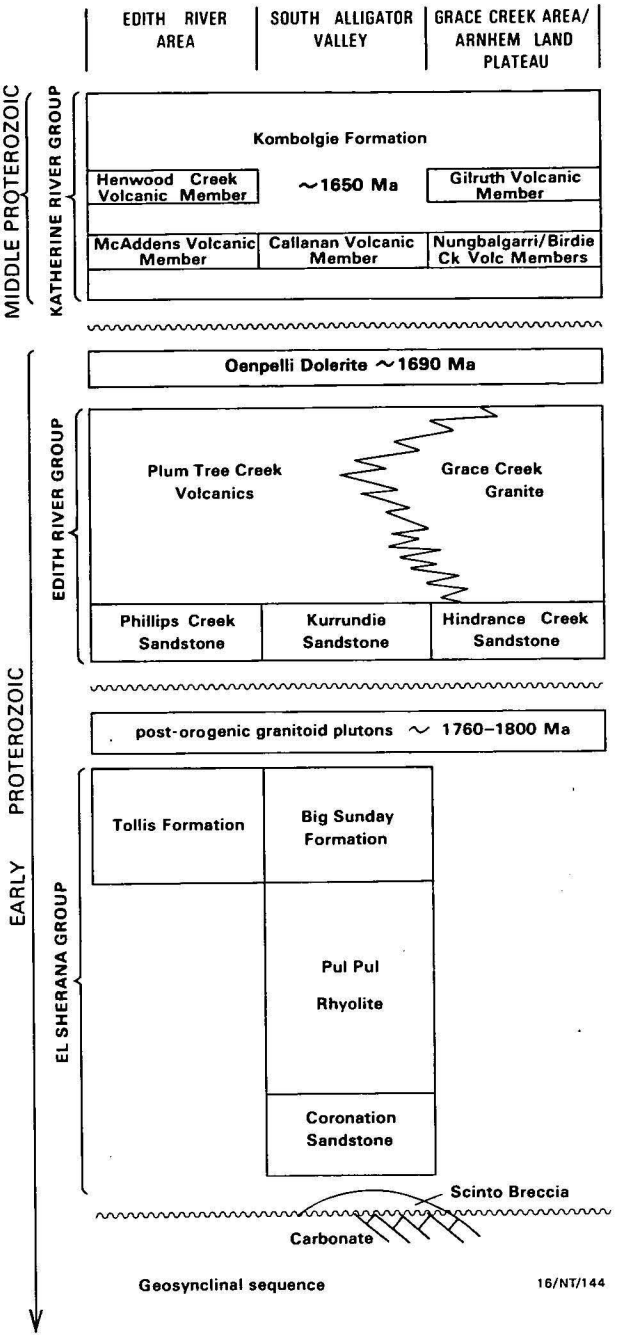

Figure 3. Diagrammatic stratigraphy of the late Early Proterozoic felsic volcanic suite and basal Middle Proterozoic platform cover.

formed by in-situ weathering and silicification of carbonate in the geosynclinal sequence, as carbonate is always present beneath or near the breccias. Consequently, their stratigraphic position is allied to weathering episodes represented by unconformity surfaces – the unconformity at the base of the Middle or Late Proterozoic **Tolmer Group at Rum Jungle** (Sweet, 1977), and the unconformity at the base of the El Sherana Group in the South Alligator Valley (Fig. 3). The 'HQB' is now formally named **Buckshee Breccia** (Crick, in preparation) and we have elevated the **Scinto Breccia** to formation status (Needham & Stuart-Smith, in preparation).

Implications for stratigraphic distribution of mineralisation

The new stratigraphic nomenclature and correlations place the

Rum Jungle U-Cu-Pb-Co-Ni mineralisation in the Whites Formation of the Mount Partridge Group instead of in the Masson Formation, as considered previously (Needham & others, 1980). Thus, the revised correlations show that the three areas of uranium mineralisation in the Pine Creek Geosyncline (Rum Jungle, South Alligator Valley, and Alligator Rivers Uranium Fields; Needham & Roarty, 1980) lie at three different stratigraphic levels, in the Whites Formation, Koolpin Formation, and Cahill Formations, respectively. Mineralisation at Rum Jungle and in the Alligator Rivers region is in the lowest calcareous/carbonaceous assemblage, and next to Archaean basement. Uranium and gold mineralisation in the South Alligator Valley is confined to carbonaceous siltstones, distant from Archaean basement, but faulted against the El Sherana Group.

References

Crick, I.H., in preparation - Rum Jungle Uranium Field, Northern Territory. *Bureau of Mineral Resources, Australia, 1:100 000 Geological Map Commentary.*

Dunn, P.R., 1962 - Alligator River, N.T. - 1:250 000 Geological Series. *Bureau of Mineral Resources, Australia, Explanatory Notes* D/53-1.

Needham, R.S., 1982 - Nabarlek Region, Northern Territory. *Bureau of Mineral Resources, Australia, 1:100 000 Geological Map Commentary.*

Needham, R.S., 1984 - Alligator River, Northern Territory - 1:250 000 Geological Series. *Bureau of Mineral Resources, Australia, Explanatory Notes* D/53-1, Second Edition.

Needham, R.S., & Roarty, M.J., 1980 - An overview of metallic mineralisation in the Pine Creek Geosyncline. *In* Ferguson, J., & Goleby, A.B., (editors). Uranium in the Pine Creek Geosyncline. *International Atomic Energy Agency, Vienna.* 154-174.

Needham, R.S., & Stuart-Smith, P.G., 1984 - The relationship between mineralisation and depositional environment in Early Proterozoic metasediments of the Pine Creek Geosyncline. *Australasian Institute of Mining and Metallurgy, Darwin Conference, 1984,* 201-211.

Needham, R.S. & Stuart-Smith, P.G., in press - The Early to Middle Proterozoic transition in Northern Australia. *Australian Journal of Earth Sciences.*

Needham, R.S., Crick, I.H. & Stuart-Smith, P.G., 1980 - Regional geology of the Pine Creek Geosyncline. *In* Ferguson, J., & Goleby, A.B. (editors), Uranium in the Pine Creek Geosyncline. *International Atomic Energy Agency, Vienna.* 1-22.

Page, R.W., Compston, W., & Needham, R.S., 1980 - Geochronology and evolution of the late-Archaean basement and Proterozoic rocks in the Alligator Rivers Uranium Field, Northern Territory, Australia. *In* Ferguson, J., & Goleby, A.B., (editors), Uranium in the Pine Creek Geosyncline. *International Atomic Energy Agency, Vienna.* 39-68.

Riley, G.H., 1980 - Granite ages in the Pine Creek Geosyncline. *In* Ferguson, J., & Goleby, A.B., (editors) Uranium in the Pine Creek Geosyncline. *International Atomic Energy Agency, Vienna.* 69-72.

Stuart-Smith, P.G., Wallace, D.A., & Roarty, M.J., 1984a - Mary River-Point Stuart Region, Northern Territory. *Bureau of Mineral Resources, Australia, 1:100 000 Geological Map Commentary.*

Stuart-Smith, P.G., Needham, R.S., Roarty, M.J. & Crick, I.H., 1984b - Mundogie, Northern Territory. *Bureau of Mineral Resources, Australia, 1:100 000 Geological Map Commentary.*

Stuart-Smith, P.G., Needham, R.S., Bagas, L., & Wallace, D.A., in preparation - Pine Creek, Northern Territory. *Bureau of Mineral Resources, Australia, 1:100 000 Geological Map Commentary.*

Sweet, I.P., 1977 - The Precambrian geology of the Victoria River region, Northern Territory. *Bureau of Mineral Resources, Australia, Bulletin* 168.

Walpole, B.P., Crohn, P.W., Dunn, P.R. & Randal, M.A., 1968 - Geology of the Katherine-Darwin region, Northern Territory. *Bureau of Mineral Resources, Australia, Bulletin* 82.

BMR Journal of Australian Geology & Geophysics, 9, 239-254

New discoveries of Devonian vertebrates from the Amadeus Basin, central Australia

G.C. Young[1]

Devonian vertebrate occurrences are reviewed from nine localities in the Amadeus Basin, of which five are new. Acanthodian, phyllolepid placoderm, rhipidistian, and dipnoan fishes are recorded from near Stokes Pass, for the first time from the Parke Siltstone of the Pertnjara Group. Several different species of the antiarch *Bothriolepis* are provisionally identified in the same faunas. An older fauna, which contains phlyctaeniid euarthrodires, other placoderms, and acanthodians, but not *Bothriolepis*, is definitely known only from an occurrence at Gosses Bluff. The stratigraphic position of this assemblage is uncertain. Comparisons of sediment thickness between broadly equivalent fossil horizons in the Dulcie Sandstone (Georgina Basin) suggest that if the Gosses Bluff fauna occurs in basal beds of the Mereenie Sandstone, then this probably does not correspond to the base of the formation in other sections where it attains a much greater thickness. It is suggested that the Gosses Bluff fauna may correlate with the *Wuttagoonaspis* assemblage from the Merrimerriwa Formation of the Mulga Downs Group in western New South Wales and the Cravens Peak Beds and lower Dulcie Sandstone in the Georgina Basin. The age of this assemblage is probably late Early Devonian. Evidence provided by palynology and vertebrate palaeontology for the age of the Parke Siltstone is reviewed, and a Givetian-Frasnian age is suggested. The placoderm *Phyllolepis* is a typical Late Devonian form, but its downward range in Australian sequences is not yet established. Acanthodian and dipnoan evidence points to a Middle Devonian age. Regarding the age of the underlying Mereenie Sandstone, it seems unlikely that the whole formation is Devonian. The Rodingan Movement was more likely a Silurian event. It is possible that the age of magnetisation measured from the lower part of the Mereenie Sandstone at Ellery Creek is Early Devonian or older, and thus consistent with a subplate model for the Palaeozoic apparent polar wander curve for Australia. The presence of *Phyllolepis* and *Wuttagoonaspis* in the central Australian Devonian fish faunas indicates affinities with southeastern Australia, where these taxa are known from many localities.

Introduction

That Devonian strata are present in the Palaeozoic sequences of central Australia was suggested almost a century ago by Chewings (1891). However, this was not confirmed by fossil evidence until Hills (1959) described fish remains of probable Late Devonian age from sandstones in the Dulcie Range, about 330 km northeast of Alice Springs, on the western margin of the Georgina Basin. Farther west, in the Amadeus Basin, another Devonian fish locality was discovered in 1963 by R.M. Hopkins (Magellan Petroleum) from a level within the Pertnjara Group (Gilbert-Tomlinson, 1968). Together with poorly preserved macroplants and the evidence of spores (Hodgson, 1968) these pointed also to a Late Devonian age for the Pertnjara Group. The significance of these and several other vertebrate localities of probable Devonian age in central Australia (Gosses Bluff in the Amadeus Basin, and the Toko Syncline area in the Georgina Basin) was discussed by Gilbert-Tomlinson (1968) in a general review of Late Devonian fish occurrences in Australia, as they were then known.

In 1973, 1974, and 1977 I visited areas of Devonian and older outcrop in the Amadeus and Georgina Basins to obtain more comprehensive collections of Palaeozoic vertebrates for biostratigraphic and systematic study. Several new localities were found, and further specimens were collected from previously known sites (Fig. 1). Sediments of the Finke Group in the southeastern part of the Amadeus Basin were also ex-

[1]Division of Continental Geology, BMR

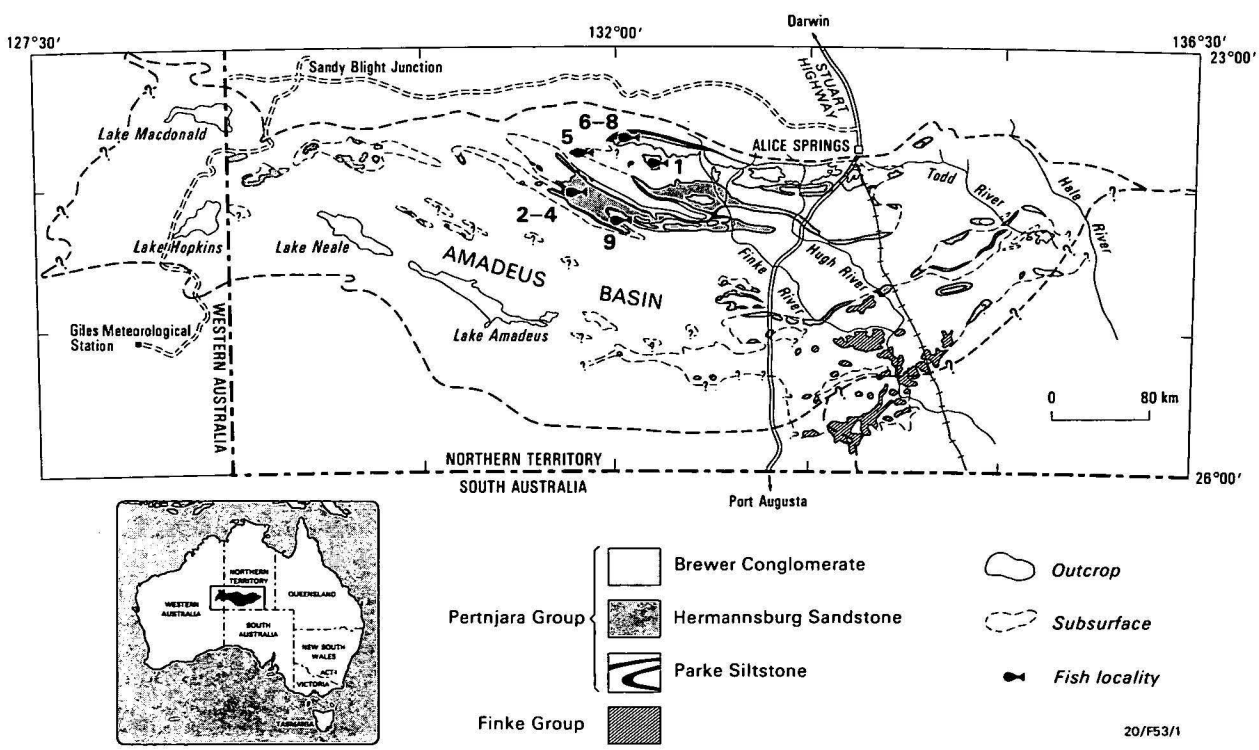

Figure 1. Distribution of the Pertnjara and Finke Groups in the Amadeus Basin, central Australia, showing general localities (1-9) for the Devonian vertebrate occurrences discussed in this paper.

amined, but vertebrate remains were not discovered. Some of the new localities have yielded substantial quantities of diverse vertebrate material, representing several different horizons within the Devonian sequence. The bulk of these collections has now been prepared, and detailed systematic study should provide much new information on the nature and significance of the assemblages from biostratigraphic, biogeographic, and evolutionary standpoints. In the course of this work I have also re-examined various samples from central Australia in the collection of the late Joyce Gilbert-Tomlinson, submitted by a number of field surveys (BMR, Frome Broken Hill, Magellan Petroleum) over the past twenty years.

This is the first of two papers providing a preliminary summary of faunal content, biostratigraphy, and locality data for the Devonian vertebrate occurrences of central Australia. A second paper will deal with new discoveries in the Georgina Basin. Systematic descriptions of the new forms in these faunas will be presented elsewhere. Since the review of Gilbert-Tomlinson (1968) there have been several contributions mentioning or discussing Palaeozoic vertebrate localities or faunas from central Australia, including Jones (1972), Young (1974, 1984a), Playford & others (1976), Ritchie (1973), Ritchie & Gilbert-Tomlinson (1977), Turner & others (1981), and Young & Gorter (1981). A general account of the geology of the Amadeus Basin was given by Wells & others (1970). A more detailed summary of Pertnjara Group stratigraphy (Jones, 1972) forms the stratigraphic framework for the present account.

With few exceptions the Devonian vertebrate remains from central Australia are deeply weathered, and all traces of bone tissue have been lost. All the specimens discussed below have been studied as latex rubber casts of impressions preserved in sandstone. The material is housed in the Commonwealth Palaeontological Collection (prefix CPC), in the Bureau of Mineral Resources, Canberra.

General stratigraphy

The Pertnjara Group, as defined by Wells & others (1970), comprises fluviatile sandstones and conglomerates and some probable lacustrine siltstone units with a maximum preserved thickness of about 3600 m and combined area in outcrop and subsurface within the Amadeus Basin of some 32 000 km² (Fig. 1). It is underlain by another widespread unit, the Mereenie Sandstone, which has a maximum preserved thickness of about 1000 m in the Gardiner Range area and extends over an area in subsurface and outcrop of about 16 000 km². Devonian vertebrates have been reported from the Mereenie Sandstone and the Parke Siltstone, the lower two of three formations making up the Pertnjara Group (Wells & others, 1970). Jones (1972) proposed a subdivision of the Pertnjara Group into eight members, the lower four constituting the Parke Siltstone of previous authors (Fig. 2). However, there are many problems of detailed stratigraphy where the geology of specific areas departs from the simple scheme indicated by this composite section. The various units within the Pertnjara Group differ considerably in thickness, and the lowermost Deering Siltstone and Harajica Sandstone Members of the Parke Siltstone – the latter containing several vertebrate localities – have only been recognised in the Ellery Creek–Deering Hills region in the central part of the northern margin of the basin (Jones, 1972, figs 5, 7). Consequently, the extrapolation of a fossiliferous datum outside its area of occurrence is not a straightforward exercise, and any generalisations about the age of such widespread units must be seen as tentative. The same applies to the Mereenie Sandstone, which is also of considerable lateral extent, and apparently of fairly consistent

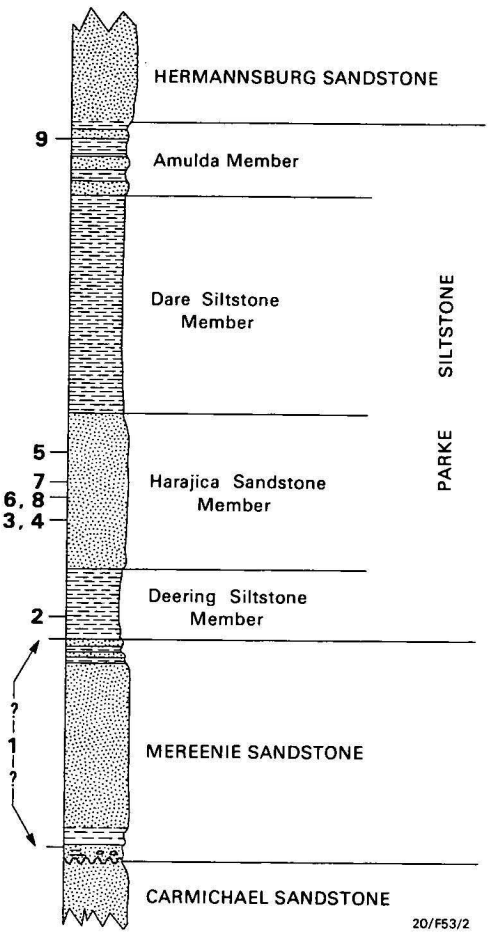

Figure 2. Composite stratigraphic column for formations in the Larapinta Group (Carmichael Sandstone), and Pertnjara Group (Parke Siltstone, Hermannsburg Sandstone), and the Mereenie Sandstone, showing all members of the Parke Siltstone as defined by Jones (1972).

Assumed relative stratigraphic levels for the Devonian vertebrate occurrences discussed in this paper shown on the left (1–9). Not to scale.

lithology. No formal subdivision of this formation has been proposed, but some problems relating to its basal beds are discussed below.

Vertebrate localities

The general location and stratigraphic horizon for each of the nine known Devonian vertebrate localities from the Amadeus Basin are summarised in Figures 1 and 2, and more detailed local geology is illustrated in Figures 3, 4, 6, and 9. Details on the occurrence, fauna, and age of each locality are summarised in turn below, as numbered in Figure 1. Considerably older vertebrate occurrences in the Stairway and Carmichael Sandstones (Ritchie & Gilbert-Tomlinson, 1977) and the Pacoota Sandstone (Early-Middle Ordovician) will be dealt with elsewhere.

Locality 1. Gosses Bluff

Occurrence. This may be the oldest Devonian vertebrate fauna so far known from the Amadeus Basin, and is of special interest because it may provide evidence for the age of the Mereenie Sandstone. However, there is uncertainty about the stratigraphic level of the occurrence, because of difficulties in interpreting the stratigraphy at Gosses Bluff. Gosses Bluff is the central uplifted part of a highly complex impact structure of

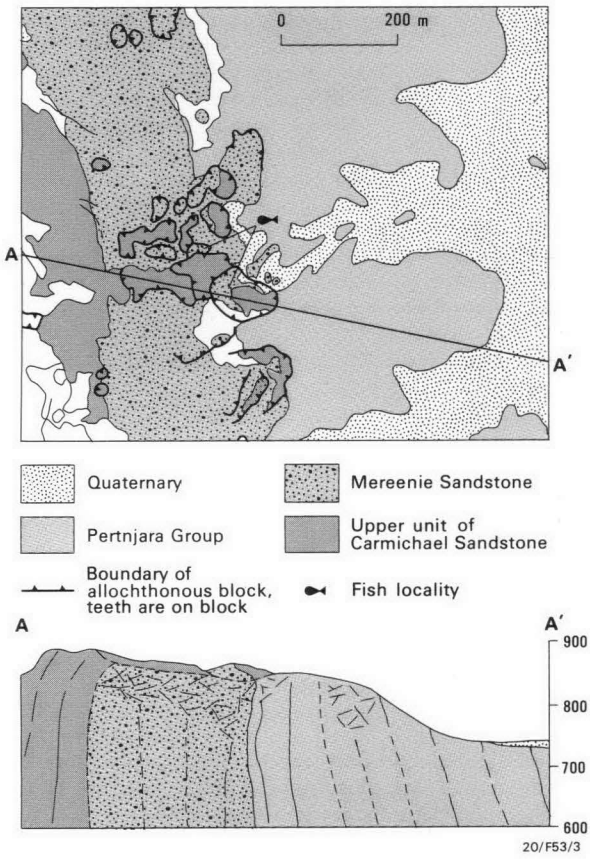

Figure 3. Geological map and section through part of the eastern rim of Gosses Bluff.

Simplified from the 1:7500 geological map 'Gosses Bluff Impact Structure, Northern Territory', published by the Bureau of Mineral Resources, 1978.

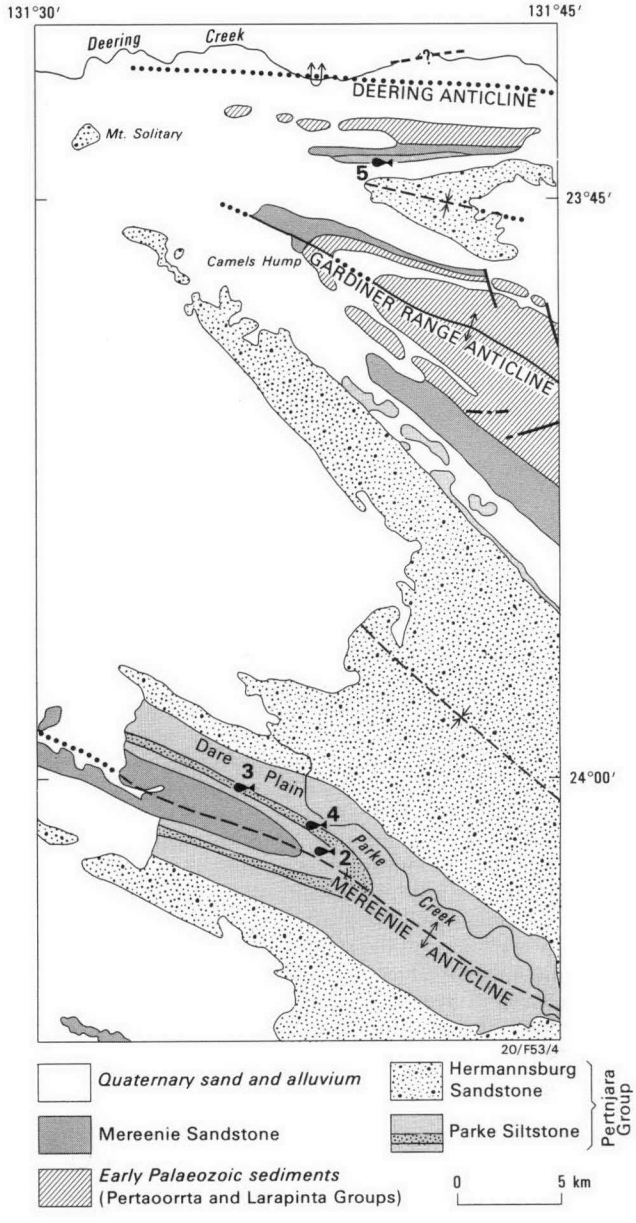

Figure 4. General geology of the Dare Plain and Deering Hills areas, simplified from the Lake Amadeus (south of 24°00'S) and Mount Liebig 1:250 000 geological sheets.

Devonian vertebrate localities shown are at Dare Plain (2–4), and Deering Hills (5, approximate).

Mesozoic age, which severely disrupted the Palaeozoic sediments in a zone about 20 km across (e.g. Crook & Cook, 1966; Milton & others, 1972).

The fish remains were discovered in 1966 by P.J. Cook in the eastern rim of Gosses Bluff, and further material was collected by D.J. Milton from an adjacent locality in 1967. The fossils are associated with allochthonous blocks of white sandstone. There is little doubt, however, that these blocks have been overturned, and that the fossiliferous red sandstone is also allochthonous and stratigraphically overlies the white sandstone, as detailed mapping by D.J. Milton has shown (Fig. 3). Milton (1967, and unpublished ms; see also Milton & others, 1972, fig. 3) identified the white sandstone, previously mapped as Mereenie Sandstone (e.g. Crook & Cook, 1966, fig. 4), as an uppermost sandstone unit belonging to the Larapinta Group (an unnamed upper member of the Carmichael Sandstone). As such, the beds containing the fish remains, which are immediately above the contact with this unnamed unit, would represent the base of the Mereenie Sandstone. However, this basal red sandstone has not been recognised as part of the Mereenie Sandstone elsewhere. A thin basal conglomerate was reported in the Mereenie Sandstone in the northeastern part of the Amadeus (Wells & others, 1970, p. 88). But the basal unit of red-brown and pale purple-brown sandstones up to 90 m thick, previously reported from areas south of Gosses Bluff (Ranford & others, 1966) and in the Mount Liebig Sheet area (Wells & others, 1965), was subsequently separated out as a new formation, the Carmichael Sandstone, and defined as the uppermost formation of the Larapinta Group (Wells & others, 1970, p. 61). The Carmichael Sandstone is largely unfossiliferous, but an Ordovician age has been suggested on trace fossil evidence (Wells & others, 1970, p. 81), and fragmentary Ordovician vertebrates have been reported (Ritchie & Gilbert-Tomlinson, 1977). As such, the apparently conformable contact in the overturned blocks at Gosses Bluff, between the white sandstone interpreted by Milton as the uppermost Larapinta unit and the red sandstone containing the Gosses Bluff fish fossils, would represent a considerable time gap (Late Ordovician–Early Devonian). Milton (unpublished ms) has interpreted this contact at Gosses Bluff as corresponding to the regional unconformity between the Mereenie Sandstone and the underlying Larapinta Group.

The unnamed sandstone unit interpreted by Milton as the upper part of the Carmichael Sandstone has also been identified by him in a 60 m interval of the Tyler No. 1 well, about 15 km northeast of Gosses Bluff, and in the MacDonnell Ranges to the north, where it is said to thicken westward from a 15–25 m unit between Goyder Pass and Tyler Pass, to about 180 m thick

at Harajica (Stokes) Pass (Milton, unpublished ms). However, the unit has not been documented in previous sections measured in this area (e.g. Wells & others, 1970). In my opinion, its lithology, at least in the allochthonous blocks containing the fossiliferous beds, is not clearly distinguishable from Mereenie Sandstone (with which it was confused in previous mapping at Gosses Bluff). A possible alternative interpretation is that this white sandstone represents the top of the Mereenie Sandstone, and the overlying fossiliferous redbeds are the base of the Pertnjara Group. In many areas the lowermost Parke Siltstone of the Pertnjara Group appears to lie conformably on Mereenie Sandstone (Jones, 1972, p. 231), and in the section at Stokes Pass, for example, the transition consists of several interbeds of white Mereenie Sandstone and red sandstone or siltstone units. In the allochthonous blocks at Gosses Bluff, as noted above, the white and red sandstones appear to be conformable.

To summarise, there are currently two possible interpretations of the stratigraphic position of these Devonian fish remains. The first, based on detailed geological mapping at Gosses Bluff, is that they occur in basal redbeds of the Mereenie Sandstone. This implies a late Early and Middle Devonian age for the whole of the Mereenie Sandstone, a considerable time gap between it and the underlying Carmichael Sandstone, and some special features in the stratigraphy at Gosses Bluff (basal redbeds of the Mereenie Sandstone, and an additional upper sandstone unit of the Carmichael Sandstone). The alternative hypothesis is that the fish remains occur in basal redbeds belonging to the Pertnjara Group, which conformably overlies the Mereenie Sandstone. This implies a pre-Middle Devonian age for the Mereenie Sandstone, but invokes a special interpretation of the allochthonous blocks containing the fish fossils, consistent with the Mereenie–Pertnjara transition as observed in some other sections, but not in accord with the detailed mapping of the rest of the Gosses Bluff structure. Discovery of new fossil localities at Gosses Bluff or elsewhere and more detailed work on lithological changes across the Carmichael–Mereenie contact should permit a decision between these alternatives. As discussed below, a comparison of sediment thickness with the Dulcie Sandstone in the Georgina Basin, the closest known occurrence of assumed correlatives of the Gosses Bluff fish fauna, indicates that, if the fish horizon does occur at the base of the Mereenie Sandstone at Gosses Bluff, this cannot be correlated with the base of the formation in other sections.

Fauna. Twenty-seven samples are available for study, but many of these are small indeterminate fragments. All are preserved as impressions in sandstone. The collection includes three larger plates with tubercular ornament from Cook's locality (CPC24664, 24665), and another from Milton's (CPC24666). These and about 10 small fragments with similar ornament may be tentatively referred to one or two closely related placoderms. However, only the originally collected specimen (CPC24664) provides any significant morphological details indicating the affinities of the material. This is a fairly large (at least 80 mm long) apparently unpaired plate, incompletely preserved in part and counterpart. The external surface (Fig. 5A) is covered with coarse tubercles, which in the posterolateral parts of the bone show a strong concentric alignment and form a crowded zone inside the posterior margin. Only the central part of the posterior margin is preserved, but the configuration of tubercle rows suggests a fairly short, broad overall shape for the bone. The counterpart shows a strong internal thickening along the posterior margin. The bone was strongly arched, with the laminae of each side enclosing an angle of about 100° at the posterior margin. These features indicate that this is a nuchal plate from the skull of a euarthrodiran placoderm. A similar but somewhat smaller specimen from the Toko Syncline in the Georgina Basin resembles the Gosses Bluff specimen in its strong arching to 100°, well-developed nuchal thickening, and tendency to alignment of tubercles in concentric rows. The nuchal thickening is seen only in certain groups of phlyctaenioid euarthrodires (e.g. groenlandaspids, brachythoracids; Young, 1981), and the relatively short and broad overall shape of the nuchal as displayed in the Georgina Basin specimen is consistent with this. A possibly distinctive feature of the ornament in CPC24664 is the concentration of larger crowded tubercles in the vicinity of the ossification centre of the bone. An associated impression, of similar size and ornamentation, may belong to the same individual, but, as none of the bone margins are preserved, its position in the skeleton could not be determined.

In addition to the smaller fragments with similar ornament mentioned above, there are three examples (CPC24667–24669) of small plate impressions with a much finer tubercular ornament, which may represent smaller individuals of this or another placoderm.

Also in the collection are several elongate or spine-like elements, mostly too poorly preserved for determination. However, one relatively well-preserved specimen is a curved spine ornamented with nine longitudinal ridges, decreasing in size posteriorly (Fig. 5B). This is possibly part of a placoderm spinal plate. Another specimen (CPC24671) shows a small area of placoderm ornament about 15 mm across, on which irregular tubercles grade into subparallel ridges. This feature is seen at the junction of the spinal and anterior lateral plates in several placoderms from the Cravens Peak Beds. CPC24672, in size (length about 70 mm) and curved shape, could be a fairly complete phlyctaenioid spinal plate, but is too poorly preserved for this to be confirmed. A number of other fragments ornamented with subparallel ridges may also be portions of spines, but it is possible that some also derive from a placoderm with a general ornament of concentric ridges. Such fragments are fairly common at certain localities in the Cravens Peak Beds in the Georgina Basin, where they are ascribed to *Wuttagoonaspis*. However, none of the distinctive features of *Wuttagoonaspis* has been observed in the Gosses Bluff material. Finally, CPC24673 is a slender, fairly straight spine about 20 mm long, on which at least three longitudinal ridges can be discerned. The proximal part is devoid of ridges and may be an inserted part of the spine, which is therefore probably referable to the Acanthodii.

In view of the poor preservation and fragmentary nature of this material, these determinations are tentative, but it seems that at least three taxa are represented: a phlyctaenioid (?groenlandaspid) euarthrodire, an acanthodian, and another form with ridged ornament, possibly *Wuttagoonaspis*.

Age. This fauna, although poorly known, may be assumed on the evidence just presented to correspond to the much more diverse fauna from the lower Dulcie Sandstone and Cravens

Figure 5.

A, incomplete nuchal plate of a phlyctaeniid euarthrodire in external view, CPC24664, x 1. B, incomplete element, probably a placoderm spinal plate, CPC24670, x 2. A & B from Gosses Bluff (locality 1). C, *Bothriolepis* sp., incomplete posterior median dorsal plate in dorsal view, CPC24678, x 1, from Deering Hills (locality 5). D,E, *Bothriolepis* sp., two posterior ventrolateral plates, probably conspecific: D, CPC24675, from locality 4, x 1; E, CPC 24688, from locality 8, x 1. F, *Bothriolepis* sp., ventrolateral plate, CPC24709, from locality 9, x 1.5. G,H, *Bothriolepis* sp., probably conspecific with D,E: G, incomplete left anterior dorsolateral, CPC6922, x 1, same specimen from locality 4 (Dare Plain) as figured by Gilbert-Tomlinson (1968, pl. 15, figs. 1, 3–5); H, incomplete left anterior ventrolateral from locality 7, CPC24689, x 1.5. I, *Bothriolepis* sp., a left posterior ventrolateral plate, belonging to another species, from locality 6, CPC24687, x 1. All specimens whitened with ammonium chloride.

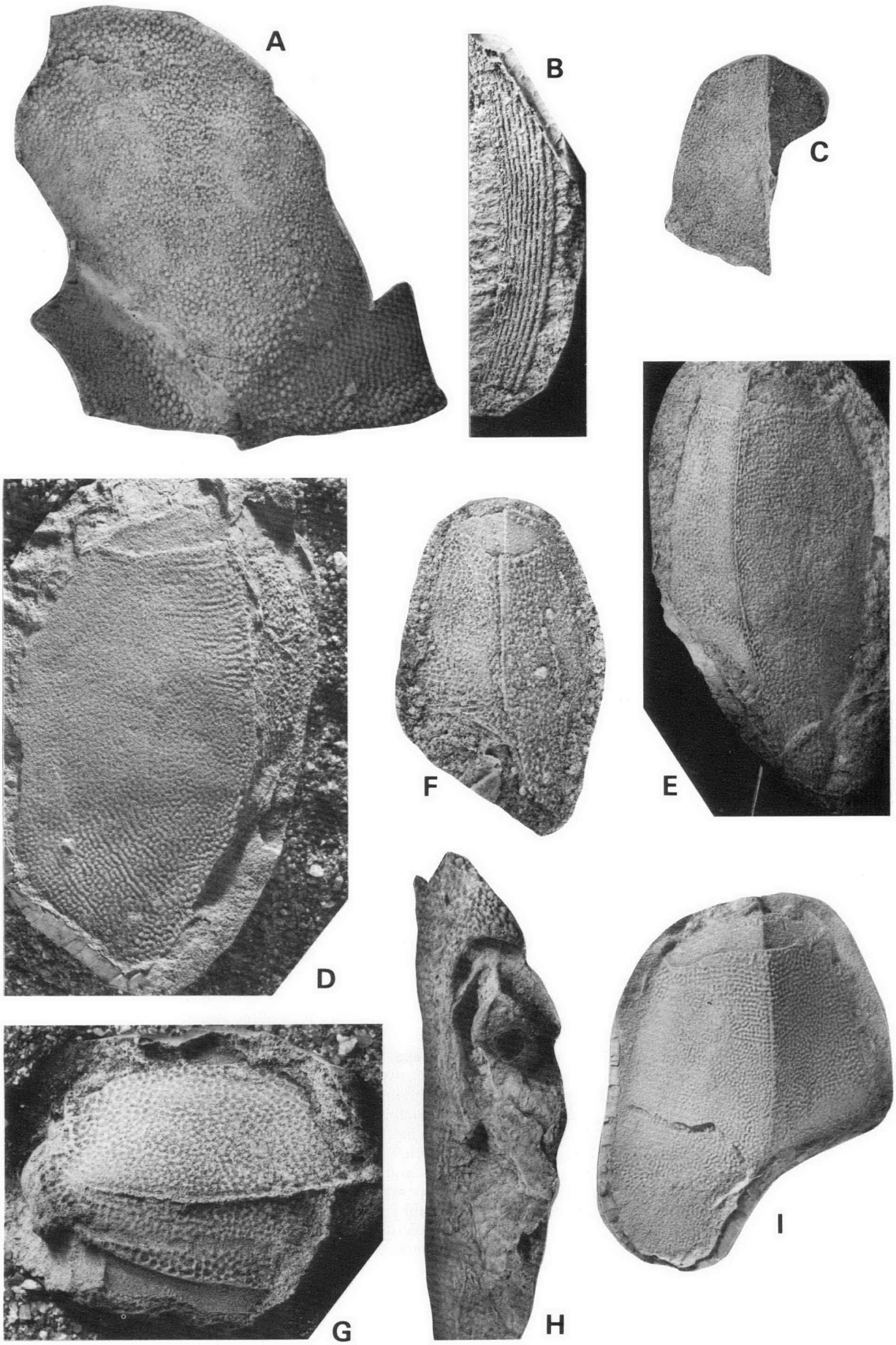
A
B
C
D
E
F
G
H
I

Peak Beds in the Georgina Basin. The latter fauna includes various placoderms (*Wuttagoonaspis*, groenlandaspids, actinolepids, antiarchs), acanthodians, crossopterygians, dipnoans, and thelodontid agnathans (Turner & others, 1981; Young, in press a). The Cravens Peak Beds fauna is assumed to correlate broadly with the *Wuttagoonaspis* fauna from the lower part of the Mulga Downs Group in western New South Wales (Ritchie, 1973), although detailed systematic work is required to confirm this. A maximum age of Emsian (late Early Devonian) is indicated for the base of the Mulga Downs Group, which overlies the marine Amphitheatre Group containing brachiopods of Pragian age (Glen, 1979, 1982).

Locality 2. Dare Plain

Occurrence. Of several fish localities on Dare Plain, along the northern flank of the Mereenie Anticline, the lowest stratigraphically is an occurrence about 5 km southeast of Gilbert-Tomlinson's (1968) Dare Plain locality (see below), found by K.A.W. Crook. This was reported by Jones (1970, 1972 p. 234) to come from a thin, massive, light reddish-brown siltstone, 38 m above the base of the type section of the Deering Siltstone Member of the Parke Siltstone (Figs 2, 4).

Fauna. The only specimen (CPC24674) is an impression of placoderm ornament measuring 10 by 30 mm, with no margins preserved. The ornament comprises fairly coarse, regularly spaced tubercles, not unlike that on some of the specimens from Gosses Bluff. In the absence of plate margins, this specimen is undeterminable, although it almost certainly does not belong to *Bothriolepis*, in which the ornament is always more reticulate. It could come from a euarthrodire like the one from Gosses Bluff, but this would need to be established with better material.

Age. If it is assumed, as is indicated by the limited available evidence, that there are two main vertebrate faunas in the Mereenie–Pertnjara sequence, this occurrence could be tentatively correlated with the Gosses Bluff assemblage and provisionally assigned a late Lower–early Middle Devonian age. However, one difficulty with such a correlation is the fact that, in the Dare Plain sequence, a higher fossiliferous horizon, apparently of late Middle or early Late Devonian age, occurs no more than 100 m stratigraphically above this occurrence. This is further discussed below.

Locality 3, Dare Plain

Occurrence. Material from this locality (Fig. 4) was described by Gilbert-Tomlinson (1968), who also gave collecting details. The specimens come from 'near the top' of the Harajica Sandstone Member of the Parke Siltstone, and about 180 m above the local base of the formation according to Gilbert-Tomlinson (1968, p.217). However, Jones (1970; 1972, p. 236) gave the stratigraphic horizon as the uppermost fine sandstone about 55 m above the base of the Harajica Member, which is about 140 m above the base of the formation according to Jones' type section (1972, fig. 4).

Fauna. Gilbert-Tomlinson (1968) described three incomplete plates of the antiarch *Bothriolepis* from this locality. Two anterior dorsolateral plates were assumed to be conspecific (Gilbert-Tomlinson, 1968, p. 219). A third incomplete and indeterminate plate was tentatively referred to the genus. This is probably a portion of a trunk-shield plate from a larger individual, as indicated by the coarser reticulate ornament.

The evidence of new material from other localities now indicates that the two anterior dorsolateral plates represent different species. Gilbert-Tomlinson (1968, p. 220) noted some differences between them, which she attributed to intraspecific variability. However, the less complete example (CPC6923) compares closely in size and ornament with a fairly complete specimen (CPC24686) from locality 6 (near Stokes Pass), which is characterised by elongate overall proportions (length-breadth index 185), and a relatively acute angle (115–125°) between laminae. The dorsolateral ridge is fairly straight, and not produced as a crest. In contrast, CPC6922 (Gilbert-Tomlinson, 1968, pl. 15, figs 1, 3–5) has coarser, more reticulate ornament, an outward curvature of the dorsolateral ridge, which forms a distinct crest, and an obtuse angle (about 140°) between laminae (the measurement previously given for this angle is too low). This plate was probably shorter and deeper in proportion than CPC6923.

Gilbert-Tomlinson (1968) also compared this material with various species of *Bothriolepis* from Australia and elsewhere, but several of her points of similarity are general features for the genus, and of no significance at the species level. It was suggested, on the basis of comparison with the Victorian species *Bothriolepis gippslandiensis* Hills, that there may be a local group of closely related species. However, the morphological features indicating this have not proved significant in a recent revision of *B. gippslandiensis* and several new species from Victoria (Long, 1983b). Some points of resemblance were also noted with the *Bothriolepis* material described by Hills (1959) from the Dulcie Range in the Georgina Basin, but new evidence now indicates that different species are also involved here.

Age. Gilbert-Tomlinson (1968) originally dated these remains as Late Devonian, and probably no older than late Frasnian, but this was questioned by Young (1974) on the evidence of the presence of *Bothriolepis* in the early Frasnian Gogo Formation in the Canning Basin. Further material from new localities described below now indicates that the two species of *Bothriolepis* represented by these remains also occur in a more diverse assemblage from the Harajica Sandstone near Stokes Pass (locality 6, below). On the assumption that the absence of associated fauna at this Dare Plain locality is ecologically rather than stratigraphically controlled or due to incomplete sampling, I suggest a correlation between this fauna and the more diverse fauna from near Stokes Pass. Evidence for assigning the latter occurrence a late Middle or early Late Devonian age is discussed below.

Locality 4. Dare Plain

Occurrence. This locality was discovered in 1973 in the Harajica Sandstone Member, about 4 km southeast of the previous locality (Fig. 4). Disarticulated fish-plates of *Bothriolepis* were collected from a 40 cm thick massive bed of fine-grained clayey sandstone, about 2 m below the top of the Harajica Sandstone, in the second last cycle of the member.

Fauna. A fairly complete left posterior ventrolateral plate (Fig. 5D), two incomplete mixilaterals preserved in part and counterpart, and a few ornamented fragments from this locality are referable to *Bothriolepis*. The posterior ventrolateral is about 88 mm long, and represents an individual of moderate size (estimated length of armour about 170 mm). The mixilaterals are also fairly large, and resemble the posterior ventrolateral in the ornament of low, rounded, anastomosing ridges, the outward curvature of the dorsolateral and ventrolateral ridges, and their development into distinct crests. Comparison with material of the same species from locality 6 (see below) indicates that these specimens are conspecific with CPC6922, described by Gilbert-Tomlinson (1968) from the previous locality.

Age. As for the previous locality, it is assumed that the absence

of associated fauna is not biostratigraphically significant, and a correlation with the faunas from localities 3 and 6 (see below) is proposed, as indicated by the occurrence of the same species of *Bothriolepis* at these localities. Evidence for a Givetian–Frasnian age is discussed below.

Locality 5, Deering Hills

Occurrence. These remains were found in 1968 by L.G.G. Pearce (Magellan Petroleum) in the Harajica Sandstone exposed in the hills south of Deering Creek (Fig. 4). Details provided with the specimens give the stratigraphic level of two fossiliferous layers at about 239 and 244 m above the top of the Mereenie Sandstone. The level is said by Jones (1972, p. 236) to be about 180 m above the base of the Harajica Sandstone Member.

Fauna. There are four specimens, preserved as moulds in a fine reddish-brown sandstone, and all referable to *Bothriolepis*. CPC29678, from the lower horizon, is a well-preserved, but incomplete, external impression of a posterior median dorsal plate (Fig. 5C). It has a breadth–length index of about 100, which compares closely with a number of posterior median dorsals from the locality 6 assemblage described below.

The other specimens, from the higher horizon, are very poorly preserved. A small ornamented fragment from an anterior dorsolateral or mixilateral, an incomplete internal impression of a posterior ventrolateral, and part of the dorsal lamina of a mixilateral or anterior median dorsal plate have been identified (CPC24579–24681). None shows any features by which useful comparisons can be made.

Age. On very limited evidence, it is again assumed that one of the *Bothriolepis* species from the Harajica Sandstone near Stokes Pass is also represented at this locality. As with the previous two localities, a Givetian–Frasnian age may be proposed on evidence presented below.

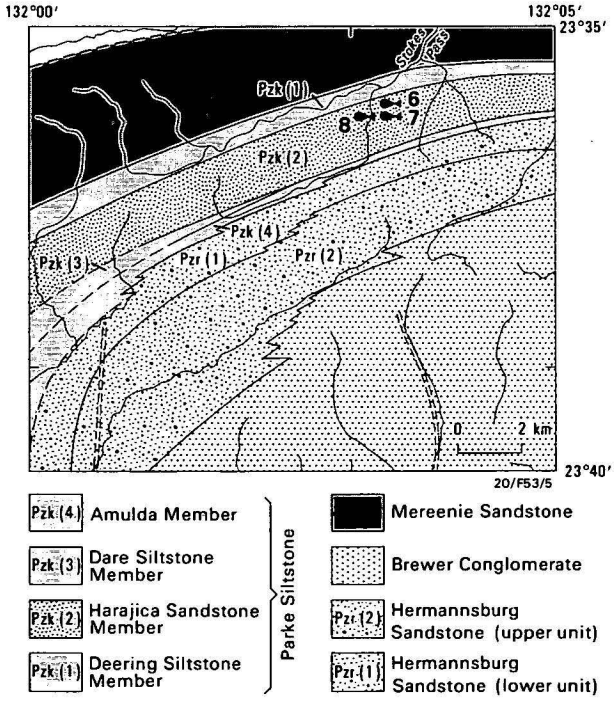

Figure 6. Geological map of the western MacDonnell Ranges, showing Devonian vertebrate localities 6–8 in the area about 2 km southwest of the southern end of Stokes Pass.

Geology from the Hermannsburg 1:250 000 geological sheet, as modified by Wells & others (1970, pl. 23) and Jones (1972, pl. 8).

Localities 6–8, southwest of Stokes Pass

Occurrence. These localities were discovered in 1973. Locality 6 is the most important vertebrate occurrence so far known from the Pertnjara Group. Again, the productive beds lie within the Harajica Sandstone Member of the Parke Siltstone, about 2 km southwest of the southern end of Stokes Pass (Fig. 6). They form the highest part of the first strike ridge of sandstone southwest of Stokes Pass, which is adjacent to the type section of the Harajica Sandstone (Jones, 1972, p.234), along the north-flowing creek immediately west of the main vertebrate locality.

Jones (1972, p. 236) gave the Harajica Sandstone a thickness of 500 m in the vicinity of Stokes Pass. The base of the member is defined as the top of the highest siltstone bed thicker than 150 mm in the underlying Deering Siltstone Member. A section measured with Jacobs staff at the main fish locality, from the lowest exposed sandstone at the base of the bluff, showed the fish remains to be mainly restricted to a 15 m zone between 75 and 90 m above the approximate top of the Deering Siltstone. In addition, a single plate of *Bothriolepis* was collected from a horizon about 50 m stratigraphically above the main locality (locality 7), and several specimens were found along strike at the same stratigraphic level as the main locality, about 500 m west of the Harajica Sandstone type section (locality 8).

At locality 6, the lowest fish horizon is characterised by fragmentary material in a sandstone containing abundant mud clasts. Above this is a greenish, medium to coarse-grained sandstone, with abundant complete plates, which are generally disarticulated, but with parts of the same individual often associated. The top of the fossiliferous zone is a fine-grained reddish sandstone, in which many complete individuals are preserved on a single bedding plane. This layer is of limited lateral extent.

Fauna. The main fish locality (6) is a very rich occurrence, in which most of the material is referable to the antiarch *Bothriolepis*. The upper fish layer includes remains of a large number of articulated individuals of this form, of which over fifty have been studied. Almost all these are preserved as external impressions of the dorsal surface of the armour (Fig. 7C, D). They have a limited size range (length of skull-roof and trunk-shield typically between 75 and 95 mm), and show various morphological features that indicate they were not fully grown. Possibly, they represent remains of a school of fish trapped in an evaporating pool. In one specimen (Fig. 7B), a faint impression of the tail is preserved behind a fairly small armour (length about 60 mm). Total length of this fish was about 140 mm, making the trunk armour relatively shorter than restored for *Bothriolepis canadensis* or *B. gippslandiensis*. These and a second Victorian species, *B. cullodenensis*, are the only other species of *Bothriolepis* in which the tail is known (Stensio, 1948; Long, 1983b). According to Long (1983b), the ratio of tail length to armour length is greater in juveniles of the Victorian species, which are also characterised by ventrolateral rows of enlarged scales. There is no sign of these in the new specimens, and the squamation was probably much reduced, as in *B. canadensis*.

Much detailed morphological information is provided by this new material, which will be dealt with elsewhere. Here, remarks are confined to comparisons with *Bothriolepis* remains from other localities in the Amadeus Basin. Such comparisons can be made particularly with the disarticulated dermal bones of the trunk armour that occur in the underlying coarse sandstone horizon. These generally are from individuals of larger size (armour length about 150 mm) than in the upper fish layer.

They include the anterior dorsolateral plate mentioned above (CPC24686) and several mixilateral plates (Fig. 8A), which are probably conspecific with one of the specimens described by Gilbert-Tomlinson (1968) from Dare Plain. Several examples of the anterior ventrolateral plate (e.g. CPC24690) show a well-preserved articular fossa for the pectoral fin. One of these, an incomplete plate from the left side (Fig. 5H) is the only specimen known from higher in the sequence in this area (locality 7). This is from a somewhat larger individual than is commonly preserved at the main horizon, but is comparable in size with the specimens from locality 4 at Dare Plain. The coarser ornament is also similar, but more material is required to confirm that this anterior ventrolateral belongs to the same species. The detailed preservation of the complex morphology of the articular fossa for the pectoral fin in these specimens is well displayed (Fig. 7A). Also from the main locality are several disarticulated bones from the pectoral fin itself, and, in the upper fish layer, several distal segments and many proximal segments of the articulated pectoral fin are preserved (Fig. 7C).

From the western locality (8, Fig. 6), *Bothriolepis* is represented by a well-preserved posterior ventrolateral (Fig. 5F), and a first ventral central plate from the right pectoral fin (Fig. 8G). The posterior ventrolateral can be definitely assigned to one of the species from the main locality.

To summarise, there are at least two, and probably three, species of *Bothriolepis* represented at localities 6–8, and, as far as can be ascertained, these include the two species represented by much more limited material from the Dare Plain and Deering Hills localities (3–5, Fig. 1).

The only other placoderm identified in this fauna is *Phyllolepis*, which is represented by five small fragments (CPC24692–24696) from locality 6. This form has a characteristic ornament of sinuous widely spaced ridges (Fig. 8C–E), but these fragments are too incomplete for more definite determination. *Phyllolepis* is also known from the Dulcie Range in the Georgina Basin (Hills, 1959; Gilbert-Tomlinson, 1968) and from many localities in eastern Australia (e.g. Young, 1974; Ferguson & others, 1979). This new occurrence extends the geographic range of the genus farther west than previously recorded.

Associated with *Bothriolepis* and *Phyllolepis*, and of special interest, are several remains of osteichthyans (bony fishes) from locality 6. Two forms are represented: a rhipidistian crossopterygian, and a dipnoan (lungfish). CPC24697 is a lungfish skull with the anterior part of the body squamation and part of the shoulder girdle preserved in dorsal view (Fig. 8J). It occurs with the articulated *Bothriolepis* in the upper fish layer. This new lungfish specimen will be described in detail elsewhere, and remarks here are restricted to some observations on the dermal bone pattern of the skull-roof. The bone sutures on the preserved part of the skull are clear, but preservation is too poor for pores of the sensory canal system to be reliably identified. The preserved portion of the skull is about 32 mm long. The snout region is missing and presumably was unossified, as is commonly the case with immature *Dipterus* (Forster-Cooper, 1937; White, 1965). From the general configuration of the bones, it is clear that this new lungfish was not a member of one of the long-snouted groups (rhynchodipterids, holodipterids, fleurantiids), which are fairly widespread in Late Devonian deposits in eastern Australia (Campbell & Bell, 1982), Western Australia (Miles, 1977), Europe (e.g. Schultze, 1969), Greenland (Lehman, 1959), and North America (Graham-Smith & Westoll, 1937). Of the remaining Middle–Late Devonian forms, *Scaumenacia*, *Phaneropleuron*, and *Pentlandia* lack a 'D' bone in the skull, but this bone is clearly present in the new specimen and in the remaining named Devonian genera (*Dipterus*, *Rhinodipterus*, *Chirodipterus*). However, *Rhinodipterus* also shows a tendency towards elongation of the prepineal region of the skull, and the only forms that show any close resemblance to the new specimen in dermal bone pattern are *Dipterus* and *Chirodipterus*. Excluding the 'dipterid' from the Late Devonian of Victoria (Hills, 1931; Long, 1983b), in which the skull-roof is not known, there are from Australia only the species of *Chirodipterus* from the Frasnian Gogo Formation (Canning Basin, W.A.) with which useful comparisons can be made. Miles (1977) described two new species of *Chirodipterus* from Gogo, but only one (*C. australis*) is represented by good skull-roof material. Given the variability in dermal bone shape in Devonian dipnoans, the new form compares well both with the various skulls of *Chirodipterus australis* (Miles, 1977, fig. 118) and also with those of *Dipterus valenciennesi* from the Middle Devonian of Scotland (e.g. White, 1965). One feature of possible significance is the apparent presence in CPC24697 of another median bone immediately in front of the unpaired D bone on the displaced anterior part of the preserved portion (Fig. 8J). Contact between the unpaired D and F bones is known in both *Dipterus* and *Chirodipterus*, but is unusual (Miles, 1977, p. 235). In comparison with one specimen of *C. australis* showing this feature (Miles, 1977, fig. 118C), the suture between these bones in CPC24697 is apparently more regular and symmetrical, and more widely separates the E bones of each side. A broad transverse contact between D and enlarged F bones is a feature of Mesozoic and younger dipnoans, in which, however, the number of bones in the skull is much reduced. In the Early Devonian lungfish *Uranolophus*, on the other hand, there are many small bones in the snout region, but, again, there is a broad transverse anterior border to the D bone, which may abut an anterior unpaired element (Denison, 1968). A similar configuration may occur in the Middle Devonian *Dipterus* (e.g. Westoll, 1949, fig. 2B). Another feature in which CPC24697 resembles *Dipterus* rather than *Chirodipterus* is the relatively large bone 3, which tends to be reduced in more advanced forms (K.S.W. Campbell, personal communication). Clearly, further specimens are required to determine whether these are individual variations or consistent features of this new form.

Two other specimens are probably also dipnoans. CPC24698 is an impression of part of a vertebral column, showing about fourteen closely spaced centra broken through the midline. These resemble in proportions the amphicoelous centra attributed to lungfish from the Late Devonian of East Greenland, as figured by Jarvik (1952, fig. 16A, B). CPC24699 shows about six similar elements associated with poorly preserved scales, and some larger rounded plates, which probably come from the opercular or gular series. These are smooth externally, except for some short radiating ridges near the margins. On some of the scales, a fine radiating sculpture is faintly preserved, resembling that figured in *Dipterus* scales from the Middle Devonian of Scotland (Forster-Cooper, 1937, pl. 2, fig. 3). Regarding the vertebral column of *Dipterus*, Denison (1968) noted that centra tend to be absent, and that the row of elements sometimes preserved may be enlarged bases of the neural arches.

Figure 7.

A–D, *Bothriolepis* sp., from locality 6, near Stokes Pass, western MacDonnell Ranges: A, left anterior ventrolateral plate in ventrolateral view showing the articular fossa for the pectoral fin, CPC24690, x 1.5; B, sandstone slab showing the steinkern of a skull and trunk armour in ventral view (top right) with an impression of the tail curving to the bottom left, CPC24684, x 1; C, articulated skull, trunk armour (incomplete) and right pectoral fin in dorsal view, partly restored after CPC24682, x 1.5; D, articulated skull and trunk armour in dorsal view, CPC24683, x 1. E, portion of body squamation of a rhipidistian or dipnoan fish, from locality 6, near Stokes Pass, CPC24705, x 1. All specimens whitened with ammonium chloride.

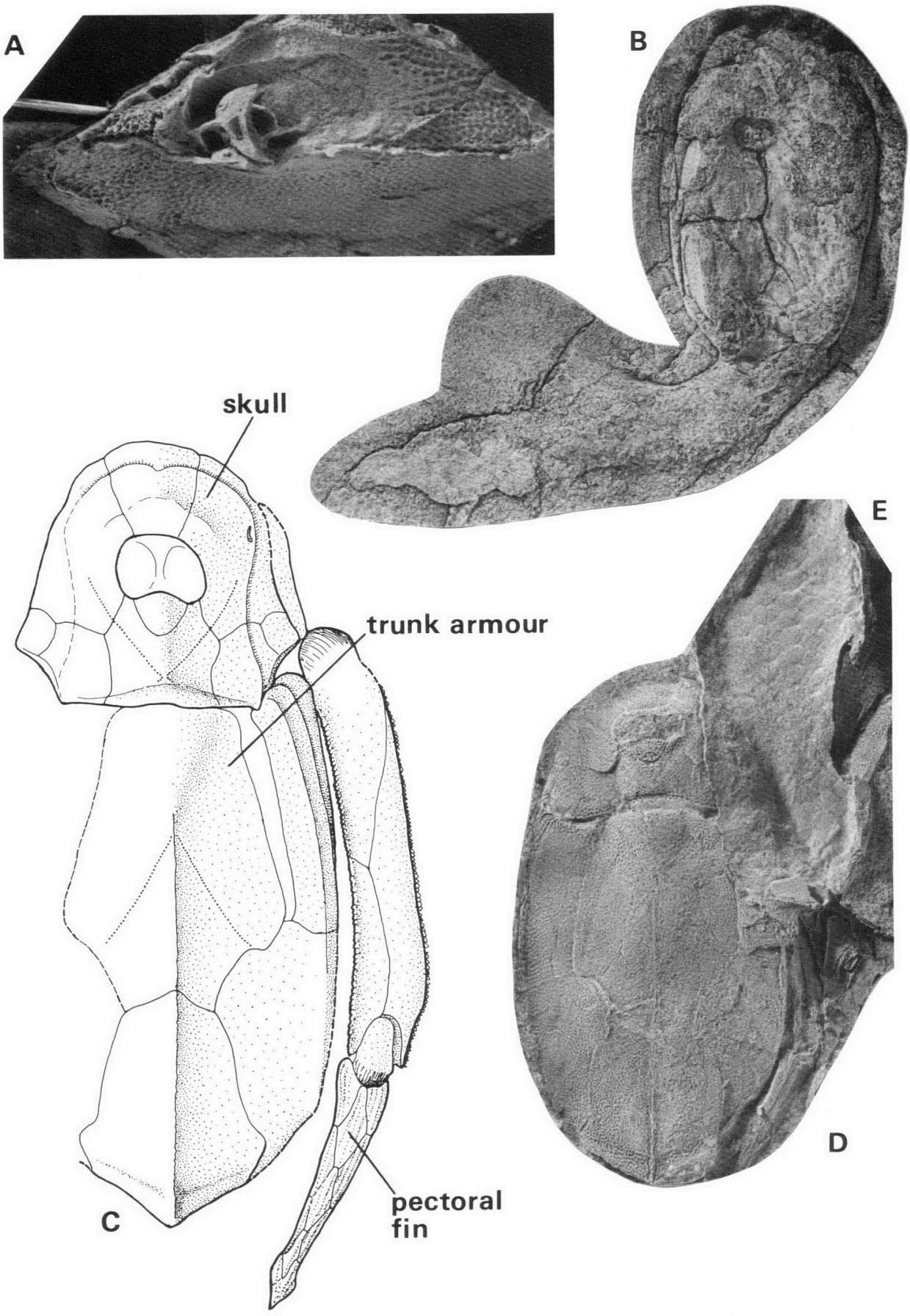
A
B
skull
trunk armour
E
D
C
pectoral
fin

The presence of a rhipidistian crossopterygian in the fauna is demonstrated by CPC24700, in which an area of squamation is associated with an elongate element at least 65 mm long (presumably the inside of a maxilla or dentary), and several teeth of two sizes. The larger teeth, of which two are well exposed, are about 5.5 mm long, with ten longitudinal ribs at the base, and smooth tips. They are apparently attached to displaced elements, presumably coronoids or elements of the dermopalatine series. Immediately adjacent is an alignment of much smaller teeth, which must represent the marginal tooth row from the upper or lower jaw. The associated scales have a maximum exposed height of about 7.5 mm, and appear to be unornamented cycloid scales, although preservation is poor. CPC24701 is another possible jaw element, 68 mm long, but lacks diagnostic morphological features, owing to incompleteness. CPC24702 is a plate some 46 mm long and partly covered with fine sharp tubercles. It may be a denticulate tooth plate from within the mouth cavity.

Three other osteichthyan remains may belong either to the dipnoan or the rhipidistian. On CPC24703, about four branching unjointed fin rays run obliquely from the edge of a small area of scales, and, presumably, represent part of the internal skeleton of an unpaired fin. The dermal fin rays of Devonian dipnoans and rhipidistians have a similar morphology (e.g. Jarvik, 1959). CPC24704 is another poorly preserved section of the body squamation of an osteichthyan, associated with some disarticulated and possibly fragmented plates, presumably, from the skull region. No significant morphological details can be discerned. Finally, CPC24705 (Fig. 7E) is a section of body squamation that includes part of the lateral line system, preserved as faint ridges along one of the scale rows (cf. Jarvik, 1950, pl. 3).

The third major group of jawed fishes identified in this assemblage are acanthodians, which are represented by three incomplete spines of two types. CPC24706 is a curved spine about 35 mm long, up to 6 mm across, and incomplete at both ends. Each lateral face is ornamented with up to thirteen nodose longitudinal ridges (Fig. 8I). Distally, the nodes are well enough preserved to show resemblance to the nodose ornament typical of climatiid acanthodians (e.g. Miles, 1973; Denison, 1979). In the degree of curvature, number and ornament of ridges, and general size, this spine resembles the spine described from the Middle Devonian near Wee Jasper, New South Wales, as a climatiid acanthodian (Young & Gorter, 1981, pl. 9, fig. 8). The second acanthodian spine type has five smooth longitudinal ridges on each lateral face, the anterior one probably being a median ridge. CPC24707 is 39 mm long with a maximum width of 2 mm. It is only slightly curved (Fig. 8H). CPC24708 is the proximal portion of a similar spine, and shows part of the unornamented base of insertion (Fig. 8F). Similar spines of the *Onchus* or *Archaeacanthus* type (e.g. Denison, 1979) are widely distributed in rocks of Silurian and Devonian age. They are known from the Cravens Peak Beds in the Georgina Basin, but have not been recorded previously from younger strata in central Australia. Spines of the same type from the Frasnian of Victoria were described by Hills (1931) as *Striacanthus sicaeformis*. Articulated material from the same deposits was described by Long (1983a) as *Culmacanthus stewarti*. However, these new spines, insomuch as preserved, appear to be more slender than the Victorian examples.

Age. A previous assessment of the age of this fauna (see Playford & others, 1976, p. 237) must now be revised, since *Phyllolepis* was not then known to be present. This fauna, as now known from the abundant material at locality 6, is characterised by many specimens of *Bothriolepis* (at least 2 species), associated with rare *Phyllolepis*, acanthodians, rhipidistians, and dipnoans. Recent work elsewhere in Australia has clarified the stratigraphic occurrence of some of these forms. The placoderm *Phyllolepis*, previously thought to be a Famennian indicator on the evidence of its European stratigraphic range, is now known to occur in Frasnian strata in southeastern Australia (Ferguson & others, 1979), and a closely related new phyllolepid has been described from basal Frasnian strata near Braidwood, New South Wales (Ritchie, 1984). An early and primitive species of *Bothriolepis* occurs in the Middle Devonian Hatchery Creek Conglomerate, near Wee Jasper, New South Wales (Young & Gorter, 1981), but other occurrences in New South Wales and Victoria are thought to be Frasnian or younger (Young, 1974; Long, 1983b). *Bothriolepis* is also known from the early Frasnian Gogo Formation in the Canning Basin (Gardiner & Miles, 1975; Young, 1984b).

Lungfishes of comparable age are known from the Carnarvon and Canning Basins in Western Australia (Seddon, 1969; Miles, 1977), where they are marine, and from Late Devonian nonmarine strata in eastern Victoria (Hills, 1931; Marsden, 1976; Long, 1983b) and New South Wales (Campbell & Bell, 1982). Except for the last-mentioned, these occurrences have been generally dated as Frasnian. Gilbert-Tomlinson (1968, p. 203) referred to 'a possible dipnoan fragment' in a fauna of putative Late Devonian age from the Georgina Basin, but this determination and the age were erroneous. However, lungfish scales do occur in an Early Devonian fauna from the Toko Syncline area of the Georgina Basin (Young, 1984a). It is noteworthy that the lungfishes from the Mount Howitt fauna in Victoria, of probable Frasnian age (Long, 1983b), resemble in their skull characters the more advanced *Scaumenacia* from the Late Devonian of Canada (Marsden, 1976, p. 122). As mentioned above, the dipnoan skull from the Harajica Sandstone is generally more primitive in its dermal bone pattern.

Rhipidistian crossopterygians are generally poorly known in Australia, but osteolepiform rhipidistians have been recorded from Middle Devonian to Carboniferous strata in eastern Australia (Woodward, 1906; Young & Gorter, 1981; Long, 1983a, 1983b; Young, 1983), and also occur in the Frasnian Gogo Formation of the Canning Basin. Porolepiform rhipidistians are known from the Early and Late Devonian of eastern Australia (Thomson, 1973; Giffin, 1980; Young, 1982, 1983, in press c). As noted above, acanthodian spines of the '*Onchus*' type occur in the Frasnian of Victoria (Long, 1983a). They are also known from rocks of similar age in southeastern New South Wales (Fergusson & others, 1979; Young, 1983) and from older strata (Early-Middle Devonian) in New South Wales (Rade, 1964; Ritchie, 1973; Young & Gorter, 1981), and in the Georgina Basin (Turner, & others, 1981; Young, 1984a).

Leaving aside the rhipidistians, which are insufficiently known in Australia to be useful biostratigraphically, the elements in this assemblage fall into two groups. The dipnoan, which resembles the Middle Devonian *Dipterus*, and the 'climatiid' acanthodian spine, very similar to one from the Hatchery Creek fauna, point to a Middle Devonian age for the assemblage. This is supported by the apparent absence of *Groenlandaspis*, which, in the Late Devonian of Victoria, is absent from earliest Frasnian and older strata, according to the

Figure 8.

A,B, *Bothriolepis* sp., associated mixilateral plate (A) and anterior median dorsal plate (B) in external view, probably conspecific with the specimen in Fig. 5I, CPC24685, x 1.5. C–E, *Phyllolepis* sp., three ornamented fragments, CPC24692, 24693, 24695, x 2. F,H, acanthodian spines of the *Striacanthus* type, CPC24708, 24707, x 3. G, *Bothriolepis* sp., first ventral central plate from a right pectoral fin, in external view, CPC24691, x 1.5. I, climatiid acanthodian spine, CPC24706 (x 3). J, dipnoan (lungfish) skull associated with part of the body squamation and pectoral girdle, in dorsal view, CPC24697, x 1.5. Specimens in H,I from locality 8; other specimens from locality 6 (both near Stokes Pass, western MacDonnell Ranges). All specimens whitened with ammonium chloride.

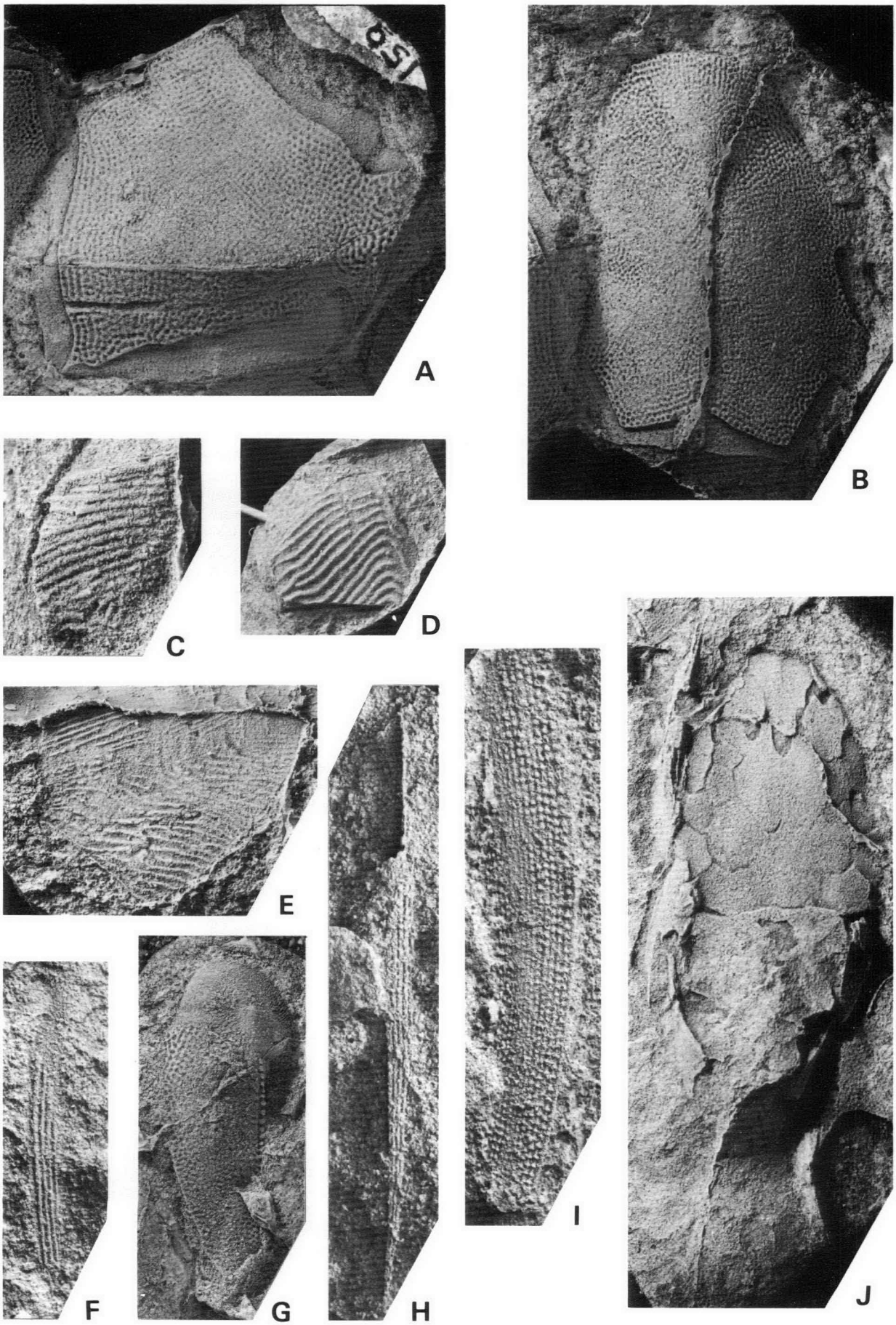
A
B
C
D
E
F
G
H
I
J

biostratigraphic analysis of Long (1983b). On the other hand, *Bothriolepis* is more typically known as a Late Devonian form in Australia. Although one species, *B. verrucosa*, occurs in the Middle Devonian (Young & Gorter, 1981), it is more primitive in several features than other known Australian occurrences of the genus, including the new species dealt with above. It should also be pointed out that these new species are not conspecific with the *Bothriolepis* from the Frasnian Gogo Formation in the Canning Basin. Finally, *Phyllolepis* is generally regarded as a Late Devonian form, and this is apparently valid for European sequences, but, as previously noted (Fergusson & others, 1979, p. 103), its occurrence in rocks as old as Frasnian in eastern Australia weakens its reliability as a Late Devonian indicator. Taken together, therefore, this vertebrate evidence points to an age possibly as old as Givetian (late Middle Devonian), but unlikely to be younger than Frasnian (early Late Devonian).

Locality 9. Walker Creek

Occurrence. This material was recently collected (1983) by J.D. Gorter (Pancontinental Petroleum) from near the top of the Parke Siltstone in the Walker Creek area (Fig. 9). This is about 40 km southeast of the Dare Plain fish localities. There are two orange sandstone lenses near the top of the Parke

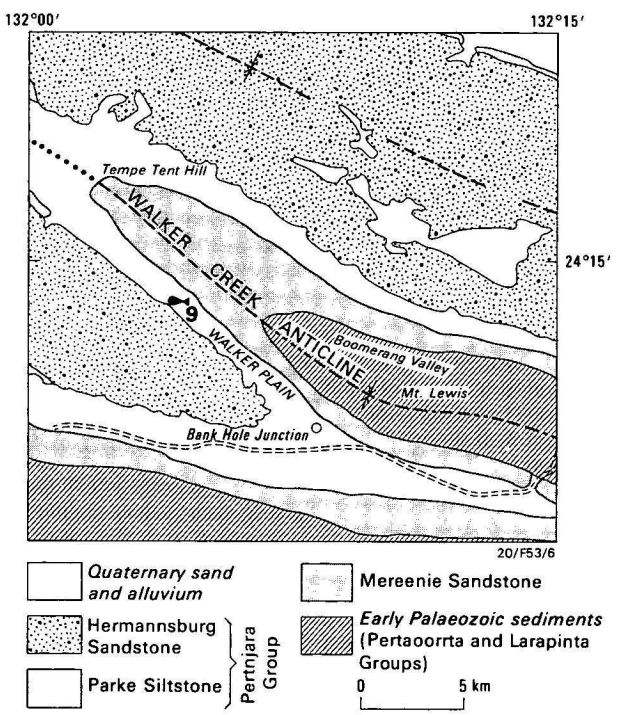

Figure 9. General geology of the Walker Creek area, simplified from the Henbury 1:250 000 geological sheet, showing Devonian vertebrate locality 9 discussed in this paper.

Siltstone at this locality, and the fish sample, which was collected as float, is thought to have come from the upper sandstone, about 20 m below the top of the Parke Siltstone. The contact between the Parke Siltstone and the overlying Hermannsburg Sandstone in this area is gradational (Ranford & others, 1965, p. 31), and Jones (1972) separated out these upper transitional beds as the Amulda Member of the Parke Siltstone. The lower Deering Siltstone and Harajica Sandstone members do not occur in this area, and the combined thickness of the Dare Siltstone and Amulda members, which make up the whole of the Parke Siltstone, is given as 300–400 m (Jones, 1972, fig. 8). This new fish occurrence from near the top of the Amulda Member is thus considerably higher stratigraphically than the other fossiliferous horizons in the Parke Siltstone.

Fauna. Associated on one sandstone block, together with a few indeterminate fragments, are seven placoderm plates, of which five, and probably six, are referable to *Bothriolepis*. The latter include small anterior and posterior median dorsals, a left mixilateral, and a right posterior ventrolateral, all probably from one individual. However, only the posterior ventrolateral (Fig. 5F) is sufficiently complete and well preserved for comparisons to be made. This plate is 38 mm long, and comparable in the proportions of its ventral lamina and prominence of the ventrolateral ridge to the much larger posterior ventrolaterals (CPC 24675, 24688) from the Stokes Pass and Dare Plain localities (see above). However, the lateral lamina is somewhat higher and shorter, and, in view of the disparity in size, these resemblances may not be significant

Two associated plates come from a much larger fish. A left posterior ventrolateral (CPC24711), incompletely preserved as an internal view of the ventral lamina, differs from typical *Bothriolepis* in the thickened internal crista along the rounded posterior border of the subanal lamina. A second lateral marginal plate from the pectoral fin (CPC24710) may be definitely assigned to *Bothriolepis*. It is 67 mm long, with a maximum breadth of 15 mm. A small sample of seven corresponding plates from locality 6 was measured for comparative purposes, and all were considerably longer in proportion to breadth than the Walker Creek example. Finally, there is an indeterminate portion, about 30 x 25 mm in size, of a placoderm plate ornamented with fairly coarse tubercles, somewhat reminiscent of euarthrodiran ornament. However, preservation is too poor for positive identification, and assignment to *Bothriolepis* cannot be excluded.

Age. It is possible that one of the Dare Plain species of *Bothriolepis* is represented in this sample, but, in view of the several distinctive morphological features exhibited by only a small number of bones, I consider it equally likely that one or two different species are represented. Further material is needed to reach a decision on this and to establish whether another placoderm with tuberculate ornament (?*Groenlandaspis*) is also present in the fauna. It is tentatively suggested that these remains are slightly younger than the *Bothriolepis* occurrences discussed above.

Discussion

As indicated by the foregoing assessment, three vertebrate horizons may be placed in two main faunas amongst the Devonian fish occurrences so far known from the Amadeus Basin. The highest horizon, very poorly known, contains *Bothriolepis* and, possibly, other placoderms. It occurs near the top of the Parke Siltstone. The middle horizon, characterised by several species of *Bothriolepis*, rare *Phyllolepis*, and dipnoans, rhipidistians, and acanthodians, comes from the Harajica Sandstone Member in the lower part of the Park Siltstone. The age of these horizons, based on the vertebrate evidence, is probably within the Givetian–Frasnian.

The lower fauna, of uncertain stratigraphic position and also very poorly known, contains a phlyctaeniid (?groenlandaspid) euarthrodire, another placodern with ridged ornament, and acanthodians. This may represent another occurrence of the late Early Devonian *Wuttagoonaspis* fauna known from western New South Wales and the Georgina Basin.

Other evidence on the age of the Pertnjara Group is provided by palynology. Playford & others (1976) described samples from the Undandita Member of the Brewer Conglomerate at the top

of the Pertnjara Group, which indicated a Famennian age, but probably older than the latest Famennian assemblage known from the lower Fairfield Formation in the Canning Basin. Previously (e.g. Wells & others, 1970; Jones, 1972; Jones & others, 1973), the top of the Pertnjara Group had been regarded as Early Carboniferous in age, in view of its preserved maximum thickness (up to 3600 m). This palynological evidence implies a high rate of sedimentation during the Late Devonian for the Pertnjara Group, given a Frasnian age for the Harajica Sandstone. For comparison, Friend & House (1964) gave known thickness maxima of about 1800 m and 3000 m for the Frasnian and Famennian, respectively. It is relevant to reiterate, therefore, that the Harajica fish fauna, as presently known, comprises a mixture of forms indicating either Middle or Late Devonian ages. The presence of *Phyllolepis* is the strongest evidence for a Late Devonian age, but, as noted above, this form appears earlier in Australia than in Europe, and its downward range in Australian sequences has not yet been established. From about the same horizon, Hodgson (1968) described spores from the Harajica Sandstone at Dare Plain, which were also assessed as indicating a late Middle or early Late Devonian age. Playford (1983) recently reviewed occurrences of the miospore genus *Geminospora*, which is relatively abundant in the Harajica spore assemblage. He concluded that the relevant species (*G. lemurata*) has a known vertical range of (?)early or middle Givetian to late Frasnian or (?)early Famennian, and is particularly abundant near the Givetian–Frasnian boundary. The vertebrate and palynological evidence is therefore consistent, but there is scope for a more refined zonation if new vertebrate faunas or spore assemblages are found.

Turning now to the older vertebrate horizon, there are, as noted above, alternative interpretations of its stratigraphic level at the type locality, Gosses Bluff. Resolution of these is rendered more difficult by the fact that older and younger fossil horizons are not presently known from any one section within the Amadeus Basin. However, inferred sediment thicknesses under these alternatives can be compared with the Dulcie Sandstone sequence in the western part of the Georgina Basin, which is the closest known occurrence of the *Wuttagoonaspis* fauna.

Gilbert-Tomlinson (1968) reported three vertebrate horizons in the Dulcie Sandstone. Further collecting in 1974 established that the lowest of these, from the northwestern end of the Dulcie Syncline, contains a species of *Wuttagoonaspis* and various other forms closely similar to those in the Merrimerriwa Formation of the Mulga Downs Group in western New South Wales (Ritchie, 1973; Glen, 1979, 1982). From the southeastern end of the Dulcie Syncline the two higher vertebrate horizons were reported (Hills, 1959; Gilbert-Tomlinson, 1968): a lower horizon in the upper part of the Dulcie Sandstone, about 487 m above its base, containing *Bothriolepis*; and an upper horizon some 122 m higher, at the top of the sequence (total thickness 620 m), containing *Bothriolepis* and *Phyllolepis*. The 1974 collections now show that *Phyllolepis* is also present in the lower horizon of the Upper Dulcie Sandstone, and an asterolepid antiarch, probably *Remigolepis*, is present with *Bothriolepis* and *Phyllolepis* in the upper horizon. Other placoderm remains, probably belonging to *Groenlandaspis*, occur in both horizons. This suggests that these faunas are somewhat younger than the *Bothriolepis* faunas so far known from the Pertnjara Group in the Amadeus Basin.

The older *Wuttagoonaspis* fauna is not known from the southeastern end of the Dulcie Syncline, but fieldwork in 1974 established that, at the northwestern end, fish remains occur at various horizons up to 60 m above the base of the formation. Thus, within the Dulcie Sandstone, there may be a broadly estimated 430 m of sediment thickness between the lower *Wuttagoonaspis* assemblage and the upper *Bothriolepis*/*Phyllolepis* assemblage (Fig. 10D). I assume here that sedimentation within the Dulcie Sandstone was continuous, as there is no convincing evidence to the contrary.

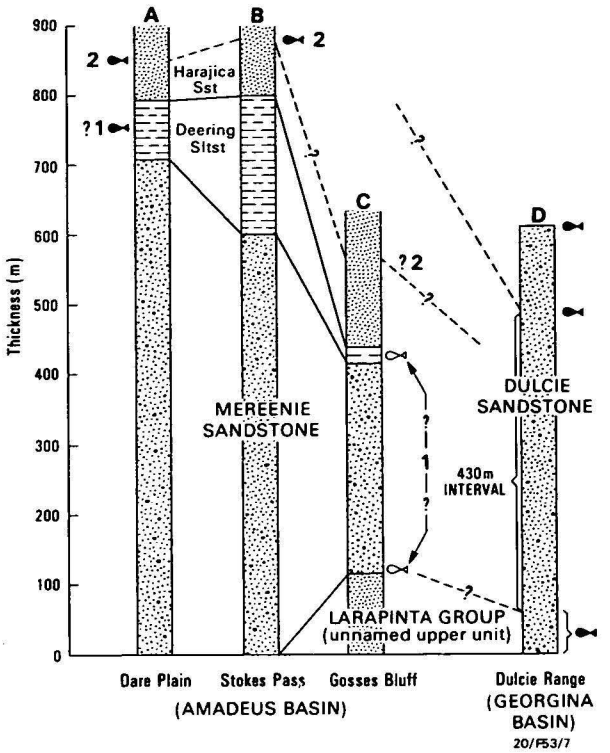

Figure 10. Comparisons of sediment thickness between three sections in the Amadeus Basin, showing relative stratigraphic levels of assumed lower (1) and upper (2) fish horizons, and the Dulcie Sandstone in the Georgina Basin.

Gosses Bluff section after D.J. Milton. All thicknesses approximate.

By comparison, the Mereenie Sandstone in the Amadeus Basin is said to be up to 915 m thick in the Gardiner Range (Wells & others, 1970). Measured sections in this region (Ranford & others, 1966) give a maximum thickness of 750 m, and in the Dare Plain area its thickness is 600–750 m (Wells & others, 1970). The *Bothriolepis* horizon at Dare Plain is about 140 m above the top of the Mereenie Sandstone and, therefore, some 850 m above its base (Fig. 10A). In the Stokes Pass area, the Mereenie Sandstone is about 600 m thick (Pritchard & Quinlan, 1962), and the thickness of the overlying Parke Siltstone is given as about 915 m (Wells & others, 1970), which probably includes part or all of the Harajica Sandstone Member, about 500 m thick in this area (Jones, 1972). The underlying Deering Siltstone Member of the Parke Siltstone is about 200 m thick (Jones, 1972, fig. 6), and the fossiliferous horizon at locality 6 is 75–90 m above the top of the Deering Siltstone and, therefore, some 880 m above the local base of the Mereenie (Fig. 10B). Finally, in a measured section on the northeastern side of Gosses Bluff, Milton (unpublished ms) reported the Mereenie Sandstone to be 286 m thick, the Deering Siltstone member to be thin (40 m) or absent, and the overlying Harajica Sandstone to be several hundred metres thick (see also Barlow, 1979, table 1). However, the Mereenie Sandstone, as interpreted in this section, is anomalously thin, considering the relatively thick sections in the western MacDonnell Ranges to the north and in the Gardiner Range to the south. Thickness data inferred from these surrounding areas place Gosses Bluff between the 760 and 915 m isopachs for the Mereenie Sandstone (Wells & others, (1970, fig. 34). This far exceeds Milton's thickness, even if the thickness of the unnamed Larapina unit

(116 m) previously mapped as Mereenie Sandstone (Crook & Cook, 1966; see above) is subtracted. By comparison with the Dare Plain and Stokes Pass *Bothriolepis* horizons, one might estimate that the equivalent horizon in the Gosses Bluff sequence is 100–200 m above the top of the Mereenie Sandstone and, therefore, some 380–480 m above its base (Fig. 10C). The base of the Mereenie Sandstone is the level of the Gosses Bluff fish horizon under Milton's interpretation.

To summarise (Fig. 10), an assumption that the Gosses Bluff fish horizon can be correlated with the base of the Mereenie Sandstone elsewhere gives sediment thicknesses at Dare Plain and Stokes Pass (850–880 m) far in excess of that between approximately equivalent fossiliferous horizons in the Dulcie Sandstone (430 m). However, a thickness comparable to that in the Dulcie Sandstone can be estimated for the corresponding part of the Gosses Bluff sequence if Milton's interpretation of Gosses Bluff stratigraphy is followed. If Mereenie Sandstone thickness inferred by Wells & others (1970) is used, the corresponding thickness is again excessive compared to the Dulcie Sandstone sequence.

Alternatively, if it is assumed that the Gosses Bluff fish horizon can be correlated with the top of the Mereenie, then inferred thicknesses (140–290 m) are less than in the corresponding interval of the Dulcie Sandstone sequence (430 m). Moreover, assuming the fossil occurrence from the Deering Siltstone at Dare Plain (Locality 2 above) represents an equivalent of the Gosses Bluff fish horizon, then the intervening thickness in the Dare Plain sequence would be as low as 100 m (Fig. 10A). However, as noted above, the fish faunas from the Upper Dulcie Sandstone may be younger than the *Bothriolepis* horizon in the Harajica Sandstone, and this could account for these differences in thickness.

Thus, these comparisons of sediment thickness do not conflict with the interpretation that the Gosses Bluff fish horizon lies at or near the Mereenie-Pertnjara transition. Nor are they inconsistent with the alternative interpretation that the fossiliferous horizon occurs at the base of the Mereenie Sandstone at Gosses Bluff, given that the Mereenie Sandstone is considerably thinner here than in other exposures in the western MacDonnell and Gardiner Ranges. The problem then becomes one of explaining this anomalous thinness, which is clearly an aspect requiring further investigation. (Seismic interpretations suggest a thickness for the Mereenie Sandstone of some 500 m under the Missionary Plain near Gosses Bluff; see Brown, 1973, fig. 10.) What is strongly suggested by these comparisons, however, is that, if the Gosses Bluff fish horizon is at the base of a much reduced Mereenie Sandstone, this does not correlate with the base of the formation in its much thicker exposures to the west.

It is recognised that formation thicknesses can vary greatly over shorter distances than involved here, as is particularly evident in the middle Palaeozoic stratigraphy of the Amadeus Basin. Comparisons based on sediment thickness are tenuous at best, and those used above would be invalidated if a hiatus within the Dulcie Sandstone could be demonstrated, as suggested by various authors (e.g. Johnstone & others, 1968; Gilbert-Tomlinson, 1968, fig. 6; cf. Wells & Moss, 1983, fig. 8). Also, any further evidence confirming that the fossiliferous horizon in the Deering Siltstone at Locality 2 is equivalent to the Gosses Bluff fauna would lend support to an interpretation of an older (Givetian) rather than younger (Frasnian) age for the Harajica fish fauna, which is only 100 m stratigraphically higher in the Dare Plain sequence (see above). Further investigations are required on both these points.

The age of the Mereenie Sandstone is relevant to some more general aspects of the geological history of the Amadeus Basin and the Australian continent. In the northern and northeastern parts of the basin the Mereenie Sandstone unconformably overlies older sediments, and the name Rodingan Movement has been applied to the causative event (Wells & others, 1970). From the above discussion, a Devonian age for this event seems unlikely, the evidence pointing to a Silurian age, as suggested by Wells & others (1970).

The palaeomagnetism of the Mereenie Sandstone has also been investigated. Results from samples in the lower 100 m of Mereenie Sandstone in the Ellery Creek section were reported by Embleton (1972), who interpreted them as Devonian in age, based on the Gosses Bluff fish occurrence. Schmidt & Morris (1977, p. 2676; also Embleton, 1981, p. 82) noted that the age of magnetisation measured in the Mereenie Sandstone was critical to a decision between two opposing interpretations for the Palaeozoic apparent polar wander curve for the Australian continent. Under the Schmidt & Morris model this magnetisation should be post-Early Devonian in age. Under the sub-plate model (McElhinny & Embleton, 1974; Embleton & others, 1974), which postulates a microplate history for southeastern Australia (see also Goleby, 1980), the Mereenie magnetisation would be older (Silurian–Early Devonian). Since it was suggested above that the fish horizon at Gosses Bluff cannot be assumed to correlate with the base of the Mereenie Sandstone elsewhere, it seems likely that the magnetisation measured in the basal part of the Mereenie Sandstone at Ellery Creek is older than Early Devonian, which is consistent with the subplate model for the Australian Palaeozoic apparent polar wander curve. However, the total thickness of Mereenie Sandstone at Ellery Creek (about 300 m) is comparable to its thickness at Gosses Bluff under Milton's stratigraphic scheme, and further evidence is required to support this conclusion. It should be noted that neither the Carmichael Sandstone, as defined by Wells & others (1970), nor its unnamed upper unit, as recognised by Milton & others (1972) at Gosses Bluff, has been identified as far east as Ellery Creek (Wells & others, 1970; Milton, unpublished ms).

Finally, some brief comments can be made on the affinities shown by the central Australian Devonian fish faunas to those from elsewhere on the continent. These affinities are generally with eastern Australia, as exemplified by the presence of *Phyllolepis* and *Wuttagoonaspis*. To the west, *Bothriolepis* has been recorded from non-marine Late Devonian strata in the Bonaparte Gulf and east Canning Basins (Gilbert-Tomlinson, 1968, p. 210; Young, unpublished), but *Phyllolepis* is apparently absent. Turner & others (1981) suggested Devonian marine and fluvial connections from the central Australian basins westward to the Canning and/or Bonaparte Gulf Basins on the evidence of thelodont scale occurrences, and current-direction measurements in the Cravens Peak Beds of the Georgina Basin. However, there is much stronger faunal evidence in the distribution of the *Wuttagoonaspis* fauna for a southeastern connection between the Dulcie Sandstone and Cravens Peak Beds of the Georgina Basin and the Mulga Downs Group of western New South Wales, and this is reinforced by the known distribution of *Phyllolepis* on the Australian continent (see also Gilbert-Tomlinson, 1968, fig. 7).

Acknowledgements

I thank J.G. McPherson, J.D. Gorter, and P.W. Davis for assistance in the field, and J.D. Gorter for submitting for study the material from the Walker Creek area. B.G. Jones made available the specimen from the Deering Siltstone, and gave advice on Pertnjara stratigraphy. Other material was submitted by Magellan Petroleum Corporation. P.J. Cook and D.J. Milton provided information on the Gosses Bluff fish locality, and

A.T. Wells gave advice and information on many aspects of Palaeozoic stratigraphy in the Amadeus Basin. I thank J.G. McPherson for discussing stratigraphy and sedimentology, and K.S.W. Campbell, P.L. Forey, D. Goujet, and A. Ritchie for advice on the vertebrate faunas and their identification. A. Haupt and W. Peters prepared the material, and H.M. Doyle, R.W. Brown and P.W. Davis carried out the photography. For reading and commenting on the manuscript I thank K.S.W. Campbell, P.J. Cook, P.J. Jones, and A.T. Wells.

References

Barlow, B.C., 1979 - Gravity investigations of the Gosses Bluff impact structure, central Australia. *BMR Journal of Australian Geology & Geophysics*, 4, 323-339.

Brown, A.R., 1973 - A detailed seismic study of Gosses Bluff Northern Territory. *Bureau of Mineral Resources, Australia, Report* 163.

Campbell, K.S.W., & Bell, M.W., 1982 - *Soederberghia* (Dipnoi) from the Late Devonian of New South Wales. *Alcheringa*, 6, 143-149.

Chewings, C., 1891 - Geological notes on the Upper Finke Basin. *Transactions of the Royal Society of South Australia*, 18, 247-255.

Cook, P.J., 1976 - The Mereenie Sandstone. *In* Wells, A.T. Geology of the Late Proterozoic-Palaeozoic Amadeus Basin. *25th International Geological Congress, Excursion Guide* 48A, 38-39.

Crook, K.A.W., & Cook, P.J., 1966 - Gosses Bluff - diapir, cryptovolcanic structure, or astrobleme? *Journal of the Geological Society of Australia*, 14, 495-516.

Denison, R.H., 1968 - The evolutionary significance of the earliest known lungfish, *Uranolophus*, *In* Ørvig, T., (editor), Current problems in lower vertebrate phylogeny. *Nobel Symposium*, 4, 247-257. *Alqvist & Wiksell, Stockholm.*

Denison, R.H., 1979 - Acanthodii. Handbook of Paleoichthyology, Volume 5. Schultze, H-P., (editor), *Gustav Fischer Verlag, Stuttgart, New York.*

Embleton, B.J.J., 1972 - The palaeomagnetism of some Palaeozoic sediments from central Australia. *Journal and Proceedings of the Royal Society of New South Wales*, 105, 86-93.

Embleton, B.J.J., 1981 - A review of paleomagnetism of Australia and Antartica. *In* McElhinny, M.W., & Valencio, D.A., (editors), Paleoreconstruction of the continents. *American Geophysical Union and Geological Society of America Geodynamics Series*, 2, 77-92.

Embleton, B.J.J., McElhinny, M.W., Crawford, A.R., & Luck, G.R., 1974 - Palaeomagnetism and the tectonic evolution of the Tasman Orogenic Zone. *Journal of the Geological Society of Australia*, 21, 187-194.

Fergusson, C.L., Cas, R.A.F., Collins, W.J., Craig, G.Y., Crook, K.A.W., Powell, C.McA., Scott, P.A., & Young, G.C., 1979 - The Late Devonian Boyd Volcanic Complex, Eden, N.S.W. *Journal of the Geological Society of Australia*, 26, 87-105.

Friend, P.F., & House, M.R., 1964 - The Devonian Period. *In* Harland, W.B., & others (editors), The Phanerozoic Time Scale. *Quarterly Journal of the Geological Society of London*, 120S (supplement), 233-236.

Forster-Cooper, C., 1937 - The Middle Devonian fish fauna of Achanarras. *Transactions of the Royal Society of Edinburgh*, 59, 223-239.

Gardiner, B.G., & Miles, R.S., 1975 - Devonian fishes of the Gogo Formation, Western Australia. *Colloques Internationaux du Centre National de la Recherche Scientifique*, 218, 73-79.

Giffin, E.B., 1980 - Devonian vertebrates from Australia. *Postilla*, 180, 1-15.

Gilbert-Tomlinson, J., 1968 - A new record of *Bothriolepis* in the Northern Territory of Australia. *Bureau of Mineral Resources, Australia, Bulletin* 80, 191-224.

Glen, R.A., 1979 - The Mulga Downs Group and its relationship to the Amphitheatre Group southwest of Cobar. *Quarterly Notes of the Geological Survey of New South Wales*, 36, 1-10.

Glen, R.A., 1982 - Nature of late-Early to Middle Devonian tectonism in the Buchambool area, Cobar, New South Wales. *Journal of the Geological Society of Australia*, 29, 127-138.

Goleby, B.R., 1980 - Early Palaeozoic palaeomagnetism in southeast Australia. *Journal of Geomagnetism and Geoelectricity*, 32, supplement 3, 11-21.

Graham-Smith, W., & Westoll, T.S., 1937 - On a new long-headed dipnoan fish from the Upper Devonian of Scaumenac Bay, P.Q., Canada. *Transactions of the Royal Society of Edinburgh*, 59, 241-266.

Hills, E.S., 1931 - The Upper Devonian fishes of Victoria, Australia, and their bearing on the stratigraphy of the state. *Geological Magazine*, 68, 206-31.

Hills, E.S., 1959 - Record of *Bothriolepis* and *Phyllolepis* (Upper Devonian) from the Northern Territory of Australia. *Journal and Proceedings of the Royal Society of New South Wales*, 92, 174-5.

Hodgson, E.A., 1968 - Devonian spores from the Pertnjara Formation, Northern Territory. *Bureau of Mineral Resources, Australia, Bulletin* 80, 65-82.

Jarvik, E., 1950 - On some osteolepiform crossopterygians from the Upper Old Red Sandstone of Scotland. *Kungliga Svenska Vetenskapsakademiens Handlingar* (4), 2, 1-35.

Jarvik, E., 1952 - On the fish-like tail in the ichthyostegid stegocephalians, with descriptions of a new stegocephalian and a new crossopterygian from the Upper Devonian of east Greenland. *Meddelelser om Grønland*, 114, 1-90.

Jarvik, E., 1959 - Dermal fin-rays and Holmgren's principle of delamination *Kungliga Svenska Vetenskapsakademiens Handlingar* (4), 6, 1-51.

Johnstone, M.H., Jones, P.J., Koop, W.J., Roberts, J., Gilbert-Tomlinson, J., Veevers, J.J., & Wells, A.T., 1968 - Devonian of Western and Central Australia. *In* Oswald, D.H., (editor)- International Symposium on the Devonian system, 1, 599-612. *Alberta Society of Petroleum Geologists, Calgary.*

Jones, B.G., 1970 - Stratigraphy and sedimentology of the Upper Devonian Pertnjara and Finke Groups, Amadeus Basin, Northern Territory. *Ph.D thesis, Australian National University.*

Jones, B.G., 1972 - Upper Devonian to Lower Carboniferous stratigraphy of the Pertnjara Group, Amadeus Basin, central Australia. *Journal of the Geological Society of Australia*, 19, 229-249.

Jones, P.J., Campbell, K.S.W., & Roberts, J., 1973 - Correlation chart for the Carboniferous System in Australia. *Bureau of Mineral Resources, Australia, Bulletin*, 156A, 1-40.

Lehman, J.P., 1959 - Les dipneustes du Devonien superieur du Groenland. *Meddelelser om Grønland*, 160, 1-58.

Long, J.A., 1983a - A new diplacanthoid acanthodian from the Late Devonian of Victoria. *Memoir of the Association of Australasian Palaeontologists*, 1, 51-65.

Long, J.A., 1983b - New bothriolepid fish from the Late Devonian of Victoria, Australia. *Palaeontology*, 26, 295-320.

Marsden, M.A.H., 1976 - Upper Devonian-Carboniferous. *In* Douglas, J.G., & Ferguson, J.A., (editors), Geology of Victoria. *Geological Society of Australia, Special Publication* 5, 77-124.

McElhinny, M.W., & Embleton, B.J.J., 1974 - Australian palaeomagnetism and the Phanerozoic plate tectonics of eastern Gondwanaland. *Tectonophysics*, 22, 1-29.

Miles, R.S., 1973 - Articulated acanthodian fishes from the Old Red Sandstone of England, with a review of the structure and evolution of the acanthodian shoulder-girdle. *Bulletin of the British Museum (Natural History), Geology*, 24, 113-213.

Miles, R.S., 1977 - Dipnoan (lungfish) skulls and the relationships of the group: a study based on new species from the Devonian of Australia *Zoological Journal of the Linnean Society*, 61, 1-328.

Milton, D.J., 1967 - Gosses Bluff crater study. *In Bureau of Mineral Resources, Australia, Record* 1967/134, 11-14.

Milton, D.J., Barlow, B.C., Brett, R., Brown, A.R., Glikson, A.Y., Manwaring, E.A., Moss, F.J., Sedmik, E.C.E., Vanson, J., & Young, G.A., 1972 - Gosses Bluff impact structure, Australia. *Science*, 175, 1199-1209.

Playford, G., 1983 - The Devonian miospore genus *Geminospora* Balme 1962: a reappraisal based on topotypic *G. lemurata* (type species). *Memoir of the Association of Australasian Palaeontologists*, 1, 311-325.

Playford, G., Jones, B.G., & Kemp, E.M., 1976 - Palynological evidence for the age of the synorogenic Brewer Conglomerate, Amadeus Basin, central Australia. *Alcheringa*, 1, 235-243.

Pritchard, C.E., & Quinlan, T., 1962 - The geology of the southern half of the Hermannsburg 1:250 000 Sheet. *Bureau of Mineral Resources, Australia, Report*, 61.

Rade, J., 1964 - Upper Devonian fish from the Mt Jack area, New South Wales, Australia. *Journal of Palaeontology*, 38, 929-931.

Ranford, L.C., Cook, P.J., & Wells, A.T., 1966 - The geology of the central part of the Amadeus Basin, Northern Territory. *Bureau of Mineral Resources, Australia, Report*, 86.

Ritchie, A., 1973 - *Wuttagoonaspis* gen. nov., an unusual arthrodire

from the Devonian of western New South Wales, Australia. *Palaeontographica A*, 143, 58-72.

Ritchie, A., in press - A new placoderm, *Placolepis* gen. nov. (Phyllolepidae) from the Late Devonian of New South Wales, Australia. *Proceedings of the Linnean Society of New South Wales.*

Ritchie, A., & Gilbert-Tomlinson, J., 1977 - First Ordovician vertebrates from the Southern Hemisphere. *Alcheringa*, 1, 351-368.

Schmidt, P.W., & Morris, W.A., 1977 - An alternative view of the Gondwana Paleozoic apparent polar wander path. *Canadian Journal of Earth Sciences*, 14, 2674-2678.

Schultze, H.-P., 1969 - *Griphognathus* Gross, ein langschnauziger Dipnoer aus dem Oberdevon von Bergisch-Gladbach (Rheinisches Schiefergebirge) und von Lettland. *Geologica et Palaeontologica*, 3, 21-79.

Seddon, G., 1969 - Conodonts and fish remains from the Gneudna Formation, Carnarvon Basin, Western Australia. *Journal of the Royal Society of Western Australia*, 52, 21-30.

Stensio, E.A., 1948 - On the Placodermi of the Upper Devonian of East Greenland. 2. Antiarchi: subfamily Bothriolepinae. With an attempt at a revision of the previously described species of that family. *Meddelelser om Grønland*, 139, 1-622.

Thomson, K.S., 1973 - Observations on a new rhipidistian fish from the Upper Devonian of Australia. *Palaeontographica A*, 143, 209-220.

Turner, S., Jones, P.J., & Draper, J.J., 1981 - Early Devonian thelodonts (Agnatha) from the Toko Syncline, western Queensland, and a review of other Australian discoveries. *BMR Journal of Australian Geology & Geophysics*, 6, 51-69.

Wells, A.T., & Moss, F.J., 1983 - The Ngalia Basin, Northern Territory: stratigraphy and structure. *Bureau of Mineral Resources, Australia, Bulletin*, 212.

Wells, A.T., Forman, D.J., & Ranford, L.C., 1965 - The geology of the northwestern part of the Amadeus Basin, Northern Territory. *Bureau of Mineral Resources, Australia, Report*, 85.

Wells, A.T., Forman, D.J., Ranford, L.C., & Cook, P.J., 1970 - Geology of the Amadeus Basin, central Australia. *Bureau of Mineral Resources, Australia, Bulletin*, 100.

Westoll, T.S., 1949 - On the evolution of the Dipnoi. *In* Jepson, G.L., Simpson, G.G., & Mayr, E., (editors), Genetics, paleontology & evolution. *University Press, Princeton*, 121-184.

White, E.I., 1965 - The head of *Dipterus valenciennesi* Sedgwick & Murchison. *Bulletin of the British Museum (Natural History), Geology*, 11, 1-45.

Woodward, A.S., 1906 - On a Carboniferous fish fauna from the Mansfield district, Victoria. *Memoirs of the National Museum, Melbourne*, 1, 1-32.

Young, G.C., 1974 - Stratigraphic occurrence of some placoderm fishes in the Middle and Late Devonian. *Newsletters on Stratigraphy*, 3, 243-61.

Young, G.C., 1981 - New Early Devonian brachythoracids (placoderm fishes) from the Taemas-Wee Jasper region of New South Wales. *Alcheringa*, 5, 245-271.

Young, G.C., 1982 - Devonian sharks from southeastern Australian and Antarctica *Palaeontology*, 25, 817-843.

Young, G.C., 1983 - A new antiarchan fish (Placodermi) from the Late Devonian of southeastern Australia. *BMR Journal of Australian Geology & Geophysics*, 8, 71-81.

Young, G.C., 1984a - An asterolepidoid antiarch (placoderm fish) from the Early Devonian of the Georgina Basin, central Australia. *Alcheringa* 8, 65-80.

Young, G.C., 1984b - Reconstruction of the jaws and braincase in the Devonian placoderm fish *Bothriolepis*. *Palaeontology*, 23(3), 635-661.

Young, G.C., in press - Further petalichthyid remains from the Taemas/Wee Jasper area of New South Wales (placoderm fish, Early Devonian) *BMR Journal of Australian Geology & Geophysics.*

Young, G.C., & Gorter, J.D., 1981 - A new fish fauna of Middle Devonian age from the Taemas/Wee Jasper region of New South Wales. *Bureau of Mineral Resources, Australia, Bulletin*, 209, 83-147.

BMR Journal of Australian Geology & Geophysics, 9, 255-260

The 1982 Wyalong earthquakes (NSW) and recent crustal deformation

D. Denham[1], T. Jones[1] & J. Weekes[2]

Since 1959, when the Snowy Mountains Network was installed in southeastern Australia, several minor (ML < 4.0) earthquakes have been located in the Wyalong–Grenfell–Cootamundra region of New South Wales. However, until the end of 1983, only two earthquakes were large enough for focal mechanisms to be determined. These were the 1972 Temora and the 1982 Wyalong earthquakes. Both had magnitudes of ML ~ 4.5 and were associated with compressive stresses in the crust. The Wyalong sequence in 1982 consisted of several hundred earthquakes, of which 26 could be located and the largest (ML ~ 4.6 on 26 November 1982) caused minor damage in the towns of Wyalong and West Wyalong. Most earthquake activity in the region appears to be associated with the boundaries of the Bland Creek drainage system, which is a shallow depression containing on average about 50 m of Cainozoic deposits. The Bland Creek drainage system used to flow north into the Lachlan River, but its path was blocked as a result of either minor uplift or local subsidence, and it now drains into Lake Cowal, which is a closed basin. However, a lack of seismicity near Lake Cowal suggests that this crustal deformation is not associated with the recent earthquakes.

Introduction

Although earthquakes were felt in New South Wales within one month of the founding of the Colony in 1788 (Clarke, 1869), we have found no reference to any significant earthquake in the Wyalong–Temora region until 1972 (Burke-Gaffney, 1951; Doyle & others, 1968; Drake, 1974). In that year an earthquake of Richter magnitude close to 4.5 occurred about 15 km north of Temora. Since then several small earthquakes have culminated in a series of moderate-sized earthquakes in 1982 (Fig. 1).

The 1982 series prompted the present investigation because it contained an earthquake large enough for a focal mechanism to be determined, and offered an opportunity to relate earthquake activity to possible recent crustal deformation in the region. Furthermore, the largest earthquake in the 1982 series caused damage in Wyalong, and the series as a whole caused considerable consternation to the local population.

Most earthquakes have occurred at the edges of the Bland Creek drainage system. There appear to be no references in the literature to the Recent physiographic history of the region, but a cursory inspection of the drainage patterns indicates that recent movements have taken place, causing the Bland Creek drainage system, which used to flow into the Lachlan River, to drain into the closed Lake Cowal.

The age of the uplift or subsidence that resulted in the formation of Lake Cowal is unknown, as is the age of the Bland Creek drainage system. However, the average thickness of Cainzoic cover in the Bland Creek drainage system is only about 40–50 m, except where the creeks flow over earlier river courses; in these instances the thickness reaches about 150 m (M. Williams, personal communication, 1983). This small thickness is confirmed by airborne magnetic data (see BMR 1:250 000 maps of the Forbes and Cootamundra areas).

Earthquake parameters

1982 Wyalong earthquakes

Figure 1 shows the simplified geology of the region and all known earthquake epicentres located by five or more stations until the end of 1982. None of the epicentres dates from before 1959, when the Australian National University (ANU) network began operating (Doyle & Underwood, 1965), and only the 1972 Temora and the largest 1982 Wyalong earthquake had magnitudes greater than 4.0. As the Riverview station has operated since 1909 (Drake, 1974) and the area has been populated for at least 100 years, it appears that no large earthquake (ML ≥ 5.5) has occurred in the region in historical times and that the Wyalong sequence represents a distinct recent increase in earthquake activity. Twenty-six earthquakes from the 1982 sequence were large enough to be located (Table 1), but because of the poor distribution of stations in all but the southeast quadrant of the region, the epicentres are probably accurate only to about 10 km. Many more earthquakes were felt near Wyalong, but not located, because the nearest permanent station, at Young, was at least 90 km from most of the sequence, and all other stations in the region were at least 150 km from Wyalong (see Denham, 1983, for locations of the seismographs).

Table 1. Wyalong earthquakes 1982

Date	Origin time	Lat °S	Long °E	Depth (km)	Magnitude (ML)	No. of stations
04 01 82	02 21 13	34.30	147.50	0	2.5	5
15 03 82	16 54 20	34.28	147.58	23	2.5	9
20 05 82	07 36 18	33.96	147.24	2	3.6	26
20 05 82	08 13 17	33.91	147.38	18	2.6	8
20 05 82	15 37 20	34.15	147.54	24	3.4	13
20 09 82	08 21 02	34.03	147.42	21	3.2	7
20 09 82	14 36 55	33.99	147.30	0	2.5	7
25 09 82	10 18 05	33.99	147.33	19	2.8	9
25 09 82	16 11 49	33.95	147.21	12	3.3	12
09 11 82	23 10 45	33.98	147.26	0	2.5	5
15 11 82	14 11 14	33.85	147.29	17	2.6	8
24 11 82	07 07 53	34.01	147.21	1	4.0	8
24 11 82	07 09 23	34.01	147.21	1	4.0	8
25 11 82	09 02 56	33.95	147.37	19	2.8	8
26 11 82	00 11 14	33.94	147.25	4	4.6	13
26 11 82	05 07 42	33.96	147.38	19	3.0	12
26 11 82	09 02 00	33.85	147.29	0	3.3	12
26 11 82	20 44 53	34.06	147.35	16	3.6	14
26 11 82	22 15 35	33.92	147.14	8	2.8	12
27 11 82	11 20 47	33.92	147.29	17	3.3	13
27 11 82	17 54 56	33.96	147.31	14	2.7	9
28 11 82	18 07 51	33.92	147.13	15	2.6	11
28 11 82	18 22 55	33.88	147.28	13	2.8	11
30 11 82	02 07 17	33.93	147.27	13	3.1	11
01 12 82	06 31 14	33.98	147.33	17	3.2	12
01 12 82	13 51 28	33.93	147.38	18	2.9	11

Although the earthquakes in January and March took place north of Temora near the 1972 event, the main sequence started on 20 May, when an earthquake with magnitude ML 3.6 took place near Wyalong. The isoseismal map for this earthquake (Fig. 2) indicates that the focus was very shallow, because the earthquake was only felt close to the epicentre. Earthquakes continued to be felt in the region throughout 1982, culminating in the magnitude ML 4.6 earthquake on 26 November.

[1]Division of Geophysics, BMR
[2]Research School of Earth Sciences, Australian National University, GPO Box 4, Canberra ACT 2601

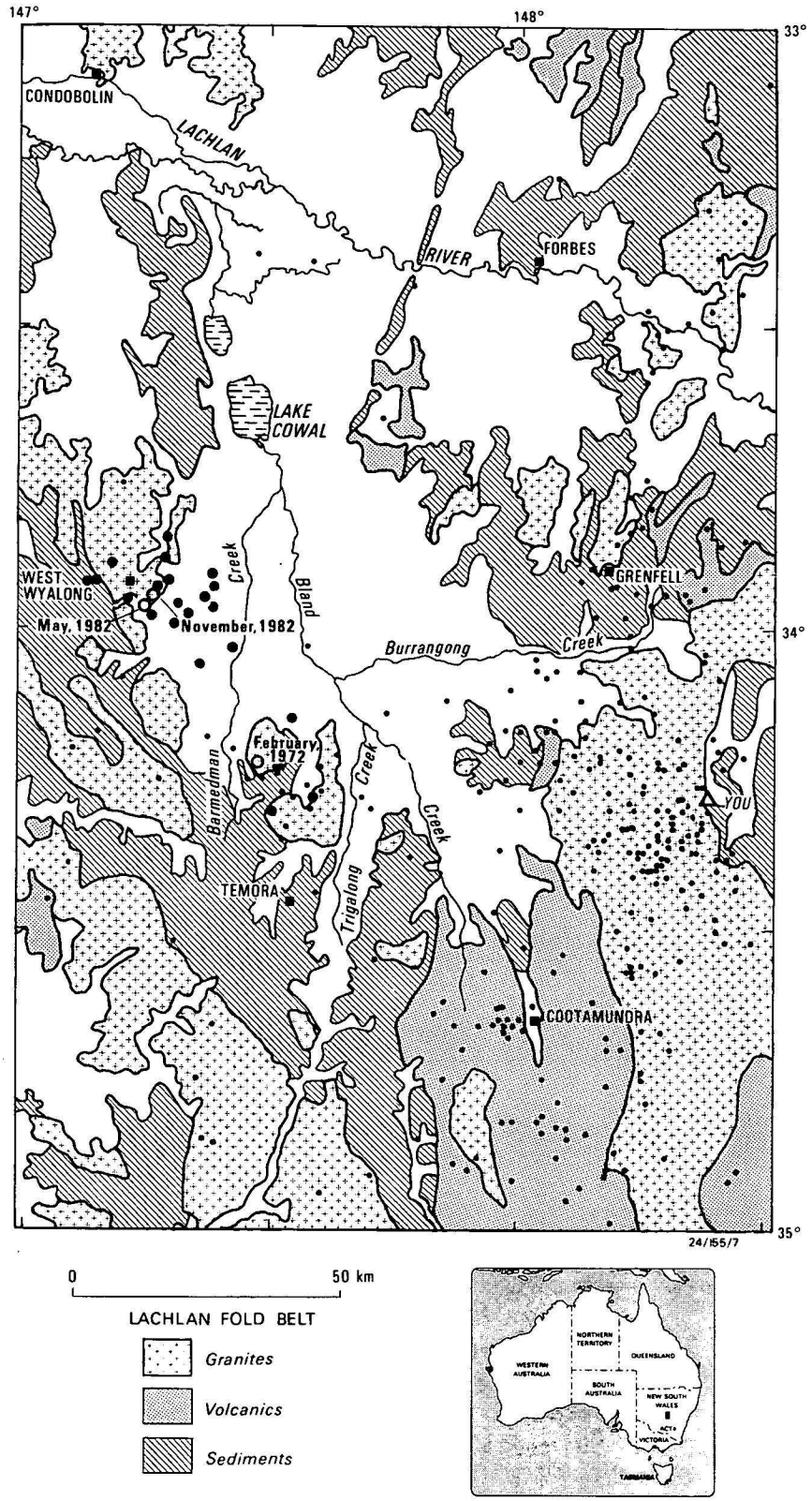

Figure 1. Simplified geology and earthquake occurrences in the Wyalong–Grenfell–Cootamundra region.
All epicentres plotted were located by five or more stations during the period 1959–1982. Only the February 1972 and the November 1982 events are larger than ML 4.0. Epicentres from the 1982 sequence are plotted as larger symbols. Unstippled areas are covered by Quaternary sediments. The seismograph at Young (YOU) is represented by the open triangle. The drainage patterns are taken from the Forbes 1:250 000 topographic map, and the geology from the Macquarie 1:500 000 sheet produced by the Geological Survey of New South Wales (1969).

The isoseismal map of the November earthquake (Fig. 3) was compiled from approximately 80 reports collected from questionnaires, and from field inspections made shortly after the earthquake. Extensive though minor damage occurred in Wyalong, West Wyalong, and neighbouring regions. In Wyalong many reports indicated cracking of internal or external walls. In some stores the stock was thrown from the shelves, and a shop awning partly collapsed. Thus, a maximum intensity of VI on the Modified Mercalli Scale was assigned (Table 2). In West Wyalong the effects of the earthquake were similar, but not so intense.

Table 2. MM VI Intensity: typical effects

Felt by all. People and animals alarmed. Many run outside. Difficulty experienced in walking steadily. Slight damage to Masonry D. Some cracks or falls. Isolated cases of chimney damage. Windows, and crockery broken. Objects fall from shelves, and pictures from walls. Heavy furniture moved. Unstable furniture overturned. Small church school bells ring. Trees and bushes shake, or are heard to rustle. Material may be dislodged from existing slips, talus slopes, or slides. (Masonry D is associated with buildings with low standards of workmanship, poor mortar, or constructed of weak materials like mud brick and rammed earth. Weak horizontally).

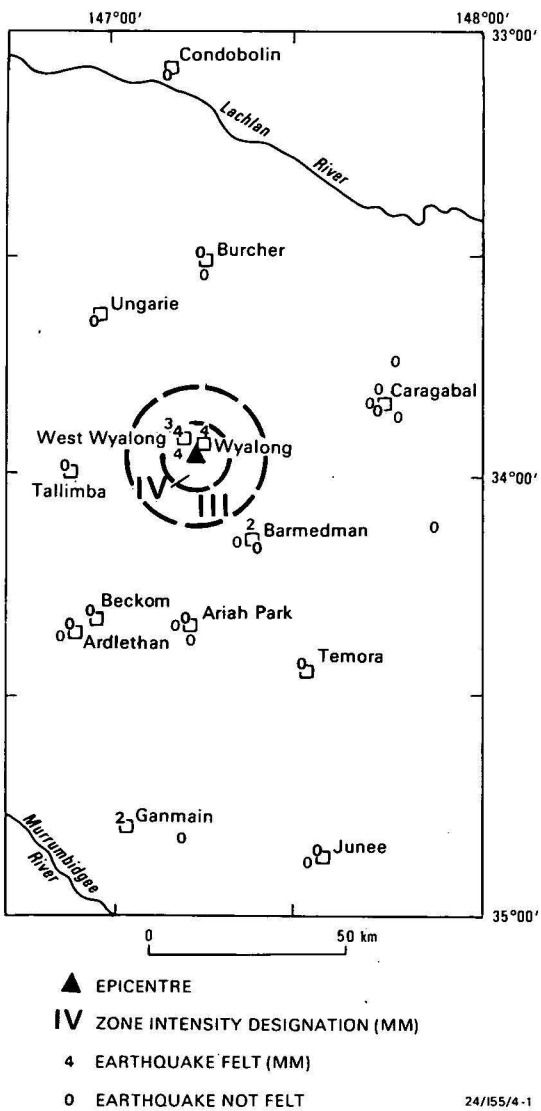

Figure 2. Isoseismal map of the Wyalong earthquake, 20 May 1982.

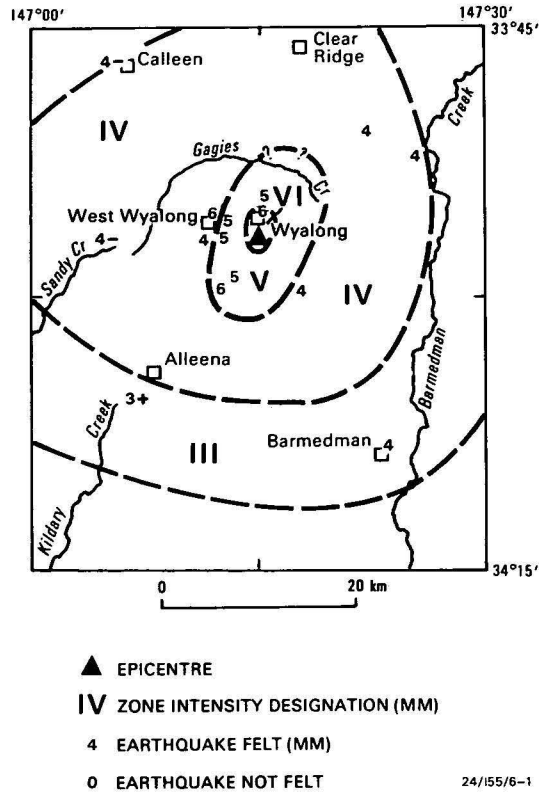

Figure 3. Isoseismal map of epicentral region for the Wyalong earthquake, 26 November 1982.

The extent of the felt area was, with a few exceptions, limited to a mean radius of about 35 km, remarkably low for an earthquake of this size. Although the isoseismal lines are not well defined, there was clearly a rapid attenuation of intensity with distance, indicating that, like the May earthquake, this also occurred at a shallow depth. The adopted epicentre of the main November earthquake (Table 1) was based on the macroseismic data, because neither of the computer generated solutions (Table 3) was consistent with the felt reports.

Table 3. Hypocentres of May 20 and November 26 1983 earthquakes and crustal models used

Source	Date	Time (UT)	Lat °S	Long °E	Depth (km)	No. of stations
ANU	20 05 82	07 36 22.9	34.14	147.55	23	13
BMR	20 05 82	07 36 17.9	33.965	147.237	2	26
MACR	20 05 82	07 36 18	33.96	147.24	~ 2	—
ANU	26 11 82	00 11 13.5	33.89	147.18	10	13
BMR	26 11 82	00 11 16.7	34.016	147.329	4	17
MACR	26 11 82	00 11 17	33.94	147.25	~ 4	—

	BMR model				ANU model		
Layer	P-velocity (km/s)	Depth (km)	Thickness (km)	Layer	P-velocity (km/s)	Depth (km)	Thickness (km)
1	5.9	0	4	1	6.03	0	37
2	6.0	4	6	2	8.16	37	
3	6.1	10	2				
4	6.2	12	8				
5	6.3	20	8				
6	6.7	28	2				
7	7.1	30	4				
8	7.4	34	5				
9	7.7	39	4				
10	8.0	43	7				
11	8.15	50					

ANU = Australian National University; BMR = Bureau of Mineral Resources; MACR = epicentre determined from felt reports, depth adopted as 4 km.

Location of hypocentres

The epicentres plotted in Figure 1 were taken from the routine solutions obtained by the ANU, except for the main earthquakes on 20 May and 26 November, where the epicentres were modified to take account of the macroseismic data. As mentioned earlier, because most of the stations are situated to the southeast of the epicentres, the epicentral control is poor. Table 3 shows different solutions obtained using different crustal models and different location programs. The uncertainties in the depths are also large; however, using the relation given by Båth (1979, p. 127), $I_0 - I = 3\log(1 + h^2/r^2)$, where I_0 is the maximum intensity, I the intensity at radius r, and h the depth, it appears that most earthquakes occurred at shallow (<12km) depth.

Magnitudes and moment

Richter (ML) and body-wave (mb) magnitudes were measured wherever possible. The ML magnitude was determined by using Richter's standard distance factors extended by Eiby & Muir (1961). Drake's (1974) distance corrections were applied to account for the differences in attenuation between southern California and southeastern Australia, and 0.1 was added to the estimate when this was derived solely from a vertical component instrument, because Richter's attenuation factors were obtained from horizontal seismographs, which record larger amplitudes than equivalent vertical instruments.

For body-waves the standard relation mb = log(A/T) + Q has been used, where A is the ground amplitude in μm, T the period in seconds, and Q the depth-distance factor given by Richter (1958, pp. 688–9). Surface waves were not observed on any of the regional long-period seismograms. This prevents the estimation of a surface-wave magnitude (Ms) and puts an upper bound of about 2.5 on it.

Table 4 lists the ML and mb estimates from sixteen stations. The errors given are the standard deviations. The mb values appear to be too large, probably because the attenuation relations for distances less than 12 degrees are different in southeastern Australia from those obtained by Richter for California. Therefore, to estimate the seismic moment Mo* and the energy release we use the ML value. Hyndman & Weichert (1983) give log Mo = 9.0 + 1.5 ML. Thus the seismic moment is approximately 8.0×10^{15} N-m. This is a larger estimate of Mo than if Ms is used to evaluate Mo. If we use Nuttli's (1983) relations for Ms–2.5, we get Mo 2×10^{14} N-m, an order of magnitude lower.

Table 4. Magnitude of the West Wyalong earthquake

Station	Distance (degrees)	mb	ML
RIV	3.2		4.7
TOO	3.8		4.0
BFD	5.0		4.3
COO	5.2		4.8
STK	5.3	5.4	4.5
WKA	6.2	4.8	4.4
MGR	6.6	5.4	4.4
ADT	7.2	5.7	4.7
UMB	7.9	6.4	4.7
NBK	7.9	5.4	4.8
WFTG	8.1	5.6	4.9
CLV	9.0	5.5	4.7
WRG	10.2	6.0	5.1
HWK	11.0	5.9	4.5
CTA	13.9	5.1	
ASP	15.7	3.5	
Mean values		5.4±0.7	4.6±0.3

*Mo = μAd, where μ = rigidity of the rock, and d the average displacement of the fault over the area A.

Focal mechanism

The ML–4.6 earthquake on 26 November was recorded at most stations in southeastern Australia, and the first motions are plotted on the lower half of the focal sphere in Figure 4. The southeasterly dipping nodal plane is well constrained because it must pass between RIV and WER and also between TOO and DRT. However, the other plane is poorly determined, and we have adopted a solution in which it passes close to the South Australian stations because the HWK and PNA arrivals give a downwards first motion and these are close to other stations where the first motion is up. Thus, we presume that these sta-

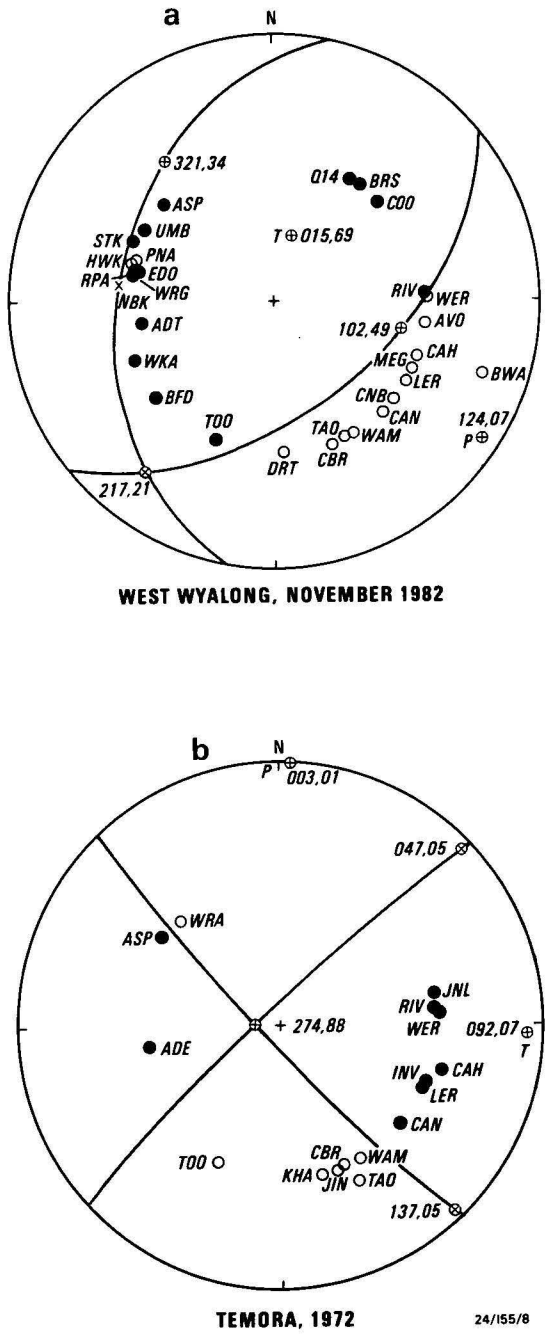

Figure 4. Fault-plane solutions for the 1972 Temora and the 1982 Wyalong earthquakes.

Solid circles, open circles, and crosses represent compressive, dilative, and emergent first motions, respectively, plotted on an equal-area projection of the lower focal hemisphere. The circumscribed crosses show the nodal poles and the pressure, tension, and null axes. The numbers represent the trend and plunge of the poles, respectively; the letters are the standard three-letter codes for Australian seismograph stations.

tions are close to a nodal plane. Unfortunately, it is not possible to determine which of the two planes is the fault plane. However, the mechanism is primarily one of thrust faulting with a small component of strike-slip movement. Table 5 lists the focal parameters. The pressure axis of 124 degrees is consistent with the average pressure axis of 120 degrees obtained by Denham & others (1981) for southeastern Australia. None of the aftershocks was large enough to obtain a focal mechanism; however, the earthquake on 20 May at 07h 36m gave rise to the same directions of first motion on the ANU network as the November 1982 earthquake, and hence it is reasonable to assume a thrust-fault mechanism for this large foreshock.

Temora earthquake 1972

The Wyalong earthquake activity prompted an examination of the 1972 Temora earthquake, (ML 4.5), which took place at 15h 22m 36s on 25 February, about 37 km from the main 1982 event. All available seismograms were examined, and Figure 4 shows the first motions for this earthquake plotted on the lower focal hemisphere. The polarities of the instruments at that time were easily determined, because a large deep Fijian earthquake took place only seven hours earlier and was well recorded as an impulsive first motion on all seismographs in eastern Australia.

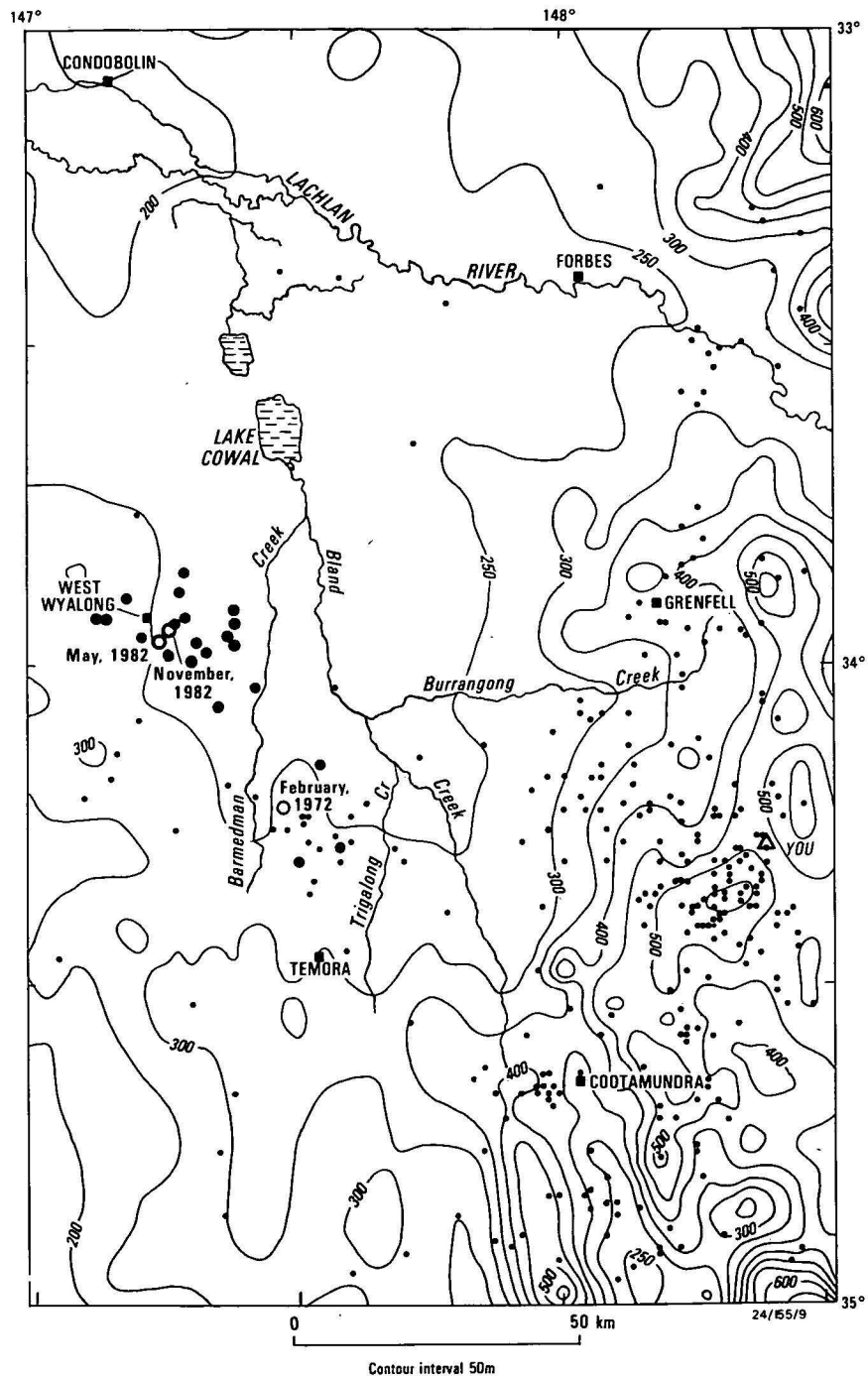

Figure 5. Topography and earthquake epicentres.
The contours are drawn at 50-m intervals. See caption to Figure 1 for key to earthquake symbols. The topography is taken from the BMR digital terrain model.

The first motions indicate a strike-slip faulting mechanism associated with almost north-south compression. Unfortunately, it is impossible to determine which nodal plane is associated with the causative fault. Table 5 lists the focal parameters.

Table 5. Adopted parameters for the Wyalong and Temora earthquakes

	Trend (degrees)	Plunge (degrees)
Wyalong, 1982		
Poles of nodal planes	102	49
	321	34
Axis of compression	124	07
Axis of tension	015	69
Null axis	217	21
Temora, 1972		
Poles of nodal planes	137	05
	047	05
Axis of compression	003	01
Axis of tension	092	07
Null axis	274	82

Discussion

Both the 1972 Temora and the 1982 Wyalong earthquakes are associated with compressive forces in the crust. However, it is difficult to relate these or any others in the region to any significant feature or features. It is not even certain that the earthquakes between Grenfell and Cootamundra are part of the same regime, because the area near Wyalong was almost aseismic until 1982, whereas the area near Young (YOU) has experienced low-level background seismicity for many years. In Figure 1 the earthquake epicentres are superimposed on the geology, and there is no obvious correlation with any rock type except perhaps for the exposed granites at the edges of the Bland Creek drainage system. Cleary (1967) noted that in the nearby Dalton-Gunning region the earthquakes appeared to correlate with a granite batholith. However, in the Wyalong region, because outcrop is so poor, any correlation between the granites and earthquake activity must be very tenuous. As most of the earthquakes appear to have occurred at the margins of the Bland Creek drainage system and very few earthquakes occur beneath the thin Cainozoic cover, it appears that there may be a correlation between topography and earthquake occurrence (Fig. 5). However, even this relationship is not strongly developed, because the eastern margin of the Bland Creek drainage system is much steeper than the western. Nevertheless, if we assume, in the absence of any other evidence, that the stress regime (north-south/northwest-southeast compression) is the same throughout the region, we can speculate on recent crustal movement associated with the earthquakes.

In this context the shallow depression associated with the Bland Creek drainage system assumes some importance, particularly with respect to the presence of Lake Cowal (Fig. 5). It is clear that the Bland Creek drainage system used to flow north into the Lachlan River, but now it drains into the closed Lake Cowal. Evidently, there has been crustal uplift between Lake Cowal and the Lachlan River, or subsidence near Cowal, which resulted in Bland Creek being unable to cut through to the north. However, if this movement was still taking place, one would expect earthquakes to occur near Lake Cowal or between Lake Cowal and the Lachlan River. At present the seismicity in this region is negligible. Therefore, we conclude that the current earthquake activity is not related to the deformation that caused the Bland Creek drainage system to change its course.

Acknowledgements

We thank H.A. Doyle, B.J. Drummond, R. Underwood, and C. Wright for reviewing the manuscript and making several suggestions to improve it.

References

Båth, M., 1979 - Introduction to seismology; 2nd edition. *Birkhauser Verlag, Basel, Boston, Stuttgart.*

Burke-Gaffney, T.N., 1951 - Seismicity of Australia. *Journal and Proceedings, Royal Society of New South Wales*, 85, 47-52.

Clarke, W.B., 1869 - On the causes and phenomena of earthquakes, especially in relation to shocks felt in New South Wales and in other provinces of Australasia. *Transactions of the Royal Society of New South Wales*, 2, 51-86.

Cleary, J.R., 1967 - The seismicity of the Gunning and surrounding areas, 1958-1961. *Journal of the Geological Society of Australia*, 14, 23-29.

Denham, D., 1983 - Australian national report to the IASPEI, 1979-1982, *Bureau of Mineral Resources, Australia, Record* 1983/20.

Denham, D., Weekes, J., & Krayshek, C., 1981 - Earthquake evidence for compressive stress in the southeast Australian crust. *Journal of the Geological Society of Australia*, 28(3), 323-332.

Doyle, H.A., Everingham, I.B., & Sutton, D.J., 1968 - Seismicity of the Australian continent. *Journal of the Geological Society of Australia*, 15(2), 295-312.

Doyle, H.A., & Underwood, R., 1965 - Seismological stations in Australia. *Australian Journal of Science*, 28, 40-43.

Drake, L., 1974 - The seismicity of New South Wales. *Journal and Proceedings, Royal Society of New South Wales*, 107, 35-40.

Eiby, G.A., & Muir, M.G., 1961 - Tables to facilitate the study of the near earthquakes. *New Zealand Department of Scientific and Industrial Research, Seismological Observatory Bulletin*, S-109.

Hyndman, R.D., & Weichert, D.H., 1983 - Seismicity and rates of relative motion on the plate boundaries of Western North America. *Geophysical Journal of the Royal Astronomical Society*, 72(1), 59-82.

Nuttli, O.W., 1983 - Average seismic source-parameter relations for mid-plate earthquakes. *Bulletin of the Seismological Society of America*, 73, 519-536.

Richter, C.F., 1958 - Elementary seismology. *Freeman & Co., San Francisco.*

BMR Journal of Australian Geology & Geophysics, 9, 261–266

Ordovician nautiloids of central Australia, with a revision of *Madiganella* Teichert & Glenister

Bryan Stait[1] & John Laurie[2]

Nautiloids mainly from the Lower Ordovician Horn Valley Siltstone of the Amadeus Basin are revised. *Madiganella* is shown to have unexpanded two-layered bullettes and well-developed endocones, the endosiphotube of which has previously been mistaken for a free siphonal tube. These features do not allow assignment of *Madiganella* to the Ruedemannoceratidae as has been suggested: instead the genus belongs to a new family of Discosorida. *Madiganella magna* Teichert & Glenister 1952 and *M.* sp. (Flower & Teichert, 1957) are shown to be synonyms of *Madiganella tatei* (Etheridge). *Endoceras warburtoni* Etheridge is assigned to *Anthoceras* Teichert & Glenister, and *Anthoceras decorum* Teichert & Glenister from Western Australia is considered a junior synonym. The specimens recently described by Crick & Teichert (1983) as *A. decorum* from Mount Arrowsmith, New South Wales, belong to a different species, herein named *A. arrowsmithense* n. sp. The type specimens of *Bactroceras gossei* (Etheridge) are redescribed and refigured. A species of *Aphetoceras* is present, but it is not *Aphetoceras delectans* Teichert & Glenister. Also present is *Lobendoceras emanuelense* Teichert & Glenister, as well as a new genus of discosorid, known also from Thailand and possibly from Queensland. '*Trochoceras recticostatum*' Tate is too poorly preserved to be assigned even to a family. *Armenoceras* is recorded from the Stairway Sandstone.

Introduction

The Ordovician nautiloid faunas of the Amadeus Basin of central Australia are still largely undescribed, with only a few papers having been published (Etheridge, 1893, 1894; Tate 1896; Teichert, 1939; Teichert & Glenister, 1952). Although these studies described the nautiloids, no attempt was made to place them into a stratigraphic framework, because, commonly, the collecting locality was not precisely known. The collections available to the present authors are also poorly located, thus precluding the erection of a biostratigraphic scheme. They do, however, permit a more detailed assessment of the morphology and taxonomic position of a number of the previously described genera and species.

Stratigraphy

The Amadeus Basin is a large sedimentary basin that occupies most of the southern quarter of the Northern Territory. The approximately 900 m thick sedimentary sequence in the basin mostly ranges in age from Proterozoic to Devono-Carboniferous, of which over 2300 m (Wells & others,1970, p. 61) belongs to the Cambro-Ordovician Larapinta Group. This group comprises five formations, in ascending order, the Pacoota Siltstone, Horn Valley Siltstone, Stairway Sandstone, Stokes Siltstone, and Carmichael Sandstone (Wells & others, 1970). Most of the nautiloids discussed here come from the late Early Ordovician Horn Valley Siltstone and the early Middle Ordovician Stairway Sandstone. The former unit is one of interbedded siltstone, calcareous siltstone, claystone, limestone, and minor sandstone, with a maximum thickness of about 250 m (Wells & others, 1970, p. 68). It contains an abundant and well-preserved fauna of trilobites, brachiopods, pelecypods, nautiloids, ostracodes, and conodonts, with some graptolites and possible vertebrates. On the basis of the included conodont fauna, Cooper (1981) showed the Horn Valley Siltstone to be Late Canadian to Whiterock in age.

The Stairway Sandstone is a unit of interbedded quartz sandstone, siltstone, mudstone, and claystone, with a maximum thickness of about 430 m (Wells & others, 1970, p. 71), and contains a rich fauna of trilobites, pelecypods, gastropods, brachiopods, nautiloids, trace fossils and vertebrates. The unit was estimated by J.G. Tomlinson (in Wells & others, 1970) to be late Llanvirnian to Llandeilian (Whiterock) in age.

[1]Geology Department, University of Tasmania, GPO Box 252C, Hobart, Tasmania 7001 (present address: Department of Earth Sciences, Memorial University of Newfoundland, St. John's, Newfoundland, Canada A1B 3X5.).
[2]Division of Continental Geology, BMR.

Collections

The specimens belonging to the Commonwealth Palaeontological Collection (CPC prefix) were collected during regional mapping of the Amadeus Basin by the BMR during the 1950s and 1960s. They were collected at spot localities and cannot be related unambiguously to any stratigraphic section; therefore, they are of little biostratigraphic utility. Of the localities, two (HY216 and NT711) lie within the Stairway Sandstone (probably the lower part), and the remainder are from the Horn Valley Siltstone (see Table 1 for locality data).

Table 1. Localities of specimens in the BMR collections from the Horn Valley Siltstone and Stairway Sandstone in the central and western Amadeus Basin.

Locality No.	Rock Unit	1:250 000 Sheet Area	Location
HY216	Stairway Sandstone	Henbury	132°59'E, 24°12'S
NT711	" "	Lake Amadeus	Eastern end of Johnny Ck Anticline
NT185	Horn Valley Siltstone	Henbury	132°15'E, 24°07'S
NT146	" " "	Hermannsburg	Stokes Pass
NY3	" " "	Henbury	132°28'E, 24°23'S
LA46	" " "	Lake Amadeus	131°49'E, 24°28'S
LA51F	" " "	" "	131°23'E, 24°07'S
ML21C	" " "	Mount Liebig	131°43'E, 23°48'S
ML132	" " "	" "	131°56'E, 23°35'S

Specimens of the Madigan collection (Geology Dept, University of Adelaide; NTO prefix) are poorly located, but, according to Teichert & Glenister (1952, p. 733), were collected mainly from Ellery Creek, 84 km by road west of Alice Springs (see Cooper 1981, p. 149 for location).

Specimens of the Tate collection (South Australian Museum, T prefix) are also poorly located, but most seem to have come from the area around Tempe Downs homestead and Petermann Creek (south of Petermann Hills).

Specimens held in the Museum of Victoria (P prefix) are similarly poorly located.

Comments on the central Australian nautiloids

A summary of the original assignments, those of Teichert & Glenister (1952), and those given herein for the central Australian nautiloids is presented in Table 2. In addition to these species, Teichert & Glenister (1952, p. 733) also mentioned the presence of specimens belonging to *Baltoceras, Cryptendocera* and *Armenoceras* in collections made by C.T. Madigan. However, they did not give specimen numbers nor did they illustrate or describe these specimens.

Table 2. Previous and present assignments of central Australian Ordovician nautiloids.

Original assignment	Teichert & Glenister (1952)	Herein
Orthoceras tatei Etheridge, 1893	*Madiganella tatei*	*Madiganella tatei*
? Orthoceras Etheridge, 1894	*Madiganella magna*	*Madiganella tatei*
Actinoceras tatei (Tate, 1896)	*Madiganella tatei*	*Madiganella tatei*
Orthoceras gossei Etheridge, 1893	*Bactroceras gossei*	*Bactroceras gossei*
Orthoceras microlineatum Tate, 1896	*Cyclendoceras? microlineatum*	*Anthoceras warburtoni*
Orthoceras larapintense Tate, 1896	gen. ind.	gen. indet.
Orthoceras ibiciforme Tate, 1896	gen. ind.	gen. indet.
Orthoceras chewingsi Tate, 1896	gen. ind.	gen. indet.
Endoceras warburtoni Etheridge, 1893	*Catoraphiceras warburtoni*	*Anthoceras warburtoni*
Endoceras warburtoni Etheridge, 1894	*Catoraphiceras warburtoni*	*Anthoceras warburtoni*
Endoceras warburtoni Etheridge (Tate, 1896)	*Endoceras* n. sp.	gen. indet.
Endoceras arenarium Tate, 1896	*Endoceras arenarium*	*Endoceras? arenarium*
Endoceras Etheridge, 1894	*Endoceras* sp. ind.	gen. indet.
Trochoceras recticostatum Tate, 1896	*Tarphyceratidae* gen. ind.	Tarphycerida fam. gen. sp. indet.
Bathmoceras australe Teichert, 1938	*Bathmoceras australe*	*Bathmoceras australe*

Below are brief comments on the taxonomic position of most of the previously described or illustrated specimens of central Australian nautiloids, followed by detailed studies on three particular genera, *Madiganella, Anthoceras*, and *Bactroceras.*

Bathmoceras australe Teichert (1939) was adequately discussed and illustrated in the original descriptive work and, in the absence of additional specimens, no further comments can be made. Only one specimen belonging to the Tarphycerida has been recorded from central Australia, and that is the type specimen of *Trochoceras recticostatum* Tate. However, examination of this specimen indicates that assignment even to a family would be unwise. No other specimens assignable to this species have been found.

The most abundant endocerid in the collections is *Lobendoceras* (specimens CPC24721, 24722 and 24724 from localities ML21C, NT185, and HY3, respectively, and specimens P. 12282, 15541, NTO 1, 3, and 11). These specimens are indistinguishable from *Lobendoceras emanuelense* Teichert & Glenister (1954). This species has been recorded from the Siberian Platform by Ogienko & others (1974).

A single specimen of *Aphetoceras*, but not *Aphetoceras delectans* Teichert & Glenister (1954), is present in the Madigan Collection (NTO 20). Description of the species must await more and better preserved material.

There are a number of poorly preserved orthoconic species in the collections (NTO 22, 23), none of which can be assigned to a genus or species. Also present are several specimens of a new large gyroconic discosorid genus (CPC24724, 24726, both from locality LA 46; CPC24725 from ML 21C and CPC24727 from LA 51F), unusual in having a dorsal siphuncle and a marked difference between the septal necks on the ventral and dorsal sides of the siphuncle. A species of this genus is also found in the lower Middle Ordovician strata of Tarutao Island, Thailand (Stait & Burrett, 1984) and possibly in the Coolibah Formation, Queensland (Wade, in press).

Whereas the bulk of the species from central Australia have been collected from the Horn Valley Siltstone, the specimens of *Armenoceras* in the BMR collections (CPC24719, 24720 from localities HY 216 and NT 711, respectively) were collected from the Stairway Sandstone. As both the specimens of *Armenoceras* are preserved in sandstone, the detail needed for a specific assignment is not available.

Systematic palaeontology

Madiganella Teichert & Glenister, 1952
Figure 1A-L

Type species. *Madiganella tatei* (Etheridge, 1893)

Specimens included in *M. tatei.*

1893 *Orthoceras tatei* Etheridge, p. 7
1894 *?Orthoceras* Etheridge p. 25, Pl. 3, Figs. 13-15
1836 *Actinoceras tatei* (Etheridge), Tate, p. 102, Pl. 1, Figs. 2a,b.
1952 *Madiganella magna* Teichert & Glenister, p. 744, Pl. 105, Figs. 1,2
1952 *Madiganella tatei* (Etheridge), Teichert & Glenister, p. 744
1957 *Madiganella magna* Teichert & Glenister, Flower & Teichert, p. 53, Pl. 4, Fig. 7.
1957 *Madiganella tatei* (Etheridge), Flower & Teichert, p. 53
1957 *Madiganella* sp. Flower & Teichert, p. 53, Pl. 14, Figs. 1-6, P. 5, Fig. 8.

Diagnosis. (emended herein). Large, straight to very slightly curved longicones with moderately concave septa and sinuous transverse sutures with a broad ventral lobe. Outside of shell has prominent growth lines and fainter longitudinal lirae. Siphuncle apically is amphora shaped, becoming symmetrical and highly expanded orad. Siphuncle varies in position from central to near the venter with growth. The siphuncle is one-fourth to one-fifth the height of the phragmocone. The septal necks are cyrtochoanitic, becoming more strongly recurved in later growth stages. The connecting rings are very thick with a granular layer on the cameral surface and a thinner, darker, denser layer on the siphonal surface. The bullettes are unexpanded, two layered, and form from differentiation of the siphonal layer of the connecting ring. There are well-developed endocones in the siphuncle, which are more strongly developed on the ventral side. They begin well orad of the endocones as small annulae around the septal necks. Episeptal and hyposeptal cameral deposits are present.

Discussion. Teichert & Glenister (1952, p. 744) established *Madiganella*, stating '*Madiganella* is probably represented by three species from five different localities in the Ordovician belt of central Australia'. However, only two species were named, *M. magna* (the type species) and *M. tatei* (based on *Orthoceras tatei). M.* sp. was figured in Flower & Teichert (1957, p. 53) and they commented that Teichert & Glenister reported '...having several undescribed species in addition to *Madiganella magna* and "*Orthoceras tatei*" Etheridge..' The main criterion used to separate the various species was the relative position of the siphuncle within the phragmocone. Recent finds by Chen & Zou (1983) in Ordos, China, Wade (in press) in Queensland, and Stait (in press) in the Ordovician of Tasmania have shown that the position and shape of the siphuncle in the early discosorids was highly variable. Examination of the collections of *Madiganella* obtained from the Bureau of Mineral Resources (CPC24728, 24729 from ML132 and NT146 respectively), University of Adelaide (NTO 7, 10, 16, 17, 24), South Australian Museum (T 1255), and the Museum of Victoria (P

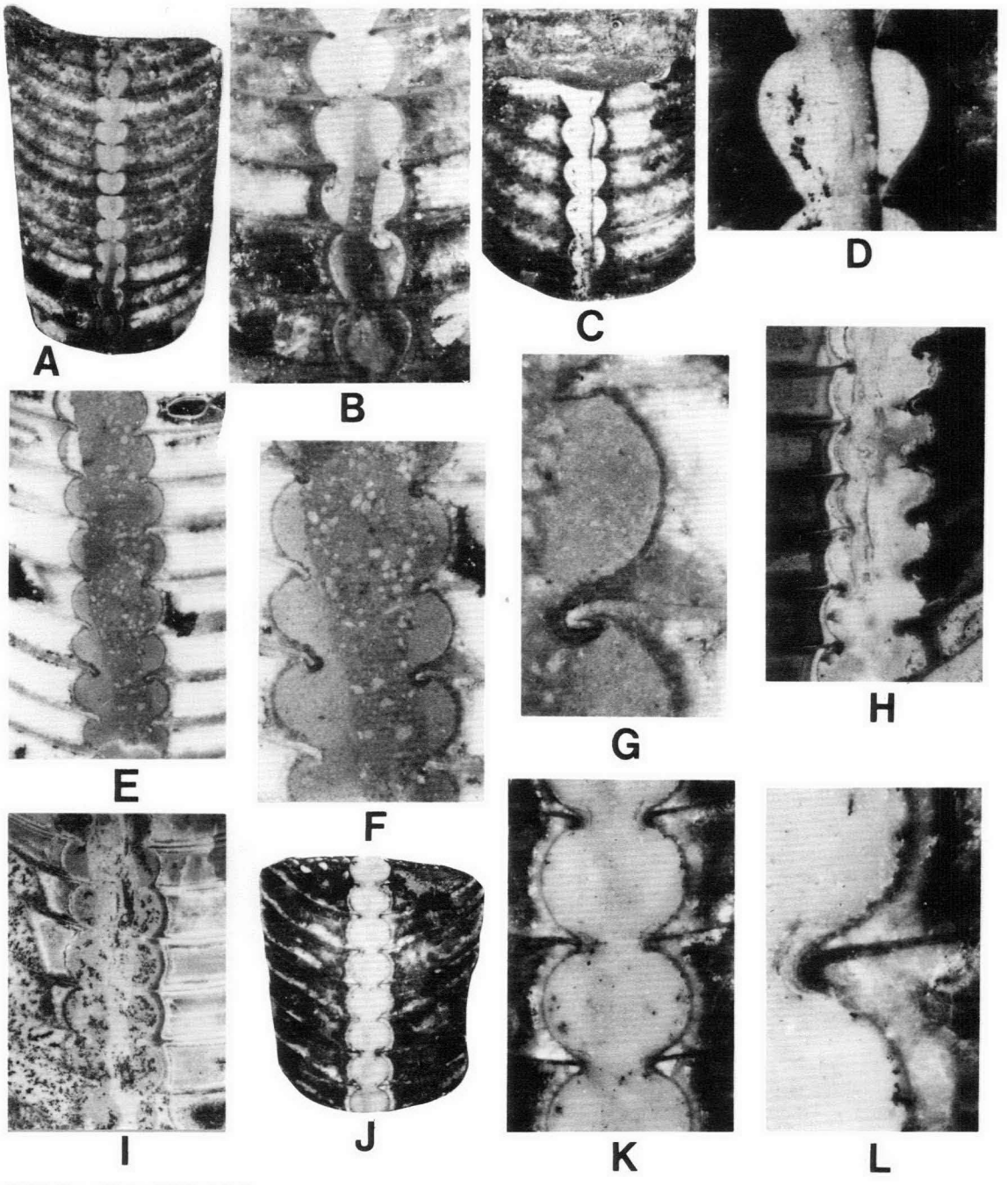

Figure 1. ***Madiganella tatei*** **(Etheridge).**
A, Sagittal section of N.T.O. 17, venter left, X2. B, Enlargement of the siphuncle of N.T.O. 17, venter left, X7. C, Sagittal section of N.T.O. 7, venter left, X3.5. D, Enlargement of the siphuncle in N.T.O. 7, venter left, X15. E, Sagittal section of the holotype of *'Actinoceras' tatei*, T1255, venter left, X1.5. F, Enlargement of the siphuncle of T1255, venter left, X3. G, Further enlargement of the dorsal side of the siphuncle, T1255, X8. H. Sagittal section of the siphuncle of N.T.O. 16, venter right, X2. I, Sagittal section of P.61762, venter left, X1.5. J, Sagittal section of N.T.O. 17, venter left, X1.8. K, Enlargement of siphuncle in N.T.O. 17, venter left, X6. L, Further enlargment of the dorsal side of the siphuncle, X15.

61762, 61763, 73049) indicates that the position of the siphuncle in *Madiganella* is also variable. The siphuncle varies from being initially central and amphora shaped (Fig. 2A–D) to more symmetrical and highly expanded in later growth stages (Fig. 2E–I). This change was not clear on the specimens used by Teichert & Glenister (1952), of which Flower & Teichert (1957, p. 52) commented 'This genus is as yet known only from relatively small portions, all appreciably large cross sections, and obviously representing relatively late portions of the phragmocone'. Owing to the highly variable shape and position of the siphuncle in *Madiganella*, it is considered that all specimens belong to one species, *Madiganella tatei.*

One of the unusual features of *Madiganella* as originally described was the presence of a free tube in the siphuncle (Fig. 1B,H). Examination of specimens in the present collections shows that the free tube is in fact the boundary between endocones and the matrix filling the endosiphotube (Fig. 1E, F, I). This is not often visible, as the endocones have been replaced by calcite, which is very similar in colour and texture to the matrix filling the endosiphotube. However, some specimens show the endosiphotube and the endocones clearly Fig. 1E, F). The endosiphotube is to the dorsal side of the centre of the siphuncle (Fig. 1H). Confusion of an endosiphotube with a free tube previously occurred with *Buttsoceras* and not until Flower (1962) undertook a detailed re-examination of the genus did the presence of the endocones and endosiphotube become apparent.

The details of the connecting rings were described by Teichert & Glenister (1952); however, a few specimens (NTO 17, T1255) show that there are also unexpanded, two-layered bullettes present, which form from differentiation of the siphonal layer (Fig. 2L). The presence of unexpanded bullettes is typical of some discosorid families, including the Ruedemannoceratidae. However, in addition, *Madiganella* has a siphuncle variable in position from centre to venter, endocones, expanded siphuncle and cyrtochoanitic septal necks, the combination of which supports an assignment to a new family of discosorids (Stait, in press). Teichert & Glenister (1952) assigned *Madiganella* to the Cyrtogomphoceratidae, and Flower & Teichert (1957) assigned it to the Ruedemannoceratidae. Both of these assignments are impossible.

Discussions of the affinities of *Madiganella* have all been tainted by the belief, expressed in Teichert & Glenister (1952, p. 733), that the age of the Larapinta Group (including the Horn Valley Siltstone) is Chazyan or younger. Recent work on the conodonts of the Horn Valley Siltstone (Cooper, 1981) has indicated the age is Late Canadian to Whiterock.

The presence of well-developed endocones, unexpanded bullettes, thick connecting rings, expanded siphuncular segments, cyrtochoanitic septal necks, and cameral deposits in Upper Canadian/Lower Whiterock discosorids such as *Madiganella* makes it difficult to believe they are the most primtive members of the order, and it must be suspected that an ancestor to these genera will be found in Middle Canadian strata.

Anthoceras Teichert & Glenister, 1954
Anthoceras warburtoni (Etheridge, 1893)
Figure 2A–F

1893 *Endoceras warburtoni* Etheridge, p. 7, Pl. 1, Figs. 11,12
1894 *Endoceras warburtoni* Etheridge, Etheridge, p. 25. Pl. 3, Figs. 19, 20
1896 *Orthoceras microlineatum* Tate, p. 39, Pl. 11, Fig. 10a, b
1952 *Cyclendoceras? microlineatum* (Tate), Teichert & Glenister, p. 733
1952 *Catoraphiceras warburtoni* (Etheridge), Teichert & Glenister, p. 733
1954 *Anothoceras decorum* Teichert & Glenister, p.63, Pl.8, Fig. 1

Discussion. Crick & Teichert (1983) described specimens of *Anthoceras* from Mount Arrowsmith, New South Wales. They considered them to belong to the type species *A. decorum.* As the external morphology of *A. decorum* was unknown, they revised the description of this species based on the Mount Arrowsmith material. This approach was reasonable, based on the data published then. However, collections of *Anthoceras* from the Horn Valley Siltstone, Amadeus Basin, indicate that the Mount Arrowsmith specimens are not conspecific with the Western Australian material. The internal morphology of the central Australian, Western Australian, and Mount Arrowsmith material is very similar. However, Crick & Teichert (1983, p. 157) indicated that 'the sutures are straight' on the Mount Arrowsmith specimens, whereas the central Australian material has distinct dorsal and ventral lobes and lateral saddles in the suture. The central Australian material (Fig. 2A–F) is virtually identical to the holotype of *A. decorum* and, because of this close similarity, *A. decorum* is considered to be a junior subjective synonym of *A. warburtoni* (Etheridge). The suture pattern of *A warburtoni* (Fig. 3A, B) is identicai to that described for *A. concavum* Lai (1965). Crick & Teichert (1983, p. 180) indicated that '*Anthoceras concavum* Lai 1965 differs from *A. decorum* by having a suture with a shallow dorsal and ventral lobe and a shallow lateral saddle. Otherwise it is identical with *A. decorum*'. However, after examination of the internal structures, Chen Junyuan (personal communication) has concluded that *A. concavum* does not belong to *Anthoceras.*

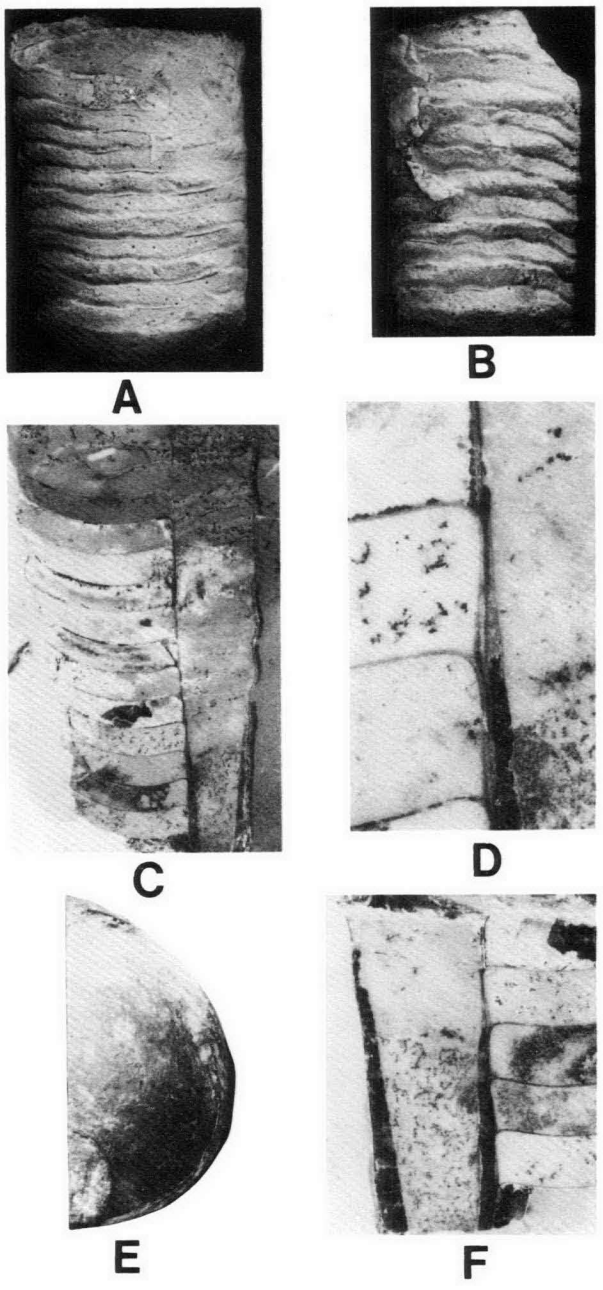

Figure 2. ***Anthoceras warburtoni*** **(Etheridge).**
A, Dorsal external view of the holotype T1257A, X2. B, Lateral external view of the holotype, venter right, X2. C, Sagittal section of P12283, venter right, X1.5. D, Enlargement of the dorsal side of the siphuncle, X10. E, Transverse section of P12283, venter below, X3. F, Sagittal section of P12283, opposite cut to that in C, venter left, X3.

Crick & Teichert (1983) have adequately discussed the other known species of *Anthoceras.* Their material from Mount Arrowsmith must now be considered as a new species.

Anthoceras arrowsmithense n. sp.

Holotype. SUP9871, paratypes SUP8801, 9855, 9867, 9884, 31892, University of Sydney Palaeontological Collection, other material, see Crick & Teichert (1983).

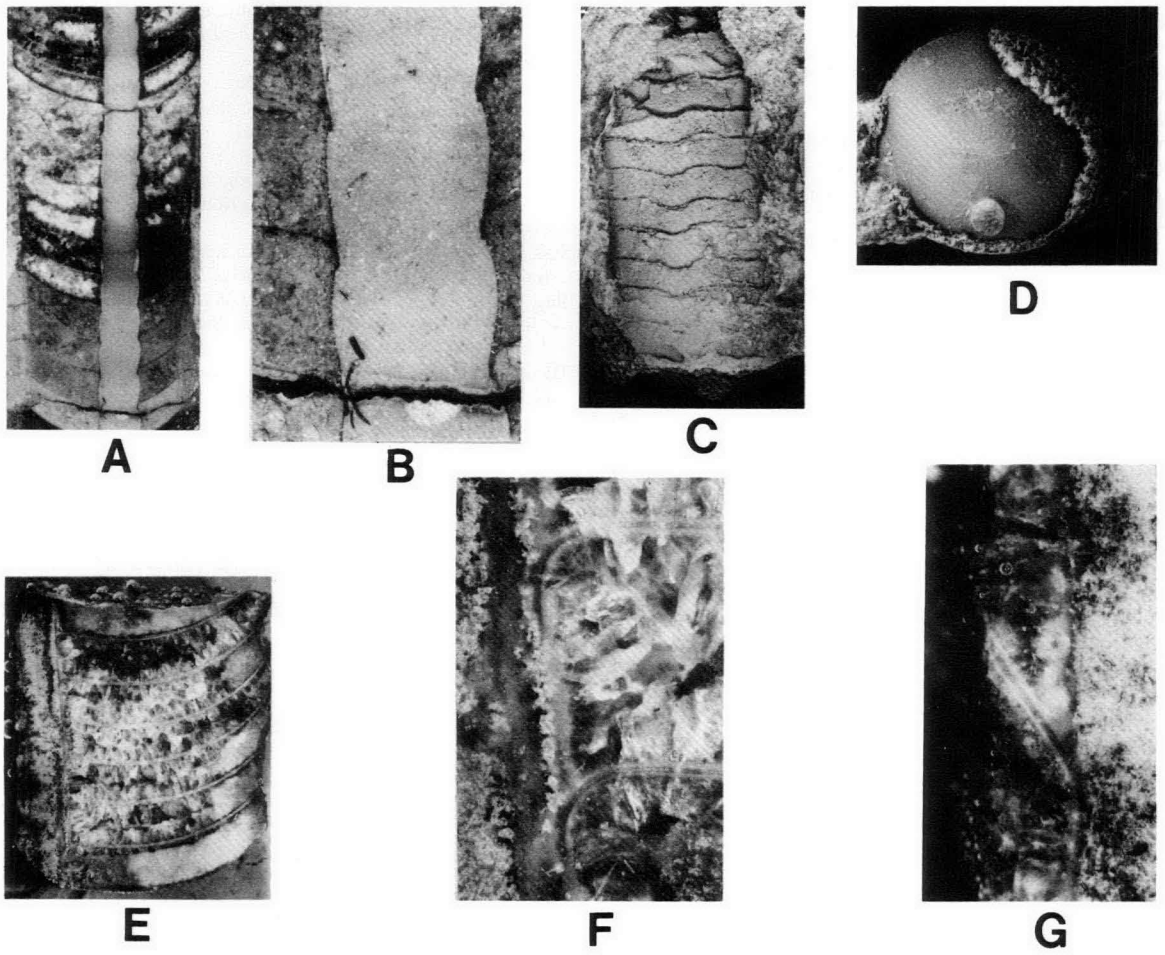

Figure 3. ***Bactroceras gossei*** **(Etheridge)**

A, Lateral section of the holotype T1216 ground from the venter, X1.8. B, An enlargement of the siphuncle in the holotype, X7. C, Ventral view of the holotype showing the suture, X1.8. D, Transverse view of the holotype showing the cross section and position of the siphuncle, X2. E, Sagittal section of T1216?, venter left, X2. F, Enlargement of the dorsal side of the siphuncle, X7. G, Enlargement of the ventral side of the siphuncle, X7.

Diagnosis. See Crick & Teichert (1983, p. 157) under diagosis of *A. decorum.*

Discussion. *Anthoceras arrowsmithense* differs from *A. warburtoni* in having straight sutures and more prominent annulations. The illustrations of the type material can be found in Crick & Teichert (1983, Figs. 4, 5).

Bactroceras Holm, 1898
Bactroceros gossei (Etheridge, 1893)
Figure 3A–G

1893 *Orthoceras gossei* Etheridge, p. 7, Pl. 1, Figs. 9–10
1952 *Bactroceras gossei* (Etheridge), Teichert & Glenister, p. 733
1964 *Bactroceras gossei* (Etheridge), Flower, p. 113

Material. Holotype T 1216, other material T1216? (sic).

Description. Phragmocone is a slowly expanding, unornamented, orthoconic longicone with a slightly compressed cross section. The siphuncle is very close to the ventral wall of the phragmocone and one-seventh of the height of the phragmocone (Fig. 3D, E). The siphuncular segments are as high as long and very slightly expanded between the septal foramina. The septa are gently curved, the radius of curvature is 25 mm.

The siphonal formula (Flower, 1968) for T1216? is 0.7/2/12:0.7/2.1/11.9,2.5. The connecting rings are only moderately thick (0.1 mm). The septal necks are orthochoanitic and moderate in length (1.0mm) (Fig. 3F, G). No cameral or siphonal deposits are present. The suture is straight across the dorsal and lateral sides. However, on the venter below the siphuncle there is a narrow lobe with a narrow saddle each side of the siphuncle (Fig. 3C).

Remarks. Teichert & Glenister (1952) suggested that *Orthoceras gossei* belonged to *Bactroceras*, but did not refigure nor describe the types. The original descriptions of Etheridge (1893) are inadequate for modern purposes; therefore, the type material is refigured and described herein.

Flower (1964) discussed *Bactroceras* and assigned four species to the genus, including *B. gossei*. *B. gossei* has a slightly larger siphuncle and less strongly curved septa than the type species of *Bactroceras*, but these are considered only to be species level differences, and the generic assignment of *B. gossei* is supported.

Acknowledgements

The authors wish to thank the following people and institutions for loan of collections; Dr P.A. Jell, Museum of Victoria; Dr N. Pledge, South Australian Museum; M. Stojanovic, University of Adelaide and Dr M.R. Banks. Dr Chen Junyuan and Dr Mary Wade are thanked for reading the manuscript and making many helpful comments.

References

Chen JunYuan & Zou Xiping, 1983 - Ordovician cephalopods from the Ordos area, China. *Memoir of the Nanjing Institute of Geology and Paleontology*, 20, 33-84.

Cooper, B.J., 1981 - Early Ordovician conodonts from the Horn Valley Siltstone, Central Australia. *Palaeontology*, 24, 147-183.

Crick, R.E. & Teichert, C., 1983. Ordovician endocerid genus Anthoceras: Its occurrence and morphology. *Alcheringa*, 7(2), 155-162.

Etheridge, R. Jr., 1893 - Contribution to the palaeontology of South Australia, No. 5; Additional Silurian and Mesozoic fossils from Central Australia. *Parliamentary Papers of South Australia*, 52, 6-8.

Etheridge, R. Jr., 1894 - Contribution to the palaeontology of South Australia, No. 7; Further additions to the Lower Silurian fauna of Central Australia. *Parliamentary Papers of South Australia*, 25, 23-26.

Flower, R.H., 1962 - Revision of Buttsoceras, Part 1. *Memoir of the New Mexico Bureau of Mines and Mineral Resources*, 10, 1-17.

Flower, R.H., 1964 - The nautiloid order Ellesmeroceratida (Cephalopoda). *Memoir of the New Mexico Bureau of Mines and Mineral Resources*, 12, 1- 234.

Flower, R.H., 1968 - The first great expansion of the Actinoceroids. *Memoir of the New Mexico Bureau of Mines and Mineral Resources*, 19, 1-16.

Flower, R.H. & Teichert, C., 1957 - The cephalopod order Discosorida. *University of Kansas Paleontological Contribution, Mollusca*, Article 6, 1-144.

Lai Caigen, 1965 - Ordovician and Silurian Cephalopods from Hanzhung and Ninghiang of Shensi. *Acta Palaeontologica Sinica*, 13, 308-342.

Ogienko, L.V., Byalyi, V.I. & Kolosnitsyna, G.R., 1974 - Biostratigrafiya Kemriyskikh i Ordovikskikh otlozheniy yuga Sibirskoy Platformy. *Vostochno-sibirsikiy nauchno-issledovatelskiy institut geologii, geofiziki i mineralnogo Syrya (Vostsiniiggims)*, 208p.

Stait, B.A., in press - Ordovician nautiloids of Tasmania, Australia - Gouldoceratidae fam. nov. (Discosorida). *Proceedings of the Royal Society of Victoria*, 97.

Stait, B.A. & Burrett, C.F., 1984 - Ordovician nautiloid faunas of Central and Southern Thailand. *Geological Magazine*, 121, 115-124.

Tate, R., 1896 - Palaeontology. *Report on the work of the Horn Scientific Expedition to Central Australia*, Part 3, Geology and Botany, *London and Melbourne*, 97-116.

Teichert, C., 1939 - The nautiloid Bathmoceras Barrande. *Royal Society of South Australia, Transactions*, 63/2, 384-391.

Teichert, C. & Glenister, B.F., 1952 - Fossil nautiloid faunas from Australia. *Journal of Paleontology*, 26(5), 730-752.

Teichert, C. & Glenister, B.F., 1954 - Early Ordovician cephalopod fauna from Western Australia. *Bulletins of American Paleontology*, 35(150), 1-112.

Wade, M., in press - Australian Lower Ordovician nautiloids: Coolibah Formation Discosorida and Tarphycerida. *Memoir of the Queensland Museum.*

Wells, A.T., Forman, D.J., Ranford, L.C. & Cook, P.J., 1970 - Geology of the Amadeus Basin, Central Australia. *Bureau of Mineral Resources, Australia, Bulletin*, 100.

CONTENTS

83/614(3) Cat. No. 84 2140 5